

**Sensing and Learning Channel State Information in a Dynamic Wireless Environment
with Cognitive Radios and Networks**

Submitted in partial fulfillment of the requirements for

the degree of

Doctor of Philosophy

in

Electrical and Computer Engineering

Reginald Lorenzo Cooper

B.S., Electrical Engineering, Southern University Baton Rouge, Louisiana

M.S., Electrical and Computer Engineering, Carnegie Mellon University

Carnegie Mellon University
Pittsburgh, PA

December, 2012

Copyright © Reginald Lorenzo Cooper 2012
All Rights Reserved



ACKNOWLEDGMENTS

First and foremost, I will like to give thanks to my Lord and savior Jesus Christ. I can do all things through Christ who strengthens me, Philippians 4:13.

My thesis research has been partially funded by Air Force Research Laboratory (AFRL) through the Minority Leaders Program (MLP), Clarkson Aerospace, and Universal Technology Corporation. Carnegie Mellon University (CMU) and DRS Signal Solutions have also financially contributed to this research. During my doctoral program I have also received financial support from General Motors, Texas Interments, and the GEM fellowship.

I will like to acknowledge my advisors, Dr. Daniel Stancil, the chair of my doctoral committee, who advised and mentored me in many aspects of my research and beyond, and Dr. Peter Steenkiste, who co-advised and helped me to think beyond the physical layer. I will also like to acknowledge the rest of my committee members, Dr. Rohit Negi and Dr. Vasu Chakravarthy, who have been instrumental in helping me develop my research as well.

Special thanks, to my undergraduate professors at Southern University Baton Rouge, your tutelage has established my fundamental understanding and respect for electrical engineering; and Dr. Ernest Walker, you have help me initiate my research within wireless communications; to professors at CMU, thank you for expanding my understanding and research within my field; and those associated with the 2006 Fusion forum, thank you as

well for all that you have done. To the team at AFRL and everyone associated with MLP, you have supported my research, mentored, and advised me. You watched my research grow from its beginnings at Southern University to my thesis research at CMU. I cannot express how grateful I am for your support, friendship, and advisement. I look forward to continuing this relationship.

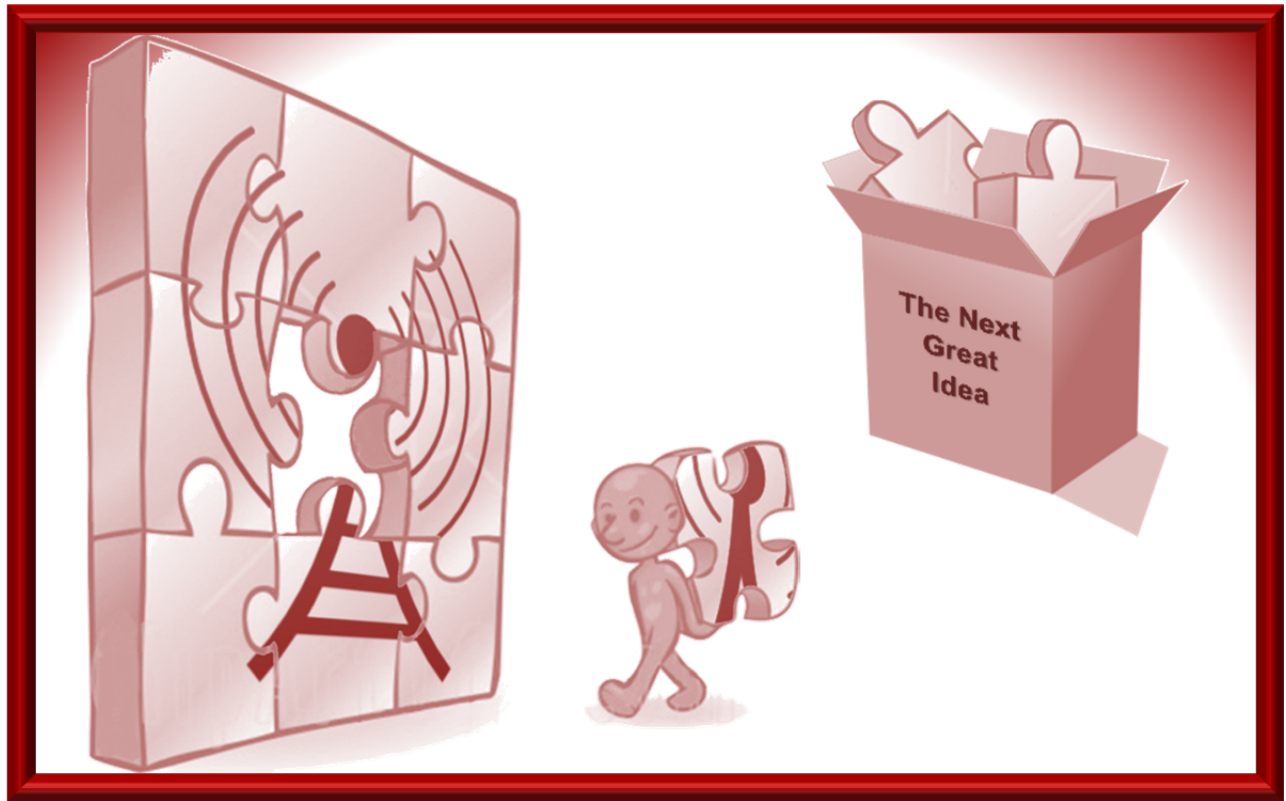
To my friends, your friendship, prayers, and support have been a blessing throughout my life. Some of you, we have been friends before we had the memory capacity to know that we were while playing at the Wee Academy. Others, we met through my matriculation through Clarendon 2 school district, “Representing that Manning Pride,” at Southern University roaming the halls of Bradford and Pinchback and around campus, in an apartment learning or teaching about a cold Tuesday night on December 04, 1906, at CMU recruiting for NSBE and enjoying Tuesday wing nights, hanging out in REH 234, grabbing a hot dog at Joe and Chris, and at Wright Patt making the most of an internship. I cherish all of your friendships and words cannot express my gratitude.

To my family, I cannot express how important your roles have been in my life. To come from a praying family, that values education, and supports each other no matter what, is a true blessing and a testimony of our faith. The numerous meals, the overnight stays, the laughter, guidance, and much more is something I can never repay. Our bond is something that goes beyond physical comprehension. Mom, Dad, Jonnifer, and Alfred you guys are the best and one word says it all CET. Dr. Jennifer Nyambura Cooper, I am truly blest to have you as my wife. Your support and understanding over this time has helped me get through so much, and I love you with all my heart and spirit.

To all, I know my hard work and dedication was not the only thing that got me here, but it was important. However, what I feel was more important is having you as professors, advisors, mentors, friends, family, and an unmovable faith. Thank you and God bless.



This thesis is dedicated to my mom, Alfreda H. Cooper, my dad, Alex L. Cooper, my brothers, Jonnifer L. Cooper and Alfred L. Cooper, my wife Jennifer. N. Cooper, and to all the other Coopers that will enter the CET in the future.



*Sometimes the next great
idea comes from those
willing to put the pieces
of the puzzle together.*



ABSTRACT

Sensing and learning channel state information (CSI) in a dynamic wireless environment (DWE) has not been a focus of the cognitive radio and network research. The focus has been on obtaining spectral resource information about the spectrum availability (i.e. spectrum sensing for dynamic spectrum access) or how to adapt radios and networks in a way that improves the effectiveness of the radio networks, for example rate adaptation. In most of these cases it is assumed that the CSI is already known or it is obtained from a method that directly measures the spectrum of interest through channel estimation, fading prediction or forecasting, blind estimation, and many others. In DWEs the wireless channel may change at high rates (i.e. fast fading), and methods that directly measure the channel will not provide accurate and timely CSI needed for a cognitive radio or network.

In this thesis a counterintuitive method is presented, indirect channel measurements. Indirect channel measuring is a technique used to determine the transfer function of a desired part of the RF spectrum, which spans several coherence bandwidths, without directly sending a signal through the spectrum of interest, but indirectly through adjacent spectrum. The indirect measuring of the channel has the ability to improve the timeliness and accuracy associated with the obtainment of the CSI in DWEs when using cognitive radios and networks.

This thesis will explain the indirect channel measurements (ICM) research and how it can be used in cognitive radio networks for SISO rate adaptation in dynamic wireless environments. Included will be an analytical and empirical analysis of the performance of the ICM technique and other comparable and contrasting techniques. This thesis will also show which technique is best suited for a particular set of parameters for a given dynamic wireless environment. A contextual explanation will also be given to provide a visual picture of a cognitive radio network that will be able to implement the ICM technique using rate adaptation, and its ability to be implemented in hardware.



TABLE OF CONTENTS

TITLE PAGE	i
ACKNOWLEDGMENTS	v
ABSTRACT	ix
TABLE OF CONTENTS	xi
LIST OF TABLES	xv
LIST OF FIGURES	xvii
PART I BACKGROUND DISCUSSION AND STATEMENT OF PROBLEM	1
Chapter 1 Introduction to Cognitive Radios	2
Chapter 2 Research Methodology	8
Section 2.1 Motivation	8
Section 2.2 Research Problem	10
Chapter 3 Thesis Outline	14
PART II REVIEW OF CONCEPTS	19
Chapter 4 Wireless Communication Channel	20
Section 4.1 Introduction.....	20

Section 4.2	Overview	21
Section 4.3	Channel Impulse Response and Transfer Function	24
	– <i>Discrete Channel Model</i>	25
	– <i>Statistical Channel Model</i>	27
	– <i>Channel Coherence</i>	35
Section 4.4	Summary	37
Chapter 5	Wireless Communication Systems	38
Section 5.1	System Model	38
	– <i>Linear System Model</i>	39
	– <i>Noise/Interference Model</i>	41
	– <i>Signal-to-Noise-Plus-Interference Ratio</i>	42
Section 5.2	Multi-Carrier Modulations	43
Section 5.3	Orthogonal Frequency Division Multiplexing (OFDM)	45
Section 5.4	Carrier-Interferometry OFDM	47
Section 5.5	Summary	48

PART III THE INDIRECT CHANNEL MEASUREMENT AND OTHER MEASUREMENT TECHNIQUES

Chapter 6	Wireless Channel Estimation and Extrapolation Techniques	50
Section 6.1	Introduction	50
Section 6.2	Traditional Estimation for OFDM	53
	– <i>Training Based Method</i>	53
	– <i>Blind and Semi-Blind Methods</i>	55
Section 6.3	Bayes and Linear Minimum Mean-Square Error (LMMSE) Estimator ..	57
Section 6.4	Fading Prediction and Time Extrapolation Techniques	60
	– <i>Linear Models</i>	61
	– <i>Time Domain Extrapolators</i>	62
Section 6.5	Super Resolution Wireless Channel Extrapolator	64
Section 6.6	Summary	64
Chapter 7	Indirect Channel Measurement Theory	67
Section 7.1	Introduction	67
Section 7.2	First Channel Measurement Research	69
Section 7.3	Indirect Channel Measurements	77
Section 7.4	Direct Channel Measurements	81
Section 7.5	No Channel and Full Channel Measurements	85
Section 7.6	Summary	87
Chapter 8	Channel Measurement and Rate Adaptation	89
Section 8.1	Introduction	89

Section 8.2	Types of Rate Adaptation Systems	91
Section 8.3	Information Update and Expiration Times	95
Section 8.4	Practical Scenario	98
Section 8.5	Rate Adaptation Mathematical Theory	102
	– <i>Squared Envelope and Rate Adaptation Thresholds</i>	103
	– <i>Rate Adaptation Metrics</i>	105
	– <i>Joint Probability Density Function of Targeted Metrics</i>	108
Section 8.6	Summary	116
Chapter 9	Channel Measurement Simulations	118
Section 9.1	Introduction	118
Section 9.2	Estimator and Extrapolator Simulator (EESIM)	119
	– <i>Explanation of EESIM Programming</i>	121
	– <i>EESIM Results</i>	124
	– <i>EESIM ICM Case Study</i>	
Section 9.3	RMSE-SE Simulator (RMSESIM)	132
	– <i>Explanation of RMSESIM Programming</i>	132
	– <i>RMSESIM Results</i>	136
Section 9.4	RMSESIM Case Study	141
Section 9.5	Summary	149
Chapter 10	Indirect Channel Measurements Experiments	151
Section 10.1	Introduction	151
Section 10.2	Experiment Setup	152
	– <i>USRP Transmitter and Receiver Design</i>	154
	– <i>Post Processing</i>	160
Section 10.3	Experiment Results	163
Section 10.4	Summary	168
PART IV	CONCLUSION	171
Chapter 11	Thesis Review	172
Section 11.1	Thesis Summary	172
	– <i>First Research Question</i>	173
	– <i>Second Research Question</i>	176
	– <i>Third Research Question</i>	177
	– <i>Simulations and Experiments</i>	178
Section 11.2	Thesis Contributions	182
	– <i>ICM Technique Contribution</i>	184
	– <i>Rate Adaptation Contributions</i>	187
Chapter 12	Future Research	189

BIBLIOGRAPHY	195
APPENDIX A MULTIPATH AND FADING MODELS	209
APPENDIX B RATE ADDAPTATION LOOK-UP TABLES	217



LIST OF TABLES

<u>Table</u>	<u>Description</u>	<u>Page</u>
6.1:	Estimator/extrapolator test	62
7.1:	Summary of the estimators and/or extrapolators in Chapter Seven.....	88
8.1:	ICM, DCM, and NCM techniques channel usage and pros and cons for rate adaptation.....	101
8.2:	Partial SNR threshold look-up table.....	104
8.3:	Initial variables and settings used in theoretical probability calculation.	112
8.4:	List of theoretical calculation of rate adaptation metrics using the ICM technique.	114
8.5:	List of theoretical calculation of rate adaptation metrics using the DCM technique.	115
8.6:	Rate adaptation metrics to compare the ICM and DCM techniques.....	117
9.1:	List of variables and GUI controls available in the EESIM.....	120
9.2:	List of EESIM GUI plots and descriptions.	124-125
9.3:	Discretize color legend for the ICM, DCM, and NCM techniques.	135
9.4:	Constant initial variables and settings used in IET_{DCM} calculation.	140
9.5:	The IET_{DCM} obtained from the first dotted line in Figure 9.11.	140
9.6:	The IET_{DCM} obtained from the second dotted line in Figure 9.11.....	141
9.7:	Initial variables and settings used in theoretical probability calculation.	142
9.8:	Case studies for a very dynamic DWE.....	146

9.9:	Case studies for a moderately dynamic DWE.	147
9.10:	Case studies for a slightly dynamic DWE.....	148
10.1:	Table outline for receiving USRP variable for the ICM technique.....	156
10.2:	Receiving USRP variable for the ICM technique and $K_{obsrv} = 128$	157
10.3:	Receiving USRP variable for the ICM technique and $K_{obsrv} = 40$	157
10.4:	Receiving USRP variable for the ICM technique and $K_{obsrv} = 16$	157
11.1:	Summary of the estimators and/or extrapolators in Chapter Seven.....	175
11.2:	Side by side comparison of the SRWC and ICM research.	183
B.1:	SNR threshold look-up table.....	217-221



LIST OF FIGURES

<u>Figure</u>	<u>Description</u>	<u>Page</u>
1.1:	Cognitive cycle presented by Joseph Mitola III.	3
1.2:	Fundamentals of cognition and the cognitive cycle presented by Joseph Mitola III.	4
1.3:	Secondary user implementing DSA with SRI in the present of primary users.....	5
1.4:	Secondary user implementing DSA with SRI and CSI in the present of primary users.....	6
2.1:	Channel gain for a multi-carrier signal.....	9
2.2:	Direct ICSI measurement method training symbol spectrum usage diagram.	11
2.3:	Indirect ICSI measurement method training symbol spectrum usage diagram.	12
4.1:	Three dimensional total coherence block diagram of the wireless channel.	23
4.2:	Two dimensional block diagram of the wireless channel.	34
4.3:	Rotated camera view of the two dimensional block diagram of the wireless channel.	35
5.1:	Wireless communication system linear model.	39
5.2:	Serial representation of the transmitted signal.	46
7.1:	MSE performance measurements for the initial and SRWC technique with and without MP reduction for the HIPERLAN/2 Model A standard.	74
7.2:	MSE performance measurements for the initial and SRWC technique with and without MP reduction for the channel model in the SRWC paper.	75

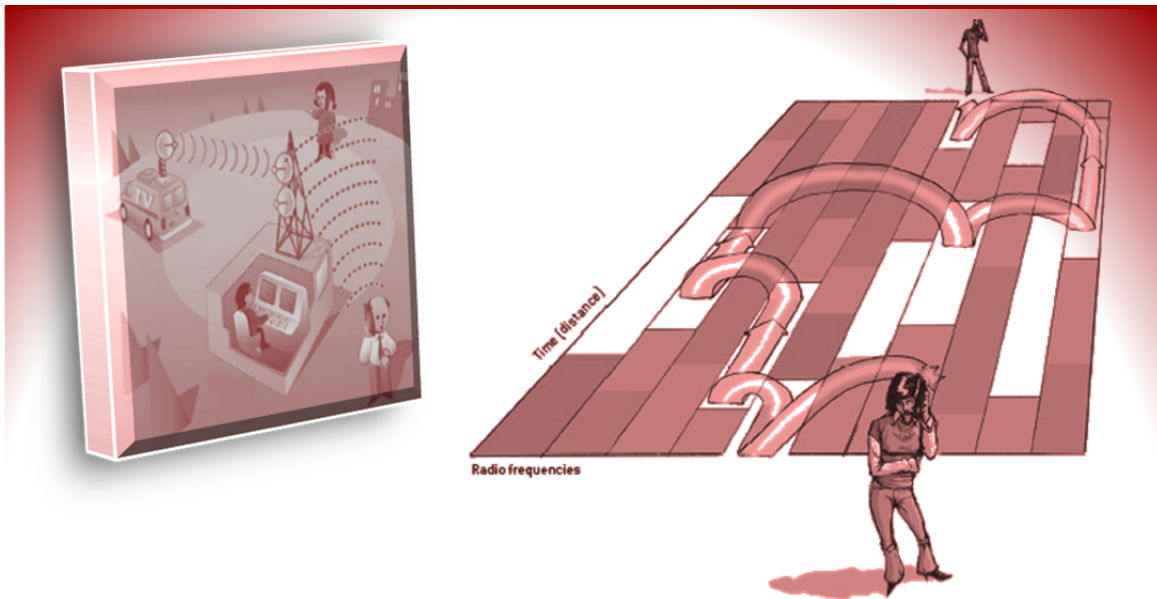
7.3:	Average CIR of the HIPERLAN/2 Model A channel standard.	76
7.4:	Average CIR of the channel model in the SRWC paper.....	76
7.5:	MSE performance measurements for LSEP without MP reduction and ICM technique for the HIPERLAN/2 Model A standard.	78
7.6:	MSE performance measurements for LSEP without MP reduction and ICM technique for an exponentially decaying tap model.	79
7.7:	CIR for an exponentially decaying channel model with a decaying slope of 36 degrees for each of the three exponentials.	80
7.8:	Jakes' Model for a max Doppler shift equal to 1 kHz and $L = 1024$, $L_1 = 64$, $N = 48$, $f_s = 62.5$ Hz.	83
7.9:	Optimal performance color map of the ICM and DCM techniques for ED delay channel model with a slope decline of 36 degrees; and a Jakes' spectral model for the frequency taps with a 1 kHz Doppler shift.	84
7.10:	MSE performance measurements for LSEP without MP reduction and ICM technique for the HIPERLAN/2 Model A standard.	87
8.1:	A block diagram of a rate adaptation system that uses present CSI observed at the receiver.	91
8.2:	A block diagram illustrating the procedure in which a rate adaption scheme using the DCM technique update the CSI at the transmitter.	92
8.3:	A block diagram illustrating the procedure in which a rate adaption scheme using the ICM technique update the CSI at the transmitter.	94
8.4:	Optimal performance color map of the ICM and DCM techniques for ED delay channel model with a slope decline of 36 degrees; and a Jakes' spectral model for the frequency taps with a 1 kHz Doppler shift.	97
8.5:	Graphical depiction of the DWE and wireless channel for one link.	100
8.6:	Joint probability of the BER and BPS for the BER Limit of $10^{-2.5}$ and the given initial values for ICM.	113
8.7:	Joint probability of the BER and BPS for the BER Limit of $10^{-2.5}$ and the given initial values for DCM.	113
9.1:	EESIM GUI.	121
9.2:	MATLAB code block diagram for EESIM.	123
9.3:	Correlation in the angular frequency domain and normalize coherence bandwidth.	128

9.4:	EESIM case 1 of a great MP model, the SRWC model, for the ICM technique.	129
9.5:	The SRWC model angular frequency domain correlation.	129
9.6:	The EDT with 90 degree slope model angular frequency domain correlation.	130
9.7:	The EDT with 36 degree slope model angular frequency domain correlation.	131
9.8:	MATLAB code block diagram for RMSESIM.	133
9.9:	Color legend for the ICM, DCM, and NCM techniques.	135
9.10:	RMSESIM GUI showing the theoretical and sampled RMSE SE.....	137
9.11:	RMSESIM GUI showing the performance comparison.	138
10.1:	Wireless communication system model for a system that is using the ICM technique.	152
10.2:	ICM experiment setup.....	153
10.3:	USRP transmit signal.	155
10.4:	USRP transmit signal for initial frequency synchronization.	155
10.5:	USRP transmit signal for initial frequency synchronization.	159
10.6:	Wireless channel estimation and extrapolations calculated in case one.	165
10.7:	Theoretical and sampled RMSE SE comparison obtained through experimentation.....	166
10.8:	Wireless channel estimation and extrapolations calculated in case two.	167
10.9:	Wireless channel estimation and extrapolations calculated in case three.	167
10.10:	Wireless channel estimation and extrapolations calculated in case four.	168
11.1:	Wireless channel two dimensional block diagram that indicates how total coherence blocks are used.	173
11.2:	Optimal performance color map of the ICM and DCM techniques for ED delay channel model with a slope decline of 36 degrees; and a Jakes spectral model for the frequency taps with a 1 kHz Doppler shift.....	176
11.3:	RMSESIM GUI showing the theoretical and sampled RMSE SE.....	179
11.4:	RMSESIM GUI showing the performance comparison.	180
11.5:	RMSESIM GUI showing the performance comparison.	181

12.1:	Generic block diagram of the author's vision of future radios.	191
12.2:	Experimental radio setup 1 (USRP1s) and 2 (USRP2s or N200s).....	191
12.3:	Diagram of experimental network setup.....	192

PART I

BACKGROUND DISCUSSION AND STATEMENT OF PROBLEM



This part of the thesis introduces the general area of study. It will also present the specific problems that will be examined and detail the precise purpose of this study. The objectives of the research will also be given in this part, along with the rationale and scope of this study. Finally, an overview of the remaining parts of this thesis will be given. After reading Part I, the reader will:

- Know the basics of cognitive radio and dynamic wireless environments.
- Gain a basic historical understanding of this research area.
- Have an understanding of sensing and learning techniques for cognitive radio.
- Understand the motivation for this study and research.
- Know the research problem and scope of this study.
- Have an overview of what to expect in the rest of the thesis.

CHAPTER ONE

INTRODUCTION TO COGNITIVE RADIO

The introduction of the concept of “cognitive radio” in the wireless communication community has stimulated significant interest in recent years. In this century we are seeing several ideas and suggestions on how to improve technology in wireless communications [1-6]. A lot of this can be accredited to the concept of personifying a radio. In essence, radios and networks of radios could possess some type of cognitive processing indicative of advanced thinking or instincts. This ability can be used to improve the effectiveness of radios and networks of radios, such as having larger network capacities and higher data rates through using adaptive or multirate OFDM, water-filling, and many other techniques [3, 7-10]. Most of these adaptive ideas and methods suggest that these radios and networks should have some type of prior knowledge of the channel state information (CSI) and/or spectral resource information (SRI) to make these adaptive or cognitive decisions possible [7, 11-15]. This thesis will show novel techniques that are timelier, more efficient, and

reasonably accurate in providing radios and networks with the needed prior knowledge to make cognitive decisions to improve radio network effectiveness (RNE).

Since the year 2000 cognitive radios and networks have been given many definitions. In 2000 Joseph Mitola III coined the term “Cognitive Radio,” defined it, and presented the idea of cognition within radios. To capture this idea of cognition Mitola presented the chart in Figure 1.1. This chart is explained in Mitola’s Thesis [4].

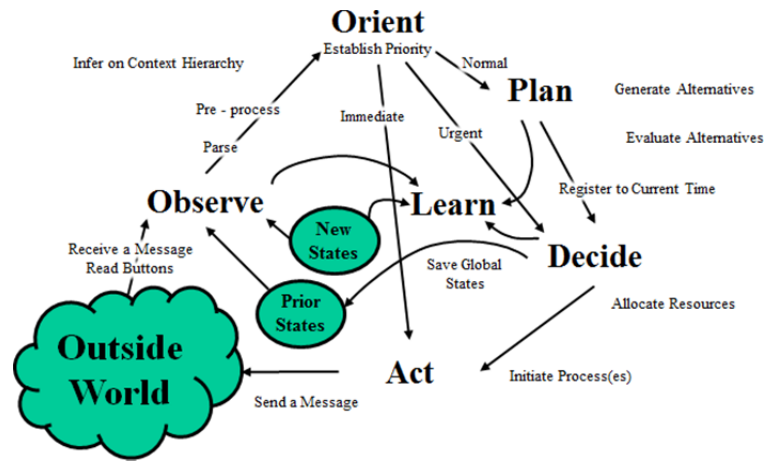


Figure 1.1: Cognitive cycle presented by Joseph Mitola III. [4]

There are other definitions and depictions that have been given for cognition [1-4, 6, 16, 17]. All the definitions and depictions try to capture one’s idea of radio cognition and intelligence, but all of them have three underlying fundamentals: sensing, learning, and adapting. Sensing involves the passive or active process that directly or indirectly gathers information about the operating environments and everything that changes the condition of the environments. The information gathered from sensing is processed to increase the radios’ or networks’ intelligence and determine what changes are needed to be made. This is considered to be the learning stage. Once learned, these changes are implemented

through adaptation. The radios and networks are reconfigured by changing the hardware, software, protocols, etc... [4, 18-26].

For example taking the depiction of cognition presented by Mitola, This depiction can be reorganized and place into this fundamental context shown in Figure 1.2.

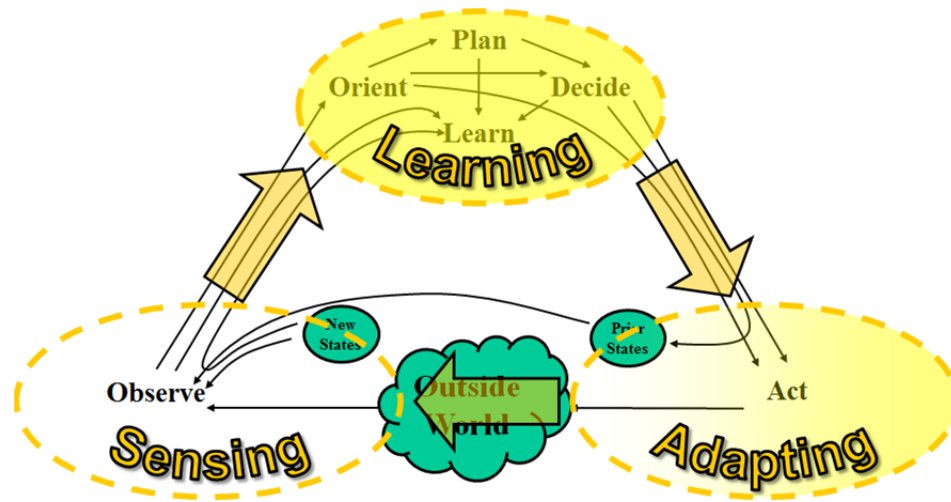


Figure 1.2: Fundamentals of cognition and the cognitive cycle presented by Joseph Mitola III.

The research presented in this thesis will focus on techniques used in the sensing and learning stages to gather CSI. In this thesis and research the sensing is done with respect to the wireless environment. This includes all the radios, networks, devices, channels and other objects or things that preside in that environment. What is learned is the channel state information. Simply, the information collected in the sensing stage can be used to learn the CSI.

The wireless communication community has long recognized the need for understanding and knowing the CSI for the physical wireless channel. The wireless channel is arguably the most critical part of a wireless communication system, because of the

ambiguity of the CSI. A wireless communication system gathers CSI by sending signals through the wireless channel and measuring the propagation effects such as path loss, fading, Doppler, multipath, etc... Within a wireless communication system these types of measurements are typically done at the radio receiver, and compensating corrections are applied to the signal after it travels through the wireless channel. This is often referred to as equalization [13, 27-29].

Along with knowing the CSI, knowing what spectral resources to use (i.e. available spectrum) has been something common with wireless radio research as well. However, knowing the dynamic nature of the spectrum resource information (SRI) has not always been a focal point of research in this community. SRI did not gain notoriety until engineers started to study and research cognitive radio systems to improve spectrum efficiency through dynamic spectrum access (DSA). This is one of the driving motives in understanding SRI [1, 4, 17, 22, 30]. There have been many emerging research areas within wireless communication that have presented new ways to use the knowledge obtained from knowing the CSI and SRI, and this can be credited to this idea of cognitive radios.

As has been stated, knowing the SRI can help a cognitive radio or network improve RNE. Figure 1.3 shows a crude drawing of how this would work.

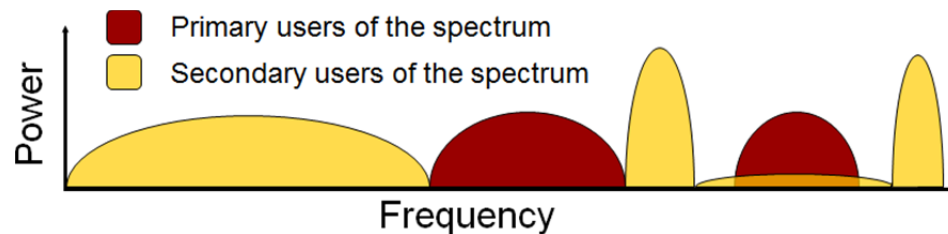


Figure 1.3: Secondary users implementing DSA with SRI in the present of primary users.

The cognitive radio or network would sense the spectrum to determine and learn what part of the spectrum is being used by the primary users of the spectrum. If the spectrum is not being used or underused, the secondary users will make use of the spectrum in a way that does not interfere with the primary user. This allows the secondary users to improve RNE for their radios and networks. CSI can be used to further improve RNE through efficient use of the used or underused spectrum or in DSA for determining what part of the spectrum is in a useable part of the channel (i.e. the spectrum is not in a null of the channel). Figure 1.4 shows this. By knowing the CSI, the secondary user can efficiently place power or data in the parts of spectrum that will give the radio or network the desired results with respect to its data rate or capacity.

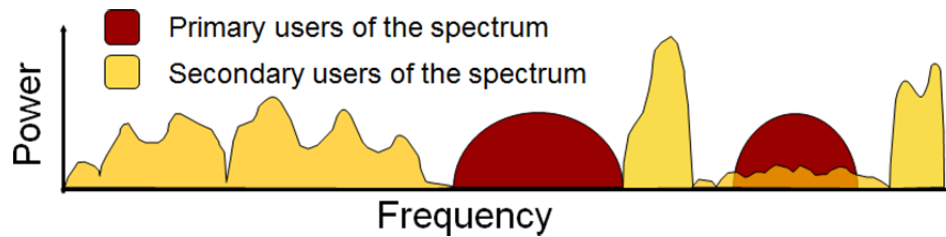


Figure 1.4: Secondary users implementing DSA with SRI and CSI in the present of primary users.

In Figure 1.4 the secondary user signal power varies with respect to frequency and this is to take advantage of the CSI.

There has been a lot of research presented on how to obtain SRI for cognitive radios [17, 28, 30]. However, there has not been much advancement in the techniques and methods used to obtain CSI, and these techniques may be inefficient or less accurate. Therefore, it is possible that there are ways to improve upon how this information is obtained, and research in this thesis will shed some light on the issues with current methods and present solutions for these issues.

The scope of this research will cover how CSI can be obtained and used in a cognitive radio and/or cognitive network context to improve RNE. Note the scope of the cognitive radio and network research extends beyond the intelligent use of the CSI. Cognitive radios and cognitive networks comprise a much grander idea [4, 26]. However, studies and research like this are important aspects in the development of this grand idea of cognitive radios and networks.

Most of this thesis will be dedicated to how cognitive radios can obtain the CSI for intelligent use, but there will be some emphasis placed on how the CSI is used in a particular adaptive technique. The next chapter will cover the research motivation and the structure of the research problem in this thesis.

CHAPTER TWO

RESEARCH METHODOLOGY

2.1 Motivation

The first motive or reason for implementing this research is captured by the background and scope presented in Chapter One. It was mentioned there has been increasing interest in the study and research of cognitive radio systems for various reasons. Over the past decade there have been numerous developments and suggestions on how to achieve this idea of cognition. The fundamentals of cognition can be viewed as the ability to sense, learn, and adapt [1, 23, 24]. To put this into context, the sensing part in this research is the measurement collected through an active signaling process that involves the sending and observing of a signal sent through a wireless channel in a wireless environment, which will be referred to as a dynamic wireless environment (DWE). Through this signaling process the channel state information (CSI) is learned from the measurements collected, and the radios and networks adapt their configuration based on this newfound knowledge. This sensing, learning, and adaptation process is in accordance with the background and

scope presented in Chapter One, and by researching this process it can and will aid in creating better cognitive devices.

Achieving this idea of cognition is not the only motivation. There are other motivators for research that study how to determine CSI. Future radio networks are pushing to improve RNE, and this is requiring more information about the environment than previously needed. This information must be timely and accurate. In dynamic wireless environments (DWEs) the timeliness and accuracy are very important [7, 8, 11-13, 31-33]. For example, Figure 2.1 shows two channels. One of the channels is static and the other is dynamic with respect to the time variation of the wireless channel. The signaling process involves the sending of something called a training symbol through the channel to measure the CSI, and this is typically done at the beginning of the transmitted signal.

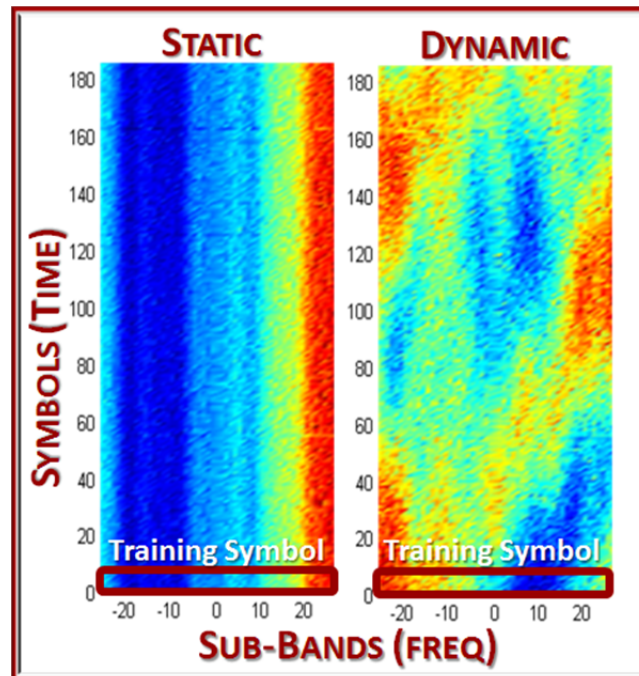


Figure 2.1: Channel gain for a multi-carrier signal.

What should be taken away from Figure 2.1 is that in the static case the channel looks the same with respect to time. Therefore, a signaling process that measures the channel state at the beginning of a transmitted signal will most likely suffice, because the channel does not vary. Whereas, in the dynamic case a signaling process that measures the channel state in the beginning most likely will not work, because the channel state varies with respect to time.

The ability to determine how to obtain the CSI in dynamic wireless channels and environments is a major motivation for this research. Figuring out how radios can overcome problems caused by dynamic channels and DWEs has always been a major part of wireless communication. In most recent years, a lot of the research in this area focused on the methods that improve RNE and not on the techniques to obtain the CSI in DWEs. For environments where this information, the CSI, is changing at rates faster than what systems or networks can convey to the respect devices, these improvements for RNE will not work. This inspired the creation of the research problem and question in the next section.

2.2 Research Problem

Two important aspects associated with the obtainment and/or measurement of CSI is timeliness and accuracy: how fast information must change with changes in the environment and how robust the information is to environmental effects. This research will use the following problem scenario. Assume that a radio or network can perform some cognitive fundamentals: sensing, learning, and adapting. Along with the spectrum resource information (SRI) or by itself, CSI can be used by the radios and/or networks to improve the overall throughput of a network through some type of cognitive process.

The first stage in the process is sensing. The network or radio collects measurements through sensing the wireless environments. This involves the sending of what is known as a training symbol through the wireless channel. Over time, this training symbol can be used to learn the statistical channel state information (SCSI). Once the SCSI is obtained, the radio and or network continues the sensing and uses the instantaneous channel state information (ICSI) and SCSI to learn how to adapt the transmitted or received waveforms to best suit the end-to-end objective of the networks and/or radios. However, the wireless environment in which the radio or network operates is very dynamic. This means the channel changes rapidly, at time lengths equal to or less than the time it takes to obtain or measure ICSI using conventional methods.

Conventional methods (direct methods) directly measure ICSI in the spectrum band or frequencies of interest through sending the training symbol through the same spectrum, shown in Figure 2.2. The ICSI obtained is with respect to frequency and time.

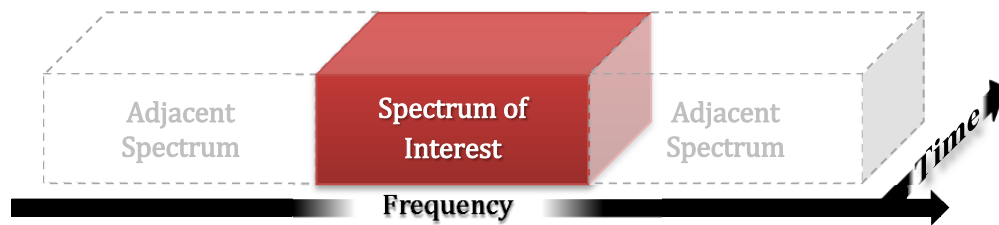


Figure 2.2: Direct ICSI measurement method training symbol spectrum usage diagram.

From Figure 2.1 and 2.2 it can be derived that the direct method could have issues with a dynamic wireless environment because of the varying nature of the ICSI. So, the first research question that arises is how can radios obtain the ICSI in a timely and accurate manner in DWEs? The direct method is one of the possible answers considered in this thesis.

Another answer to the question, the counter to the conventional method, and the main contribution of this thesis, is to obtain the same ICSI by using the adjacent spectrum. This will be referred to as the indirect method, and it is depicted in Figure 2.3.

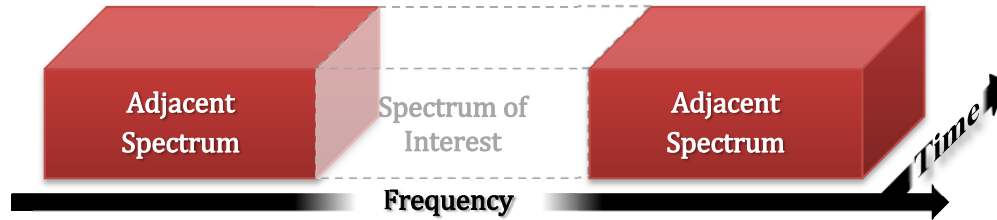


Figure 2.3: Indirect ICSI measurement method training symbol spectrum usage diagram .

In the indirect method, the adjacent spectrum is used to obtain the ICSI of the spectrum of interest. This is counter intuitive. In common practice researchers and engineers often assume that to obtain spectral information a radio must directly measure the spectrum for which the radio wishes to obtain ICSI. In this thesis it will be proven that in some cases it is possible to accurately obtain ICSI indirectly. It will also be shown that this can resolve the timeliness issues that can be caused by DWEs.

The research questions that will be addressed in this thesis are:

- How can radios obtain the ICSI in a timely and accurate manner in DWEs?
- What method is the best in DWEs: the Direct Channel Measurement (DCM) method, Indirect Channel Measurement (ICM) method, or neither?
- How is this related to RNE in cognitive radio networks?

These questions will be answered through presenting the theory created and the simulations and experiments performed throughout the course of this research. With

general respect to the questions, it was hypothesized that the ICM method will prove to be the preferred technique for very dynamic DWEs because it will not have issues with the timeliness of the ICSI updates, and the DCM method is going to be better for less dynamic DWEs because timeliness is not as important. The next chapter gives an overview of the entire thesis.

CHAPTER THREE

THESIS OUTLINE

This thesis has four parts and twelve chapters. Chapters 1 – 3 make up Part I. Part I has covered the background and the statement of the research problem. Part II will cover several concepts important to the research in this thesis. Part III is the main part of the thesis. It focuses on the main contribution, the indirect channel measurement (ICM) technique. Part IV summarizes and concludes everything that was presented.

Part II, the concept review, covers two concepts: wireless communication channels and wireless communication systems. The two chapters in Part II give a basic review that aid in the understanding of these concepts if lacking, but more importantly they build the notational framework that will be used throughout the entire thesis. In the case of Chapter Four, a less common, maybe even uncommon, framework for the wireless communication system is presented. This framework gives insight into how the wireless channel is viewed for this research. This view will help give intuition in how the ICM and other techniques

work. Chapter Five expands upon this framework and shows how the wireless channel models fit within a communication system with transmitted and received signals. Chapter Five also covers the types of signals used. In this thesis all signals are multi-carrier signals.

Part III is the most important part of this thesis. It covers the ICM technique as well as other preceding, contrasting, and complementing techniques. Part III includes Chapters 6 – 10. Chapter Six is mostly a literature review, but included are some important equations created during the course of this research to unify all these techniques for comparison purposes. In Chapter Six all the relevant techniques that preceded the ICM technique are presented. In this chapter the fundamentals of the direct channel measurement (DCM) method is also presented. Along with these fundamentals, a linear equation that fits the ICM and DCM technique is also given. This linear equation allows for direct comparison of the two techniques. This linear equation also fits the other preceding, contrasting, and comparable techniques.

Chapter Seven covers the mathematical theory of the ICM and DCM techniques. This chapter also gives the first metrics to test the accuracy of the ICM technique. The metrics given in this chapter are very important to this research. They are used to make a determination of what technique is the best. In this research these metrics were vetted through rigorous simulations and experiments which will be discussed later.

In the beginning of Chapter Seven a very similar technique to the ICM technique is discussed. This technique was created by researchers at Mitsubishi Electric Research Laboratories [34]. This technique also uses adjacent spectrum to determine the ICSI for the spectrum of interest. The ICM research and Mitsubishi research are somewhat similar ideas, but with respect to their theories there are some significant differences when it

comes to accuracy. The rest of the thesis will not cover the Mitsubishi technique because it is similar to the ICM technique, although significantly less accurate. The rest of the thesis will focus on the ICM and DCM techniques because they are contrasting techniques.

Three fundamental stages of cognition have been presented. The ICM and DCM techniques are implemented in the sensing and learning stages, but they have a direct effect on what is done in the adaptive stage. In Chapter Eight an adaptive technique that could improve RNE by using the ICM and/or DCM techniques is presented. These types of adaptive techniques are categorized as rate adaptation. Rate adaptation is when the transmitted signal's data rate is adapted by changing some aspect of the transmitted signal with respect to the CSI. In this chapter a rate adaptation scenario is given. For this scenario several tools are presented to help researchers and engineers make decisions on what technique will be best for improving RNE. The usage of the tools and metrics are not limited to the scope of the thesis. The reason for presenting these tools is to inspire researchers and engineers to come up with other novel ways of how to use them with respect to the ICM and DCM techniques in real world scenarios. So, in this research these rate adaptation metrics were not vetted through simulations or experiments.

Chapter Nine goes over a couple of the simulations created during this research. There were numerous simulations develop through this research study. For this thesis two of the most interesting simulations were chosen. The first simulation allows researchers and engineers to vary channel and radio parameters and then implement the ICM and DCM techniques and obtain the CSI. The second simulation verifies that the theory presented is accurate. The second simulation also gives researchers the ability to compare the ICM and DCM techniques and this comparison is used in the case studies, also to show when the ICM

and DCM techniques have the best performance. These case studies based on the second simulations are a very informative part of Chapter Nine. In these case studies various channel and radio parameters are changed and the best channel measurement technique is determined for each case and presented in the form of a look-up table. Readers will be able to pick various scenarios and determine what technique is the best.

Chapter Ten is the last chapter in Part III. Chapter Ten goes over one of the experiments conducted for this research. This experiment used universal software radio peripherals (USRPs) and software developed by students at Carnegie Mellon University [23]. The experiment complements the two simulations. The experiment only covers the ICM technique. The ICM technique was implemented using the hardware and software setup mentioned. From this implementation, the wireless channel was determined and the accuracy metric was verified. The experiment that is presented in Chapter Ten shows that the ICM technique can be implemented in real hardware.

The last part of this thesis, Part IV, is the conclusion. In this part all that was presented will be briefly reviewed and summarized. Also, a vision for future research will be given. Note, even though a lot of the mathematical theory overlaps with respect to the chapters and parts, each chapter and/or part is written to be read sequentially and individually.

PART II

REVIEW OF CONCEPTS



This part of the thesis will give a detailed explanation of several wireless communication concepts that are relevant to the research in this thesis. A mathematical foundation for these concepts will also be given. These concepts are important for the subsequent parts. This part will cover:

- The wireless communication channel concept in this thesis.
- How to obtain the statistical model for the wireless communication channel.
- Mathematical equations that define the wireless channels for this research.
- Fundamentals of a wireless communication system that are used.
- Multi-carrier modulations, in particular OFDM and CI-OFDM.
- The use of OFDM and CI-OFDM in this research

CHAPTER FOUR

WIRELESS COMMUNICATION CHANNELS

4.1 Introduction

This part of the thesis, *The Concept Review*, starts by discussing one of the most fundamental parts of this research, the wireless channel. The wireless channel is at the center of a wireless communication system. The wireless communication system will be defined in the next chapter. The wireless channel is often characterized by its bandwidth (e.g. narrowband and wideband channels). The wireless channel is defined as the physical link (temporal, spectral, and/or spatial) between RF transmitting and receiving radios. Due to its variability, the wireless channel is a particularly critical part of a wireless communication system. Transmitters and receivers can be designed to meet the communication needs of a wireless communication network, but the wireless channel is an unknown factor often set by uncontrollable events that are dependent on temporal, spectral, and spatial factors in the wireless environment [27, 35-37].

First, this chapter will give a graphical overview and intuitive understanding, because the way wireless channel was viewed was an important factor in how the mathematical concepts were formulated for this thesis. Then a mathematical representation of the analog and digital wireless channel will be presented, followed by a statistical representation. In conclusion this chapter will cover the coherence associated with the domains of the wireless channel.

4.2 Overview

This section will provide a view of the wireless channel that will be helpful in understanding other parts of the thesis. One of the more typical ways to view the wireless channel is by looking at it as a time varying tapped delay line model. Note that these taps are also space dependent. Each tap represents a multipath component for a particular space, time, and delay. Multipath is when two or more replicas of the transmitted signal reach the receiver at different times and amplitudes. Each replica is referred to as a multipath component. Multipath is caused by objects in the environment that scatter and/or reflect RF signals [27, 36, 38-40].

As mentioned, the channel's multipath components are directly related to this time varying tapped delay line model, often referred to as the channel impulse response (CIR). By taking a Fourier transform of the delay domain the CIR becomes the transfer function (TF) [27, 38, 39, 41]. The view of the channel presented in this thesis is based off these common views of the channel.

The view of the wireless channel in this thesis starts with the transfer function of the wireless channel. The transfer function is a useful place to start because it allows coherence

to be directly viewed in each domain (coherence time, coherence bandwidth, and coherence distance). Coherence distance will not be discussed in this thesis. However, later in this chapter a more detail definition of coherence time and bandwidth will be given. For now, a simple definition of coherence will be used.

Coherence means that for a given distance, time, or bandwidth the wireless channel does not vary for the respective domain [27]. For example, there is coherence within the spatial domain when the wireless channel does not vary over a particular distance. Total coherence is simply defined as coherence in all domains. This is where the visual depiction starts.

Consider a three dimensional block where each of the dimensions represents one of the three domains mentioned. Suppose that the space is discretized into rectangular blocks such that the variation of the channel within the block can be neglected. Therefore, the effect of the channel on any RF signal occurring within a given block can be multiplied by a constant complex value. Such a block will be referred to as a total coherence block. Within a wireless channel there may be several total coherence blocks. The combination of these total coherence blocks symbolizes the transfer function of the channel with respect to time and space.

In this thesis the wireless channel is further divided into six types of channels, depicted in Figure 4.1. Note that the time references of past, present, and future are with respect to the time the data or signal arrives at the receiver. Each block in the diagram is a total coherence block and it represents the channel's complex gain at a particular time, frequency, and spatial location. The darker colored blocks signify the complex channel gains at the geographical location of interest, and the lighter colored blocks are the complex

channel gains at other geographical locations surrounding the location of interest. However, the use of the spatial domain will not be covered in this thesis.

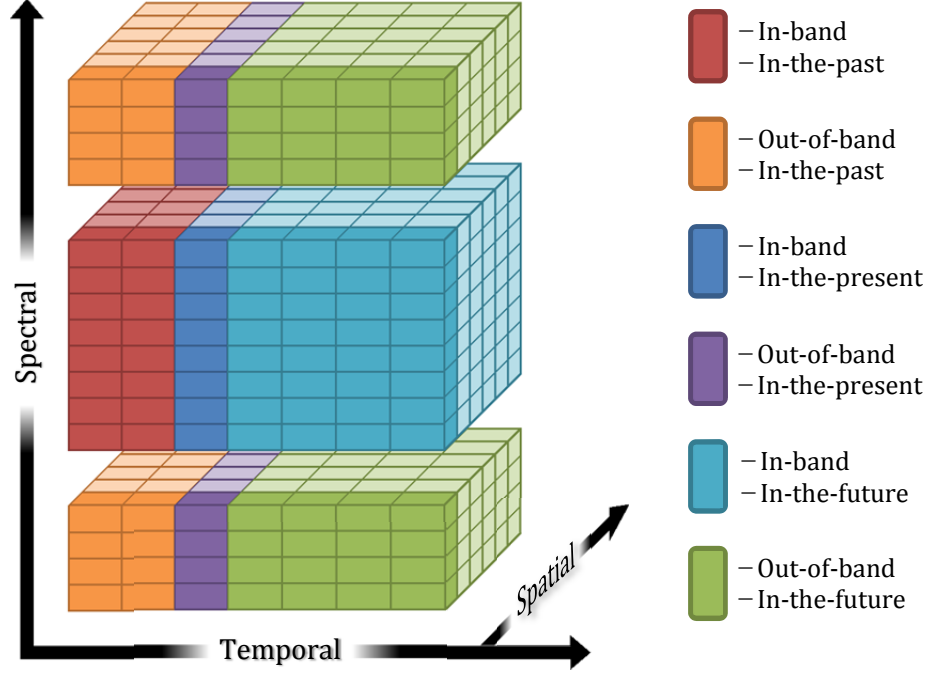


Figure 4.1: Three dimensional total coherence block diagram of the wireless channel.

The in-band (IB) channel refers to the wireless channel used to transmit data from the respective users, while the out-of-band (OOB) channel does not carry any data. In wireless communication the IB channel typically impairs the data. Instantaneous channel state information (ICSI) is commonly used to reverse or reduce the effects of these impairments. Typically, the ICSI that is used is the CIR and/or TF [27, 42-46].

In this thesis we will also talk about statistical channel state information (SCSI). This information is gathered over a long period of time (i.e. over the duration of many coherence times). In contrast, ICSI is obtained over periods of time shorter than a coherence time. By

observing the wireless channel over long periods of time, the fading characteristics and distributions can be determined [27, 41, 44, 45].

In this thesis, all the observed wireless channels are with respect to a single receiver and single transmitter, single-input-single-output (SISO) wireless communication system. This means that the spatial domain can be disregarded and from here forward the focus will be on the time and frequency domains.

4.3 Channel Impulse Response and Transfer Function

As stated, the ICSI used in this thesis is the CIR and TF. The CIR and TF can be used to show the effects the wireless channel have on the transmitted signal. Equation 4.1 shows the CIR with respect to time (time-delay domain). It also represents the analog wireless channel for a particular wireless communication system,

$$g_g(t, \tau) = \sum_{n=0}^{\infty} \sum_{k=0}^{\infty} c_c(t_n, \tau_k) \delta(\tau - \tau_k) \delta(t - t_n). \quad 4.1$$

This equation can be displayed in three other ways: the CIR at frequency f (frequency-delay domain) and the TF at time t (time-angular-frequency domain) or frequency f (frequency-angular-frequency domain),

$$g_G(f, \tau) = \sum_{n=0}^{\infty} \sum_{k=0}^{\infty} c_c(t_n, \tau_k) \delta(\tau - \tau_k) e^{-j2\pi f t_n}, \quad 4.2$$

$$G_g(t, \omega) = \sum_{n=0}^{\infty} \sum_{k=0}^{\infty} c_c(t_n, \tau_k) \delta(t - t_n) e^{-j\omega \tau_k}, \quad 4.3$$

$$G_G(f, \omega) = \sum_{n=0}^{\infty} \sum_{k=0}^{\infty} c_c(t_n, \tau_k) e^{-j\omega \tau_k} e^{-j2\pi f t_n}. \quad 4.4$$

In using these equations, some assumptions are made about the wireless channel, CIR, and TF. It is assumed that τ_k is positive, and that $\Delta\tau = \tau_k - \tau_{k-1}$ and $\Delta t = t_n - t_{n-1}$ have infinitesimal values. It is also assumed that there is causality in the delay and time domains,

and that the wireless channel has a maximum excess delay of τ_{\max} . Also, the frequency domain values are only present between the interval $[f_{\min}, f_{\max})$. For simplicity, in this paper f_{\min} will equal $-f_{\max}$. The variables f_{\min} and f_{\max} are the minimum and maximum excess frequencies. The absolute values of these frequencies are equal to or greater than that of the maximum Doppler shift, f_D .

The maximum excess delay is a well-known term that signifies the delay where the power delay profile drops below a certain threshold value [27, 40]. The minimum and maximum excess frequencies are terms created for this thesis. Similar to the maximum excess delay, these terms signify frequencies where the Doppler spectrum drops below a certain threshold value. The use of the maximum excess delay and frequencies values will be further explained later in this section.

Discrete Channel Model

Equations 4.1 – 4.4 represent a wireless channels that has infinite bandwidth and time in all the respective domains. However, Figure 4.1 is a discrete representation of the wireless channel. To obtain the discrete representations the following assumptions are made.

First, it is assumed that the wireless channel is band limited in the angular frequency domain. The channel is then complex-sampled and windowed in the time and delay domains with frequency resolution of f_s and ω_s , in the respective frequency domains, and $\omega_k = k\omega_s$ and $f_n = nf_s$. The span for the frequency domains are $[\omega_{-K_0}, \omega_{K_0})$ and $[f_{-L_0/2}, f_{L_0/2})$. The respective sample rates are $1/t_s$ and $1/\tau_s$, where $t_l = lt_s$ and $\tau_m = m\tau_s$.

The respective time windows are $[t_{L_1}, t_{L_0+L_1})$ and $[0, \tau_{2K_0})$, where the number of time samples is

$$L = L_0 + 2L_1 = \frac{1}{f_s t_s}, \quad 4.5$$

and the max number of delay samples are

$$K = 2(K_0 + K_1) = \frac{2\pi}{\omega_s \tau_s}. \quad 4.6$$

The need for variables L_1 and K_1 , will be explained later. They are important for improving the estimation when using the statistical model.

With these assumptions the following discrete representation of the CIR and TR can be derived,

$$h_h(t, \tau) = \begin{cases} a_a(t_l, \tau_m) & , t = t_l \text{ and } \tau = \tau_m \\ 0 & , \text{elsewhere} \end{cases}, \quad 4.7$$

$$h_H(f, \tau) = \begin{cases} a_A(f_n, \tau_m) & , f = f_n \text{ and } \tau = \tau_m \\ 0 & , \text{elsewhere} \end{cases}, \quad 4.8$$

$$H_h(t, \omega) = \begin{cases} A_a(t_l, \omega_k) & , t = t_l \text{ and } \omega = \omega_k \\ 0 & , \text{elsewhere} \end{cases}, \quad 4.9$$

$$H_H(f, \omega) = \begin{cases} A_A(f_n, \omega_k) & , f = f_n \text{ and } \omega = \omega_k \\ 0 & , \text{elsewhere} \end{cases}, \quad 4.10$$

where

$$a_a(t, \tau) = w(t, \tau) [g_g(t, \tau) * b(\tau)]. \quad 4.11$$

In Equation 4.11 function $b(\tau)$ is an arbitrary band limiting filter, and function $w(t, \tau)$ is an arbitrary sampling and windowing function. The filter and window are not set by the wireless environment. The band limiting filter and time window are determined by the design of the transmitting and receiving radios. The discrete channel model presented can be used to create a statistical model that can aid in estimating, extrapolating, and predicting the value of a_a .

Statistical Channel Model

The variable a_a is a random process that varies with respect to the time and delay. There are a few common assumptions that are made about the statistical model. The first being that the statistical model is Rayleigh distributed. This means that for every time and delay value, a_a is a zero-mean complex Gaussian random variable (RV) and its envelope is defined as the magnitude of a_a . Rayleigh fading is a common phenomenon within in wireless communication [27, 41-47].

The reasoning for the assumption for complex Gaussian RV stems from Equation 4.11. The variable g_g is also a random process. Variables b and w are deterministic variables. Using Equations 4.1 and 4.11, and given that g_g is a random process and b and w are deterministic, the following equation can be shown for a_a ,

$$a_a(t_l, \tau_m) = w(t_l, \tau_m) \sum_{k=-\infty}^{\infty} b(\tau_m - \tau_k) c_c(t_l, \tau_k). \quad 4.12$$

The variable $c_c(t_l, \tau_k)$ is the only RV. Assuming that $w(t_l, \tau_m)$ is not equal to zero and that there are a very large number of delay values for which $b(\tau_m - \tau_k)$ is not equal to zero, a variant of the central limit theorem can be invoked and used to prove that a_a can be modeled with a complex Gaussian RV. In part, this also justifies the Rayleigh fading assumption and its use in this research and thesis. However, these techniques can be adapted for other statistical models [41, 42, 44, 47].

The next assumptions are based on the number of RV needed to define a_a . In the delay domain it is assumed that values of a_a are negligible if τ is greater than τ_{\max} , and those values of a_a are assumed to be zero. Therefore, the maximum number of nonzero delay components, τ_m , that can be observed by the receiving radio is

$$M = \left\lfloor \frac{\tau_{\max} - \Delta\tau}{\tau_s} \right\rfloor + 1. \quad 4.13$$

In the frequency domain the number of RV depends on the maximum number of nonzero frequency components, f_n , that can be observed by the receiving radio, and that value will be

$$N = \left\lfloor \frac{2f_{\max} - \Delta f}{f_s} \right\rfloor. \quad 4.14$$

A statistical model can be derived by using these assumptions. These derivations will be done in matrix form. The variable A_a used in the discrete channel model can be written in the following matrix form. Note that these matrix forms can be in reference to column vectors or row vectors.

$$\begin{aligned} \mathbf{A}_{A_a} &= \begin{bmatrix} \mathbf{a}_{\mathbf{c},A_a,(0)} & \cdots & \mathbf{a}_{\mathbf{c},A_a,(L_0-1)} \end{bmatrix} \\ &= \begin{bmatrix} A_a(t_{L_1}, \omega_{-K_0}) & \cdots & A_a(t_{L_0+L_1-1}, \omega_{-K_0}) \\ \vdots & \ddots & \vdots \\ A_a(t_{L_1}, \omega_{K_0-1}) & \cdots & A_a(t_{L_0+L_1-1}, \omega_{K_0-1}) \end{bmatrix}, \end{aligned} \quad 4.15$$

$$\mathbf{A}_{A_a} = \begin{bmatrix} \mathbf{a}_{\mathbf{r},A_a,(0)} \\ \vdots \\ \mathbf{a}_{\mathbf{r},A_a,(2K_0-1)} \end{bmatrix} = \begin{bmatrix} A_a(t_{L_1}, \omega_{-K_0}) & \cdots & A_a(t_{L_0+L_1-1}, \omega_{-K_0}) \\ \vdots & \ddots & \vdots \\ A_a(t_{L_1}, \omega_{K_0-1}) & \cdots & A_a(t_{L_0+L_1-1}, \omega_{K_0-1}) \end{bmatrix}. \quad 4.16$$

The matrix in these equations represents a multivariate complex Gaussian RV with zero mean. Therefore, it can be defined by its covariance matrix. To find the covariance matrix for the matrix \mathbf{A}_{A_a} two-dimensional correlation analysis is typically used. This matrix also can be obtained by concatenating several small covariance and cross-covariance matrices. Let the covariance and cross-covariance matrix for the column vectors $\mathbf{a}_{\mathbf{c},A_a,(i)}$ and $\mathbf{a}_{\mathbf{c},A_a,(j)}$ be defined as

$$\mathbf{R}_{\mathbf{c},\mathbf{A}_{A_a},(i,j)} = E\{\mathbf{a}_{\mathbf{c},A_a,(i)} \mathbf{a}_{\mathbf{c},A_a,(j)}^H\}, \quad 4.17$$

and for the row vectors $\mathbf{a}_{\mathbf{r},A_a,(i)}$ and $\mathbf{a}_{\mathbf{r},A_a,(j)}$ be defined as

$$\mathbf{R}_{\mathbf{r},\mathbf{A}_{A_a},(i,j)} = E\{\mathbf{a}_{\mathbf{r},A_a,(j)}^H \mathbf{a}_{\mathbf{r},A_a,(i)}\}. \quad 4.18$$

The covariance matrix, using the column vector arrangement, of \mathbf{A}_{A_a} can be shown as

$$\mathbf{R}_{\mathbf{c},\mathbf{A}_{A_a}} = \begin{bmatrix} \mathbf{R}_{\mathbf{c},\mathbf{A}_{A_a},(0,0)} & \cdots & \mathbf{R}_{\mathbf{c},\mathbf{A}_{A_a},(L_0-1,0)} \\ \vdots & \ddots & \vdots \\ \mathbf{R}_{\mathbf{c},\mathbf{A}_{A_a},(0,L_0-1)} & \cdots & \mathbf{R}_{\mathbf{c},\mathbf{A}_{A_a},(L_0-1,L_0-1)} \end{bmatrix}, \quad 4.19$$

and for the row vector arrangement

$$\mathbf{R}_{\mathbf{r},\mathbf{A}_{A_a}} = \begin{bmatrix} \mathbf{R}_{\mathbf{r},\mathbf{A}_{A_a},(0,0)} & \cdots & \mathbf{R}_{\mathbf{r},\mathbf{A}_{A_a},(2K_0-1,0)} \\ \vdots & \ddots & \vdots \\ \mathbf{R}_{\mathbf{r},\mathbf{A}_{A_a},(0,2K_0-1)} & \cdots & \mathbf{R}_{\mathbf{r},\mathbf{A}_{A_a},(L_0-1,2K_0-1)} \end{bmatrix}. \quad 4.20$$

These matrices can be used in generating the statistical model for the multivariate complex Gaussian RV \mathbf{A}_{A_a} . One of the ways this can be done is by taking the Cholesky decomposition of either of the covariance matrices, and then multiplying the matrix obtained from the decomposition with a vector of i.i.d. standard complex Gaussian RVs,

$$\begin{bmatrix} \mathbf{a}_{\mathbf{c},\mathbf{A}_{A_a},(0)} \\ \vdots \\ \mathbf{a}_{\mathbf{c},\mathbf{A}_{A_a},(L_0-1)} \end{bmatrix} = \mathbf{C}_{\mathbf{c},\mathbf{A}_{A_a}}^H \begin{bmatrix} \mathcal{N}_0 \\ \vdots \\ \mathcal{N}_{2K_0L_0-1} \end{bmatrix}, \quad 4.21$$

$$[\mathbf{a}_{\mathbf{r},\mathbf{A}_{A_a},(0)} \quad \cdots \quad \mathbf{a}_{\mathbf{r},\mathbf{A}_{A_a},(L_0-1)}] = [\mathcal{N}_0 \quad \cdots \quad \mathcal{N}_{2K_0L_0-1}] \mathbf{C}_{\mathbf{r},\mathbf{A}_{A_a}}. \quad 4.22$$

In Equations 4.21 and 4.22, the variable \mathcal{N} is a standard complex Gaussian random variable, and \mathbf{C} is an upper triangular matrix obtained from the Cholesky decomposition.

Equations 4.21 and 4.22 represent the common statistical model used in two dimensional analysis [41, 44]. In this thesis a more manageable form is used. The documentation of this more manageable model has not been found in any of the current literature, but the intuition behind it is commonly used. Due to the mathematical complexity, the relationship between the two models will not be discussed.

Equations 4.15 and 4.16 define the column and row vectors that are used to define the wireless channel. The column vectors represent the TF at the time value associated with the respective column. The row vectors represent the Rayleigh fading with respect to the

angular-frequency associated with the row. Using equation 4.17 and 4.18, a simpler statistical model for the time dependent TF can be created.

Equations 4.17 and 4.18 give the covariance and cross-covariance matrices for the column and row vectors. For this statistical model the cross-covariance matrices are not needed. Disregarding the cross-covariance, the matrices become

$$\mathbf{R}_{\mathbf{c}, \mathbf{A}_{A_a}(i)} = E\{\mathbf{A}_{\mathbf{c}, A_a(i)} \mathbf{A}_{\mathbf{c}, A_a(i)}^H\}, \quad 4.23$$

$$\mathbf{R}_{\mathbf{r}, \mathbf{A}_{A_a}(j)} = E\{\mathbf{A}_{\mathbf{r}, A_a(j)}^H \mathbf{A}_{\mathbf{r}, A_a(j)}\}. \quad 4.24$$

For further simplification only, wide sense stationarity (WSS) is assumed in all domains. By assuming WSS and making the assumption that c_c can be divided into two independent one variable functions, the following simplification can be made

$$\mathbf{R}_{\omega, \mathbf{A}_{A_a}} = E\left\{\frac{1}{L_0} \mathbf{A}_{A_a} \mathbf{A}_{A_a}^H\right\} = \mathbf{R}_{\mathbf{c}, \mathbf{A}_{A_a}(i)}, \quad 4.25$$

$$\mathbf{R}_{t, \mathbf{A}_{A_a}} = E\left\{\frac{1}{2K_0} \mathbf{A}_{A_a}^H \mathbf{A}_{A_a}\right\} = \mathbf{R}_{\mathbf{r}, \mathbf{A}_{A_a}(j)}. \quad 4.26$$

Given these assumptions the following statistical model can be derived

$$\mathbf{A}_{A_a} = \mathbf{C}_{\omega, \mathbf{A}_{A_a}}^H \underbrace{\begin{bmatrix} \mathcal{N}_{0,0} & \cdots & \mathcal{N}_{L_0-1,0} \\ \vdots & \ddots & \vdots \\ \mathcal{N}_{0,2K_0-1} & \cdots & \mathcal{N}_{L_0-1,2K_0-1} \end{bmatrix}}_{\mathbf{N}} \mathbf{C}_{t, \mathbf{A}_{A_a}}. \quad 4.27$$

Once again, the matrixes represented by the variable \mathbf{C} are Cholesky decompositions of the respective covariance matrices \mathbf{R} . The model in Equation 4.27 is given in the time-angular-frequency domain, signified by the variable A_a . The rows represent the angular-frequencies and the columns represent the times. There are a couple of reasons that the time-angular-frequency domain was used to present the statistical model thus far. One being that this is the domain the channel will be measured in, but more importantly to

help visualize the use of the extra samples mentioned in the previous section denoted by the variables L_1 and K_1 .

These extra samples are added to minimize the value of M and N . The science behind this minimization, within context to this research, has not been scientifically studied to determine the optimal values that should be used to extend the wireless channel. However, its affects have been observed. The extended transfer function takes the following form,

$$\mathbf{B}_{A_a} = \begin{bmatrix} A_a(t_0, \omega_{-K_0-K_1}) & \cdots & A_a(t_{L_0+2L_1-1}, \omega_{-K_0-K_1}) \\ \vdots & \ddots & \vdots \\ A_a(t_0, \omega_{K_0+K_1-1}) & \cdots & A_a(t_{L_0+2L_1-1}, \omega_{K_0+K_1-1}) \end{bmatrix} = \begin{bmatrix} \ddots & \vdots & \ddots \\ \cdots & \mathbf{A}_{A_a} & \cdots \\ \ddots & \vdots & \ddots \end{bmatrix}. \quad 4.28$$

An extended version of each of the four matrix domains (i.e. time-delay domain, frequency-delay domain, etc.) can be derived from one another by multiplying one of the column domains, the delay or angular-frequency domain, by a modified and shifted fast Fourier transform (FFT) and/or multiplying one of the row domains, the time or frequency domain, by a modified and shifted inverse FFT (IFFT) matrix:

$$\mathbf{B}_{a_a} = \frac{1}{K} \mathbf{F}_F^H \mathbf{B}_{A_a} = \mathbf{B}_{a_A} \mathbf{F}_I = \frac{1}{K} \mathbf{F}_F^H \mathbf{B}_{A_A} \mathbf{F}_I, \quad 4.29$$

$$\mathbf{B}_{a_A} = \frac{1}{K} \mathbf{F}_F^H \mathbf{B}_{A_A} = L \mathbf{B}_{a_a} \mathbf{F}_I^H = \frac{L}{K} \mathbf{F}_F^H \mathbf{B}_{A_a} \mathbf{F}_I^H, \quad 4.30$$

$$\mathbf{B}_{A_a} = \mathbf{F}_F \mathbf{B}_{a_a} = \mathbf{B}_{A_A} \mathbf{F}_I = \mathbf{F}_F \mathbf{B}_{a_A} \mathbf{F}_I, \quad 4.31$$

$$\mathbf{B}_{A_A} = \mathbf{F}_F \mathbf{B}_{a_A} = L \mathbf{B}_{A_a} \mathbf{F}_I^H = L \mathbf{F}_F \mathbf{B}_{a_a} \mathbf{F}_I^H. \quad 4.32$$

The matrix \mathbf{F}_F is a row shifted $K \times M$ FFT matrix, and \mathbf{F}_I is the row shifted $N \times L$ IFFT matrix:

$$\mathbf{F}_F = \begin{bmatrix} 1 & \alpha_K^{-\left(\frac{K}{2}-1\right)} & \alpha_K^{-2\left(\frac{K}{2}-1\right)} & \dots & \alpha_K^{-(M-1)\left(\frac{K}{2}-1\right)} \\ \vdots & \vdots & \vdots & \ddots & \vdots \\ 1 & \alpha_K^{-1} & \alpha_K^{-2} & \dots & \alpha_K^{-(M-1)} \\ 1 & 1 & 1 & \dots & 1 \\ \vdots & \vdots & \vdots & \ddots & \vdots \\ 1 & \alpha_K^{\left(\frac{K}{2}-1\right)} & \alpha_K^{2\left(\frac{K}{2}-1\right)} & \dots & \alpha_K^{(M-1)\left(\frac{K}{2}-1\right)} \end{bmatrix}, \quad 4.33$$

$$\mathbf{F}_I = \frac{1}{L} \begin{bmatrix} 1 & \alpha_L^{\left(\frac{N}{2}-1\right)} & \alpha_L^{2\left(\frac{N}{2}-1\right)} & \dots & \alpha_L^{(L-1)\left(\frac{N}{2}-1\right)} \\ \vdots & \vdots & \vdots & \ddots & \vdots \\ 1 & \alpha_L^1 & \alpha_L^2 & \dots & \alpha_L^{(L-1)} \\ 1 & 1 & 1 & \dots & 1 \\ \vdots & \vdots & \vdots & \ddots & \vdots \\ 1 & \alpha_L^{-\left(\frac{N}{2}-1\right)} & \alpha_L^{-2\left(\frac{N}{2}-1\right)} & \dots & \alpha_L^{-(L-1)\left(\frac{N}{2}-1\right)} \end{bmatrix}, \quad 4.34$$

$$\alpha_K = e^{-j\frac{2\pi}{K}}, \quad 4.35$$

$$\alpha_L = e^{-j\frac{2\pi}{L}}. \quad 4.36$$

The covariance matrices for the vector domains (i.e. the column and row domains) of the extended transfer function will have a similar form to Equation 4.28,

$$\mathbf{R}_\omega = \mathbf{R}_{\omega, \mathbf{B}_{A_a}} = \mathbf{R}_{\omega, \mathbf{B}_{A_A}} = E\{\frac{1}{L} \mathbf{B}_{A_a} \mathbf{B}_{A_a}^H\} = E\{\frac{1}{N} \mathbf{B}_{A_A} \mathbf{B}_{A_A}^H\} = \begin{bmatrix} \ddots & & \vdots & & \ddots \\ \cdots & & \mathbf{R}_{\omega, A_{A_a}} & & \cdots \\ \ddots & & \vdots & & \ddots \end{bmatrix}, \quad 4.37$$

$$\mathbf{R}_t = \mathbf{R}_{t, \mathbf{B}_{A_a}} = \mathbf{R}_{t, \mathbf{B}_{a_a}} = E\{\frac{1}{K} \mathbf{B}_{A_a}^H \mathbf{B}_{A_a}\} = E\{\frac{1}{M} \mathbf{B}_{a_a}^H \mathbf{B}_{a_a}\} = \begin{bmatrix} \ddots & & \vdots & & \ddots \\ \cdots & & \mathbf{R}_{t, A_{A_a}} & & \cdots \\ \ddots & & \vdots & & \ddots \end{bmatrix}. \quad 4.38$$

Note that the statistical relationships between the non-extended values are the same. By doing this, the maximum excess delay and number of frequency values are reduced, changing the statistics of the non-extended values that will be observed. This happens because the extending in time is similar to windowing, and the extending in the angular frequency domain is like filtering. These extended values will never be observed in the

physical measurements. These values are only used to improve the estimation, extrapolation, and prediction.

The covariance matrix for the other two vector domains, the delay and frequency domains, can be define as

$$\mathbf{R}_\tau = \mathbf{R}_{\tau, \mathbf{B}_{a_a}} = \mathbf{R}_{\tau, \mathbf{B}_{a_A}} = E\left\{\frac{1}{L} \mathbf{B}_{a_a} \mathbf{B}_{a_a}^H\right\} = E\left\{\frac{1}{N} \mathbf{B}_{a_A} \mathbf{B}_{a_A}^H\right\}, \quad 4.39$$

$$\mathbf{R}_f = \mathbf{R}_{f, \mathbf{B}_{A_A}} = \mathbf{R}_{f, \mathbf{B}_{a_A}} = E\left\{\frac{1}{K} \mathbf{B}_{A_A}^H \mathbf{B}_{A_A}\right\} = E\left\{\frac{1}{M} \mathbf{B}_{a_A}^H \mathbf{B}_{a_A}\right\}. \quad 4.40$$

The vector domains also have the following relationship to one another respectively:

$$\mathbf{R}_\tau = \frac{1}{K^2} \mathbf{F}_F^H \mathbf{R}_\omega \mathbf{F}_F, \quad 4.41$$

$$\mathbf{R}_\omega = \mathbf{F}_F \mathbf{R}_\tau \mathbf{F}_F^H. \quad 4.42$$

$$\mathbf{R}_t = L^2 \mathbf{F}_I^H \mathbf{R}_f \mathbf{F}_I, \quad 4.43$$

$$\mathbf{R}_f = \mathbf{F}_I \mathbf{R}_t \mathbf{F}_I^H. \quad 4.44$$

By using the extended sample version of the wireless channel the number of values needed to define the channel in the delay-frequency domain can be reduced and the following new statistical model includes this reduction.

$$\mathbf{H}_{h_H} = \mathbf{B}_{a_A} = \mathbf{C}_\tau^H \underbrace{\begin{bmatrix} \mathcal{N}_{0,0} & \cdots & \mathcal{N}_{N-1,0} \\ \vdots & \ddots & \vdots \\ \mathcal{N}_{0,M-1} & \cdots & \mathcal{N}_{N-1,M-1} \end{bmatrix}}_{\mathbf{N}_{(M \times N)}} \mathbf{C}_f. \quad 4.45$$

The random variables, $\mathcal{N}_{n,m}$, are i.i.d. standard complex Gaussian. The variables \mathbf{C}_τ , and \mathbf{C}_f are the upper triangular matrices for the respective domains that can be obtained by taking the Cholesky decomposition of the corresponding covariance matrices, \mathbf{R}_τ and \mathbf{R}_f .

Using Equation 4.45, a statistical model for the wireless channel with respect to any of the other matrix domains can be derived. Most importantly, the time-angular-frequency

domain model, shown in Equation 4.46, using the Cholesky decompositions for the covariance matrices of the time and angular-frequency vector domains, can be simplified.

$$\mathbf{H}_{H_h} = \mathbf{B}_{A_a} = \mathbf{C}_\omega \mathbf{N}_{(K \times L)} \mathbf{C}_t, \quad 4.46$$

Equations 4.31 and 4.45 can be used to simplify the model. Only requiring N times M unknown values or RVs to defined the channel instead of L times K . Therefore the statistical channel model for the wireless channel of Figure 4.2 can be shown as

$$\begin{aligned} \mathbf{H}_{H_h} &= \mathbf{B}_{A_a} \\ &= \mathbf{F}_F \mathbf{B}_{a_A} \mathbf{F}_I \\ &= \mathbf{F}_F \mathbf{H}_{h_H} \mathbf{F}_I \\ &= \mathbf{F}_F \mathbf{C}_\tau \mathbf{N}_{(M \times N)} \mathbf{C}_f \mathbf{F}_I \end{aligned} \quad 4.47$$

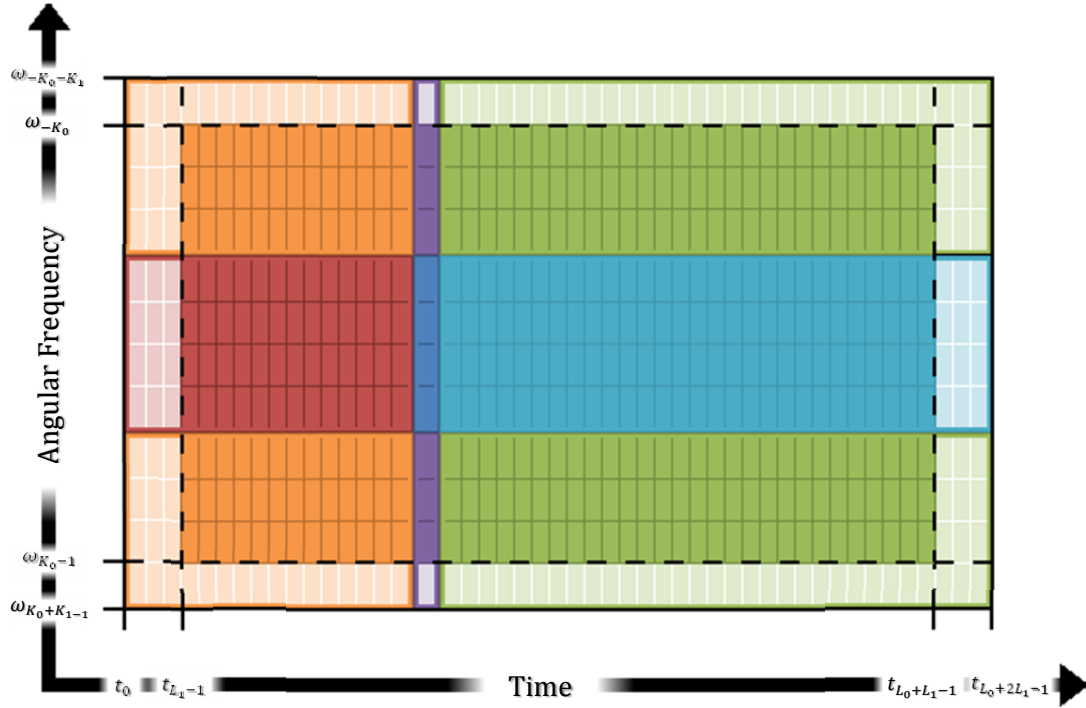


Figure 4.2: Two dimensional block diagram of the wireless channel.

Figure 4.2 gives a depiction of the wireless channel with respect to some of the variables defined in this section thus far. In this figure the lighter colored blocks represent the

extended blocks, and the darker blocks are the non-extended blocks. This time each block in the figure represents multiple total coherence blocks.

Figure 4.3 shows the wireless channel in Figure 4.2 from a different camera angle. The purpose of this view is to show how the extended parts of the channel decay towards zero. It also provides depiction of the magnitude of the TF changing with respect to the time.

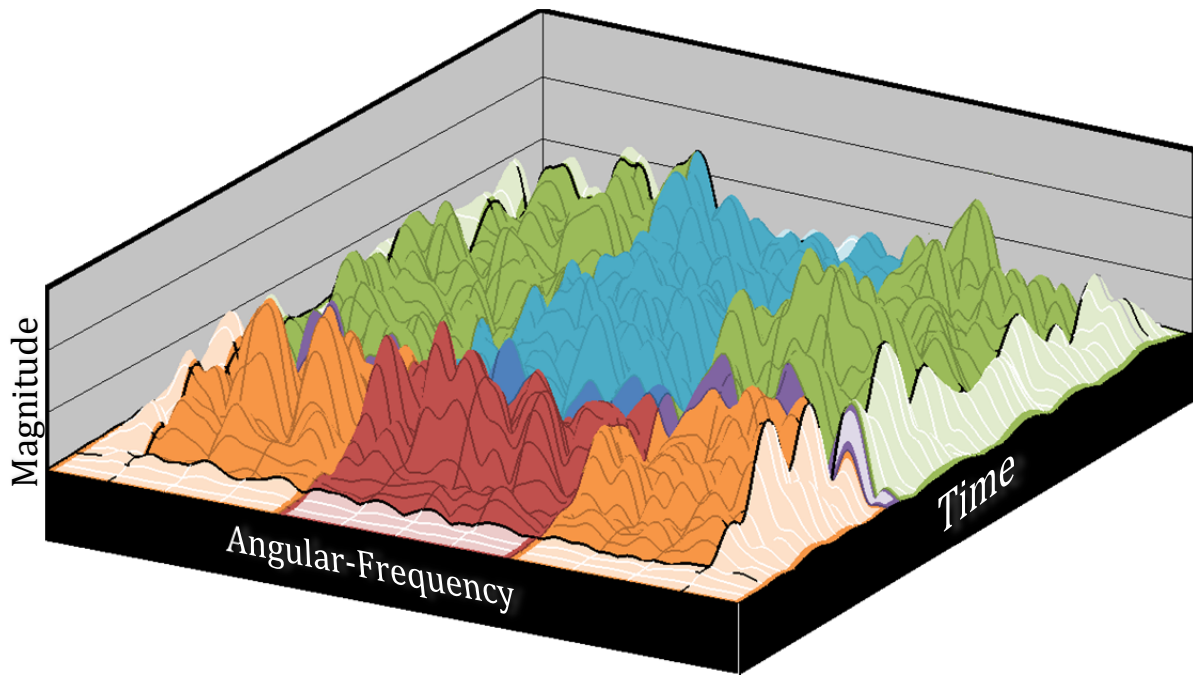


Figure 4.3: Rotated camera view of the two dimensional block diagram of the wireless channel.

Channel Coherence

Each of the domains shown in Figure 4.2 will be normalized to their coherence time or bandwidth in the plots in subsequent sections. Since the channel is time varying, each instance of the channel is valid for a given time window known as the coherence time, t_c .

Another property of the wireless channel is the coherence bandwidth. The coherence bandwidth is inversely proportional to τ_{\max} . There are common heuristics used to approximate these values, but in this paper the actual average coherence values for the model will be determined by using the actual correlation values. In this thesis, for the angular-frequency the average 90% coherence bandwidth is defined as,

$$\rho_{\mathbf{R}_\omega} = \lim_{\gamma \rightarrow 0} \lim_{K \rightarrow \infty} \frac{\pi}{K} \arg \min_{k \geq 0} \left(\left[\frac{\text{Tr}(\mathbf{S}_k \mathbf{R}_\omega)}{\text{Tr}(\mathbf{R}_\omega)} - 0.9 \right]^2 + \gamma k \right). \quad 4.48$$

Here, \mathbf{S}_k is an identity matrix that is circularly shifted and k denotes the number of times the rows are shifted upwards. Also, in determining the coherence time it is assumed that K is very large. The term γk is used to select the first local minimum, and the value of γk obeys the following inequality,

$$\gamma k < \min \left(\frac{[\text{Tr}(\mathbf{S}_k \mathbf{R}_\omega) - \text{Tr}(\mathbf{R}_\omega)]^2 - [\text{Tr}(\mathbf{S}_{k-1} \mathbf{R}_\omega) - \text{Tr}(\mathbf{R}_\omega)]^2}{[\text{Tr}(\mathbf{R}_\omega)]^2} \right). \quad 4.49$$

The actual average 90% coherence bandwidth is typically obtained by taking the sliding auto-correlation of multiple instances of the wireless channel and then averaging them. The point at which the correlation drops to 90% becomes the average 90% coherence BW [27, 41, 42, 44, 45]. This same value can be obtained by using Equation 4.48.

The average 90% coherence time obtained from the time domain data has a similar form. It is also assumed that $L \gg 1$, and the term γl is similar to the term γk and obeys the same inequality but with respect l instead of k .

$$\rho_{\mathbf{R}_t} = \lim_{\gamma \rightarrow 0} \lim_{L \rightarrow \infty} \frac{1}{L f_s} \arg \min_{l \geq 0} \left(\left[\frac{\text{Tr}(\mathbf{S}_l \mathbf{R}_t)}{\text{Tr}(\mathbf{R}_t)} - 0.9 \right]^2 + \gamma l \right). \quad 4.50$$

This concludes the concept review section pertaining to the wireless channel. The equations and concept presented in this Chapter will be important to understanding the theory that will be given later in this thesis.

4.4 Summary

In summary, this chapter provided an overview of the wireless channel. In this thesis the wireless channel should be viewed as set of total coherence blocks that can be divided in to six groups (i.e. either IB or OOB at a time reference of past, present, or future). These total coherence blocks can also be organized into a matrix representation of the channel that is best viewed in the time-angular-frequency matrix domain.

The time-angular-frequency domain is the chosen matrix domain to view, observe, or measure the wireless channel. However, in modeling the wireless channel, the frequency-delay matrix domain is deemed better because it requires fewer unknown values or RVs. It is important that the equations that are associated with these matrix domains are understood. These equations will be cross-referenced in subsequent chapters.

The understanding of the Rayleigh fading statistical model is also helpful. Equation 4.47 is very important to the research theory that will be presented. However, the research can be adapted to work with other statistical models, and even other models that are not based on a zero mean multivariate complex Gaussian RV. These types of models give simple and workable examples for this research and thesis, and they are a very accurate representation of the wireless channel.

CHAPTER FIVE

WIRELESS COMMUNICATION SYSTEMS

5.1 System Model

In Chapter Four the wireless channel was discussed. The wireless channel is just one of the elements of the wireless communication system. Within a network setting, wireless communication systems are often referred to as a point-to-point link, and there are four fundamental elements of a wireless communication system: transmitter, receiver, channel, and noise/interference blocks. Each of these four elements can also be viewed as subsystems, but for now they will be view as elements only [48, 49].

A wireless communication system models the wireless connection between a transmitting and receiving node, shown in Figure 5.1. Wireless communication systems are often modeled as linear systems, and can be represented by the following discrete linear models,

$$y_y(t_l, \tau) = h_h(t_l, \tau) \circledast x_x(t_l, \tau) + w_w(t_l, \tau), \quad 5.1$$

$$Y_y(t_l, \omega) = H_h(t_l, \omega)X_x(t_l, \omega) + W_w(t_l, \omega). \quad 5.2$$

Where $Y_y(t_l, \omega)$ is the discrete Fourier transform (DFT) of $y_y(t_l, \tau)$. In this thesis, all of the mathematical models will make use of the linear model given in Equation 5.2.

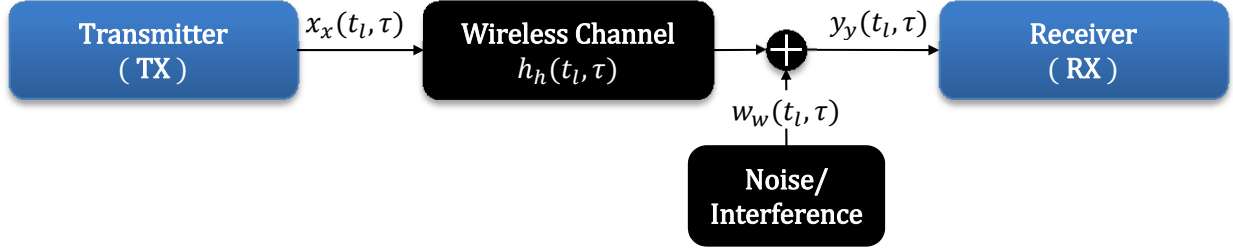


Figure 5.1: Wireless communication system linear model.

Linear System Model

In this thesis the linear model will be presented in a couple different matrix forms. In one of the forms, the transmit signal, receive signal, and noise/interference will be represented by a time-angular-frequency domain matrix. Equation 5.3 shows the transmitted signal. All the other respective matrices will have a similar form,

$$\mathbf{X}_{X_x, t_l, \tau_G} = \begin{bmatrix} X_x(t_l, \omega_{-\frac{K}{2}}) \big|_{[\tau_G, \tau_{K+G})} & X_x(t_l, \omega_{-\frac{K}{2}}) \big|_{[\tau_{K+2G}, \tau_{2K+2G})} & \cdots & X_x(t_l, \omega_{-\frac{K}{2}}) \big|_{[\tau_{(K+G)N-K}, \tau_{(K+G)N})} \\ \vdots & \vdots & \ddots & \vdots \\ X_x(t_l, \omega_{\frac{K}{2}-1}) \big|_{[\tau_G, \tau_{K+G})} & X_x(t_l, \omega_{\frac{K}{2}-1}) \big|_{[\tau_{K+2G}, \tau_{2K+2G})} & \cdots & X_x(t_l, \omega_{\frac{K}{2}-1}) \big|_{[\tau_{(K+G)N-K}, \tau_{(K+G)N})} \end{bmatrix}. \quad 5.3$$

Here, the variable τ_G is the delay between the respective intervals of each column, and $X_x(t_l, \omega_{-K}) \big|_{[\tau_0, \tau_K)}$ is the DFT of $x_x(t_l, \tau)$ evaluated on the interval $[\tau_0, \tau_K)$. Therefore, the time-delay matrix domain representation can be obtained by taking the inverse DFT (IDFT) of matrix \mathbf{X}_{X_x, t_l} . The result is

$$\mathbf{X}_{x_x, t_l, \tau_G} = \begin{bmatrix} x_x(t_l, \tau_G) & x_x(t_l, \tau_{K+2G}) & \cdots & x_x(t_l, \tau_{(K+G)N-K}) \\ \vdots & \vdots & \ddots & \vdots \\ x_x(t_l, \tau_{K+G-1}) & x_x(t_l, \tau_{2K+2G-1}) & \cdots & x_x(t_l, \tau_{(K+G)N-1}) \end{bmatrix}. \quad 5.4$$

For this model, the wireless channel that is linked to the transmit signal is represented by the diagonal matrix

$$\mathbf{H}_{H_h, t_l} = \text{diag}(\mathbf{b}_{c, A_a, (l)}) = \begin{bmatrix} H_h(t_l, \omega_{-\frac{K}{2}}) & & \mathbf{0} \\ & \ddots & \\ \mathbf{0} & & H_h(t_l, \omega_{\frac{K}{2}-1}) \end{bmatrix}. \quad 5.5$$

The column vector $\mathbf{b}_{c, A_a, (l)}$ is the l^{th} column of matrix \mathbf{H}_{H_h} and the function $\text{diag}(\cdot)$ is the diagonal function, it converts a vector into a diagonal matrix or a diagonal matrix to a column vector. Remember, it is assumed that $h_h(t_l, \tau)$ can be completely defined by the frequency components in Equation 5.5. Therefore, one of the matrix forms of the linear model for the wireless communication system in this thesis is

$$\mathbf{Y}_{y, t_l, \tau_G} = \mathbf{H}_{H_h, t_l} \mathbf{X}_{x, t_l, \tau_G} + \mathbf{W}_{w, t_l, \tau_G}. \quad 5.6$$

The second linear model is slightly different with respect to the matrices and linear equation. The new channel matrix will be

$$\mathbf{H}_{H_h} = \begin{bmatrix} H_h(t_0, \omega_{-\frac{K}{2}}) & \cdots & H_h(t_{L-1}, \omega_{-\frac{K}{2}}) \\ \vdots & \ddots & \vdots \\ H_h(t_0, \omega_{\frac{K}{2}-1}) & \cdots & H_h(t_{L-1}, \omega_{\frac{K}{2}-1}) \end{bmatrix}. \quad 5.7$$

The receive signal and noise/interference will be similar but with respect to a time interval,

$$\mathbf{X}_{x, \tau_m} = \begin{bmatrix} X_x(t_0, \omega_{-K})|_{[\tau_m, \tau_{K+m})} & \cdots & X_x(t_{L-1}, \omega_{-K})|_{[\tau_m, \tau_{K+m})} \\ \vdots & \ddots & \vdots \\ X_x(t_0, \omega_{K-1})|_{[\tau_m, \tau_{K+m})} & \cdots & X_x(t_{L-1}, \omega_{K-1})|_{[\tau_m, \tau_{K+m})} \end{bmatrix}. \quad 5.8$$

However, the transmit signal can be simplify to a diagonal matrix when

$$X_x(t_0, \omega)|_{[\tau_m, \tau_{K+m})} = X_x(t_l, \omega_{-K_0})|_{[\tau_m, \tau_{K+m})}. \quad 5.9$$

The received signal and the noise/interference cannot be simplified. The diagonal matrix for the transmitted signal is

$$\mathbf{X}_{X_x} = \begin{bmatrix} X_x \left(t_0, \omega_{-\frac{K}{2}} \right) \Big|_{[\tau_G, \tau_{K+G})} & \mathbf{0} \\ & \ddots \\ \mathbf{0} & X_x \left(t_0, \omega_{\frac{K}{2}} \right) \Big|_{[\tau_G, \tau_{K+G})} \end{bmatrix}. \quad 5.10$$

Therefore, the linear equation for the second model is

$$\mathbf{Y}_{Y_y} = \mathbf{X}_{X_x} \mathbf{H}_{H_h} + \mathbf{W}_{W_w}, \quad 5.11$$

where, $\mathbf{Y}_{Y_y} = \mathbf{Y}_{Y_y, \tau_G}$ and $\mathbf{W}_{W_w} = \mathbf{W}_{W_w, \tau_G}$.

Noise/Interference Model

Noise in this thesis can be additive white Gaussian noise (AWGN) or additive colored noise. The interference is also assumed to be additive. Therefore the noise and interference is represented by one variable. In this thesis there is no mathematical distinction made to distinguish the noise from interference, but the source of the interference is different from that of the noise. The interference is mainly caused by primary users and maybe secondary user.

It is also assumed that the noise and interference can be made to be a zero-mean complex multivariate Gaussian RV by designing the transmitter and receiver in a particular way. This will be shown later in this chapter. Therefore, the only statistic that is needed is the covariance matrix of the noise/interference term, and it is assumed to be known.

The statistical model of the noise/interference term is similar to the wireless channel model given in Equation 4.46. So, the covariance matrices of the noise term can be determined using the same method in Equations 4.37 and 4.38,

$$\mathbf{R}_{\omega\mathbf{w}} = \mathbf{R}_{\omega, \mathbf{w}_{W_w}} = E\{\frac{1}{L} \mathbf{W}_{W_w} \mathbf{W}_{W_w}^H\}, \quad 5.12$$

$$\mathbf{R}_{t\mathbf{W}} = \mathbf{R}_{t, \mathbf{W}_{W_w}} E\left\{\frac{1}{K} \mathbf{W}_{W_w}^H \mathbf{W}_{W_w}\right\}. \quad 5.13$$

These matrices also have a similar relationship to their respective vector domain transforms as presented in Equations 4.41 – 4.44 except that the FFT and IFFT are not modified and they are shifted.

Referring back to Equation 4.46, the statistical model for the noise can be defined using the Cholesky decomposition of the covariance matrices,

$$\mathbf{W}_{W_w} = \mathbf{C}_{\omega\mathbf{W}} \underbrace{\begin{bmatrix} \mathcal{N}_{0,0} & \cdots & \mathcal{N}_{L-1,0} \\ \vdots & \ddots & \vdots \\ \mathcal{N}_{0,K-1} & \cdots & \mathcal{N}_{L-1,K-1} \end{bmatrix}}_{\mathbf{N}_{(K \times L)}} \mathbf{C}_{t\mathbf{W}}. \quad 5.14$$

For AWGN, the statistical model becomes

$$\mathbf{W}_{W_w} = \sqrt{K\sigma_{\mathbf{W}}^2} \mathbf{N}_{(K \times L)}. \quad 5.15$$

The variable $\sigma_{\mathbf{W}}^2$ is the noise variance and average power. It is also worth noting that the matrix domain relationships of the noise/interference term matrices are similar to that in Equations 4.29 – 4.32.

Signal-to-Noise-Plus-Interference Ratio

The signal-to-noise-plus-interference ratio (SNIR) can now be defined since the model of the noise/interference term has been given. The SNIR is simply a ratio of the power of a transmitted signal that has been convolved with the wireless channel and the noise/interference term. In this thesis the average SNIR for a particular time and angular-frequency is

$$\begin{aligned}
SNIR_{t_l, \omega_k} &= \frac{\overbrace{K^2 E\left\{\frac{1}{K^2}|H_h(t_l, \omega_k)|^2\right\}}^{\text{Channel Avg. Power Gain}} \overbrace{E\left\{\frac{1}{K^2}|X_x(t_l, \omega_k)|^2\right\}}^{\text{Signal Avg. Power}}}{\underbrace{E\left\{\frac{1}{K^2}|W_w(t_l, \omega_k)|^2\right\}}_{\text{Noise/Interference Avg. Power}}} \\
&= \frac{E\{|H_h(t_l, \omega_k)|^2\}E\{|X_x(t_l, \omega_k)|^2\}}{E\{|W_w(t_l, \omega_k)|^2\}}
\end{aligned} \tag{5.16}$$

If the noise/interference term is just AWGN then the SNIR becomes the signal-to-noise ratio (SNR),

$$SNR_{t_l, \omega_k} = \frac{E\{|H_h(t_l, \omega_k)|^2\}E\{|X_x(t_l, \omega_k)|^2\}}{K\sigma_w^2}. \tag{5.17}$$

The channel models, the statistical model of this noise/interference term, SNIR and SNR are important parts of the system model. All the statistical models presented for the wireless communication system will be used in determining the wireless channel.

The system models that have been presented define the mathematical and statistical relationship between the four elements of the wireless communication system. These relationships will be used as stated. The final part of the wireless communication system that will be covered in *The Concept Review* is the received and transmitted signal. The signals used in this research are multi-carrier signals. The rest of this chapter will discuss multi-carrier modulation schemes.

5.2 Multi-Carrier Modulations

In multi-carrier modulation (MCM) schemes a signal that is transmitted serially is converted into parallel streams and transmitted over multiple sub-bands on respective modulated sub-carriers. This idea of multi-carrier modulations dates back to 1950s to the Kinplex Modem. The most common MCM scheme is Orthogonal Frequency Division Multiplexing (OFDM). OFDM dates back to the 60s, and like many other things in wireless

communication did not gain high levels of deployment until the digital era. The digital advancement during the time span of the late 70s to the late 90s has brought on many changes in wireless communication. OFDM and other MCM schemes are just a few of them [27, 38, 39, 48, 50-53].

OFDM is a combination of multiple ideas for MCM schemes, the oldest of them being the ability to use a bank of sub-carrier oscillators to transmit a signal without inter channel interference (ICI) or inter symbol interference (ISI) caused by the wireless channel. This idea showcases one of the most prominent advantages of OFDM, its robustness to frequency selective fading. Another idea that was behind OFDM is the processing of the base-band signal using Fourier transforms instead of using a bank of oscillators on the RF signal. To maintain the robustness to ISI and ICI using the Fourier transform method, the idea of guard intervals (GI) was also introduced. However, there was still the requirement for multiple filters and oscillators until the idea of a more efficient digital implementation that used some type of digital Fourier transform, was conceived. The advancement during the digital era made it possible for this digital implementation [51-53].

Many wireless communication systems use OFDM for their modulation scheme, because of its spectrum efficiency and especially its robustness to fading. There are some disadvantages to OFDM. One of the disadvantages is the peak-to-average-power ratio (PAPR) because it requires linear amplifiers with a high dynamic range. To combat PAPR some have suggested carrier interferometry (CI). CI-OFDM is a MCM scheme that also uses spread spectrum to spread data across each of the sub carriers [54-56]. Both OFDM and CI-OFDM were used in this research.

The next couple of sections in this chapter are outline as follows. First the mathematical formulas for the transmitted OFDM signal will be given. Then some of the OFDM disadvantages with respect to this research will be presented. Finally, the mathematical formulas for CI-OFDM will be given.

5.3 Orthogonal Frequency Division Multiplexing

The OFDM formulation starts with a serial data stream. This data is mapped to a set of data symbols determined by a particular modulation scheme. These data symbols are then converted to multiple parallel streams, $S_n(t_l, \omega_k)$. In this case the variable n is the OFDM symbol index. The matrix form of the data symbol is

$$\mathbf{S}_{t_l} = \begin{bmatrix} S_0(t_l, \omega_{-K}) & \cdots & S_{N-1}(t_l, \omega_{-K}) \\ \vdots & \ddots & \vdots \\ S_0(t_l, \omega_{K-1}) & \cdots & S_{N-1}(t_l, \omega_{K-1}) \end{bmatrix}. \quad 5.18$$

Using Equation 5.18, the OFDM transmit signal in the time-angular-frequency domain is defined as

$$\mathbf{X}_{X_x, t_l, \tau_G} = \mathbf{S}_{t_l}. \quad 5.19$$

With OFDM τ_G becomes the length of the GI for each OFDM symbol. The transmitted signal in the time-delay domain with the guard interval inserted is

$$\mathbf{X}_{x_x, t_l} = \begin{bmatrix} x_x(t_l, \tau_{2K}) & x_x(t_l, \tau_{4K+G}) & \cdots & x_x(t_l, \tau_{(2K+G)N-G}) \\ \vdots & \vdots & \ddots & \vdots \\ x_x(t_l, \tau_{2K+G-1}) & x_x(t_l, \tau_{4K+2G-1}) & \cdots & x_x(t_l, \tau_{(2K+G)N-1}) \end{bmatrix}. \quad 5.20$$

$\mathbf{X}_{x_x, t_l, \tau_G}$

If the length of the GI is greater than or equal to the maximum excess delay, $\tau_G \geq \tau_{\max}$, the receive signal can be defined using Equation 5.6 and 5.11. This simplification is one of the primary benefits of OFDM [51-53].

Figure 5.2 shows a serial delay representation of Equation 5.20 with guard intervals. This figure also makes note of special symbols known as training symbols that are used to determine the wireless channel.

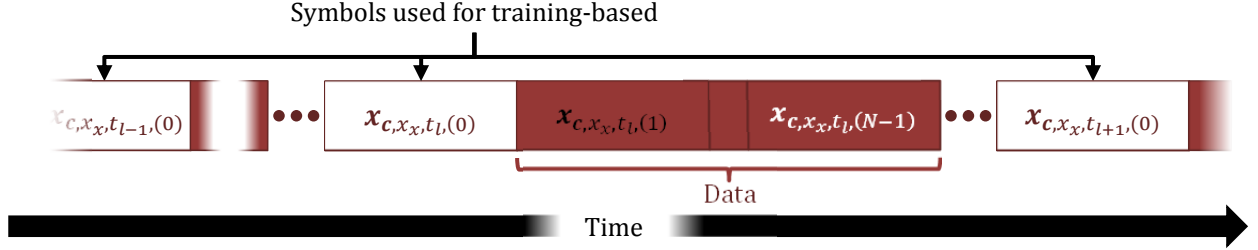


Figure 5.2: Serial representation of the transmitted signal.

The vector $\mathbf{x}_{c,x_x,t_l,(n)}$ is the n^{th} column of the matrix \mathbf{X}_{x_x,t_l} which is the transmitted signal a time t_l over the delay interval $[\tau_{n(K+G)}, \tau_{(n+1)(K+G)}]$. The white blocks are known and used for training and the red blocks in the data section are the data symbols. Training symbols typical occur at the beginning of a packet, but in this thesis the training symbol and data symbol arrangement may be a little different. In OFDM some of the sub-carriers are also use for training and frequency synchronization. These sub-carriers are known as pilot tones [51-53].

As it was previously mentioned, one of the disadvantages of OFDM is that it has a higher PAPR than single carrier modulations. Higher PAPR can cause nonlinear effects in the receiving radio. CI-OFDM can be used to mitigate this problem [54, 55]. However, that is not the reason that CI-OFDM is used in this thesis. This reason will be explained in the next section.

5.4 Carrier-Interferometry OFDM

Before explaining the reason for using CI-OFDM, the formulation of the transmit signal will be given. CI-OFDM formulation is the same as OFDM but with one difference: each of the parallel data streams are coded with a code matrix, \mathbf{Z}_{t_l} , such that

$$\mathbf{Z}_{t_l} = \mathbf{F} \begin{bmatrix} e^{-j2\pi U_{l,0}} & & \mathbf{0} \\ & \ddots & \\ \mathbf{0} & & e^{-j2\pi U_{l,N}} \end{bmatrix} \mathbf{F}^{-1}, \quad 5.21$$

$$\mathbf{X}_{X_x, t_l, \tau_G} = \mathbf{S}_{t_l} \mathbf{Z}_{t_l}. \quad 5.22$$

The variable $U_{l,n}$ is a Uniform RV. The code sequence used in this thesis has the following properties,

$$\mathbf{Z}_{t_l} \mathbf{Z}_{t_l}^H = \mathbf{I}. \quad 5.23$$

$$E\{\mathbf{Z}_{t_l} \mathbf{1}\} \approx \mathbf{0}. \quad 5.24$$

Next, to address the reason for using CI-OFDM Equations 5.6 and 5.22 will be used,

$$\mathbf{Y}_{Y_y, t_l, \tau_G} = \mathbf{H}_{H_h, t_l} \mathbf{S}_{t_l} \mathbf{Z}_{t_l} + \mathbf{W}_{W_w, t_l, \tau_G}. \quad 5.25$$

It is typically assumed that $\mathbf{W}_{W_w, t_l, \tau_G}$ is AWGN and there is no interference. In this thesis $\mathbf{W}_{W_w, t_l, \tau_G}$ is not necessarily AWGN and there will be interference present. Therefore, $\mathbf{W}_{W_w, t_l, \tau_G}$ may not be zero mean complex multivariate Gaussian RV, but $\mathbf{W}_{W_w, t_l, \tau_G} \mathbf{Z}_{t_l}^H$ can be model as AWGN (i.e. a zero mean complex multivariate RV) [54-58]. Therefore, the receive signal will be modified to,

$$\mathbf{Y}_{Y_y, t_l, \tau_G} \mathbf{Z}_{t_l}^H = \mathbf{H}_{H_h, t_l} \mathbf{S}_{t_l} + \mathbf{W}_{W_w, t_l, \tau_G} \mathbf{Z}_{t_l}^H. \quad 5.26$$

This shows that all models that do not have AWGN can be simplified to a model with AWGN if CI-OFDM is used.

5.5 Summary

In summary, this chapter has provided an understanding of the linear system model used to represent the wireless channel. The equations associated with these models were also given. There are two equations that are used to represent the wireless channel, Equations 5.11 and 5.6.

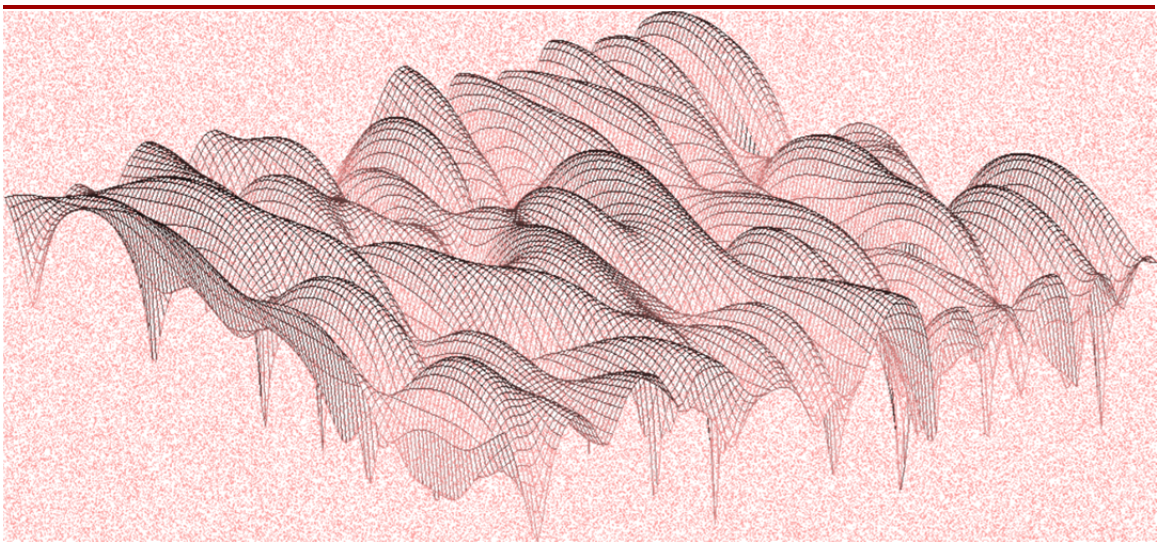
This chapter also covered the noise and interference in the channel and gave a statistical model for the noise/interference terms. Using these models the average SNIR and SNR were defined. It is assumed that the statistics of noise and the average SNIR or SNR is known at the time of transmission.

The last three sections in this chapter covered two MCM schemes: OFDM and CI-OFDM. The transmitted signals in the research and this thesis are either an OFDM or CI-OFDM signal. CI-OFDM is used to whiten the noise and interference terms.

The next part of this thesis will cover the main contribution of this thesis, the Indirect Channel Measurement (ICM) technique. The ICM technique was analyzed and compared to other techniques. In Part III, along with several other things, this analysis and comparison is discussed

PART III

THE INDIRECT CHANNEL MEASUREMENT AND OTHER MEASUREMENT TECHNIQUES



Part III of the thesis will cover the contributions of this research. The main contribution is the indirect channel measurement (ICM) technique. It contributes and adds to channel measurement research for cognitive radios in dynamic wireless environments. Other contributions with respect to rate adaptation will also be presented. A literature review, theory formulation, application design, simulations, and an experiment for the ICM and other techniques will be given. This part will cover:

- Linear estimator and/or extrapolators for OFDM wireless communication systems.
- The theory behind the ICM technique and several other techniques for comparison.
- The use of the ICM technique in a rate adaptation scheme.
- A detailed design of a rate adaptation system.
- Simulations of the ICM and other techniques and of the rate adaptation scheme.
- An experiment that validates the accuracy of the ICM technique's theory.

CHAPTER SIX

WIRELESS CHANNEL ESTIMATION AND EXTRAPOLATION TECHNIQUES

6.1 Introduction

This part of the thesis covers most of the contributions, but the main contribution is the ability to indirectly measure the wireless channel. In this thesis the wireless channel can be estimated and/or extrapolated. The indirect channel measurement (ICM) technique is a form of extrapolation. To understand and compare the ICM technique to other techniques, an understanding of the other estimation and extrapolation techniques must be given.

So, before presenting the main contribution, a literature review on relevant research will be given. The relevant research areas that will be discussed are wireless channel estimation and wireless channel extrapolation. In this thesis, wireless channel estimation is defined as any technique that collects measured values (i.e. complex gains) of a set of total coherence blocks, and uses these same values to determine the actual complex gains of some or all of the complex gains in the same set of total coherence blocks. In contrast,

wireless channel extrapolation is defined as any technique that collects measured values of a set of total coherence blocks, and uses these measured values to determine the complex gains of another set of total coherence blocks [13, 57, 59-65].

Figure 4.1 displays six sets of total coherence blocks. The estimation techniques in this thesis uses a set of present IB and maybe in addition past IB total coherence blocks to estimate the present IB blocks. Using the sets of total coherence blocks in Figure 4.1, three types of extrapolations, that will be discussed later, can be defined. The first, the ICM technique uses the present and future OOB total coherence blocks to extrapolate present and future IB blocks. The ICM technique will be compared with two other types of extrapolation techniques. The first type technique uses the past and present IB blocks to extrapolate the future blocks. There are multiple techniques that can place into this category, but they will all be represented by what will be called the “direct channel measurement” technique. The terms direct and indirect are with respect to the channel measurements being IB or OOB respectively. The second type of technique that will be used for comparison does not use either IB or OOB. Instead, a null set of total coherence blocks is used to extrapolate the future IB channel. This type of technique will be called the “no channel measurement” technique.

Furthermore, the estimation and extrapolation techniques discussed can be categorized into two other groups: classical and Bayesian techniques. Both classical and Bayesian techniques make use of either analog or discrete models of the wireless channel to determine the actual values from measured values. However, Bayesian techniques make assumptions about the statistics of the actual values, and classical techniques do not. For this reason some people may view Bayesian techniques as being more controversial

because the statistical assumption may not be true. In wireless communication, the statistics associated with the wireless channel can often be determined through a measurement campaign. As stated in Chapter Four, a very common model, and the model used in this thesis, is the Rayleigh fading model [27, 42, 44-46].

As stated in Part I, the wireless communication community has noticed the need for understanding more about the wireless channel than just the effects of path loss; and somewhere between the 1970s and the 1980s the first propagation measurement techniques emerged. There were three measurement techniques born during this time period: direct pulse, swept frequency, and sliding correlator propagation measurement systems. The techniques used today to measure multipath and propagation can be derived from one of these three techniques. In this thesis, these three historical techniques are classified as classical channel estimation techniques [27, 40].

In this chapter, the historical and mathematical connection to these techniques will not be covered. However, a detailed explanation of the current techniques in each of the four categories will be discussed with respect to a wireless channel for OFDM signals. The rest of this chapter will be organized as follows: first classical wireless channel estimation and extrapolation techniques will be discussed, as well as Bayesian wireless channel estimation and time extrapolation techniques. Following this, a discussion of a technique that is most like the ICM technique in what is measured and extrapolated is discussed, and a summary concludes the chapter.

6.2 Traditional Estimation for OFDM

For a wireless communication system that uses OFDM, traditional channel estimation is most commonly used for channel equalization. Channel equalization is a well-defined and researched area in wireless communication. There are several different techniques that have been suggested and researched over the past decades. In this thesis just the fundamental example will be given for the traditional techniques. It is recommended to read the referenced literature in this chapter to understand the state-of-the-art in this area [13, 29, 32, 60-62, 66-81].

With the traditional techniques it is often assumed that the wireless environment is not dynamic. With this assumption it can be proven that the channel does not vary over one or multiple packets. Therefore, channel estimation will suffice.

These traditional techniques will be separated into the following categories: training-based methods and blind/semi-blind methods. All the estimation and extrapolation techniques can be categorized in this way. However all techniques in the other sections will be presented as training-based. The most common convention in estimating the channel is the training based method.

Training Based Method

To explain these methods the diagram in Figure 5.2 will be used. As stated, in this figure the lighter colored blocks represent symbols used purely for training the estimator, and the darker blocks are symbols that contain information. It also assumed that the first block is

used for the training based method, and the receive signal, channel, and noise/interference in Equation 5.11 can be represent by the following equations,

$$\mathbf{Y}_{Y_y} = [\mathbf{y}_{c,Y_y,t_0} \quad \mathbf{y}_{c,Y_y,t_1} \quad \cdots \quad \mathbf{y}_{c,Y_y,t_l} \quad \cdots \quad \mathbf{y}_{c,Y_y,t_{N-1}}], \quad 6.1$$

$$\mathbf{H}_{H_h} = [\mathbf{h}_{c,H_h,t_0} \quad \mathbf{h}_{c,H_h,t_1} \quad \cdots \quad \mathbf{h}_{c,H_h,t_l} \quad \cdots \quad \mathbf{h}_{c,H_h,t_{N-1}}], \quad 6.2$$

$$\mathbf{W}_{W_w} = [\mathbf{w}_{c,W_w,t_0} \quad \mathbf{w}_{c,W_w,t_1} \quad \cdots \quad \mathbf{w}_{c,W_w,t_l} \quad \cdots \quad \mathbf{w}_{c,W_w,t_{N-1}}]. \quad 6.3$$

Equation 4.31 can be used to get the following equation

$$\mathbf{y}_{c,Y_y,t_l} = \mathbf{X}_{X_x} \mathbf{h}_{c,H_h,t_l} + \mathbf{w}_{c,W_w,t_l}. \quad 6.4$$

The estimated value of \mathbf{h}_{c,H_h,t_l} can be obtained by using the maximum likelihood estimator (MLE). The principals behind MLEs are some of the most common principals used in estimating the wireless channel. With the MLE the channel is assume to be deterministic. The only RV in the received signal is the noise/interference term, \mathbf{w}_{c,W_w,t_l} . Therefore, the proabilty density function (pdf) of the received signal, $f_{\boldsymbol{\theta}}(\mathbf{y}_{c,Y_y,t_l})$, takes the pdf of the noise/interference term but with an added unknown mean of, $\mathbf{X}_{X_x} \mathbf{h}_{c,H_h,t_l}$. Note that the transmitted signal \mathbf{X}_{X_x} is known because it is a trainning signal. Also, the variable $\boldsymbol{\theta}$ in this thesis represents the value that will be estimated or extrapolated, and in this case $\boldsymbol{\theta}$ equals \mathbf{h}_{c,H_h,t_l} . To find the unknown channel The MLE can be used. The MLE is defined as

$$\hat{\mathbf{h}}_{c,\text{MLE},H_h,t_l} = \arg \max_{\boldsymbol{\theta}} \left[f_{\boldsymbol{\theta}}(\mathbf{y}_{c,Y_y,t_l}) \right] \Big|_{\boldsymbol{\theta}=\mathbf{h}_{c,H_h,t_l}}. \quad 6.5$$

The solution to MLEs can be found in various textbooks and research papers [57, 82, 83]. These solutions vary depending on how you define the noise/interference term. This term is often defined as AWGN. When this term is AWGN the solution to the maximization function is

$$\hat{\mathbf{h}}_{\mathbf{c},\text{MLE},H_h,t_l} = \mathbf{X}_{X_x}^{-1} \mathbf{y}_{\mathbf{c},Y_y,t_l}. \quad 6.6$$

To quantify the performance of these estimators, the mean squared error (MSE) is often used [57].

$$\begin{aligned} \text{MSE}_{\mathbf{h}_{\mathbf{c},H_h,t_l}} &= \frac{1}{K} \text{Tr} \left(E \left\{ (\hat{\mathbf{h}}_{\mathbf{c},H_h,t_l} - \mathbf{h}_{\mathbf{c},H_h,t_l})(\hat{\mathbf{h}}_{\mathbf{c},H_h,t_l} - \mathbf{h}_{\mathbf{c},H_h,t_l})^H \right\} \right) \\ &= \sigma_W^2 \text{Tr} \left(\mathbf{X}_{X_x}^{-1} (\mathbf{X}_{X_x}^{-1})^H \right). \end{aligned} \quad 6.7$$

As seen in Equation 6.6 the MLE can be very easy to compute. To improve the MLE it is not uncommon to use multiple training symbols to get a more accurate result. However, MLEs are often known to have higher errors because of the inversion of \mathbf{X}_{X_x} . In the case of training-based traditional channel estimation for OFDM, inversion issues are not that much of a problem, because \mathbf{X}_{X_x} is designed to be easily inverted, but there are other issues with using MLEs in training-based traditional channel estimation. One of these issues is that the MLE is only good for channels within the time interval $[t_l, t_c + t_l)$ at the least. Where t_c is the coherence time. So, at least one training symbol must be in each of these intervals. When multiple training symbols are not available to improve the estimation, data symbols must be used, and data symbols are unknown.

Therefore, to estimate the channel in these cases researchers have used blind and semi-blind techniques. Just like the training-based method the blind and semi-blind methods are areas that have been heavily researched and only a textbook example will be given with respect to Equation 6.6 and the AWGN assumption.

Blind and Semi-Blind Methods

Similar to the ICM technique blind and semi-blind methods try to determine the wireless channel in very dynamic wireless environments. One of the common ways to

perform blind and semi-blind estimation is an iterative method known as the expectation maximization (EM) algorithm. The EM algorithm can be used to estimate the channel $\hat{\mathbf{h}}_{\mathbf{c},H_h,t_l}$ for a time interval less than or more than the coherence time, given that you have a model for the channel you are trying to estimate. This model will be discussed later in this chapter, and this model is with respect to the time domain.

The first step is initialization: an initial value of $\hat{\mathbf{h}}_{\mathbf{c},H_h,t_l}$ is obtained or assigned, $\hat{\mathbf{h}}_{\mathbf{c},H_h,t_0}$. The second step is expectation: the expected value for all the symbols, $(\hat{\mathbf{X}}_{X_x}^{-1})^{(0)}$, used for blind or semi-blind estimation is calculated. Note that with the EM algorithm some or none of the values of the transmitted signals are known, and the values change with each time iteration because of the data. In the third step, maximization, the expected value of the symbols is used to get the MLE of the channel again, $\hat{\mathbf{h}}_{\mathbf{c},H_h,t_1}$. Then, the second and third steps are repeated increasing the time step, t_l , until the channel estimate converges [57, 84].

The equations used in this three-step EM process for an OFDM signal is given in the following bulleted listings:

- **Initialization:** The estimate $\hat{\mathbf{h}}_{\mathbf{c},H_h,t_0}$ is determined from the training data
- **Expectation:**

$$f_{\theta}(\mathbf{X}_{X_x} | \mathbf{y}_{\mathbf{c},Y_y,t_l}) = \prod_{k=-\frac{K}{2}}^{\frac{K}{2}-1} f_{\theta} \left(X_x \left(t_l, \omega_{-\frac{K}{2}} \right) \middle|_{[\tau_G, \tau_{K+G})} \middle| Y_y \left(t_l, \omega_{-\frac{K}{2}} \right) \right). \quad 6.8$$

- **Maximization:**

$$\hat{\mathbf{h}}_{\mathbf{c},\text{EM},H_h,t_l} = \arg \max_{\theta} \left[f_{\theta}(\mathbf{X}_{X_x} | \mathbf{y}_{\mathbf{c},Y_y,t_l}) \right] \Big|_{\theta = \hat{\mathbf{h}}_{\mathbf{c},H_h,t_l}}. \quad 6.9$$

The traditional, blind, and semi-blind techniques can be further improved by using statistical information about the channel [57, 84]. The next section will discuss these techniques.

6.3 Bayes and Linear Minimum Mean-Square Error Estimation

The Bayes and linear minimum mean-square error (LMMSE) estimators use Bayesian statistics. The LMMSE estimator is not the Bayes estimator (BE), but in some cases it is equal to the Bayes estimator. However, the BE is the best estimator given that the assumptions of the statistics are correct. The use of these estimators in OFDM systems can be dated back to the 90's. There have been many papers published between then and now suggesting how to improve channel estimates using different variations of the LMMSE and Bayes Estimators, but the fundamentals are the same. Once again the textbook example will be given, but the reference section contains many of the researched variations [13, 66, 67, 85-96].

In the previous section, with the traditional estimators, the statistics of the channel were not taken into consideration and it was treated as a deterministic value that if chosen correctly could maximize the likelihood of the received signal. At most the only assumption made about the channel in the previous section is a model that relates different time instances of the channel. In this section the statistics of the channel are taken into consideration, and the channel is assumed to have what is called a prior distribution (the BE). At the very least the first and second order statistics of the wireless channel is known or defined by a known equation (the LMMSE estimator).

As stated in Chapter Four the pdf of the wireless channel is a zero-mean complex multivariate Gaussian (i.e. normal) RV. Normal pdf's are defined by their first and second order statistics. The wireless channel in this thesis is also defined by a linear model. These two things, the wireless channel being defined by a linear model and its pdf defined by the first and second order statistics, along with another criteria that will be defined in the next paragraphs makes the LMMSE Estimator equal to the BE [57]. Though the LMMSE estimator is the most commonly used, the BE will be defined in this section because it is a more general and accurate estimator.

To explain the Bayes estimator, first a discussion of the joint distribution will be covered. Before, the wireless channel was assumed to be deterministic, and because of this a joint distribution was not needed. For the BE the channel has a pdf. Therefore, the joint pdf for the channel and the received signal is represented by the function $f(\mathbf{y}_{\mathbf{c},Y_y,t_l}, \mathbf{h}_{\mathbf{c},Y_y,t_l})$.

The accuracy of the BE for the wireless channel is determined by a loss function $L(\mathbf{h}_{\mathbf{c},Y_y,t_l}, \hat{\mathbf{h}}_{\mathbf{c},Y_y,t_l}(\mathbf{y}_{\mathbf{c},Y_y,t_l}))$. Note that the estimate $\hat{\mathbf{h}}_{\mathbf{c},Y_y,t_l}$ is a linear function with respect to $\mathbf{y}_{\mathbf{c},Y_y,t_l}$. The most common loss function used for Bayes estimators is the quadratic loss function that measured Euclidean distance between the estimator and the actual channel.

$$L(\mathbf{h}_{\mathbf{c},Y_y,t_l}, \hat{\mathbf{h}}_{\mathbf{c},Y_y,t_l}(\mathbf{y}_{\mathbf{c},Y_y,t_l})) = [\mathbf{h}_{\mathbf{c},Y_y,t_l} - \hat{\mathbf{h}}_{\mathbf{c},Y_y,t_l}(\mathbf{y}_{\mathbf{c},Y_y,t_l})]^H [\mathbf{h}_{\mathbf{c},Y_y,t_l} - \hat{\mathbf{h}}_{\mathbf{c},Y_y,t_l}(\mathbf{y}_{\mathbf{c},Y_y,t_l})]. \quad 6.10$$

This definition of the loss function is another criteria that is required for the LMMSE estimator to be Equal to the BE [57, 84].

To finish defining the BE, something called the Bayes risk must be defined. The Bayes risk can be viewed as the average Loss, given a particular loss function, over the joint distribution,

$$\text{Bayes Risk} = \int \int L\left(\mathbf{h}_{\mathbf{c},Y_y,t_l}, \hat{\mathbf{h}}_{\mathbf{c},Y_y,t_l}(\mathbf{y}_{\mathbf{c},Y_y,t_l})\right) f(\mathbf{y}_{\mathbf{c},Y_y,t_l}, \mathbf{h}_{\mathbf{c},Y_y,t_l}) d\mathbf{y}_{\mathbf{c},Y_y,t_l} d\mathbf{h}_{\mathbf{c},Y_y,t_l}. \quad 6.11$$

The Bayes estimate can be define as the estimate that minimizes the Bayes risk. Using some other theorems, the minimization function can be shown as [57, 84]

$$\hat{\mathbf{h}}_{\mathbf{c},\text{BE},Y_y,t_l} = \arg \max_{\hat{\mathbf{h}}_{\mathbf{c},Y_y,t_l}} \left\{ \int L\left(\mathbf{h}_{\mathbf{c},Y_y,t_l}, \hat{\mathbf{h}}_{\mathbf{c},Y_y,t_l}(\mathbf{y}_{\mathbf{c},Y_y,t_l})\right) f(\mathbf{h}_{\mathbf{c},Y_y,t_l} | \mathbf{y}_{\mathbf{c},Y_y,t_l}) d\mathbf{h}_{\mathbf{c},Y_y,t_l} \right\}. \quad 6.12$$

The BE is the most accurate estimate of the wireless channel given that the assumptions about the statistics and Loss functions are accurate [57, 84]. However, it can be difficult to compute for a few reasons. The first difficulty is defining the conditional probability in Equation 6.12. In this thesis the conditional probability is of a complex and multivariate normal RV. This is a special case of the BE that involves conjugate priors. The references can be used to obtain a better understanding [57, 84]. The other complication could occur if the integration in Equation 6.12 is difficult to compute and/or the maximization function is hard to determine. In this thesis the choice of a quadratic loss function makes this computation simple, and Equation 6.12 can be simplified to

$$\hat{\mathbf{h}}_{\mathbf{c},\text{BE},Y_y,t_l} = E\left\{\mathbf{h}_{\mathbf{c},Y_y,t_l} | \mathbf{y}_{\mathbf{c},Y_y,t_l}\right\}. \quad 6.13$$

This means that for the wireless channel defined in this thesis, the BE is equal to the mean or expected value of the wireless channel given the received signal. Also, the LMMSE estimator is the same given that the assumptions about the channel and Loss function are true. Without these assumptions the calculation of the BE may be complicated by the reasons given before: not being able to use conjugate priors and/or not having an easily

integrable loss function. However, the LMMSE estimator always makes these assumptions no matter the validity of the assumptions [57, 84].

As shown by Equation 6.13 the mean of the conditional pdf $f(\mathbf{h}_{c,Y_y,t_l}|\mathbf{y}_{c,Y_y,t_l})$ is the Bayes estimator. What can also be shown is that the Trace of the covariance of the conditional pdf is the MSE of the BE, [57, 84]

$$MSE_{\hat{\mathbf{h}}_{c,BE,Y_y,t_l}} = \frac{1}{K} \text{Tr} \left(\text{Var} \left\{ \mathbf{h}_{c,Y_y,t_l} | \mathbf{y}_{c,Y_y,t_l} \right\} \right). \quad 6.14$$

All the measurement techniques covered this far have been estimators. In the next section extrapolators will be discussed.

6.4 Fading Prediction and Time Extrapolation Techniques

In this thesis, the terms “extrapolate” and “predict” are interchangeable with respect to the time domain because only future parts of the channel will be extrapolated. The definition of extrapolation given earlier in this chapter states that extrapolation means more than just determining the future measurements of the wireless channel. For this section only, this view can be simplified to a technique that can determine future values of the wireless channel from present and/or past measurements or estimates. Note that future, past, and present are time domain references with respect to the received signal.

Similar to the estimators, the extrapolators can be either classical or Bayesian, and of course the classical extrapolators are the most common because of their simplicity. However, adding some complexity by using the second order statistics is desirable because of the accuracy it provides, but before determining the extrapolator for a wireless channel it is necessary to define a linear model for extrapolating and estimating the channel.

Linear Models

In the previous section a reference is made to linear models for estimators and extrapolators. These linear models are defined in this section because they are more relevant for the extrapolators that will be covered. One of the important aspects about the wireless channels in this paper and most of the research in this area is that it can be estimated or extrapolated from a linear equation of the measured, and in some cases estimated, values. So, the estimate or extrapolations of the wireless channel will always have one of the following forms.

$$\underbrace{\mathbf{O}_{\mathbf{h}_{\mathbf{c}},(\text{LEE}),t_l} \hat{\mathbf{h}}_{\mathbf{c},H_h,t_l}}_{\hat{\mathbf{h}}_{\mathbf{c},(\text{LEE}),H_h,t_l}} = \mathbf{G}_{\mathbf{y}_{\mathbf{c}},(\text{LEE}),t_l} \underbrace{\mathbf{O}_{\mathbf{y}_{\mathbf{c}},(\text{LEE}),t_l} \mathbf{y}_{\mathbf{c},Y_y,t_l}}_{\mathbf{y}_{\mathbf{c},(\text{LEE}),Y_y,t_l}} \quad 6.15$$

$$\underbrace{\hat{\mathbf{h}}_{\mathbf{r},H_h,\omega_k} \mathbf{O}_{\mathbf{h}_{\mathbf{r}},(\text{LEE}),\omega_k}}_{\hat{\mathbf{h}}_{\mathbf{r},(\text{LEE}),H_h,\omega_k}} = \underbrace{\mathbf{y}_{\mathbf{r},Y_y,\omega_k} \mathbf{O}_{\mathbf{y}_{\mathbf{r}},(\text{LEE}),\omega_k}}_{\mathbf{y}_{\mathbf{r},(\text{LEE}),Y_y,\omega_k}} \mathbf{G}_{\mathbf{y}_{\mathbf{r}},(\text{LEE}),\omega_k} \quad 6.16$$

Here, (LEE) denotes a particular linear estimation or extrapolation (LEE) technique and model used, as well as the linear the relationship it has with the measured data. This linear relationship is defined by the matrices, $\mathbf{G}_{\mathbf{y}_{\mathbf{c}},(\text{LEE}),t_l}$ or $\mathbf{G}_{\mathbf{y}_{\mathbf{r}},(\text{LEE}),\omega_k}$.

The LEE model also suggests what measured values are used and what values are estimated. The values to estimate or measure are determined by the omission matrix pairs: $\mathbf{O}_{\mathbf{h}_{\mathbf{c}},(\text{LEE}),t_l}$ and $\mathbf{O}_{\mathbf{y}_{\mathbf{c}},(\text{LEE}),t_l}$; and $\mathbf{O}_{\mathbf{h}_{\mathbf{r}},(\text{LEE}),\omega_k}$ and $\mathbf{O}_{\mathbf{y}_{\mathbf{r}},(\text{LEE}),\omega_k}$. At most, each column and row vector of these omission matrices have an element with the value of one. The rest of the elements that are not ones are zeroed, and none of the estimated channel omission matrices, denoted by $\hat{\mathbf{h}}_{\mathbf{c}}$ or $\hat{\mathbf{h}}_{\mathbf{r}}$, are zero matrices of any size, $\mathbf{0}_{(\text{Row} \times \text{Col})}$. The vectors and rows are organized such that that all the ones elements row and column indices are all in descending order. From the omission matrices it can be determined if the LEE model is an

estimator extrapolator or both. The following table shows how to determine this particular aspect of the LEE model.

Domain	Test	Estimator , Extrapolator, or Both
Angular-Frequency Domain	$O_{y_c,(\text{LEE}),t_l} O_{\hat{h}_c,(\text{LEE}),t_l}^H = \begin{bmatrix} I_{(\text{Row} \times \text{Col})} \\ 0_{(\text{Row} \times \text{Col})} \end{bmatrix}$	<i>estimator</i>
	$O_{y_c,(\text{LEE}),t_l} O_{\hat{h}_c,(\text{LEE}),t_l}^H = 0_{(\text{Row} \times \text{Col})}$	<i>extrapolator</i>
	$O_{y_c,(\text{LEE}),t_l} O_{\hat{h}_c,(\text{LEE}),t_l}^H = \text{Any other matrix}$	<i>estimator-extrapolator</i>
Time Domain	$O_{y_r,(\text{LEE}),\omega_k} O_{\hat{h}_r,(\text{LEE}),\omega_k}^H = \begin{bmatrix} I_{(\text{Row} \times \text{Col})} & 0_{(\text{Row} \times \text{Col})} \end{bmatrix}$	<i>estimator</i>
	$O_{y_r,(\text{LEE}),\omega_k} O_{\hat{h}_r,(\text{LEE}),\omega_k}^H = 0_{(\text{Row} \times \text{Col})}$	<i>extrapolator</i>
	$O_{y_r,(\text{LEE}),\omega_k} O_{\hat{h}_r,(\text{LEE}),\omega_k}^H = \text{Any other matrix}$	<i>estimator-extrapolator</i>

Table 6.1: Estimator/extrapolator test.

Time Domain Extrapolators

Any “fading” prediction technique will be a time domain extrapolator in this thesis. However, there is a relationship between the time domain and spatial domain with respect to fading. Therefore, in research papers fading prediction or extrapolation techniques could also reference extrapolations in the spatial domain. As stated in other sections, there are several techniques that fall into this category [60-65, 97-106]. Even nonlinear techniques are suggested in some research papers, the difference between nonlinear and linear techniques is that the relationship between the extrapolated and measured values are nonlinear. Although nonlinear techniques are discussed in other literature, this research only considered linear extrapolators. Therefore, the relationship between the extrapolated and measured values can be represented by the matrix $\mathbf{G}_{y_r,(\text{LEE}),\omega_k}$.

There are many interesting papers that discuss fading prediction and extrapolation models, but the two most common of these models are the radio channel model that treats the time domain channel as a sum of sinusoids and the models that describe an autoregressive or filtering process [64, 65, 107-109]. There are still many sub-variations of these models. These models and their relationship to the matrix $\mathbf{G}_{\mathbf{y}_r, (LEE), \omega_k}$ will not be presented or discussed in this thesis, but they are referenced in this section for further reading.

A very prominent reason for fading prediction or time extrapolation techniques is to aid in rate adaptation. As discussed in Part I of the thesis the knowledge about the channel can be crucial in implementing higher data rate schemes and applications.

In rate adaptation schemes the transmitted signal is adapted to increase the amount of data that can be sent through the channel. To do this, the wireless channel must be known. If the wireless channel is changing rapidly (i.e. fast fading), it is hard to estimate the channel at the receiver, and then send the estimate back to the transmitter and used the estimated for an accurate representation of the channel before the channel changes. This is why time domain extrapolations are important.

The next section references an angular-frequency domain extrapolator. However, the reference for this extrapolator does not suggest an application for angular-frequency domain extrapolators. As part of this contribution of the thesis, angular-frequency domain extrapolators are suggested for rate adaptation and this will be explained later in the thesis.

6.5 Super Resolution Wireless Channel Extrapolator

The super resolution wireless channel (SRWC) extrapolator is what is known in this thesis as an angular-frequency domain estimator-extrapolator. To the best of the author's knowledge, the SWRC extrapolator is the only angular-frequency domain extrapolator that has been reported in literature [34].

The SRWC extrapolator refers to the extrapolated channel as the blind region. To extrapolate the blind region this technique uses the adjacent sub-bands. However, this technique does not use a MCM scheme. Instead it uses PN sequences. A PN sequence is sent through each sub-band. At the receiver each sub-band goes through the following processing steps. First the receive signal is placed through a classification algorithm known as TLS-ESPRIT (total least squares version of estimation of signal parameters via rotational invariance technique) to determine the prominent delay components for estimating the wireless channel from the respective sub-band. The knowledge of the most prominent delay components obtained is used to create a least squared extrapolation and estimate of the wireless channel. In this thesis the least squared extrapolation is similar to the MLE for the same reasons the LMMSE is similar to the Bayes. The final step is a process called soft combining, where each channel measurement is summed together with a weighting filter [34]. The comparison of the SRWC technique and the ICM technique will be given in the next chapter.

6.6 Summary

This Chapter has covered channel estimation and/or extrapolation techniques used in OFDM systems. Mathematical representations were given. The accuracy and inaccuracy of

these techniques were also discussed. The main cause for inaccuracy discussed in this thesis was identified as the dynamic nature of the wireless environment. This causes CIR and TF to change rapidly and/or be more complicated (i.e. Multipath rich, fast fading, etc...). Also a unifying mathematical framework was presented. All estimators and/or extrapolators in this thesis can be defined by this mathematical framework as well as categorized. Also in this chapter the DCM and NCM techniques were introduced. These two techniques are contrasting techniques to the indirect channel measurement technique that will be presented in the next chapter.

The mathematical equations presented in this chapter are all important for understanding the equations and discussions in other chapters. However, the equations for the Bayes estimator and linear models are of particular importance. Equation 6.13 and 6.14 can yield closed form expressions for the estimator-extrapolator and the MSE in the ICM technique. Equation 6.13 shows that the Bayes estimator and/or extrapolator for wireless channels in this research and thesis is just the mean of a conditional pdf, and Equation 6.14 shows that the MSE is the variance of the same pdf.

Along with the Bayes estimator equations a linear model for the estimators and extrapolators were given. These linear forms allow for the comparison of all relevant techniques. Table 6.1 also gives a way to determine if the linear model used is an estimator, extrapolator, or both. From this linear model it can also be determined if the estimator and/or extrapolator is classical or Bayesian. If either of the terms in matrices $\mathbf{G}_{\mathbf{y}_c(\text{LEE}),t_l}$ and $\mathbf{G}_{\mathbf{y}_r(\text{LEE}),\omega_k}$, from the linear model Equation 6.15 or 6.16, uses any statistical information about the channel it can be viewed as a form of Bayesian statistic. Otherwise, it is of the

classical variety. In the next chapter these equations really aid in unifying all the techniques for comparison.

One of the techniques for comparison is the super resolution wireless channel measurement technique. This technique was briefly described in this chapter, but the mathematical representation is given in Chapter Seven. The SRWC technique is the most comparable technique to the ICM technique as far as what is measured and what is extrapolated, but it suffers from in-accuracy in multipath rich environments. This will be shown in the next chapter.

Fading predictors are the other techniques that the ICM technique is compared to. This technique is the most contrasting technique to the ICM technique. The ICM technique will be an angular-frequency domain estimator and/or extrapolator, and fading predictors will be time domain extrapolators. Time extrapolators are the main techniques that will be used in comparison with the ICM technique, and the linear model will aid in obtaining comparable accuracy metrics.

CHAPTER SEVEN

INDIRECT CHANNEL MEASUREMENT THEORY

7.1 Introduction

In Chapter Seven the wireless channel measurement theory that was created during the course of this research will be discussed. As stated in Part I the motivation for this research is to create a channel measurement technique that allows radios to have the most up-to-date and accurate channel state information (CSI) while maintaining a high-data-rate communication link.

Most estimation and extrapolation techniques measure the in-band (IB) channel directly. This is seen in the case of traditional estimation techniques and fading prediction techniques. Note that fading prediction techniques are the same as time extrapolation techniques presented in this thesis. Time extrapolation techniques are used to provide more up-to-date CSI, but in a dynamic wireless environment (DWE) these measurements may not be the most accurate. What has been proposed in this thesis is a technique that

uses the out-off-band (OOB) channel in a way that allows the measurement of the IB channel while maintaining data communications on the same IB channel. In the DWES, the technique should also provide a more up-to-date and accurate measurement of the CSI.

It is evident that the super resolution wireless channel (SRWC) extrapolator could use the OOB channel to measure the IB channel, even though this was not explicitly discussed [34]. Therefore, if this technique is used, it could also allow for data communication on the IB channel. Similar to the time extrapolation techniques, the SRWC technique can provide more up-to-date CSI, but it suffers from inaccuracy. SRWC extrapolators cannot handle certain types of multipath rich environments. In the next section this will be shown.

The next section will discuss the first estimator and extrapolator developed during the course of this research and the SRWC extrapolator. Similar to the SRWC extrapolator, the first estimator and extrapolator researched had issues with accuracy in certain types of multipath rich environment, but it is still more accurate than the SRWC technique because of how the measurements are used. These two techniques both indirectly measure the wireless channel, and there could be many other variations of an indirect channel measurement (ICM) technique. However, in this thesis the term ICM technique refers to a Bayes estimator-extrapolator that indirectly measures the wireless channel.

The following three sections will go over four techniques that will be used in the chapter regarding the simulations. Two of the techniques represent the best and worst case with respect to accuracy. The indirect channel measurement (ICM) technique, the proposed technique, will be the first section. The ICM technique is an angular-frequency-domain estimator-extrapolator that uses Bayesian statistics. The direct channel measurement (DCM) technique will be the next section of the three. The DCM technique is used to

represent the fading extrapolators in other research, but maintains notation similar to that given in this thesis. It also uses Bayesian statistics. The third section will cover the two techniques that represent the best and worst case: a technique that does not use any channel measurements, the no channel measurement (NCM) technique, and a technique that uses the full channel measurement (FCM). The NCM technique represents the lowest accuracy that would be observed by the ICM or DCM technique, and the FCM technique, a Bayes Estimator (BE) not a extrapolator, represents the highest accuracy. The DCM, NCM, and FCM techniques were introduced for comparison purpose.

The NCM addresses an important notion: in some cases the accuracy of the ICM or DCM techniques could be obtained without taking any channel measurements, and assuming a constant value for all total coherence blocks. Therefore, the NCM technique assumes a constant value for the channel, and if the same accuracy can be obtained without making a measurement then the simpler NCM technique could preferable to the ICM or DCM technique. The FCM technique will always be the best, but obviously would not allow a portion of the band to be simultaneously used for data transmission. After the discussion of these four techniques (i.e. ICM, DCM, NCM, and FCM), a summary will be given to conclude this chapter. Note, in the summary there is a list of all the techniques in this chapter.

7.2 First Channel Measurement Research

The first channel measurement technique researched was designed to take advantage of one particular aspect of a sampled band-limited and delay-limited wireless channel. Recalling Chapter Four, this type of wireless channel has “at most” M multipath components determined by the maximum excess delay and delay sample rate, and K angular-frequency samples determined by the delay and angular-frequency sample rate. The variables M and

K can be determined from Equation 4.13 and 4.14 respectively. Therefore, there are M delay values that are used to defined K angular-frequency values. This mathematical relationship is captured in Equation 4.31. Using Equation 4.31, Equation 7.1 can be obtained with respect to one of the time indices of the channel:

$$\mathbf{h}_{\mathbf{c},H_h,t_l} = \mathbf{F}_F \mathbf{h}_{\mathbf{c},h_h,t_l}. \quad 7.1$$

Equation 7.1 can be used in conjunction with Equation 6.4 to create the following column representation of the receive signal,

$$\mathbf{y}_{\mathbf{c},Y_y,t_l} = \mathbf{X}_{X_x} \mathbf{F}_F \mathbf{h}_{\mathbf{c},h_h,t_l} + \mathbf{w}_{\mathbf{c},W_w,t_l}. \quad 7.2$$

Assuming that $M < K$, then Equation 7.2 creates an overdetermined linear system (i.e. there are more equations than unknown values). Therefore, it is possible to remove some of the equations from the system and still obtain a solution, and if noise was not an issue, $K - M$ equations could be removed. So in theory (i.e. noise not being an issue), a radio could still measure the channel if it omits a maximum of $K - M$ angular-frequency samples.

The first channel measurement technique uses this aspect of the wireless channel. Thus far, it has been said that this estimator-extrapolator measures the OOB channel at a particular time and estimates the OOB and extrapolates the IB channel at the same time. Using Equation 7.2 a more detailed explanation of what is happening can be given. What is actually happening is the channel impulse response (CIR), $\mathbf{h}_{\mathbf{c},h_h,t_l}$, is being estimated from the OOB channel measurements, and these measurements are used to estimate the OOB and extrapolate the IB channels at the same time. Determining the CIR is considered to be estimation since the measure OOB channel values have the same time reference as the CIR.

This makes it possible to omit a set of angular-frequency samples in the central portion of the transfer function (TF) of the wireless channel and still obtain the entire TF. By

omitting this central portion it will allow this band to be used for data communication. If this central portion is used for data communications then it is the IB channel. In other words, this technique will allow a radio to observe the OOB channel and obtain the TF for the IB channel while using the IB channel for data communications.

To define the angular-frequency estimator and extrapolator for the first technique created during this research, Equation 6.15 will be used. In this chapter all the wireless channel omission matrices, \mathbf{O}_{h_c} or \mathbf{O}_{h_r} , will always be identity matrices. Also for this chapter, all the column representation of the received signal omission matrices, \mathbf{O}_{y_c} , have the following form

$$\mathbf{O}_{y_c} = \begin{bmatrix} \mathbf{0}_{(K_{obsrv} \times K_2)} & \mathbf{I}_{(K_{obsrv})} & \mathbf{0}_{(K_{obsrv} \times 2K_{omit})} & \mathbf{0}_{(K_{obsrv})} & \mathbf{0}_{(K_{obsrv} \times K_2)} \\ \mathbf{0}_{(K_{obsrv} \times K_2)} & \mathbf{0}_{(K_{obsrv})} & \mathbf{0}_{(K_{obsrv} \times 2K_{omit})} & \mathbf{I}_{(K_{obsrv})} & \mathbf{0}_{(K_{obsrv} \times K_2)} \end{bmatrix}, \quad 7.3$$

where,

$$K_2 \geq K_1, \quad 7.4$$

$$K - K_2 \geq K_{obsrv} \geq \frac{M}{2}, \quad 7.5$$

$$K_{omit} = \frac{K - 2K_{obsrv} - 2K_2}{2}. \quad 7.6$$

Using this omission matrix a least squared (LS) estimator/extrapolator for the initial measurement technique was created.

$$\begin{aligned} \hat{\mathbf{h}}_{c,LSEP,H_h,t_l} &= \underbrace{\mathbf{F}_F (\mathbf{F}_F^H \mathbf{X}_{X_x}^H \mathbf{O}_{y_c}^H \mathbf{O}_{y_c} \mathbf{X}_{X_x} \mathbf{F}_F)^{-1} (\mathbf{O}_{y_c} \mathbf{X}_{X_x} \mathbf{F}_F)^H}_{\mathbf{G}_{y_c,LSEP}} \underbrace{\mathbf{O}_{y_c} \mathbf{y}_{c,Y_y,t_l}}_{\mathbf{y}_{c,t_l}}. \\ &= \mathbf{G}_{y_c,LSEP} \mathbf{y}_{c,t_l} \end{aligned} \quad 7.7$$

The SRWC technique also uses LS estimators and extrapolators [34]. In order to compare the SRWC extrapolator, a few differences must be pointed out. First, the step that finds the most prominent delays is not needed. This step would have given the omission matrix. Since it is assumed that the statistical CSI (SCSI) is known, the omission matrix can

be obtained from the SCSL. The omission matrix used in the research paper does not quite follow the same omission matrix form given in this thesis in Equation 7.3. This is because each “sub-band” is treated as a different estimator-extrapolator, but when the estimator-extrapolators are combined, the omission matrix does take the same form as the omission matrix in Equation 7.3. So, for the estimator-extrapolator for each of the sub-bands, the slight difference is that the identity matrices are multiply by a constant and the other elements remain zero,

$$\mathbf{O}_{\mathbf{y}_c(i)} = [\mathbf{0}_{(K_{obsrv} \times K_2)} \quad (1-i)\mathbf{I}_{(K_{obsrv})} \quad \mathbf{0}_{(K_{obsrv} \times 2K_{omit})} \quad (i)\mathbf{I}_{(K_{obsrv})} \quad \mathbf{0}_{(K_{obsrv} \times K_2)}]. \quad 7.8$$

Here, the variable i represents the i^{th} sub-band. So, by replacing the omission matrix in Equation 7.7 with the omission matrix in Equation 7.8 a least squared estimator-extrapolator can be created for the respective sub-bands,

$$\hat{\mathbf{h}}_{\mathbf{c}, \text{LSEP}, H_h, t_l(i)} = \mathbf{G}_{\mathbf{y}_c, \text{LSEP}, (i)} \mathbf{y}_{\mathbf{c}, t_l}, \quad 7.9$$

$$\mathbf{G}_{\mathbf{y}_c, \text{LSEP}, (i)} = \mathbf{F}_F (\mathbf{F}_F^H \mathbf{X}_{X_x}^H \mathbf{O}_{\mathbf{y}_c(i)}^H \mathbf{O}_{\mathbf{y}_c(i)} \mathbf{X}_{X_x} \mathbf{F}_F)^{-1} (\mathbf{O}_{\mathbf{y}_c(i)} \mathbf{X}_{X_x} \mathbf{F}_F)^H. \quad 7.10$$

The final step in the SRWC technique is the soft combining of the two estimator-extrapolators to get SRWC estimator-extrapolator.

$$\begin{aligned} \hat{\mathbf{h}}_{\mathbf{c}, \text{SRWC}, H_h, t_l} &= \sum_{i=0}^1 \underbrace{\begin{bmatrix} |i - p_{-K/2}| & & \mathbf{0} \\ & \ddots & \\ \mathbf{0} & & |i - p_{K/2-1}| \end{bmatrix}}_{\mathbf{G}_{\mathbf{y}_c, \text{SRWC}, (i)}} \mathbf{G}_{\mathbf{y}_c, \text{LSEP}, (i)} \underbrace{\mathbf{O}_{\mathbf{y}_c(i)} \mathbf{y}_{\mathbf{c}, t_l}}_{\mathbf{y}_{\mathbf{c}, t_l(i)}}, \\ &= \underbrace{[\mathbf{G}_{\mathbf{y}_c, \text{SRWC}, (0)} \quad \mathbf{G}_{\mathbf{y}_c, \text{SRWC}, (1)}]}_{\mathbf{G}_{\mathbf{y}_c, \text{SRWC}}} \underbrace{\begin{bmatrix} \mathbf{y}_{\mathbf{c}, t_l(0)} \\ \mathbf{y}_{\mathbf{c}, t_l(1)} \end{bmatrix}}_{\mathbf{y}_{\mathbf{c}, t_l}}, \\ &= \mathbf{G}_{\mathbf{y}_c, \text{SRWC}} \mathbf{y}_{\mathbf{c}, t_l} \end{aligned} \quad 7.11$$

where,

$$p_k = \begin{cases} 1, & -K \leq k < -K_{omit} \\ \frac{K_{omit}-k}{2K_{omit}+1}, & -K_{omit} \leq k \leq K_{omit}, \\ 0, & K_{omit} \leq k < K \end{cases} \quad 7.12$$

$$\Sigma_{i=0}^1 \begin{bmatrix} |i - p_{-K/2}| & & \mathbf{0} \\ & \ddots & \\ \mathbf{0} & & |i - p_{K/2-1}| \end{bmatrix} = \mathbf{I}_{(K \times K)}. \quad 7.13$$

The theoretical performance of these two techniques in AWGN can be obtained by calculating the MSE. The respective MSEs are

$$MSE_{\mathbf{h}_c, H_h, \text{LSEP}} = \sigma_{\mathbf{W}}^2 \text{Tr} \left(\mathbf{G}_{\mathbf{y}_c, \text{LSEP}} (\mathbf{G}_{\mathbf{y}_c, \text{LSEP}})^H \right). \quad 7.14$$

$$MSE_{\mathbf{h}_c, H_h, \text{SRWC}} = \sigma_{\mathbf{W}}^2 \text{Tr} \left(\mathbf{G}_{\mathbf{y}_c, \text{SRWC}} (\mathbf{G}_{\mathbf{y}_c, \text{SRWC}})^H \right). \quad 7.15$$

To reduce error, another form of these techniques can be used. In this form another omission matrix is introduced to remove any multipath (MP) components whose power is less than that of the maximum excess delay power value. This will be called the multipath reduced (MPR) channel model. This changes Equation 7.1 to

$$\begin{aligned} \mathbf{h}_{c, \text{MPR}, H_h, t_l} &= \underbrace{\mathbf{F}_F \mathbf{O}_{\text{MPR}}^T}_{\mathbf{F}_{F, \text{MPR}}} \underbrace{\mathbf{O}_{\text{MPR}} \mathbf{h}_{c, h_h, t_l}}_{\mathbf{h}_{c, \text{MPR}, h_h, t_l}} \\ &= \mathbf{F}_{F, \text{MPR}} \mathbf{h}_{c, \text{MPR}, h_h, t_l} \end{aligned} \quad 7.16$$

The matrix \mathbf{O}_{MPR} has a similar structure as the matrix $\mathbf{O}_{\mathbf{y}_c}$. For this matrix, the number of rows is equal to the number of MP components that have power less than that of the maximum excess delay. For some wireless channel models this can provide significant improvements. The research paper on the SRWC technique also uses a similar matrix. The estimator and MSE are listed below.

$$\mathbf{G}_{\mathbf{y}_c, \text{LSEP} \setminus \text{MPR}} = \mathbf{F}_{F, \text{MPR}} (\mathbf{F}_{F, \text{MPR}}^H \mathbf{X}_{X_x}^H \mathbf{O}_{\mathbf{y}_c}^H \mathbf{O}_{\mathbf{y}_c} \mathbf{X}_{X_x} \mathbf{F}_{F, \text{MPR}})^{-1} (\mathbf{O}_{\mathbf{y}_c} \mathbf{X}_{X_x} \mathbf{F}_{F, \text{MPR}})^H. \quad 7.17$$

$$\mathbf{G}_{\mathbf{y}_c, \text{LSEP} \setminus \text{MPR}, (i)} = \mathbf{F}_{F, \text{MPR}} (\mathbf{F}_{F, \text{MPR}}^H \mathbf{X}_{X_x}^H \mathbf{O}_{\mathbf{y}_c, (i)}^H \mathbf{O}_{\mathbf{y}_c, (i)} \mathbf{X}_{X_x} \mathbf{F}_{F, \text{MPR}})^{-1} (\mathbf{O}_{\mathbf{y}_c, (i)} \mathbf{X}_{X_x} \mathbf{F}_{F, \text{MPR}})^H. \quad 7.18$$

$$\mathbf{G}_{\mathbf{y}_c, \text{SRWC} \setminus \text{MPR}} = \left[\underbrace{\begin{bmatrix} |i - p_{-K/2}| & & \mathbf{0} \\ & \ddots & \\ \mathbf{0} & & |i - p_{K/2-1}| \end{bmatrix}}_{\mathbf{G}_{\mathbf{y}_c, \text{SRWC} \setminus \text{MPR}, (0)}} \mathbf{G}_{\mathbf{y}_c, \text{LSEP} \setminus \text{MPR}, (0)} \quad \mathbf{G}_{\mathbf{y}_c, \text{SRWC} \setminus \text{MPR}, (1)} \right]. \quad 7.19$$

$$MSE_{\mathbf{h}_c, H_h, \text{LSEP} \setminus \text{MPR}} = \sigma_{\mathbf{W}}^2 \text{Tr} \left(\mathbf{G}_{\mathbf{y}_c, \text{LSEP} \setminus \text{MPR}} (\mathbf{G}_{\mathbf{y}_c, \text{LSEP} \setminus \text{MPR}})^H \right). \quad 7.20$$

$$MSE_{\mathbf{h}_c, H_h, \text{SRWC} \setminus \text{MPR}} = \sigma_{\mathbf{W}}^2 \text{Tr} \left(\mathbf{G}_{\mathbf{y}_c, \text{SRWC} \setminus \text{MPR}} (\mathbf{G}_{\mathbf{y}_c, \text{SRWC} \setminus \text{MPR}})^H \right). \quad 7.21$$

To show a theoretical comparison of these two techniques two channel models will be used. The channel parameters for these two models are given in the Appendix A. The first channel model is taken from Model A of the HIPERLAN/2 standard. The method to calculate the covariance matrix can be found in Appendix A. This covariance matrix was used to determine the omission matrix, \mathbf{O}_{MPR} . Using Equations 7.14, 7.15, 7.20 and 7.21 the theoretical performance of the four techniques are shown with respect to the number of average 90% coherence bandwidths omitted. The coherence bandwidth is determined from Equation 4.48. The average SNR per angular-frequency was set to be 30 dB, $K = 640$, and $K_1 = K_2 = 0$.

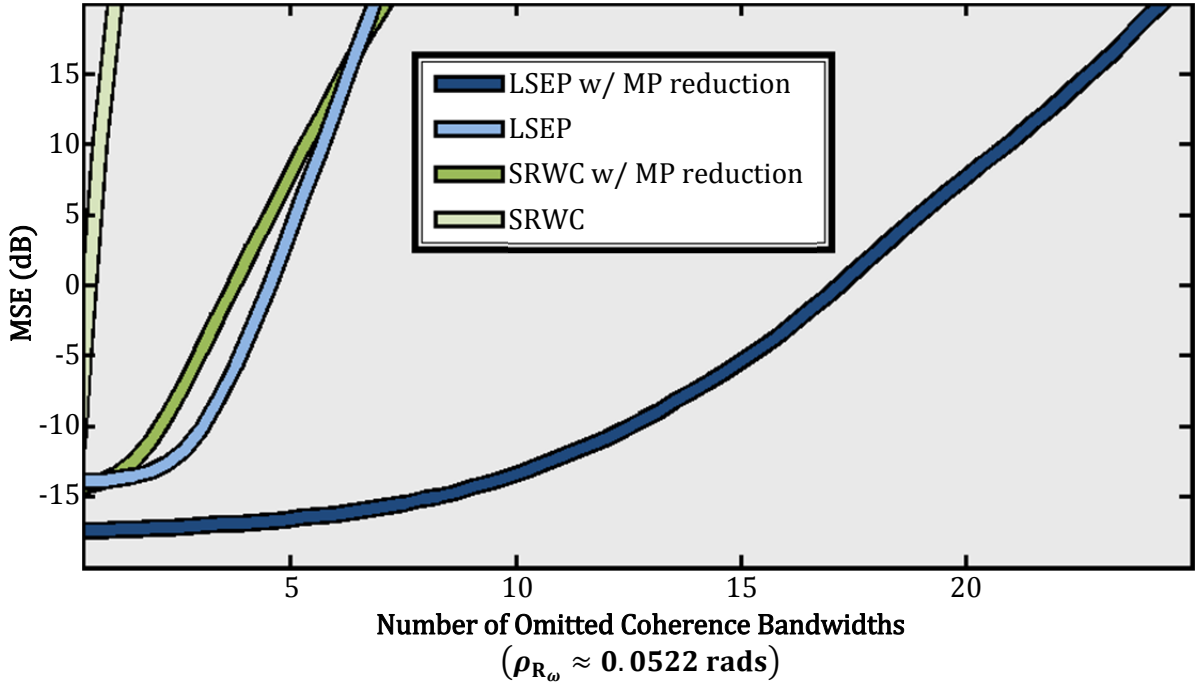


Figure 7.1: MSE performance measurements for the initial and SRWC technique with and without MP reduction for the HIPERLAN/2 Model A standard.

As seen in Figure 7.1, The LSEP technique with MP reduction is the best of the four. As stated before, the SRWC does not perform well in certain types of multipath rich environment and this can be seen with the channel model used. In Figure 7.2 the channel model was changed to mimic a model presented in the SRWC research paper, and the performance is greatly improved.

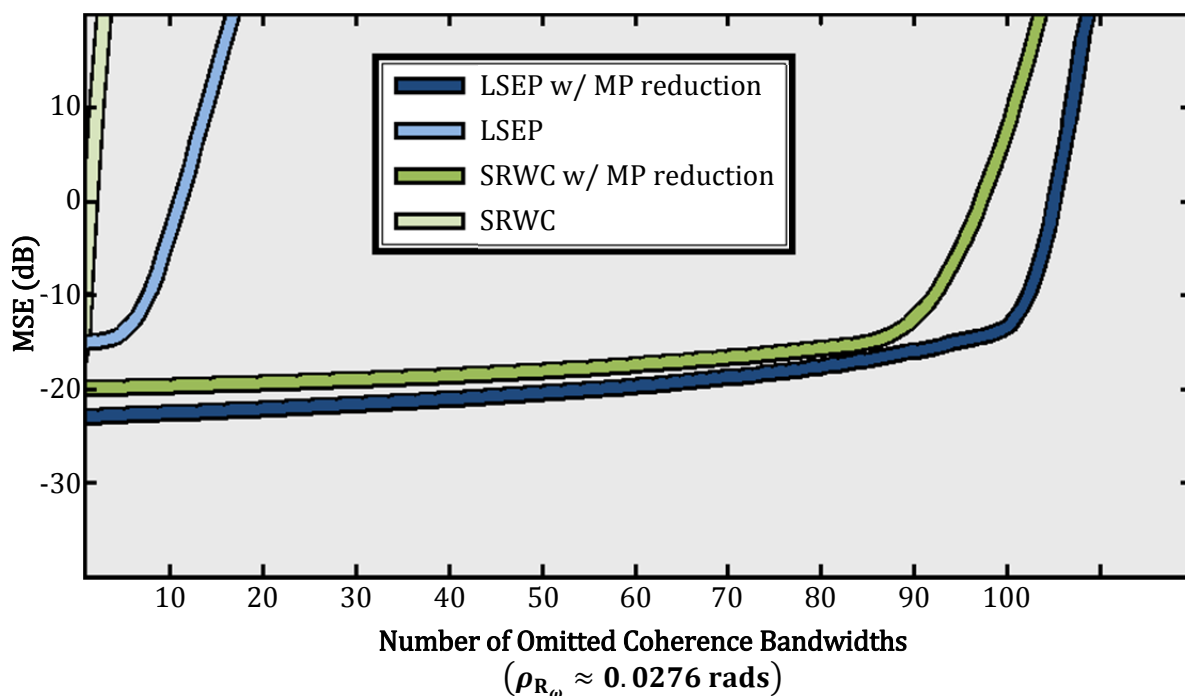


Figure 7.2: MSE performance measurements for the initial and SRWC technique with and without MP reduction for the channel model in the SRWC paper.

The multipath components in the model in the SRWC paper is further spread out than that in the HIPERLAN/2 Standard Model, and these techniques perform well in these situations. CIR of the two models is shown in Figures 7.3 and 7.4. The lighter regions in the plot represent the taps that are estimated in a technique that use MP reduction. In these techniques the darker regions are not estimated, but when MP reduction is not used the darker regions are estimated. The MSE is increased because all of the values in the CIR, even the zeroed taps, are estimated.

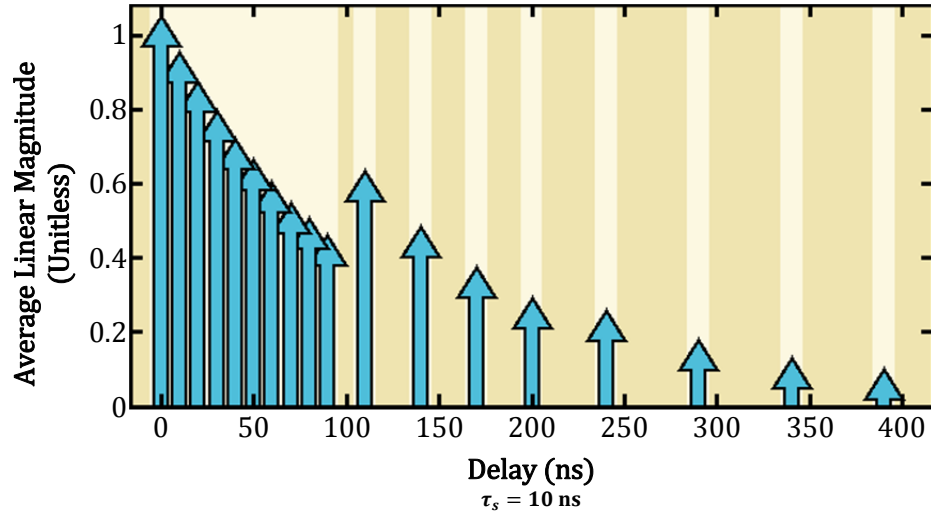


Figure 7.3: Average CIR of the HIPERLAN/2 Model A channel standard.

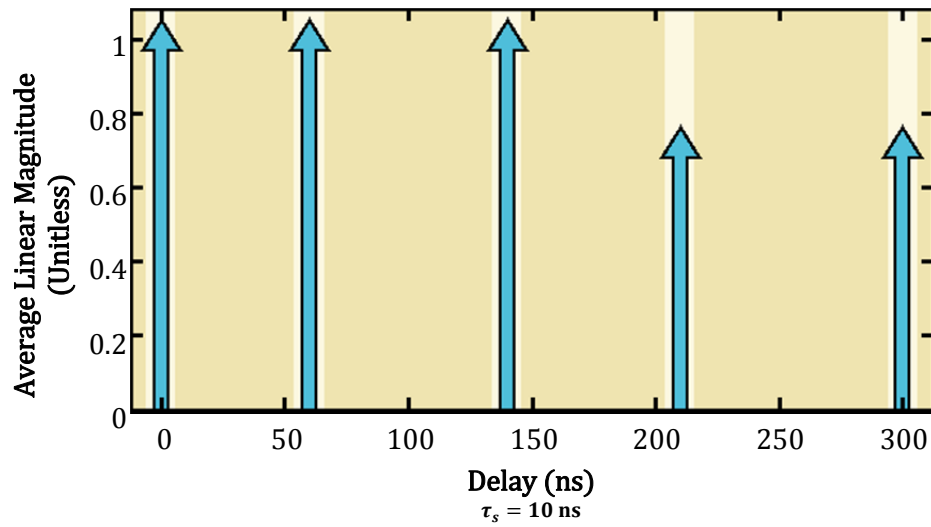


Figure 7.4: Average CIR of the channel model in the SRWC paper.

Due to the band-limiting filters and other effects in the radio, a CIR or TF represented by Equation 7.16 is not always seen in practice. Therefore, MP reduction will not work. This has been observed during this research. To improve the estimation and extrapolation in these cases the ICM technique was created.

7.3 Indirect Channel Measurements

The ICM technique uses the same concepts as the first channel measurement technique as well as the same channel model as in Equation 7.2, but the noise/interference term is a zero mean complex multivariate normal RV that is not necessarily AWGN.

The ICM technique uses Bayesian statistics. As stated in Chapter Six, by using Bayesian statistics a more accurate estimator-extrapolator can be created. To create the estimator-extrapolator, the conditional pdf, $f(\mathbf{h}_{c,Y_y,t_l} | \mathbf{y}_{c,Y_y,t_l})$ must be determined by using the mathematical definition for conditional pdf's, an understanding of multivariate normal RVs, and Equation 7.2. The result is

$$\begin{aligned} f(\mathbf{h}_{c,Y_y,t_l} | \mathbf{y}_{c,Y_y,t_l}) &= \frac{f(\mathbf{h}_{c,Y_y,t_l}, \mathbf{y}_{c,Y_y,t_l})}{f(\mathbf{y}_{c,Y_y,t_l})} \\ &= \pi^K |\det(\mathbf{P}_\omega)| \exp \left\{ \left(\mathbf{h}_{c,Y_y,t_l} - \mathbf{G}_{\mathbf{y}_c, \text{ICM}, t_l} \underbrace{\mathbf{O}_{\mathbf{y}_c} \mathbf{y}_{c,Y_y,t_l}}_{\mathbf{y}_{c,t_l}} \right)^H \mathbf{P}_\omega^{-1} \right. \\ &\quad \left. \times \left(\mathbf{h}_{c,Y_y,t_l} - \mathbf{G}_{\mathbf{y}_c, \text{ICM}, t_l} \mathbf{y}_{c,t_l} \right) \right\} \end{aligned} \quad 7.22$$

where,

$$\mathbf{G}_{\mathbf{y}_c, \text{ICM}, t_l} = \mathbf{G}_\omega = \mathbf{F}_F \mathbf{P}_\tau (\mathbf{O}_{\mathbf{y}_c} \mathbf{X}_{X_x} \mathbf{F}_F)^H (\mathbf{O}_{\mathbf{y}_c} \mathbf{R}_{W_w} \mathbf{O}_{\mathbf{y}_c}^T)^{-1}, \quad 7.23$$

$$\mathbf{P}_\tau = \left[(R_{t,t_l} \mathbf{R}_\tau)^{-1} + (\mathbf{O}_{\mathbf{y}_c} \mathbf{X}_{X_x} \mathbf{F}_F)^H (\mathbf{O}_{\mathbf{y}_c} \mathbf{R}_{W_w} \mathbf{O}_{\mathbf{y}_c}^T)^{-1} (\mathbf{O}_{\mathbf{y}_c} \mathbf{X}_{X_x} \mathbf{F}_F) \right]^{-1}, \quad 7.24$$

$$\mathbf{P}_\omega = \mathbf{F}_F \mathbf{P}_\tau \mathbf{F}_F^H. \quad 7.25$$

The matrices \mathbf{P}_τ and \mathbf{P}_ω are the Schur complements of \mathbf{R}_τ and \mathbf{R}_ω respectively. As stated in Chapters Four and Five, the matrices $\mathbf{R}_{\omega w}$, \mathbf{R}_τ , and \mathbf{R}_ω are the covariance matrices of the noise/interference term and the delay and angular-frequency domains of the wireless channels. The variable R_{t,t_l} is the t_l diagonal element of the \mathbf{R}_t covariance matrix. These

variables and matrices are SCSI; it is assumed that this information is known, because of the capabilities of cognitive radios. This simplifies the estimation and extrapolation. If the SCSI was unknown then another step must be taken to measure it before estimating and/or extrapolating the channel. Any inaccuracy in the measurement could affect the estimator and/or extrapolator drastically.

Once the SCSI is known, Equations 7.22 – 7.25 can be used to create the ICM estimator-extrapolator using Equation 6.13,

$$\hat{\mathbf{h}}_{\mathbf{c},\text{ICM},t_l} = \mathbf{G}_\omega \mathbf{y}_{\mathbf{c},t_l}. \quad 7.26$$

The accuracy of the estimator-extrapolator can be quantified by using the MSE. In the case of the Bayes estimators and/or extrapolators, the MSE is a function of the variance, \mathbf{P}_ω , of the density in Equation 7.22,

$$MSE_{\hat{\mathbf{h}}_{\mathbf{c},\text{ICM},t_l}} = \frac{1}{K} \text{Tr}(\mathbf{P}_\omega). \quad 7.27$$

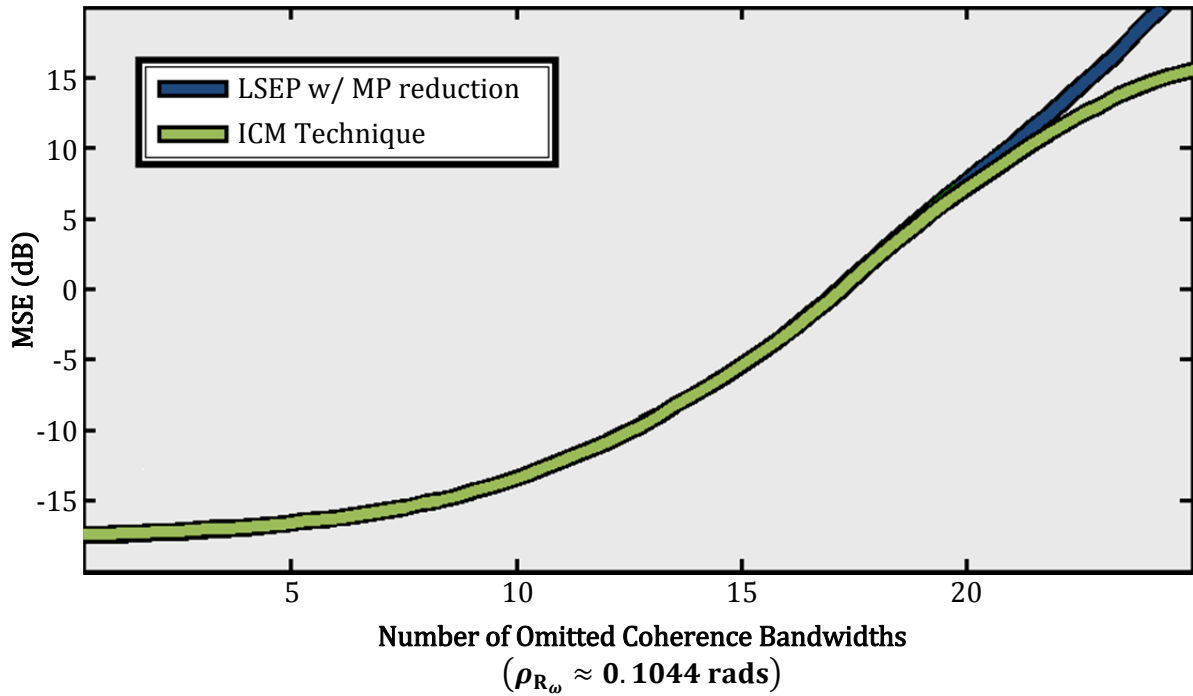


Figure 7.5: MSE performance measurements for LSEP without MP reduction and ICM technique for the HIPERLAN/2 Model A standard.

Figure 7.5 shows how the ICM technique performance compares to the LSEP with MP reduction for the same channel in Figure 7.1. As seen in the figure, the ICM estimator-extrapolator does not provide significant improvement over the LSEP when the LSEP can use MP reduction. However, if MP reduction cannot be used the performance difference between the LSEP and the ICM estimator-extrapolator is even greater, as shown in Figure 7.6. In Figure 7.6 an exponentially decaying channel model is used. Its CIR is shown in Figure 7.7.

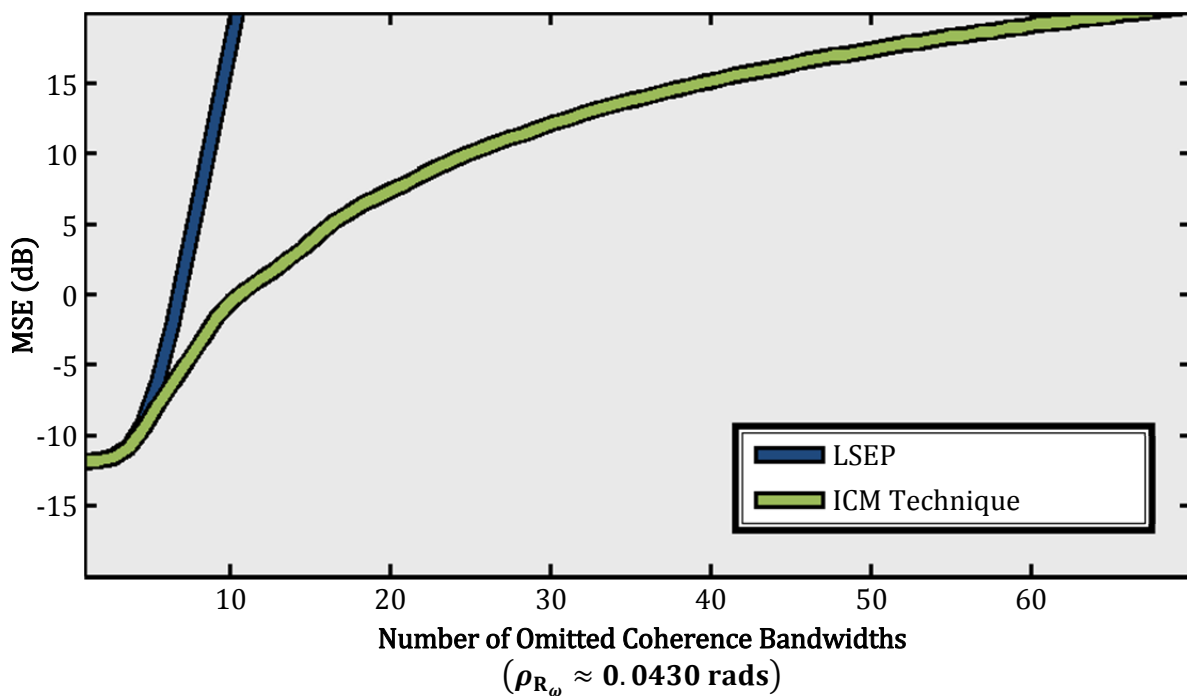


Figure 7.6: MSE performance measurements for LSEP without MP reduction and ICM technique for an exponentially decaying tap model.

The exponentially decaying (ED or EDT) channel model has a maximum number of taps M . This model was created for this research to create an easily varied channel. The channel is varied by changing the degree of decline for the slope, and the slope values can be mapped to performance. The exponentially decaying channel model is further explained in

the appendix. Unlike the HIPERLAN/2 model, MP reduction cannot be done on these models.

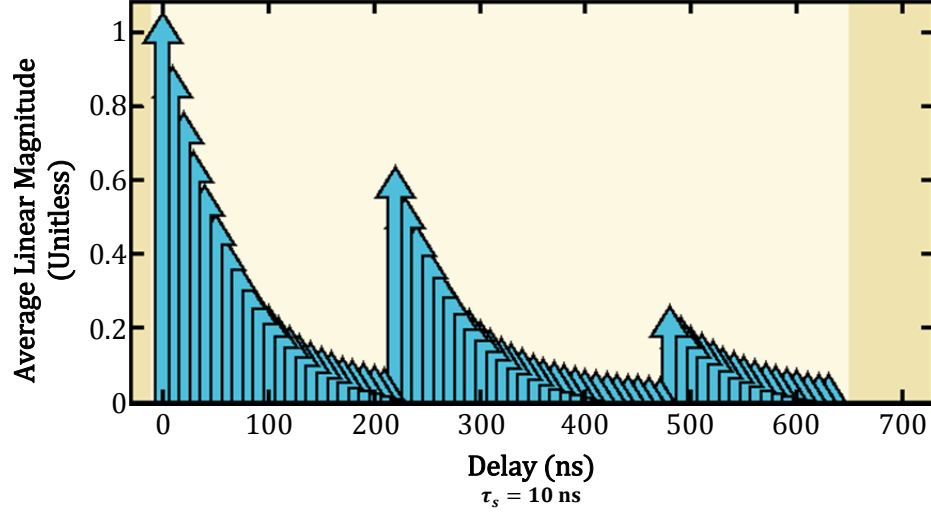


Figure 7.7: CIR for an exponentially decaying channel model with a decaying slope of 36 degrees for each of the three exponentials.

Another quantification of accuracy that will be used in this thesis is the square root of the MSE of the squared envelope (RMSE-SE),

$$\mathbf{z}_{\mathbf{c},(\text{LEE}),t_l} = \sqrt{\text{diag}\left(E\left\{\left|\hat{\mathbf{h}}_{\mathbf{c},(\text{LEE}),t_l} \circ \hat{\mathbf{h}}_{\mathbf{c},(\text{LEE}),t_l}^* - \mathbf{h}_{\mathbf{c},Y_y,t_l} \circ \mathbf{h}_{\mathbf{c},Y_y,t_l}^*\right|^2\right\}\right)}. \quad 7.28$$

Note that the square root function is an element wise square root function for this equation. This measurement of accuracy gives a way to view the performance of the envelope of the estimate. In the case of rate adaptation the envelope may be used to make adaptive decisions.

Note in other papers the error term used is the MSE of the envelope itself [64, 65, 107]. The reason for using the MSE of the squared envelope is because a closed form equation could be derived for all measurement techniques for comparison purposes. These equations that are related to the envelope values are important for rate adaptation algorithms that will be discussed later in this section.

For the ICM technique the RMSE-SE is

$$\mathbf{z}_{\mathbf{c},\text{ICM},t_l} = \sqrt{\text{diag} \left(E \left\{ \left| \hat{\mathbf{h}}_{\mathbf{c},\text{ICM},t_l} \circ \hat{\mathbf{h}}_{\mathbf{c},\text{ICM},t_l}^* - \underbrace{\mathbf{h}_{\mathbf{c},\text{ICM},t_l}}_{(\hat{\mathbf{h}}_{\mathbf{c},Y_y,t_l} + \hat{\mathbf{w}}_{\mathbf{c},\text{ICM},t_l})} \circ \mathbf{h}_{\mathbf{c},Y_y,t_l}^* \right|^2 \right\} \right)}. \quad 7.29$$

The vector $\hat{\mathbf{w}}_{\mathbf{c},\text{ICM},t_l}$ is the error of the ICM estimator-extrapolator. This error value is a zero-mean complex multivariate normal RV with covariance matrix \mathbf{P}_ω . Equation 7.29 can be further simplified,

$$\begin{aligned} \mathbf{z}_{\mathbf{c},\text{ICM},t_l} &= \sqrt{\text{diag} \left(E \left\{ \left| \hat{\mathbf{h}}_{\mathbf{c},Y_y,t_l}^* \circ \hat{\mathbf{w}}_{\mathbf{c},\text{ICM},t_l} + \hat{\mathbf{h}}_{\mathbf{c},Y_y,t_l} \circ \hat{\mathbf{w}}_{\mathbf{c},\text{ICM},t_l}^* - \hat{\mathbf{w}}_{\mathbf{c},\text{ICM},t_l} \circ \hat{\mathbf{w}}_{\mathbf{c},\text{ICM},t_l}^* \right|^2 \right\} \right)} \\ &= \sqrt{\text{diag} \left(\underbrace{2 E \left\{ \left| \hat{\mathbf{h}}_{\mathbf{c},Y_y,t_l} \right|^2 \right\}}_{(R_{t,t_l} \mathbf{R}_\omega - \mathbf{P}_\omega)} \circ \underbrace{E \left\{ \left| \hat{\mathbf{w}}_{\mathbf{c},\text{ICM},t_l} \right|^2 \right\}}_{\mathbf{P}_\omega} + \underbrace{E \left\{ \left| \hat{\mathbf{w}}_{\mathbf{c},\text{ICM},t_l} \circ \hat{\mathbf{w}}_{\mathbf{c},\text{ICM},t_l}^* \right|^2 \right\}}_{(\mathbf{P}_\omega \circ \mathbf{P}_\omega^*) + \text{diag}(\mathbf{P}_\omega) \text{diag}(\mathbf{P}_\omega)^H} \right)} \quad 7.30 \\ &= \sqrt{\text{diag} (2(R_{t,t_l} \mathbf{R}_\omega - \mathbf{P}_\omega) \circ \mathbf{P}_\omega + (\mathbf{P}_\omega \circ \mathbf{P}_\omega^*) + \text{diag}(\mathbf{P}_\omega) \text{diag}(\mathbf{P}_\omega)^H)} \end{aligned}$$

Through simulations this Equation will be verified to show its validity, and in the next section a theoretical comparison to the other techniques will be given using these equations.

7.4 Direct Channel Measurements

The ICM technique was designed to be complementary to the time extrapolation techniques mentioned in Chapter Six. The direct channel measurement (DCM) technique was created, for comparison purposes, to represent the time extrapolators. The DCM technique follows a similar formulation to the ICM technique but with respect to the time domain instead of the angular-frequency domain. This makes the DCM technique a time domain estimator-extrapolator similar to the time extrapolators. In comparison to the time extrapolator techniques the DCM technique is the optimal estimator-extrapolator for the Gaussian RV channel model given in this thesis. Similar to the SRWC technique, time

extrapolators often have a step where some type of channel statistics is determined. For the DCM technique this is not the case. The second order statistic is assumed to be known, and it is used to create the estimator-extrapolator.

Linear time domain extrapolators and/or estimators like the DCM technique have similar mathematical form to that in Equation 6.16. As mentioned, the wireless channel omission matrix is an identity matrix. However, this time the received signal omission matrix takes a different form,

$$\mathbf{O}_{y_r} = \begin{bmatrix} \mathbf{0}_{(L_2 \times L_{obsrv})} \\ \mathbf{I}_{(L_{obsrv} \times L_{obsrv})} \\ \mathbf{0}_{(L_{omit} \times L_{omit})} \\ \mathbf{0}_{(L_2 \times L_{obsrv})} \end{bmatrix}, \quad 7.31$$

where,

$$L_2 \geq L_1, \quad 7.32$$

$$L - L_2 \geq L_{obsrv} \geq N, \quad 7.33$$

$$L_{omit} = L - L_{obsrv} - 2L_2. \quad 7.34$$

Using this omission matrix and a similar Bayes estimator/extrapolator as given in the last section, a Bayes estimator/extrapolator for the DCM technique can be created.

$$f(\mathbf{h}_{r,Y_y,\omega_k} | \mathbf{y}_{r,Y_y,\omega_k}) = \pi^K |\det(\mathbf{P}_t)| \exp \left\{ \left(\mathbf{h}_{r,Y_y,\omega_k} - \underbrace{\mathbf{y}_{r,Y_y,\omega_k} \mathbf{O}_{y_r}}_{\mathbf{y}_{r,\omega_k}} \mathbf{G}_{y_r,DCM,\omega_k} \right)^H \mathbf{P}_t^{-1} \right. \\ \left. \times \left(\mathbf{h}_{r,Y_y,\omega_k} - \mathbf{y}_{r,\omega_k} \mathbf{G}_{y_r,DCM,\omega_k} \right) \right\}, \quad 7.35$$

where,

$$\mathbf{G}_{y_r,DCM,\omega_k} = \mathbf{G}_t = X_{x,\omega_k} (\mathbf{O}_{y_r}^T \mathbf{R}_{W_w} \mathbf{O}_{y_r})^{-1} (\mathbf{F}_l \mathbf{O}_{y_r})^H \mathbf{P}_f \mathbf{F}_l, \quad 7.36$$

$$\mathbf{P}_f = \left[(R_{\omega,\omega_k} \mathbf{R}_f)^{-1} + X_{x,\omega_k}^2 (\mathbf{F}_l \mathbf{O}_{y_r}) (\mathbf{O}_{y_r}^T \mathbf{R}_{W_w} \mathbf{O}_{y_r})^{-1} (\mathbf{F}_l \mathbf{O}_{y_r})^H \right]^{-1}, \quad 7.37$$

$$\mathbf{P}_t = \mathbf{F}_I^H \mathbf{P}_f \mathbf{F}_I, \quad 7.38$$

$$X_{x,\omega_k} = X_x(t_0, \omega_k)|_{[\tau_G, \tau_{K+G})}. \quad 7.39$$

The matrices \mathbf{P}_f and \mathbf{P}_t are the Schur complements of \mathbf{R}_f and \mathbf{R}_t respectively, and R_{ω,ω_k} is the ω_k diagonal element of the \mathbf{R}_ω covariance matrix. Using Equations 7.35 – 7.39 the Bayes estimator-extrapolator can be formed,

$$\hat{\mathbf{h}}_{\mathbf{r},\text{DCM},\omega_k} = \mathbf{y}_{\mathbf{r},\omega_k} \mathbf{G}_t. \quad 7.40$$

Similar to the ICM technique the two accuracy metrics, the MSE and RMSE-SE, can be represented by the following equations,

$$MSE_{\hat{\mathbf{h}}_{\mathbf{r},\text{DCM},\omega_k}} = \frac{1}{L} \text{Tr}(\mathbf{P}_t). \quad 7.41$$

$$\mathbf{z}_{\mathbf{r},\text{DCM},\omega_k} = \sqrt{\text{diag}(2(R_{\omega,\omega_k} \mathbf{R}_t - \mathbf{P}_t) \circ \mathbf{P}_t + (\mathbf{P}_t \circ \mathbf{P}_t^*) + \text{diag}(\mathbf{P}_t) \text{diag}(\mathbf{P}_t)^H)^T}. \quad 7.42$$

With these metrics, the DCM technique provides an optimal method similar to a time extrapolator that can directly compared to the ICM technique.

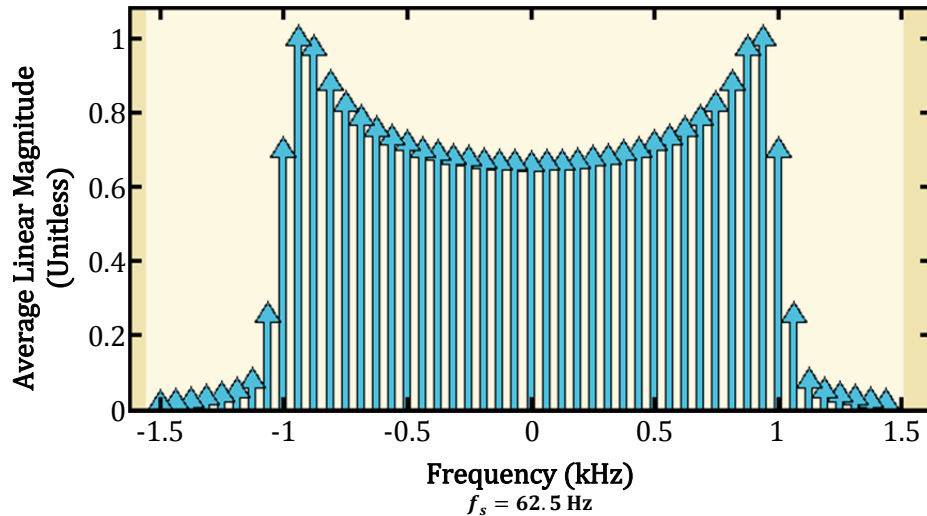


Figure 7.8: Jakes' Model for a max Doppler shift equal to 1 kHz and $L = 1024$, $L_1 = 64$, $N = 48$, $f_s = 62.5$ Hz.

To give a theoretical comparison a Jakes' Doppler spectrum model was used [41, 44]. This model is also shown in the Appendix A. The max Doppler shift was set to equal 1 kHz and the respective variables are $L = 1024$, $L_1 = 64$, $N = 48$, $f_s = 62.5$ Hz, and the covariance matrix for these variables is defined in the appendix. The frequency (i.e. Doppler spectrum taps) are shown in Figure 7.8. The Doppler model in this Figure was used for the frequency domain in Figure 7.9. For the Delay domain the ED model in Figure 7.7 was used.

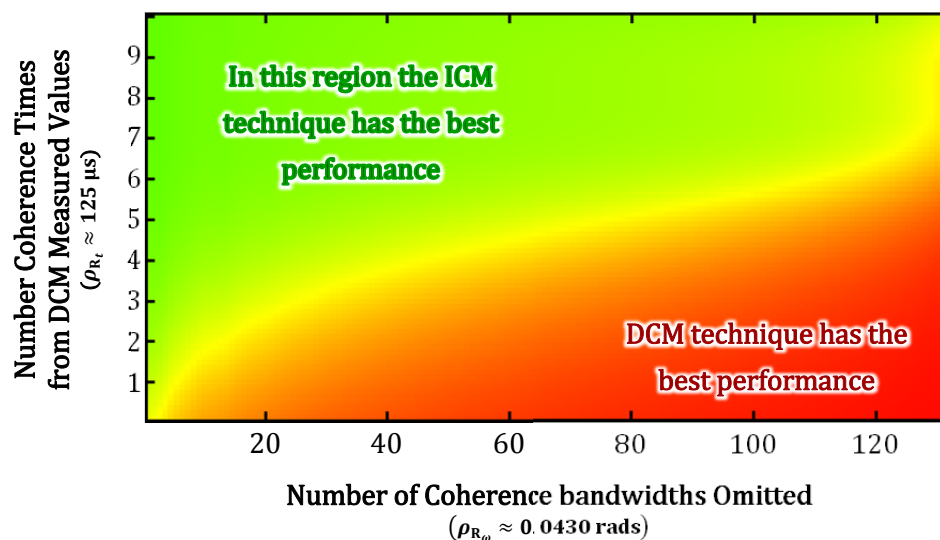


Figure 7.9: Optimal performance color map of the ICM and DCM techniques for ED delay channel model with a slope decline of 36 degrees; and a Jakes' spectral model for the frequency taps with a 1 kHz Doppler shift.

The MSE comparison for the ICM and DCM estimator-extrapolator is shown in Figure 7.9. The y-axis is the number of coherence times the extrapolation is away from the DCM estimates. The x-axis is the number of coherence bandwidths omitted. In this case the MSE for the DCM technique is the MSE value at the time index that corresponds to the respective coherence time. For the ICM technique the MSE is the average MSE over the central omitted bandwidth. These MSEs are color weighted to theoretically show what conditions would one technique out performs the other. As hypothesized, in the case of a DWE were the

extrapolation is several coherence times away from the estimate the ICM technique will outperform the DCM technique.

In this section the ICM technique was compared to the DCM technique that represents the time extrapolators. In the next section the ICM technique will be compared to the techniques with the best and worst accuracy

7.5 No Channel and Full Channel Measurements

The NCM and FCM techniques were created to show two accuracy extremes: the highest amount accuracy that can be obtained, FCM, and the lowest level of accuracy, NCM. The section will start with the NCM technique.

The NCM technique extrapolates the channel without taking any instantaneous measurement of the wireless channel. The NCM technique gives a worst case estimator-extrapolator for comparison with the ICM and/or DCM techniques. If the ICM and/or DCM techniques do not perform significantly better than the NCM technique it brings up the question of “why to make a measurement at all?” Therefore, in these cases neither technique will be needed, because the same results can be obtained without making a measurement.

In the NCM technique no training signal is transmitted and the channel is estimated to be equal to Equations 7.43 or 7.44. This is a completely flat channel in the angular-frequency domain and a delta function in the delay domain

$$\hat{\mathbf{h}}_{\mathbf{c},\text{NCM},t_l} = \sqrt{K}\mathbf{1}_K, \quad 7.43$$

$$\hat{\mathbf{h}}_{\mathbf{r},\text{NCM},\omega_k} = \sqrt{K}\mathbf{1}_L^T, \quad 7.44$$

where the variable $\mathbf{1}_K$ is a K element ones column vector. For the NCM as well as the FCM technique the MSE was not used for comparison. The RMSE-SE was used instead. The RMSE-SE for the NCM technique is given in Equations 7.45 and 7.46.

$$\mathbf{z}_{\mathbf{c},NCM,t_l} = \sqrt{\text{diag}(2(R_{t,t_l}^2 \mathbf{R}_\omega \circ \mathbf{R}_\omega) - 2K(R_{t,t_l} \mathbf{R}_\omega) + K^2)}. \quad 7.45$$

$$\mathbf{z}_{\mathbf{r},NCM,\omega_k} = \sqrt{\text{diag}(2(R_{\omega,\omega_k}^2 \mathbf{R}_t \circ \mathbf{R}_t) - 2K(R_{\omega,\omega_k} \mathbf{R}_t) + K^2)}. \quad 7.46$$

These equations are determined by using Equations 7.28, 7.45, and 7.46.

The final technique that will be discussed in this chapter is the FCM technique. The FCM technique uses all the complex gains of the channel, \mathbf{H}_{H_h} to do a Bayes estimate. This is the best performance that can be obtained given the conditions presented in this paper.

The FCM technique can be either an angular-frequency or time domain estimator. To create this estimator Equations 7.22 – 7.25 or 7.35 – 7.39 can be used. To obtain the estimator the omission matrices must be identity matrices. The matrix $\mathbf{O}_{\mathbf{y}_c}$ will be a $K \times K$ identity matrix and $\mathbf{O}_{\mathbf{y}_r}$ a $L \times L$. The RMSE-SE can be obtained from Equation 7.30 or 7.42.

Using the same ED model, The RMSE-SE for the ICM, NCM, and FCM techniques are shown in Figure 7.10. As seen in the figure, as K_{omit} increases it approaches the NCM technique, and when it decreases it approaches the FCM technique. Note that the frequency values are normalized by the coherence bandwidth.

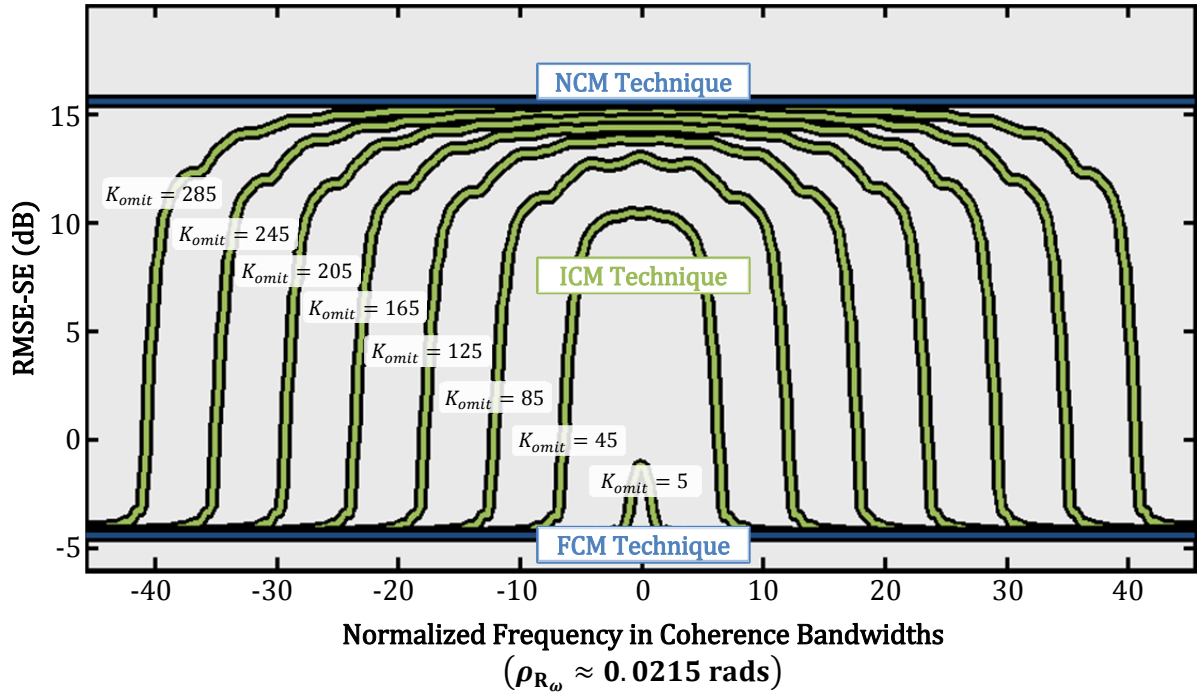


Figure 7.10: MSE performance measurements for LSEP without MP reduction and ICM technique for the HIPERLAN/2 Model A standard.

7.6 Summary

In this chapter the theory supporting the research for the first contribution has been given. This Chapter covered eight different estimators and/or extrapolators. These estimators and/or extrapolators are summarized in Table 7.1. This table lists the techniques, the linear estimator and/or extrapolator and omission matrices, and the theoretical accuracy and inaccuracy conditions. The ICM, DCM, NCM, and to some extent the FCM techniques will be used in the rate adaption, simulation, and/or experimentation chapters to follow.

Technique	Type	Linear Matrix	Omission Matrices	Theoretical Accuracy and/or Inaccuracy conditions
LSEP	Ang.-Freq. Extrapolator	$\mathbf{G}_{y_c, \text{LSEP}}$ (Equation 7.7)	\mathbf{O}_{y_c} (Equation 7.3)	This technique is accurate when M (number of multipath) is small. Inaccuracy occurs because of singularity issues
LSEP w/MP Reduction	Ang.-Freq. Extrapolator	$\mathbf{G}_{y_c, \text{LSEP} \setminus \text{MPr}}$ (Equation 7.17)	\mathbf{O}_{y_c} and \mathbf{O}_{MPR} (Equation 7.16)	This technique is more accurate than the LSEP. It removes any insignificant multipath components. This removes some of the singularity issues. However, MP reduction cannot be used in multipath rich environments
SRWC	Ang.-Freq. domain Extrapolator	$\mathbf{G}_{y_c, \text{SRWC}}$ (Equation 7.11)	\mathbf{O}_{y_c}	Not as accurate as the LSEP technique because it is not the true MLE or LS of the entire channel. By breaking the channel into sub bands it magnifies the singularity issues with LS
SRWC w/MP Reduction	Ang.-Freq. Domain Extrapolator	$\mathbf{G}_{y_c, \text{SRWC} \setminus \text{MPr}}$ (Equation 7.19)	\mathbf{O}_{y_c} and \mathbf{O}_{MPR}	Not as accurate to the LSEP w/MP reduction for the same reason.
ICM	Ang.-Freq. Domain Extrapolator	\mathbf{G}_ω (Equation 7.23)	\mathbf{O}_{y_c}	Is most accurate, in comparison to the DCM, in DWEs.
DCM	Time Domain Extrapolator	\mathbf{G}_t (Equation 7.36)	\mathbf{O}_{y_r} (Equation 7.31)	Is most accurate, in comparison to the ICM, in non DWEs.
NCM	Ang.-Freq. and Time Domain Extrapolator	Constant value	$\mathbf{0}_{(\text{Row} \times \text{Col})}$	Most inaccurate under all conditions.
FCM	Ang.-Freq. or Time Domain Extrapolator	\mathbf{G}_ω or \mathbf{G}_t	\mathbf{O}_{y_c} or \mathbf{O}_{y_r}	Most accurate under all conditions.

Table 7.1: Summary of the estimators and/or extrapolators in Chapter Seven.

CHAPTER EIGHT

CHANNEL MEASUREMENT AND RATE ADAPTATION

8.1 Introduction

It has been stated that the introduction of the concept of “cognitive radio” in the wireless communication community has stimulated significant interest in recent years. Cognitive radios can improve the effectiveness of radios and networks of radios (RNE), such as having larger network capacities, higher data rates, and better reliability through using adaptive or multirate OFDM, water-filling, and many other rate adaptation techniques [1-5, 7-10]. In this thesis rate adaptation techniques are defined as any method that varies the transmission parameters to change the data rate based on the channel state information (CSI).

This chapter will cover a rate adaptation system created for the purpose of this research. The rate adaptation system in this research was design to give a generic framework for which the ICM, DCM and/or NCM techniques could be deployed. This generic

system can be further adapted to better suit the particular needs are requirement of an actual rate adaptation system. This chapter will also give the reader tools to use to make decisions in how to design a rate adaptation system. The tools presented in this chapter are metrics developed during the course of this research that can be used and/or adapted to compare the ICM, DCM, and some cases NCM techniques.

The structure of this chapter is as follows: in the first section three types of rate adaptation systems will be given along with a block diagram that illustrates how the respective wireless communication system works. Two of the types will be rate adaptation systems that use the ICM or DCM technique. Also, this section will progressively show why each system is needed with respect to the dynamic nature of dynamic wireless environments (DWEs).

The second section will talk about the first metrics in this chapter the information update time (IUT) and the information expiration time (IET). The IUT and IET are not only relevant to rate adaptation. These metrics can be adapted and used in other context as well. This chapter also cover metrics that are only germane to rate adaptation. These metrics are covered in the fourth section of this chapter, but before these metrics are covered. The practical rate adaptation scenario used in this research is presented in the third section.

The IUT, IET, and the rate adaptation metrics are purposely given as tools or “blueprints” for tools that can aid the reader in creating a rate adaptation system for actual use. In this chapter these tools will not be used in a way that directly indicates if the ICM, DCM, or NCM technique is best for rate adaptation, because that is not the scope of this thesis. However, in Chapter Nine the IUT and IET will be used to show which of the three techniques is best based on these metric, dynamic nature of the DWE, and other factors.

8.2 Types of Rate Adaptation Systems

There are three types of rate adaptation systems that are presented in this section: a system that uses present (in-band) IB CSI to adapt the transmission data rate, a system that uses past and/or present IB CSI (this system uses the DCM technique), and a system that uses present OOB CSI (this system uses the ICM technique).

A wireless communication system that uses the present CSI to adapt the transmission data rate is shown in Figure 8.1. This is the desired situation: having a system that can send back the present CSI while the transmitter is still transmitting the present rate adapted signal. Note Figure 8.1 uses the color scheme in Figure 4.1, but the light blocks represent training signals and each block contains multiple total coherence blocks.

In Figure 8.1 the transmitter is transmitting the present rate adapted signal. The receiver extracts the rate adapted data, uses the training signal to estimate the channel and determine the rates, and feeds this information back to the transmitter. The transmitter processes this information and determines the CSI and/or rates that the receiver calculated, and uses this information for rate adaptation and makes the adjustments.

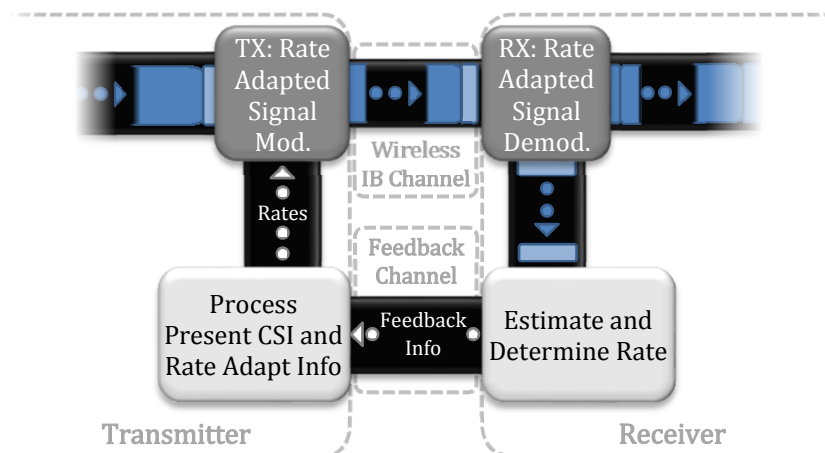


Figure 8.1: A block diagram of a rate adaptation system that uses present CSI observed at the receiver.

The use of present CSI to control rate adaptation is effective only if the DWE is slightly dynamic. A slightly dynamic DWE means that the channel is varying very slowly or virtually not at all compared with the time it takes to feedback and process the CSI, and the channel changes can be neglected. Slightly dynamic DWEs are also an indication of very slow fading. However, when the variations of the channel on this time scale cannot be neglected, fading prediction techniques, similar to time extrapolators in this research, can be used [64, 65, 107]. This is true in the case of moderately dynamic DWEs. Note, in moderately dynamic DWEs the wireless channel can be viewed as a slow or fast fading channel. Therefore, in slow or fast fading wireless channels in moderately dynamic DWEs the variation of the channel cannot be neglected and time extrapolation techniques must be used. Time extrapolation techniques require the system to have some type of channel state memory and some type of extrapolation algorithm. In this thesis the DCM technique is used to represent time extrapolation techniques, and the block diagram of the DCM rate adaptation system is given in Figure 8.2.

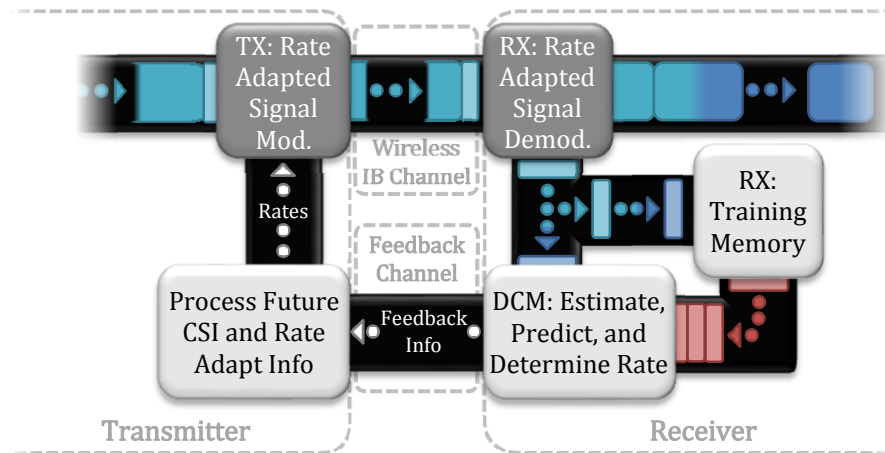


Figure 8.2: A block diagram illustrating the procedure in which a rate adaption scheme using the DCM technique update the CSI at the transmitter.

In Figure 8.2, the transmitter has begun to send the future rate adapted signal. The Receiver, using the present and past training symbols implements the DCM technique and sends the future feedback information to the transmitter. Therefore, the transmitter can successfully adapt to the channel in moderately dynamic DWEs.

Thus far the dynamic nature of the DWEs has been shown to be slightly or moderately dynamic. In slightly or moderately dynamic DWEs the DCM technique will work. However, if the DWE is very dynamic the DCM technique cannot accurately extrapolate the CSI beyond a particular time index, limiting the time into the future in which extrapolations can be made. This gives a time interval for which the DCM technique can be deemed accurate with respect to the RMSE-SE and compared to the lowest accuracy level. The lowest accuracy level is the accuracy of the NCM technique. At these accuracy level the DCM technique is not need to do rate adaptation the NCM technique can be used.

The DCM technique is inaccurate in very dynamic DWE because in very dynamic DWEs the wireless channel changes very fast in comparison to the time it takes to feedback and process CSI. This is indicative of a very fast fading channel. Note this does not mean that DCM techniques cannot be used in DWEs that are very dynamic. This means that for part of the rate adapted signal the accuracy will be at its lowest and for all or that part of the signal instead of using the DCM technique the NCM technique could be used for all or part of the extrapolation process.

One of the ways to address this feedback delay issue is to limit the information that needs to be sent back to the transmitter which also reduces the accuracy of the DCM technique. This thesis will not cover limited feedback channels [14]. Instead the use of the ICM technique will be considered as way to resolve this issue. Consequently, comparisons

will be made between the ICM technique and a DCM technique that does not limit feedback information.

Figure 8.3 shows a block diagram that uses the ICM technique to obtain the CSI. By using the ICM technique radios and networks can significantly reduce the time it takes to update the CSI. This is done by removing the need to send any feedback information from the receiver about the transmitted signal. Instead, the receiver sends training information in the adjacent wireless OOB channels while the present rate adapted signal is being sent. This allows for a virtually instantaneous update of the CSI limited only by the time it takes to transmit and process the training signal from the receiver. Since it still takes time to transmit and process the training signal, algorithms based on memory and extrapolation may still be useful. However, for this thesis, the time delay is assumed to be less than a coherence time, and the memory and extrapolation from the ICM scheme is omitted.

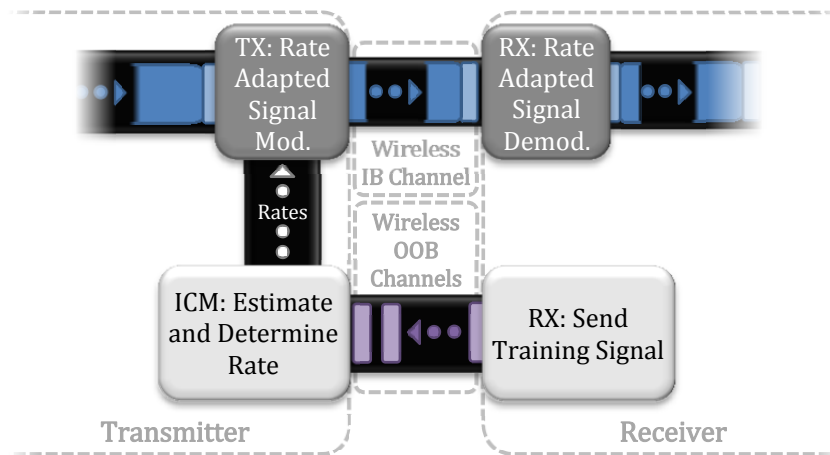


Figure 8.3: A block diagram illustrating the procedure in which a rate adaption scheme using the ICM technique update the CSI at the transmitter.

8.3 Information Update and Expiration Times

The issues with updating the CSI can be quantify using two metrics. The time it takes to update the information for the rate adaptation, referred to as the information update time (IUT). The IUT can be caused by different delay sources and can probably be quantify in many ways, but in this thesis it will be quantified as the number of coherence times it takes to update the transmitter.

The second metric is the information expiration time (IET). The IET is the period of time for which the CSI remains valid. If the time it takes to obtain the new information, the IUT, is greater than the lifetime of the information, the IET, the rate adaption technique will not be most effective in its goal. In this discussion, the IET will also be given in coherence times.

In the case of a rate adaptation technique that uses the ICM technique, the approximate IUT is given by

$$IUT_{ICM} = \frac{b_{TR}}{R_{TR}} + \tau_e, \quad 8.1$$

where b_{TR} is the number of bits in the training sequence, R_{TR} is the bit rate of the training sequence (bits/coherence time), and τ_e is the electronic processing time.

In contrast, the IUT for the DCM technique is

$$\begin{aligned} IUT_{DCM} &= \frac{b_{TR}}{R_{TR}} + \tau_e + \frac{b_{DCM}}{R_{DCM}} \\ &= IUT_{ICM} + \frac{b_{DCM}}{R_{DCM}}, \end{aligned} \quad 8.2$$

where b_{DCM} is the number of information and overhead bits needed to be sent to the transmitter to update the CSI, and R_{DCM} is the feedback bit rate (bits/coherence time). It is also assumed that the total electronic processing delays are comparable in the DCM and ICM

schemes, even though the computation may be split between the receiver and the transmitter in the DCM technique, while taking place entirely at the transmitter for the ICM technique. In the following discussion it will also be assumed that the systems have been designed so that the IUT_{ICM} is much less than one coherence time, such that

$$IUT_{ICM} \approx 0, \quad 8.3$$

$$IUT_{DCM} \approx \frac{b_{DCM}}{R_{DCM}}. \quad 8.4$$

The IET for the ICM case without memory or extrapolation is simply one coherence time, or $IET_{ICM} = 1$. In contrast, IET for the DCM case is define as the time interval over which the DCM performance is superior to a particular ICM comparison case. For example, referring to the case illustrated in Figure 7.9, a rate adaptation system that deploys the ICM technique and omits 14.6 coherence bandwidths is compared to a rate adaptation system that uses the DCM technique. In this case the DCM technique performs better for about 3 coherence times, and $IET_{DCM} \approx 3$. On the other hand if the system that uses the DCM technique is compared with a system that uses ICM technique with 30 coherence bandwidths omitted, then $IET_{DCM} \approx 4$.

The DCM technique is also affected by the number of coherence times of measured values stored in memory and used in the extrapolation process. In Figure 7.9 the rate adaptation system must store 32 coherence times of measured values in memory and use all these values in the extrapolation process. Maintaining this amount of information could be difficult. So at minimum, it is assume that the DCM technique can at least collect one coherence time of measured values and use it in the extrapolation process. So at minimum, changing the memory to one coherence time and keeping the other values used to create

Figure 7.9 the same, Figure 8.4 can be created. So, if a rate adaptation system that uses the DCM technique in Figure 8.4 is compared to a system that uses the ICM technique with 14.6 coherence times omitted, then $IET_{DCM} \approx 1.5$, and for an ICM technique that omits 30 coherence times $IET_{DCM} \approx 2.25$.

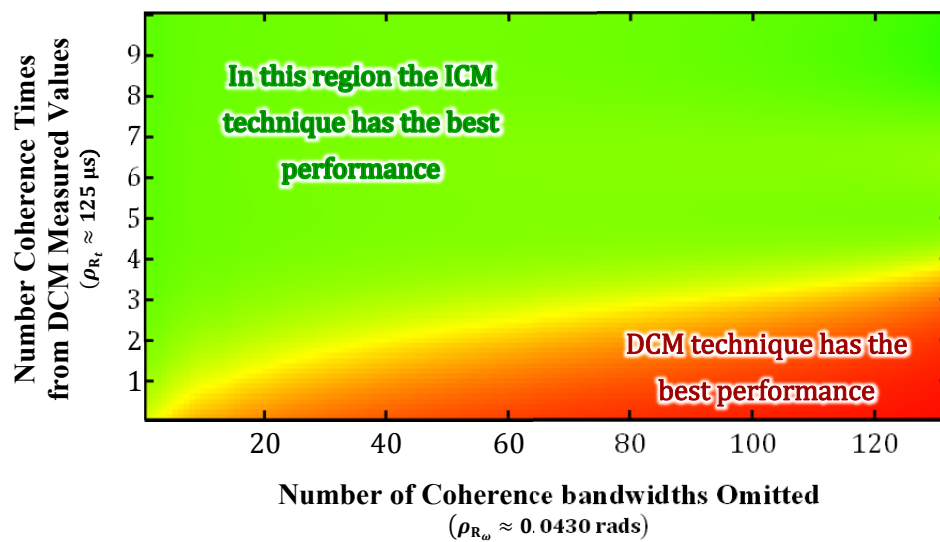


Figure 8.4: Optimal performance color map of the ICM and DCM techniques for ED delay channel model with a slope decline of 36 degrees; and a Jakes' spectral model for the frequency taps with a 1 kHz Doppler shift.

IET also imposes a minimum data rate requirement for the DCM feedback channel. The minimum data rate requirement is shown in the inequality in Equation 8.5,

$$\begin{aligned}
 IUT_{DCM} &\leq IET_{DCM} \\
 \frac{R_{DCM}}{\rho_{R_t}} &\geq \frac{b_{DCM}}{\rho_{R_t} IET_{DCM}} \\
 &\Downarrow \\
 \text{Minimum Feedback Bit Rate} &= \frac{b_{DCM}}{\rho_{R_t} IET_{DCM}}
 \end{aligned} \tag{8.5}$$

The previous case where the DCM technique had limited memory and the ICM technique omitted 14.6 coherence times will be used to do an example calculation of the minimum bit rate. The variable b_{DCM} is determined from Equation 8.6,

$$b_{DCM} = \lceil b_{sc}(2K_{omit}) \rceil. \quad 8.6$$

Equation 8.6 takes into account the number of subcarriers for which information is needed. The variable b_{sc} is the number of information and overhead bits needed per subcarrier. In this case it has already been shown that $K_{omit} = 32$, $LET_{DCM} = 1.5$, and $\rho_{R_t} = 0.125$ ms. Chapter Seven explains K_{omit} , and Chapter Seven and Four explain ρ_{R_t} . The variable b_{sc} is proportional to the amount adaptation present in the rate adaptive system. So the lower the number of bit the less adaptation there is in the system. In this case b_{sc} is set to equal 4 bits. Using Equation 8.6, $b_{DCM} = 384$. Therefore, the minimum R_{DCM} is 256 bits/coherence time or 2048 kb/s.

Note that in addition to information bits, b_{DCM} may also include overhead bits needed for synchronization, communication with multiple users, and other things needed for control. Accommodation of this feedback link within the IB channel will necessarily reduce the data rate of the forward channel, for example, by interrupting the channel in time or dedicating some portion of the spectrum to the feedback channel. Another option for the feedback channel is to use a non-existing infrastructure. To implement such a link could be expensive [14].

8.4 Practical Scenario

There are many available papers on rate adaption [7-9, 15, 64, 109-111]. In this thesis the focus will not be on the rate adaption algorithm itself, even though a rate adaption algorithm will be presented. Instead, the focus will be on how the ICM technique can improve rate adaptation given the algorithm.

To visualize these adaptive ideas in a cognitive radio context the following scenario is presented. These ideas and scenarios were created for this research. In this scenario there exists a cognitive radio network operating in a DWE. There are many things that can change the state of the wireless environment, but in this scenario and thesis the focus will be on fading and multipath.

Continuing with the scenario, the cognitive radio network has many end-to-end objectives, but for this scenario it will exclusively focus on the objectives of obtaining a particular data rate or link quality between radios within the network [1-5, 25, 26].

Similar to the end-to-end objective there are several techniques that a cognitive radio or radio network could use to meet its objectives [1-5, 25, 26]. However, in this scenario rate adaptation will be used. More specifically, an adaptive modulation technique for SISO-OFDM will be used.

In order to perform these adaptations at rates comparable to that of the dynamic nature of the wireless environment, the CSI must be known. The process of obtaining the CSI is as follows: first the network or radio collects measurements through sensing the wireless environment and over time learning the SCSi. Through its continuous sensing, the network or radios can use ICSI and SCSi to learn how to adapt the transmitted or received waveforms to best suit the end-to-end objective of the network or radio. The SCSi obtained from this continuous long-term sensing process is the covariance matrices, and SNR or SNIR.

In this scenario, the network is assumed to have a star topology. In the network there is a base station or access point and multiple user nodes. In the network the OOB channel is

used for downlink (DL) communication and the IB channel is used for uplink (UL) communication, making the radios full duplexed. For this scenario it is assumed that the feedback channel is not only used to send shared information in the DCM case but it is also used to send shared information for the rate adaptation or for any other cognitive needs unmentioned [1, 3]. Figure 8.5 shows the channel and network configuration explained. This configuration will be the same for the ICM, DCM, and NCM techniques. The depiction of the wireless link does not show the feedback link. It is assumed that the feedback link carries negligible information compared to the data.

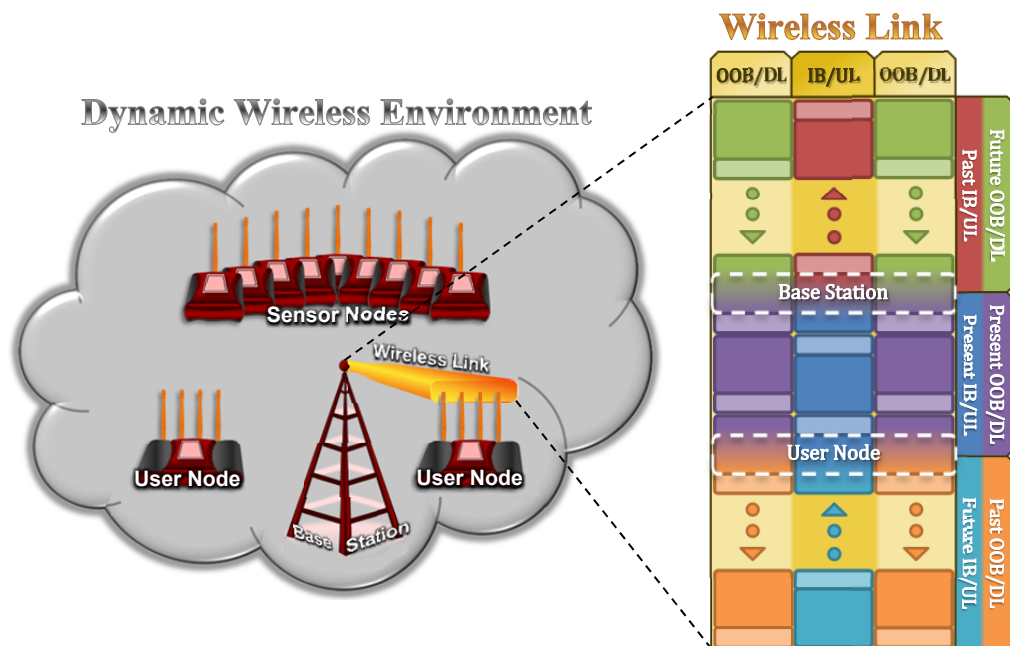


Figure 8.5: Graphical depiction of the DWE and wireless channel for one link.

In Figure 8.5 the sensor nodes are the part of the cognitive radio network that obtains the SCSi over the long-term sensing process explained earlier. The sensor nodes may have other sensing and/or learning responsibilities not mentioned in this thesis [1, 3, 23]. Note with the wireless link, the color scheme is similar to the color scheme in Figure 4.1, and as before the lighter blocks represent the training symbols and each block represents multiple

total coherence blocks. Also note, with the assumption of reciprocity, the wireless channel model for the future OOB downlink is the same as the future IB uplink.

Table 8.1 goes into more detail about usage of the respective parts of the wireless channel by the three techniques, and gives an overview of what performance to expect in a rate adaptation system that applies one of the three techniques in the given scenario. This table will also cover the pros and cons for each technique. These pros and cons will be highlighted in the simulations of these techniques as well. This table also

Technique	Wireless Channel Usage			Pros	Cons
	Past IB/UL	Present OOB/DL Future OOB/DL	Present IB/UL Future IB/UL		
ICM	Does not use this information	Uses the training symbols, the future training symbols are used when they become present training symbols	Extrapolates the optimal data rates at their respective present times	<ul style="list-style-type: none"> • Always has the respective present ICSI • Provides high accuracy in very dynamic cases • Memory of training syms. is not needed • Needs minimal additional control 	<ul style="list-style-type: none"> • May require the OOB channel bandwidth to be much larger than the IB channel bandwidth • May only work for IB channels with small bandwidths
DCM	Uses the training symbols	Does not use this information	Extrapolates the optimal data rate for present OR future data.	<ul style="list-style-type: none"> • No IB channel bandwidth limitations • Very accurate for present ICSI 	<ul style="list-style-type: none"> • Requires past memory • Not very accurate for future ICSI • May require a lot of control
NCM	Does not use this information	Does not use this information	Assumes constant data rate based on the current SNR	<ul style="list-style-type: none"> • Minimum control needed • No training is required for rate adapting • Less complex 	<ul style="list-style-type: none"> • ICSI used is inaccurate

Table 8.1: ICM, DCM, and NCM techniques channel usage and pros and cons for rate adaptation.

In the next section the details of the rate adaptation used for the scenario are discussed. There will also be some metrics given that can be used to compare these techniques for the given scenario.

8.5 Rate Adaptation Mathematical Theory

It has been stated, the cognitive radio network objective is to obtain a particular data rate or link quality. Therefore the goal for the rate adaptation is to obtain a target average bit error rate (BER) or a target average bit per subcarrier (BPS). The idea behind this is that a cognitive radio network may need to adjust its transmission to meet certain reliability or capacity requirements to obtain radio network effectiveness, such as: quality of service, efficiency, and many other unmentioned metrics. In place of the average BER the average bits in error (BIE) will be used because it is easier to use in a summation series and this will become obvious later.

Equations to calculate the average BIE and BPS will be provided to aid in this decision process for cognitive radios. Before getting to these equations, the rate adaptation algorithm must be given. As noted, this thesis will not make any claims on the novelty of this rate adaptation algorithm or make any comparisons to other algorithms. The algorithm presented here is an unpublished algorithm designed by the author. However, the contribution lies in the equations created to show the performance of the ICM, DCM, and NCM techniques, and the metrics used to make the decision on which technique is best.

It is assumed that cognitive radios can choose between 13 different QAM modulation schemes that would allow them to transmit between 0 and 12 bits on each sub-carrier independently. In other words, the decision of what modulation scheme to use is made per

sub-carrier. This is done by first taking the estimated or extrapolated envelope of the respective channel at that subcarrier. Note these equations will not be presented in matrix form for all subcarriers but could be easily adapted for ease of calculation.

Squared Envelopes and Rate Adaptation Thresholds

One of the most important things to know for rate adaptation is the squared envelope of the channel. The actual or extrapolated squared envelope is calculated from the actual or extrapolated channel respectively. The actual and extrapolated envelope for a particular subcarrier ω_k and time index t_l is,

$$\begin{aligned} E_{H_h}(t_l, \omega_k) &= |H_{H_h}(t_l, \omega_k)|^2 \\ &= |\hat{H}_{H_h}(t_l, \omega_k) + \hat{W}_{W_w}(t_l, \omega_k)|^2, \end{aligned} \quad 8.7$$

$$\hat{E}_{H_h}(t_l, \omega_k) = |\hat{H}_{H_h}(t_l, \omega_k)|^2. \quad 8.8$$

The optimal way to obtain the extrapolated squared envelope for the ICM and DCM technique is to change the loss function for the Bayesian statistical analysis to the square of the RMSE-SE given in Equation 7.29. By doing this, the optimal estimate to minimize the RMSE-SE becomes

$$\hat{E}_{H_h}(t_l, \omega_k) = |\hat{H}_{H_h}(t_l, \omega_k)|^2 + P_{LEE}(t_l, \omega_k). \quad 8.9$$

The variable $P_{LEE}(t_l, \omega_k)$ is the MSE for the respective time and angular-frequency indices, determined from the Schur complement for the respective linear estimator/extrapolator. However, this insight occurred after the simulations presented in this thesis, and have not been verified through simulation.

The squared envelope is used to obtain the square root of the SNR. The decision on the modulation scheme to select is made by using the calculated value of the actual and extrapolated SNR, but the square root is presented in Equations 8.10 and 8.11,

$$S_{l,k} = \frac{1}{\sqrt{K}\sigma_{\mathbf{w}}}\sqrt{E_{H_h}(t_l, \omega_k)}. \quad 8.10$$

$$\hat{S}_{l,k} = \frac{1}{\sigma_{\mathbf{w}_K}}\sqrt{\hat{E}_{H_h}(t_l, \omega_k)}. \quad 8.11$$

The reason for using the square root is to make the RVs $S_{l,k}$ and $\hat{S}_{l,k}$ Rayleigh or Rician distributions. If the SNR value is between a particular set of SNR thresholds a certain modulation scheme will be used. There are multiple threshold values to give the radio options in order to pick the desired BIE and BPS.

These threshold values are obtained by setting a targeted BER limit. Note, this is not the BER for the subcarrier but just a limit used to select the SNR thresholds. In this thesis there will be 67 BER limits between $[10^{-7}, 10^{-0.4}]$. The thresholds for each of these BER limits are given in Appendix B in the form of a look-up table. For each of these limits 12 SNR threshold values are determined by selecting the SNR value where the BER for the respective QAM schemes will be under the selected BER limit. For zero bits the BER is undefined.

$\begin{matrix} j \\ i \end{matrix}$		Modulation Schemes											
		00	01	02	03	04	05	06	07	08	09	10	11
BER Limits	00	11.31	14.32	19.03	21.22	25.32	27.37	31.35	33.37	37.33	39.34	43.30	45.31
	01	11.24	14.25	18.96	21.15	25.25	27.30	31.28	33.30	37.25	39.27	43.22	45.23
	02	11.16	14.17	18.89	21.07	25.17	27.22	31.20	33.22	37.17	39.19	43.14	45.15
	03	11.09	14.10	18.81	21.00	25.10	27.14	31.12	33.14	37.09	39.11	43.06	45.07

Table 8.2: Partial SNR threshold look-up table.

Table 8.2 shows a part of the SNR look-up table that is in the appendix. In this table, the SNR thresholds are rounded to the second decimal place. In practice, this value will have greater arithmetic precision. The index i represents the i^{th} BER limit, and the index j represents the j^{th} SNR bound. Therefore, the i - j^{th} SNR threshold, $Q_{i,j}$, is with respect to the corresponding BER limit and SNR bound.

Rate Adaptation Metrics

There are three types of rate adaptation metrics created for this research. The first two that have been mentioned earlier are the BPS and BIE, and the third, which will be presented in this subsection, is the probability of obtaining a target BPS and BER on any given subcarrier at a particular time. Note that the purpose of these metrics is to help engineers and researchers determine what technique will be best suited for a given situation before designing the system.

Using the indexed SNR threshold values and the actual and extrapolated SNR of the channel, the equations for the BPS and average BIE can be defined with respect to the index of the BER limit,

$$BPS_i(\hat{S}_{l,k}) = 12 - \sum_{j=1}^{12} \mathbf{1}_{Q_{i,j}}(\hat{S}_{l,k}^2), \quad 8.12$$

$$BIE_i(S_{l,k}, \hat{S}_{l,k}) = BPS_i(\hat{S}_{l,k}) BER_{(M)}(S_{l,k}^2) \Big|_{M=2^{BPS_i(\hat{S}_{l,k}^2)}}. \quad 8.13$$

Where,

$$\mathbf{1}_{Q_{i,j}}(x) = \begin{cases} 1 & , x \leq Q_{i,j} \\ 0 & , \text{otherwise} \end{cases}, \quad 8.14$$

and the function $BER_{(M)}(S^2)$ gives the average BER for a M-QAM scheme at an SNR value equal to S^2 .

The following statements can be derived from Equations 8.12 and 8.13. The extrapolated SNR will determine the modulation scheme to use. However, the actual SNR, given the modulation scheme, will determine the BIE.

To determine the expected average BIE and BPS the expectation of the joint pdf, $f\left(BPS_i(\hat{S}_{l,k}), \frac{BIE_i(S_{l,k}, \hat{S}_{l,k})}{BPS_i(\hat{S}_{l,k})}\right)$, must be calculated. A closed form representation of this expectation value may be complicated to obtain because of the mathematical definitions of BPS and BIE. However, given the SCS of the wireless channel and assuming Rayleigh or Rician fading, a discrete closed form equation can be obtained by using a variation of the equations presented for bivariate and multivariate Rayleigh and Rician distribution presented in various research papers [112-115]. This also opens the door for many other theoretical calculations such as the overall data rates and BERs for the respective techniques, and many other things.

The joint pdf is already discrete in terms of the BPS. To simplify the calculation the joint pdf will be made discrete in terms of the BER as well. There will be 67 BER ranges with BER labels between $[10^{-7}, 10^{-0.4}]$, and the values are linear in the log scale, and there is an extra label, $10^{-\text{Inf}}$, bringing the label count to 68. The label signifies the lower bound of the BER range and the next greater label signifies the upper bound. For example, label 10^{-7} signifies a BER range of $[10^{-7}, 10^{-7.1})$. Note, the upper bound for 10^{-4} is 10^0 , but 10^0 is not a label.

These BER ranges and BPS values correspond to SNR boundaries. The look-up table mentioned earlier will be used to obtain SNR boundaries with respect to these BER ranges and BPS values. These boundaries will be needed to calculate the following probability in

Equation 8.15. Equation 8.15 is the discrete form of the joint pdf mentioned. The next sub section derives this pdf.

$$\Pr\left\{BPS_i(\hat{S}_{l,k}) = T_{BPS}, \frac{BIE_i(S_{l,k}, \hat{S}_{l,k})}{BPS_i(\hat{S}_{l,k})} \in T_{BER,BPS}\right\} = \Pr\{\hat{S}_{l,k} \in \mathbb{S}_{T_{BPS}}, S_{l,k} \in \mathbb{S}_{T_{BER,BPS}}\}. \quad 8.15$$

In Equation 8.15, T_{BPS} and $T_{BER,BPS}$ are the target BPS and BER, and $\mathbb{S}_{T_{BPS}}$ and $\mathbb{S}_{T_{BER,BPS}}$ are subsets that contain a range of SNR values that correspond to the respective target BPS and BER values.

This calculation is only for the i^{th} level mentioned earlier. So, before doing the rate adaptation the cognitive radio would have to determine the SNR threshold values for the rate adaptation. This is accomplished through the following procedural steps done during the sensing stage once the SCSi is known. First the radio or network determines a target BER and/or BPS. This is done in two ways. In the case where either the BPS or BER is targeted, Equation 8.15 can be used to determine the expected value of the non-targeted metric. In the other case this is not needed because both BPS and BER are targeted and known.

After the targeted value is selected two other values can be determined, the expected value and the mode (i.e. the value with the highest probability) of the non-targeted metric. The i^{th} level that will give the highest probability and/or best BPS and BER values is selected. Note that Equation 8.15 is for one subcarrier at a particular time value. However, given the linear property of expectation, the multiple expected values can be calculated and then summed together to get the expected value of the overall sum. Note the BER must be converted to the BIE for the sum, because the summation of the BER could be normalized to different BPS values.

This can be done for each of the measurement techniques. Then the measurement technique that gives the highest probability and/or best expected value of the non-targeted or targeted metric should be selected.

For example, suppose the radio is shooting for a target BER of 10^{-3} , and all the SCS and other important information has been determined to obtain the joint pdf. The radio or network will use Equation 8.15 to determine what measurement technique provides the highest expected BPS for the spectrum of interest for a given length of time. If in this case it is ICM, the radios will implement the ICM technique to do the measurements.

Instead of using the expected value of the non-targeted metric, a probabilistic value for the metric at a particular subcarrier for a given time value could be obtained and used. Unlike the expectation operation, the probability operation is nonlinear and independence between probability values cannot be exerted due to the nature of the channel. Therefore it cannot be summed together like the expectation. Therefore, it may be harder to use in the selection process of choosing the best measurement technique. It still can give some insight, but this will not be discussed here. So the case where there is only one targeted value is used for simplicity.

In order to get these probability values or expected values, a closed form representation of Equation 8.15 needs to be given. The next sub-section provides this equation.

Joint Probability Density Function of Targeted Metrics

In this sub section the joint probability of the two targeted metrics, BPS and BER, is given. This equation is very powerful. It can allow researchers to quantify and categorize

the performance of the ICM, DCM, and NCM techniques for rate adaption. This equation is not featured in any of the simulations that will be presented. However, to show its validity this sub-section will go through a proof to verify the pdf's accuracy.

The proof starts with the joint pdf in Equation 8.16. Equation 8.16 is the joint pdf of the extrapolated channel, $\hat{H}_{H_h}(t_l, \omega_k)$, and extrapolation error, $\hat{W}_{W_w}(t_l, \omega_k)$, which will be represented by \hat{H} and \hat{W} respectively. The variables \hat{H} and \hat{W} are complex. Therefore, the real and imaginary variables are $\hat{H}_r, \hat{H}_i, \hat{W}_r$, and \hat{W}_i . Such that,

$$\begin{aligned} f(\hat{h}_r, \hat{h}_i, \hat{w}_r, \hat{w}_i) &= f(\hat{h}_r)f(\hat{h}_i)f(\hat{w}_r)f(\hat{w}_i) \\ &= \frac{1}{4\pi^2\sigma_{\hat{H}}^2\sigma_{\hat{W}}^2} \exp\left\{-\frac{\hat{h}_r^2+\hat{h}_i^2}{2\sigma_{\hat{H}}^2}\right\} \exp\left\{-\frac{\hat{w}_r^2+\hat{w}_i^2}{2\sigma_{\hat{W}}^2}\right\}, \end{aligned} \quad 8.16$$

$$\hat{H} = \hat{H}_r + i\hat{H}_i, \quad 8.17$$

$$\hat{W} = \hat{W}_r + i\hat{W}_i. \quad 8.18$$

To avoid using complex values in the pdf and to make the transformation of variables easier, the real and imaginary variables are used to define the joint pdf of the extrapolated channel and extrapolation error. In this thesis, these four variables are independent and normally distributed zero-mean RVs. Note, the lowercase variables in Equation 8.16 does not signify a change in domain. The notation is simply used to represent arguments to the density functions.

The next step in the proof is to perform a variable transformation. Equations 8.19 — 8.26 are used in this transformation. This transformation will create the joint pdf in Equation 8.27.

$$S_r = \frac{1}{\sigma_{W_K}} \sqrt{[(\hat{H}_r + \hat{W}_r)^2 + (\hat{H}_i + \hat{W}_i)^2]}, \quad 8.19$$

$$\hat{S}_r = \frac{1}{\sigma_{W_K}} \sqrt{(\hat{H}_r^2 + \hat{H}_i^2)}, \quad 8.20$$

$$S_\theta = \tan^{-1} \left(\frac{\hat{H}_i + \hat{W}_i}{\hat{H}_r + \hat{W}_r} \right), \quad 8.21$$

$$\hat{S}_\theta = \tan^{-1} \left(\frac{\hat{H}_i}{\hat{H}_r} \right). \quad 8.22$$

$$\hat{H}_r = \sigma_{\mathbf{W}_K} \hat{S}_r \cos(\hat{S}_\theta), \quad 8.23$$

$$\hat{H}_i = \sigma_{\mathbf{W}_K} \hat{S}_r \sin(\hat{S}_\theta). \quad 8.24$$

$$\hat{W}_r = \sigma_{\mathbf{W}_K} [S_r \cos(S_\theta) - \hat{S}_r \cos(\hat{S}_\theta)], \quad 8.25$$

$$\hat{W}_i = \sigma_{\mathbf{W}_K} [S_r \sin(S_\theta) - \hat{S}_r \sin(\hat{S}_\theta)]. \quad 8.26$$

The variables S_r and \hat{S}_r are simplified notations for the square roots of the SNRs in Equations 8.10 and 8.11. The variables S_θ and \hat{S}_θ are the phases of the actual and extrapolated channels. Furthermore, using the Jacobian, $J(s_r, \hat{s}_r, s_\theta, \hat{s}_\theta)$, the following variable transformation can be defined to obtain the joint pdf of the S variables,

$$f(s_r, \hat{s}_r, s_\theta, \hat{s}_\theta) = \underbrace{|J(s_r, \hat{s}_r, s_\theta, \hat{s}_\theta)|}_{\sigma_{\mathbf{W}_K}^2 s_r \hat{s}_r} \left[f(\sigma_{\mathbf{W}_K} \hat{s}_r \cos(\hat{s}_\theta)) f(\sigma_{\mathbf{W}_K} s_r \sin(\hat{s}_\theta)) \cdots \right. \quad 8.27$$

$$\left. \cdots f(\sigma_{\mathbf{W}_K} [s_r \cos(s_\theta) - \hat{s}_r \cos(\hat{s}_\theta)]) f(\sigma_{\mathbf{W}_K} [s_r \sin(s_\theta) - \hat{s}_r \sin(\hat{s}_\theta)]) \right]$$

$$f(s_r, \hat{s}_r, s_\theta, \hat{s}_\theta) = \frac{\sigma_{\mathbf{W}_K}^2 s_r \hat{s}_r}{4\pi^2 \sigma_H^2 \sigma_W^2} \exp \left\{ \underbrace{\frac{-\sigma_{\mathbf{W}_K}^2 (\sigma_H^2 + \sigma_W^2)}{2\sigma_H^2 \sigma_W^2}}_{\alpha_s^2} \hat{s}_r^2 \right\} \exp \left\{ \underbrace{\frac{-\sigma_{\mathbf{W}_K}^2}{2\sigma_W^2}}_{\alpha_s^2} s_r^2 \right\} \exp \left\{ \frac{\sigma_{\mathbf{W}_K}^2 s_r \hat{s}_r \cos(\hat{s}_\theta - s_\theta)}{\sigma_W^2} \right\}. \quad 8.28$$

The next joint pdf that will be presented is the joint pdf of the square root of the actual and extrapolated SNR. This is accomplished by integrating out the phase term,

$$f(s_r, \hat{s}_r, s_\theta, \hat{s}_\theta) = \frac{\sigma_{\mathbf{W}_K}^2 s_r \hat{s}_r}{4\pi^2 \sigma_H^2 \sigma_W^2} \exp\{\alpha_s^2 \hat{s}_r^2\} \exp\{\alpha_s^2 s_r^2\} \iint_{-\pi}^{\pi} \exp \left\{ \frac{\sigma_{\mathbf{W}_K}^2 s_r \hat{s}_r \cos(\hat{s}_\theta - s_\theta)}{\sigma_W^2} \right\} d\hat{s}_\theta ds_\theta. \quad 8.29$$

The following steps were used to solve the integral in Equation 8.29,

$$\begin{aligned}
\iint_{-\pi}^{\pi} \exp\left\{\frac{\sigma_{\mathbf{W}_K}^2 s_r \hat{s}_r \cos(\hat{s}_\theta - s_\theta)}{\sigma_{\mathbf{W}}^2}\right\} d\hat{s}_\theta ds_\theta &= 2\pi \int_{-\pi}^{\pi} \exp\left\{\frac{\sigma_{\mathbf{W}_K}^2 s_r \hat{s}_r \cos(s_\theta)}{\sigma_{\mathbf{W}}^2}\right\} ds_\theta \\
&= 4\pi \int_{-\frac{\pi}{2}}^{\frac{\pi}{2}} \cosh\left\{\frac{\sigma_{\mathbf{W}_K}^2 s_r \hat{s}_r \cos(s_\theta)}{\sigma_{\mathbf{W}}^2}\right\} ds_\theta \\
&= 4\pi \sum_{n=0}^{\infty} \frac{1}{(2n)!} \left(\frac{\sigma_{\mathbf{W}_K}^2 s_r \hat{s}_r}{\sigma_{\mathbf{W}}^2}\right)^{2n} \underbrace{\int_{-\frac{\pi}{2}}^{\frac{\pi}{2}} \cos^{2n}(s_\theta) ds_\theta}_{\left[\frac{\pi(2n)!}{2^{2n}(n!)^2}\right]} \\
&= 4\pi^2 \sum_{n=0}^{\infty} \left[\frac{\sigma_{\mathbf{W}_K}^2 s_r^n \hat{s}_r^n}{2^n \sigma_{\mathbf{W}}^{2n} (n!)}\right]^2
\end{aligned} \tag{8.30}$$

Using this solution the following series was created for the joint distribution of the SNR variables,

$$f(s_r, \hat{s}_r) = \sum_{n=0}^{\infty} \underbrace{\left[\frac{\sigma_{\mathbf{W}_K}^4}{2^{2n} \sigma_{\hat{\mathbf{B}}}^2 \sigma_{\mathbf{W}}^{4n+2} (n!)^2}\right]}_{\beta_n} \hat{s}_r^{2n+1} \exp\{\alpha_s^2 \hat{s}_r^2\} s_r^{2n+1} \exp\{\alpha_s^2 s_r^2\}. \tag{8.31}$$

The final step is to find the probability in Equation 8.15. Before doing this the subsets $\mathbb{S}_{T_{BPS}}$ and $\mathbb{S}_{T_{BER,BPS}}$ must be defined. The subset $\mathbb{S}_{T_{BPS}}$ is the range of \hat{s}_r values, $[\hat{s}_{r,0}, \hat{s}_{r,1})$, for which $BPS_i(\hat{S}_{l,k}) = T_{BPS}$, and the subset $\mathbb{S}_{T_{BER,BPS}}$ is the range of s_r values, $[s_{r,0}, s_{r,1})$, for which $\frac{BIE_i(S_{l,k}, \hat{S}_{l,k})}{BPS_i(\hat{S}_{l,k})} \in T_{BER,BPS}$ and $T_{BER,BPS}$ is a range of BER values. Therefore, the following equation can be defined,

$$\begin{aligned}
\Pr\{\hat{S}_{l,k} \in \mathbb{S}_{T_{BPS}}, S_{l,k} \in \mathbb{S}_{T_{BER,BPS}}\} &= \int_{s_{r,0}}^{s_{r,1}} \int_{\hat{s}_{r,0}}^{\hat{s}_{r,1}} f(s_r, \hat{s}_r) d\hat{s}_r ds_r \\
&= \sum_{n=0}^{\infty} \beta_n \int_{\hat{s}_{r,0}}^{\hat{s}_{r,1}} \hat{s}_r^{2n+1} \exp\{\alpha_s^2 \hat{s}_r^2\} d\hat{s}_r \cdots \\
&\quad \cdots \int_{s_{r,0}}^{s_{r,1}} s_r^{2n+1} \exp\{\alpha_s^2 s_r^2\} ds_r \quad . \tag{8.32} \\
&= \sum_{n=0}^{\infty} \left[\frac{\beta_n}{4(\alpha_s^2 \hat{s}_s^2)^{n+1}}\right] \Gamma(n+1, \alpha_s^2 \hat{s}_r^2) \Big|_{\hat{s}_{r,0}}^{\hat{s}_{r,1}} \cdots \\
&\quad \cdots \Gamma(n+1, \alpha_s^2 s_r^2) \Big|_{s_{r,0}}^{s_{r,1}}
\end{aligned}$$

Here, the function $\Gamma(\cdot, \cdot)$ is the upper incomplete gamma function.

From this equation a discrete probability of the joint pdf of the targeted metric can be created using the various subsets obtained from the look-up table in Appendix B. There are 13 subset, $\mathbb{S}_{T_{BPS}}$, that can be created by varying T_{BPS} , and there are 817 subsets, $\mathbb{S}_{T_{BER,BPS}}$,

that can be created by varying T_{BER} and T_{BPS} . Using these subsets, this theoretical calculation was done for the ICM and DCM technique with the variables listed in Table 8.3.

Assuming a BER limit of $10^{-2.5}$, the probability plots in Figures 8.6 and 8.7 can be created using Equation 8.32 and the values in Table 8.3. Figure 8.6 is the probability for the ICM technique. This Figure shows that for this BER limit it is most probable to have a BER in the range of $[10^{-2.8}, 10^{-2.7})$ and a BPS of 8 bits per subcarrier. There is approximately a 2 % chance of this most probable occurrence. The expected BIE and BPS, which are not as visible, are approximately 0.0077 bits in error and 6.59 bits per subcarrier respectively.

Wireless Channel	
Multipath Model: EDT with 18 degree Slope	
Fading Model: Jakes'	
$\tau_s = 10$ ns	
$f_s = 62.5$ Hz	
Theoretical Average SNR: 30 dB	
ICM Technique	DCM Technique
$K = 640$	$L = 1024$
$M = 64$	$N = 48$
$K_1 = 0$	$L_1 = 64$
$K_{obsrv} = 64$	$L_{obsrv} = 64$
$K_{omit} = 32$	$L_{omit} = 128$
$K_2 = 224$	$L_2 = 416$
$\tau_s = 10$ ns	$f_s = 62.5$ Hz
$\omega_{ind_0} = 0$	$t_{ind_0} = 1$
- Angular-frequency normalized to the coherence bandwidth - Use to determine the angular-frequency index	- Number of coherence times from the measured DCM values - Use to determine the time index

Table 8.3: Initial variables and settings used in theoretical probability calculation.

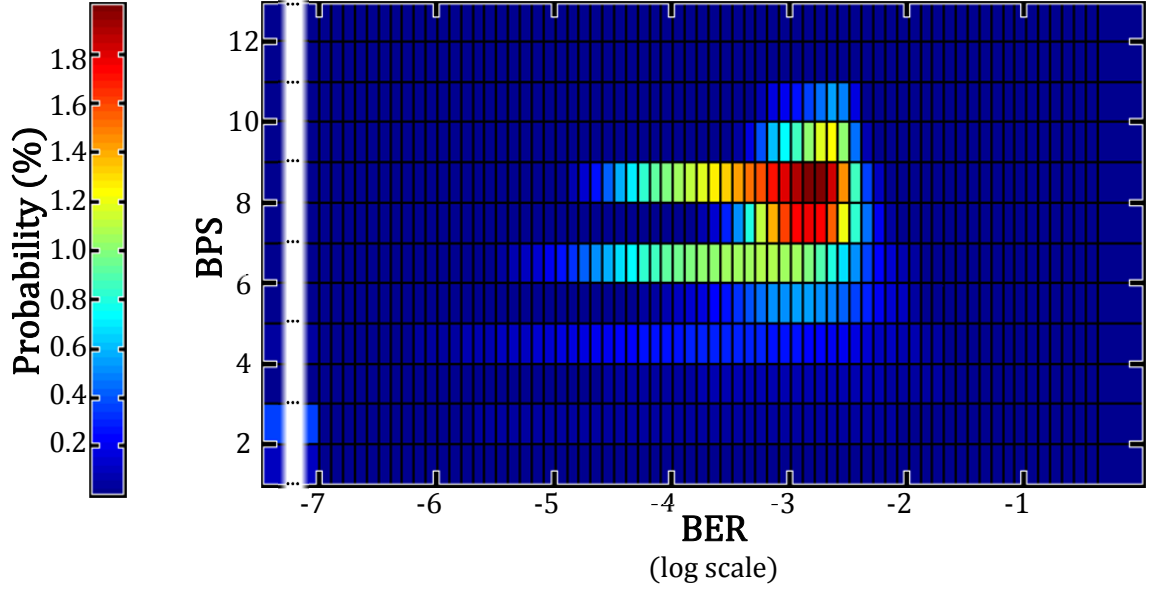


Figure 8.6: Joint probability of the BER and BPS for the BER Limit of $10^{-2.5}$ and the given initial values for ICM.

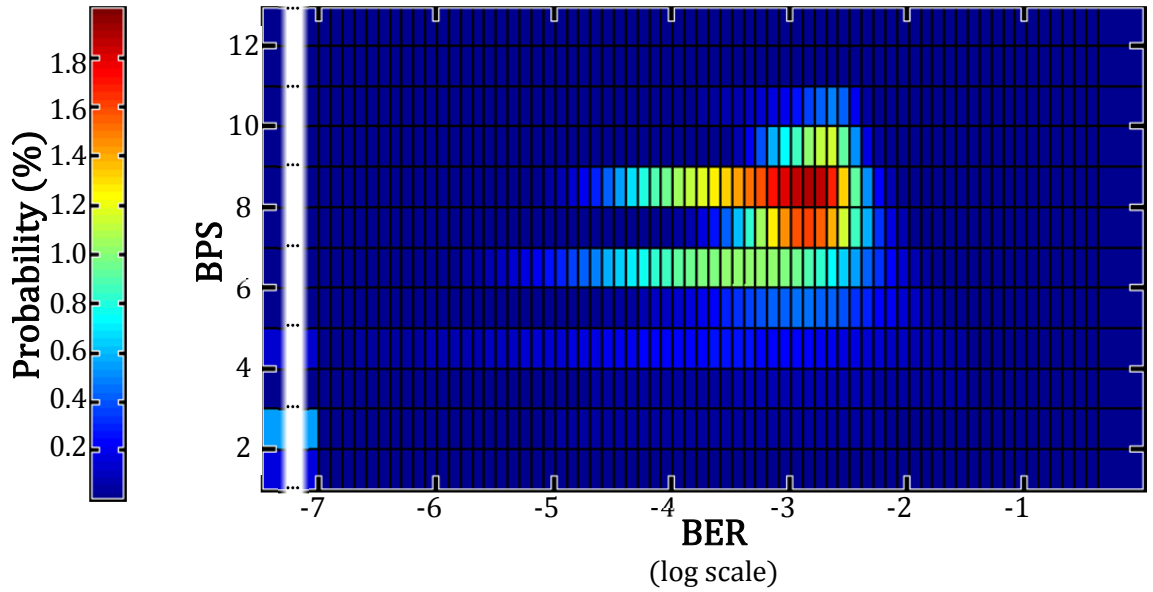


Figure 8.7: Joint probability of the BER and BPS for the BER Limit of $10^{-2.5}$ and the given initial values for DCM.

Figure 8.7 shows a similar plot for the DCM technique. For the DCM technique there is a 1.9 % chance of the most probable target values, a BER range of $[10^{-2.9}, 10^{-2.8})$ and 8 bits per subcarrier. The expected values for the pdf shown in the DCM figure are approximately

0.0088 for the expected targeted BIE and 6.64 bits per subcarrier for the expected targeted BPS.

These expected values are calculated using Equations 8.33 and 8.34. Since the BER is not truly discrete, the expected BIE is not the actual expected value but an approximation.

$$E\{BPS_i(\hat{S}_{l,k})\} = \sum_{T_{BER}} \sum_{T_{BPS}} BPS_i(\hat{S}_{l,k}) \Pr\{\hat{S}_{l,k} \in \mathbb{S}_{T_{BPS}}, S_{l,k} \in \mathbb{S}_{T_{BER,BPS}}\}, \quad 8.33$$

$$E\{BIE_i(S_{l,k}, \hat{S}_{l,k})\} = \sum_{T_{BER}} \sum_{T_{BPS}} BIE_i(S_{l,k}, \hat{S}_{l,k}) \Pr\{\hat{S}_{l,k} \in \mathbb{S}_{T_{BPS}}, S_{l,k} \in \mathbb{S}_{T_{BER,BPS}}\}. \quad 8.34$$

The most probable values and the expected values are a couple of the things that can be determined from the equations provided. There could be other metrics or values derived from these equations which could be obtained through further research. Having this pdf is a very powerful tool for evaluating the expected behavior of such a system.

ICM						
MP Model	SNR	Probability of the most probable values	Most Probable BPS	Most Probable BER range	Expected BPS	Expected BIE
EDT 18°	10 dB	49.15 %	00	Undefined	00.7728	0.0012
EDT 18°	20 dB	06.34 %	00	Undefined	03.3223	0.0044
EDT 18°	30 dB	02.00 %	08	$[10^{-2.8}, 10^{-2.7})$	06.5925	0.0077
EDT 18°	40 dB	02.27 %	11	$[10^{-2.8}, 10^{-2.7})$	09.9698	0.0101
EDT 18°	50 dB	55.49 %	12	$[0, 10^{-7})$	11.7232	0.0029
EDT 36°	10 dB	54.85 %	00	Undefined	00.6529	0.0034
EDT 36°	20 dB	06.98 %	00	Undefined	03.1953	0.0155
EDT 36°	30 dB	02.57 %	04	$[10^{-Inf}, 10^{-7})$	06.4859	0.0258
EDT 36°	40 dB	01.81 %	08	$[10^{-Inf}, 10^{-7})$	09.8836	0.0326
EDT 36°	50 dB	55.43 %	12	$[10^{-Inf}, 10^{-7})$	11.7063	0.0190
EDT 90°	10 dB	99.18 %	00	Undefined	00.0061	0.0001
EDT 90°	20 dB	24.78 %	00	Undefined	01.5752	0.0154
EDT 90°	30 dB	14.07 %	04	$[10^{-Inf}, 10^{-7})$	05.1152	0.0418
EDT 90°	40 dB	11.88 %	08	$[10^{-Inf}, 10^{-7})$	08.8571	0.0596
EDT 90°	50 dB	48.06 %	12	$[10^{-Inf}, 10^{-7})$	11.4592	0.0328

Table 8.4: List of theoretical calculation of rate adaptation metrics using the ICM technique.

Using the four metrics just presented some of the channel and extrapolator parameters were varied to show the different performances. Note that in the Figures 8.6 and 8.7 the probabilities for the 0 BPS are not shown, but they do exist. At 0 BPS the BER is undefined. Therefore, the probability is not shown. In the table you will see that in some cases it is most probable that the system does not transmit any bits at all. Also, any of the variables associated with Table 8.3 that is not listed in Tables 8.4 and 8.5 remain the same as in Table 8.3. The intent of Tables 8.4 and 8.5 is to show values of four metrics with respect to various. The values in Tables 8.4 are independent of the values in Table 8.5 and vice versa.

DCM						
t_{ind_0}	SNR	Probability of the most probable values	Most Probable BPS	Most Probable BER range	Expected BPS	Expected BIE
1	10 dB	51.73 %	00	Undefined	00.7323	0.0022
1	20 dB	06.45 %	00	Undefined	03.3313	0.0066
1	30 dB	01.90 %	08	$[10^{-2.9}, 10^{-2.8})$	06.6368	0.0088
1	40 dB	02.26 %	11	$[10^{-2.8}, 10^{-2.7})$	09.9988	0.0102
1	50dB	54.99 %	12	$[10^{-Inf}, 10^{-7})$	11.6637	0.0027
3	10 dB	74.55 %	00	Undefined	00.3197	0.0045
3	20 dB	10.70 %	02	$[10^{-Inf}, 10^{-7})$	02.9146	0.0276
3	30 dB	04.04 %	04	$[10^{-Inf}, 10^{-7})$	06.4057	0.0375
3	40 dB	01.80 %	08	$[10^{-Inf}, 10^{-7})$	09.8823	0.0325
3	50 dB	54.99 %	12	$[10^{-Inf}, 10^{-7})$	11.6565	0.0131
8	10 dB	98.09 %	00	Undefined	00.0154	0.0003
8	20 dB	23.96 %	00	Undefined	01.6143	0.0160
8	30 dB	17.20 %	04	$[10^{-Inf}, 10^{-7})$	04.7575	0.0348
8	40dB	17.41 %	08	$[10^{-Inf}, 10^{-7})$	08.2201	0.0459
8	50 dB	40.41 %	12	$[10^{-Inf}, 10^{-7})$	11.2086	0.0312

Table 8.5: List of theoretical calculation of rate adaptation metrics using the DCM technique.

8.6 Summary

In summary, this chapter has provided an understanding of how rate adaptation can be used in conjunction with the ICM, DCM, and NCM techniques. This chapter provides a blue print for developing a rate adaptation system for cognitive radio networks. It provides some fundamental metrics to determine performance, as well as a mathematical framework for a rate adaption system and performance metrics.

As shown with Table 8.1, each of the three techniques has some perceived pros and cons. This makes the need for a metric to determine which technique is better for a given case greater. That is why this chapter provides a few metrics t further research. They are listed in the table below. Table 8.6 goes over all the metrics created in this research and presented in this thesis and gives the related equations and explanation of the metric and its use.

Out of the metrics listed in the table, the Joint PDF presented in this chapter could possibly have the most value to researchers and engineers interested in rate adaptation. It gives an accurate theoretical calculation of the probability of obtaining a particular BPS and BER or BIE. Further research of this theoretical equation is needed. However, this thesis does not go beyond the theory associated with this pdf. A non-series representation could possibly be obtained to improve the calculation precision.

Metric	Equations	Description
IUT_{DCM}	Equation 8.2	The time it takes the DCM technique to update the ICSI. Inversely proportional to the feedback channel data rate. Due to low data rates and potentially large amounts of information the IUT can be large.
IET_{DCM}	Equations 7.25 and 7.38	Time for which the ICSI, obtained from DCM, is considered valid. Depends on the performance of the ICM technique. Gives an indication of what IUT is needed.
IUT_{ICM}	—	The time it takes the ICM technique to update the ICSI. Given the scenario in this chapter, it is always less than or equal to one coherence time.
IET_{ICM}	—	Time for which ICSI, obtained from ICM, is considered valid. Given the scenario in this chapter, it is always one coherence time.
BPS	Equation 8.12	Number of bits per subcarrier.
BIE	Equation 8.13	Number of bits in error per subcarrier. This metric is used because it is easily summed.
BER	Equations 8.12 and 8.13	The bit error per subcarrier. Is equal to BIE/BPS. Not as easily summed as the BIE.
Target BPS	—	The desired BPS for RNE. A metric defined by the researcher or engineer.
Target BER	—	The desired BIE for RNE. A metric defined by the researcher or engineer.
Joint Probability of the BPS and BER	Equations 8.15 and 8.32	A pdf created for this research that approximates the actual joint pdf of the BPS and BER by using a discrete joint pdf. A very powerful tool for rate adaptation.
Most Probable BPS	Equations 8.15 and 8.32	The BPS with the highest chances of occurring on a given subcarrier at a particular time index.
Most Probable BER	Equations 8.15 and 8.32	The BER with the highest chance of occurring on a given subcarrier at a particular time index.
Expected BPS	Equations 8.33	The expected or average BPS for a given subcarrier and time index.
Expected BER	Equations 8.34	The expected or average BIE for a given subcarrier and time index.

Table 8.6: Rate adaptation metrics to compare the ICM and DCM techniques.

CHAPTER NINE

CHANNEL MEASUREMENT SIMULATIONS

9.1 Introduction

For this research several simulations were created and performed but in this thesis only two of the simulations will be discussed. All of the simulations were done using the MATLAB software created by Mathworks. This software was used because it is optimized to handle matrix based operations. All the equations that have been presented in this thesis have been designed in a way that would make implementation easy in matrix optimized software like MATLAB.

The first simulation that will be covered in this chapter is the Estimator and Extrapolator Simulator. This simulation is based on the estimators and extrapolators in Chapter Seven, excluding the NCM and FCM techniques. This simulation allows the user to select a channel model for multipath and fading, as well as select what estimator-extrapolators to use for the simulation. This simulation shows the plot of the

channel models selected. More importantly it shows a plot of the actual estimates. The purpose of this simulation is to allow the user to visually see how the estimations and extrapolations look.

The second simulation that is in this thesis is designed to test the accuracy of the performance of the RMSE-SE metric created in Chapter Seven for the ICM, DCM, and NCM techniques. This simulation performs multiple estimations and extrapolations and calculates the sampled average of the squared error of the squared envelope. Then the square root is taken of this average, (i.e. the sampled RMSE-SE). The sampled RMSE-SE for each of the techniques should be approximately equal to the respective theoretical RMSE-SE for the respective techniques.

The second simulation also has another part. Both the sampled and the theoretical RMSE-SE for the ICM, DCM, and NCM techniques are compared to determine which technique will have the best performance. This comparison is similar to that in Figure 7.9. However, in this plot the comparison is with respect to the number of coherence times from the DCM measured values (x-axis) and the angular-frequency normalized to the coherence bandwidth (y-axis). The next two sections will explain these two simulators and go over the results generated by these simulations.

9.2 Estimator and Extrapolator Simulator

The estimator and extrapolator simulator (EESIM) is a MATLAB GUI interface that gives researchers and engineers (users) the ability to see how the estimator-extrapolators, presented in Chapter Seven, perform in a simulated environment. The GUI is shown in Figure 9.1. There are several variables corresponding to the variables in Chapter Seven that

can be changed to obtain a different channel or estimator-extrapolator. Table 9.1 lists all the variables and gives some descriptive information about each of them.

Variables and Controls	Description
Multipath Models	Allow user to choose from 4 HIPERLAN2 Models, 3 LTE Models, 5 ITU Models, 5 EDT Models, or the model in the SRWC paper.
Fading Models	Allow user to choose between Jakes' model or a flat spectrum model.
M	Number of taps in the multipath model, changes with multipath model selection.
N	Number of taps in fading model, always set to 48 taps.
K	Number of indices in the delay and angular-frequency domain, always 640.
L	Number of indices in the frequency and time domain, always 1024.
$K1$	The extend values for the angular-frequency domain, K_1 , always 0.
$L1$	The extend values for the time domain, L_1 , always 64.
SNR	Average theoretical SNR in dB.
Coherence	The percentage value used to determine the coherence bandwidth and time.
tausamp	The delay sample rate, τ_s .
freqsamp	The frequency sample rate, f_s .
Komit	The number of angular-frequency indices omitted in the spectrum of interest on both sides of the zeroth index, K_{omit} .
Kobsv	The number of angular-frequency indices observed and measured on both side of the zeroth index, K_{obsrv} .
L2	The number of time indices omitted but not in the time of interest, L_2 .
Lobsv	The number of time indices observed and measured, L_{obsrv} .
# of Coh. times...	# of coherence times the extrapolation is away from the measured DCM values.
Checkboxes	Allows the users to select the estimator-extrapolators to observe in the plot, the noise and actual channel is always shown.
Sim. Button	Runs a single simulation or continuous simulation if the checkbox is marked.
MATLAB tools	Allow users to adjust the view of the plot and mark data points.

Table 9.1: List of variables and GUI controls available in the EESIM.

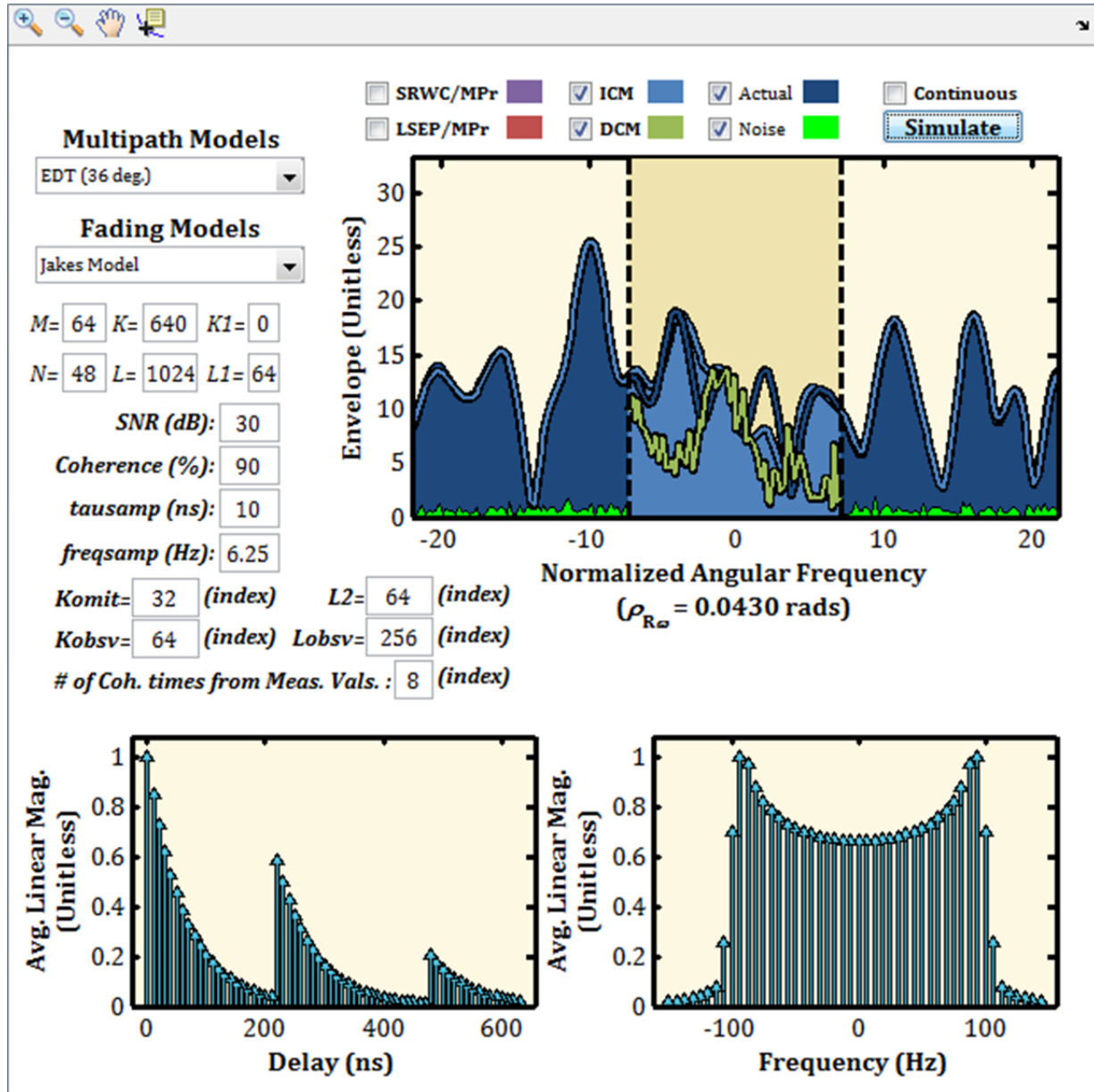


Figure 9.1: EESIM GUI.

Explanation of EESIM Programming

In this subsection a concise explanation of the program that runs the EESIM will be explained. The GUI interface programming is handled by MATLAB. A flow chart is given in Figure 9.2 to accompany the explanation.

Before starting the simulation the user has the option of changing some of the values in Table 9.1. Once the desired values are placed into the GUI, the program execution is begun by pressing the simulation button. The first step in the program is to define the initial values for the program variables shown in the GUI and others that are internal to the program.

After the initial values have been defined and set, the next step is to set or create the channel statistics and some other initial variables related to the channel statistics. The multipath model is set based on the model label selected from the pull down menu. The selection of multipath model also determines the value of the variable M , but the values pertaining to the omission matrix are set by the users. Similarly, the omission matrix corresponding to the fading model and the time extrapolator are defined by the user, and the variable N is predetermined. The variable N is always 48, because it has minimal effect on the extrapolator. Using the initial values, the values set by the model selection, and equations that have been presented in this thesis the following quantities are computed: \mathbf{F}_F , \mathbf{F}_I , \mathbf{O}_{y_c} , \mathbf{O}_{y_r} , \mathbf{O}_{MPR} , \mathbf{C}_τ , \mathbf{C}_f , \mathbf{R}_τ , \mathbf{R}_f , ρ_ω , ρ_t .

The next step is to create the linear estimator-extrapolator variable, \mathbf{G}_{LEE} . This process just uses the equations presented for the respective extrapolator since that is already shown in matrix form. After this step a random instance of the channel is created using Equation 4.47. The RV matrix, $\mathbf{N}_{(M \times N)}$, is created using MATLAB's random number generator for a standard normal distribution.

With all the variables that have been already defined, the channel estimates and extrapolations can be calculated using Equations 6.15 and 6.16. Next the MSE of only the

spectrum of interest is calculated to determine which estimator-extrapolator has the best performance. After the calculations, the final part of the program is the plotting of the various waveforms.

The legend for the plot is given in the GUI. The plot in the upper right hand corner of the GUI of the estimator-extrapolators has some things that are not as self-explanatory. The darker shaded plot region, flanked by the dotted lines and the lighter shaded region, signifies the spectrum of interest. The actual channel and all the extrapolators, excluding the extrapolator with the best performance, has a line plotted in this region. The extrapolator with the best performance, has a line plotted in this region. The extrapolator with the best performance has an area plot in this region. The extrapolator with the best performance has a line plotted in the regions on both sides of the spectrum of interest. Also in this region are the area plots of the actual channel and of the noise in the channel. The viewing area of the plot along the angular-frequency domain is limited to the observed spectrum and spectrum of interest. The other plots are the same as the plots shown in Figure 7.3 and 7.8, but without the shaded regions.

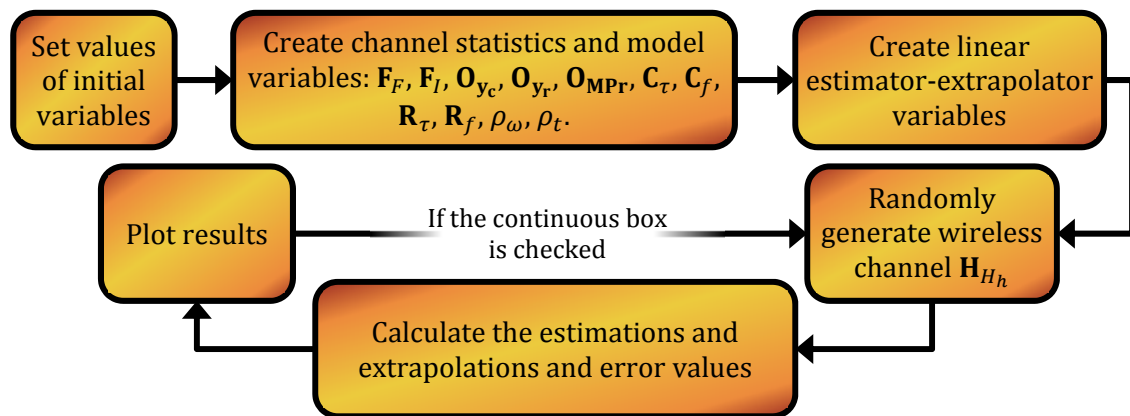
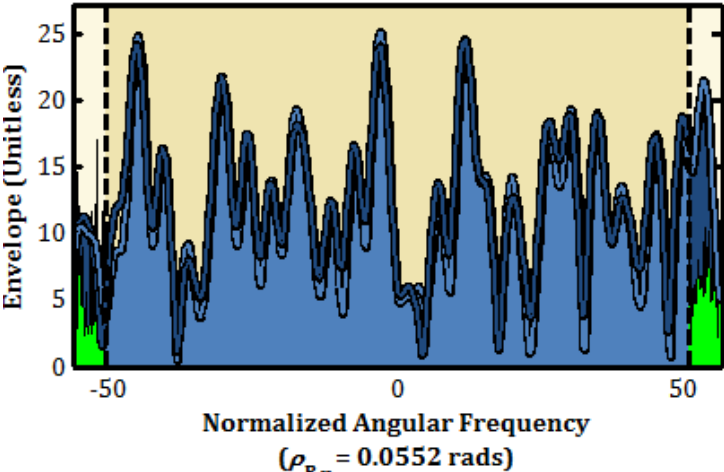
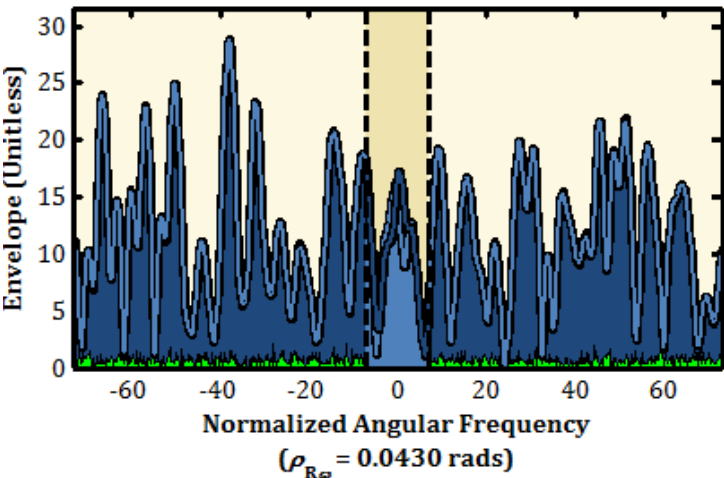


Figure 9.2: MATLAB code block diagram for EESIM.

EESIM Results

There are many variables that can be changed, and any of these variant cases can be observed with a “click of a button.” The results presented will be limited to a few plots in an effort to not obfuscate the most interesting results. These results will be presented in a listing format that shows the plot and variable selection on the left and a description and discussion of the plot on the right.

Plots	Descriptions
<p>Multipath Models SNR (dB): 10 10 288</p> <p>SRWC M= 31 K= 640 K1= 0 Kobsv= 32</p>  <p style="text-align: center;">Normalized Angular Frequency ($\rho_{R\omega} = 0.0552$ rads)</p>	<p>In this plot most of the spectrum is omitted and the ICM technique can still determine the omitted spectrum from the observed spectrum. The SRWC channel model, as well as many of the channel models presented in standards, have a type of sparsity where some or all of the taps are at least twice the sample delay from any adjacent taps. When this type of sparsity is prevalent in the channel model, the ICM technique will have great performance.</p>
<p>Multipath Models SNR (dB): 30 30 32</p> <p>EDT (36 deg.) M= 64 K= 640 K1= 0 Kobsv= 288</p>  <p style="text-align: center;">Normalized Angular Frequency ($\rho_{R\omega} = 0.0430$ rads)</p>	<p>The EDT channel models do not have this sparsity, and may be more indicative of what is seen in practice. In these cases only a smaller portion of the modeled channel can be omitted and maintain good performance. This plot also shows that 90% ($K_{obsrv} = 288$) of the model spectrum is observed to extrapolate the 10% of desired spectrum, and this could pose an issue in implementation.</p>

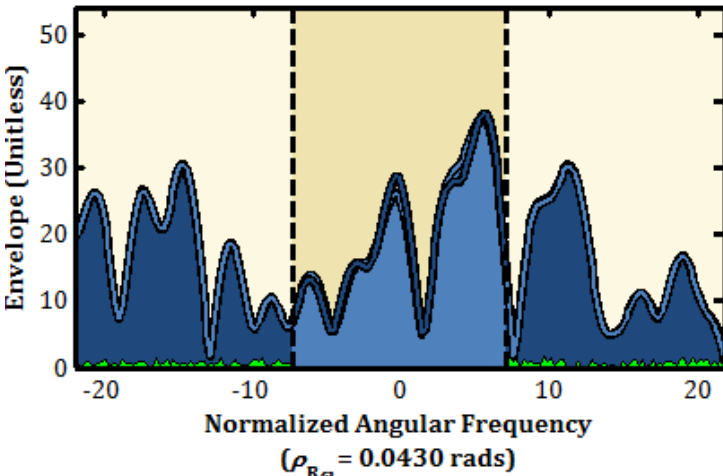
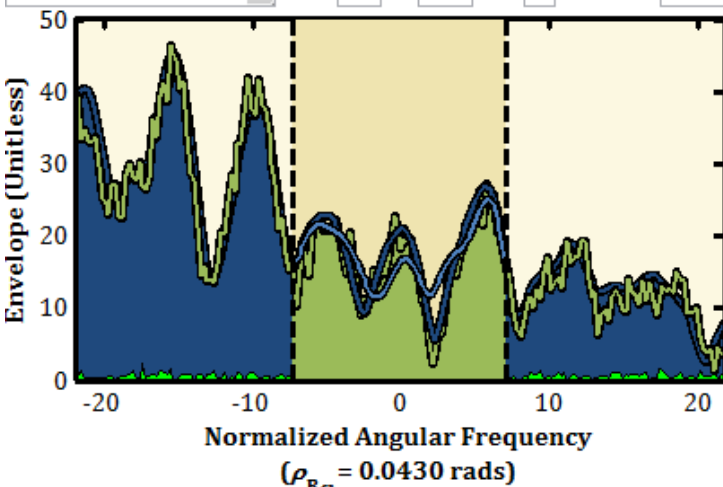
Plots (continued)				Descriptions (continued)
Multipath Models		SNR (dB): 30	Komit= 32	This plot was generated by changing the amount of the modeled spectrum observed to 20% ($K_{obsrv} = 64$) of the overall spectrum, and keeping all other variables the same. The purpose of this plot is to show 90% ($K_{obsrv} = 288$) of the overall spectrum does not need to be observed, as in the previous plot, to obtain reasonable performance. This is because most of the information needed to determine the spectrum of interest is in the spectrum closest to it.
EDT (36 deg.)	M= 64 K= 640 K1= 0	Kobsv= 64		
				
<hr/>				
Multipath Models		SNR (dB): 30	Komit= 32	This plot shows the DCM technique and the ICM technique the observed. As shown in the previous plots and in this plot. Kobsv can be reduced from the 288 index values to 64 and still maintain reasonable performance. The other thing that is noticeable in this plot and other plots displaying the DCM technique is the lack of smoothness to the estimated channel. This is because in the DCM technique each subcarrier is modeled independently. The DCM technique can be improved by changing this model and/or doing some smoothing. However, the same thing can be done with the ICM technique to improve its performance. If the ICM technique were viewed in the time domain it would also lack smoothness. Due to time constraints these improvements were not explored.
EDT (36 deg.)	M= 64 K= 640 K1= 0	Kobsv= 64		
Fading Models		# of Coh. times... : 2	L2= 416	
Jakes Model	N= 48 L= 1024 L1= 64	Lobsv= 64		
				

Table 9.2: List of EESIM GUI plots and descriptions.

EESIM ICM Case Study

In this case study several models for the ICM techniques were explored. Several examples are presented in this section along with explanations of their performance. There are many parameters in EESIM that can be change to affect the performance of the ICM technique, but the parameter with the most effect on the ICM technique's performance is the multipath model parameter, which is the first parameter listed in Table 9.1. In this section this parameter is varied and its effect is explained through the correlation of the angular-frequency spectrum.

Before discussing the case study the correlation of the angular-frequency spectrum will be explained. As given in Chapter Four, the discrete angular-frequency spectrum at time t_l is

$$H_h(t_l, \omega) = \begin{cases} A_a(t_l, \omega_q) & , \omega = \omega_q \\ 0 & , elsewhere \end{cases} \quad 9.1$$

The correlation of the angular-frequency spectrum can be defined as the expectation of the convolution of $H_h(t_l, \omega_q)$ with the conjugate of $H_h(t_l, \omega_q - \omega_k)$,

$$\rho(\omega_k) = E\{H_h(t_l, \omega_q)H_h^*(t_l, \omega_q - \omega_k)\} = \frac{\text{Tr}(\mathbf{S}_k \mathbf{R}_\omega)}{\text{Tr}(\mathbf{R}_\omega)}, \quad 9.2$$

As noted in Chapter Four, \mathbf{S}_k is an identity matrix that is circularly shifted and k denotes the number of times the rows are shifted upwards. Equation 4.48 is rewritten here using Equation 9.2,

$$\rho_{\mathbf{R}_\omega} = \lim_{\gamma \rightarrow 0} \lim_{K \rightarrow \infty} \frac{\pi}{K} \arg \min_{k \geq 0} ([\rho(\omega_k) - 0.9]^2 + \gamma k). \quad 9.3$$

Using the definitions in Equations 9.2 and 9.3, the correlation and 90% correlation bandwidth for the angular-frequency spectrum can be calculated respectively. For example, using three different two-tap delay line models with each tap having equal average power, two statistically independent taps that are complex and normally distributed, the first tap

occurring at τ_0 , and the second tap occurring at different delay indices: Model A (τ_1), Model B (τ_3), and Model C (τ_7). The delay domain covariance matrix, \mathbf{R}_τ , for the respective models are,

$$\mathbf{R}_{\tau, \text{Mod.A}} = \begin{bmatrix} \frac{K}{2} & 0 \\ 0 & \frac{K}{2} \end{bmatrix}, \quad 9.4$$

$$\mathbf{R}_{\tau, \text{Mod.B}} = \begin{bmatrix} \frac{K}{2} & 0 & 0 & 0 \\ 0 & 0 & 0 & 0 \\ 0 & 0 & 0 & 0 \\ 0 & 0 & 0 & \frac{K}{2} \end{bmatrix}, \quad 9.5$$

$$\mathbf{R}_{\tau, \text{Mod.C}} = \begin{bmatrix} \frac{K}{2} & 0 & 0 & 0 & 0 & 0 & 0 & 0 \\ 0 & 0 & 0 & 0 & 0 & 0 & 0 & 0 \\ 0 & 0 & 0 & 0 & 0 & 0 & 0 & 0 \\ 0 & 0 & 0 & 0 & 0 & 0 & 0 & 0 \\ 0 & 0 & 0 & 0 & 0 & 0 & 0 & 0 \\ 0 & 0 & 0 & 0 & 0 & 0 & 0 & 0 \\ 0 & 0 & 0 & 0 & 0 & 0 & 0 & 0 \\ 0 & 0 & 0 & 0 & 0 & 0 & 0 & \frac{K}{2} \end{bmatrix}, \quad 9.6$$

Note for Model A ($M = 2$), Model B ($M = 4$), and Model C ($M = 8$). Using Equations 4.33 and 4.42, the angular-frequency domain covariance matrix, \mathbf{R}_ω , for the respective models can be determined,

$$\mathbf{R}_{\omega, \text{Mod.A}} = \mathbf{F}_F \mathbf{R}_{\tau, \text{Mod.A}} \mathbf{F}_F^H, \quad 9.7$$

$$\mathbf{R}_{\omega, \text{Mod.B}} = \mathbf{F}_F \mathbf{R}_{\tau, \text{Mod.B}} \mathbf{F}_F^H, \quad 9.8$$

$$\mathbf{R}_{\omega, \text{Mod.C}} = \mathbf{F}_F \mathbf{R}_{\tau, \text{Mod.C}} \mathbf{F}_F^H, \quad 9.9$$

Note, since the M values for each model are different, the size of the \mathbf{F}_F matrix is also different for each model, though the notation is the same.

Using the angular frequency-domain covariance matrices and Equations 9.2 and 9.3, also letting $K = 1024$, Figure 9.3 was created. This shows a plot of the angular-frequency

correlation with respect to angular-frequency index k . It also shows the coherence bandwidth normalized to $\frac{\pi}{K}$.

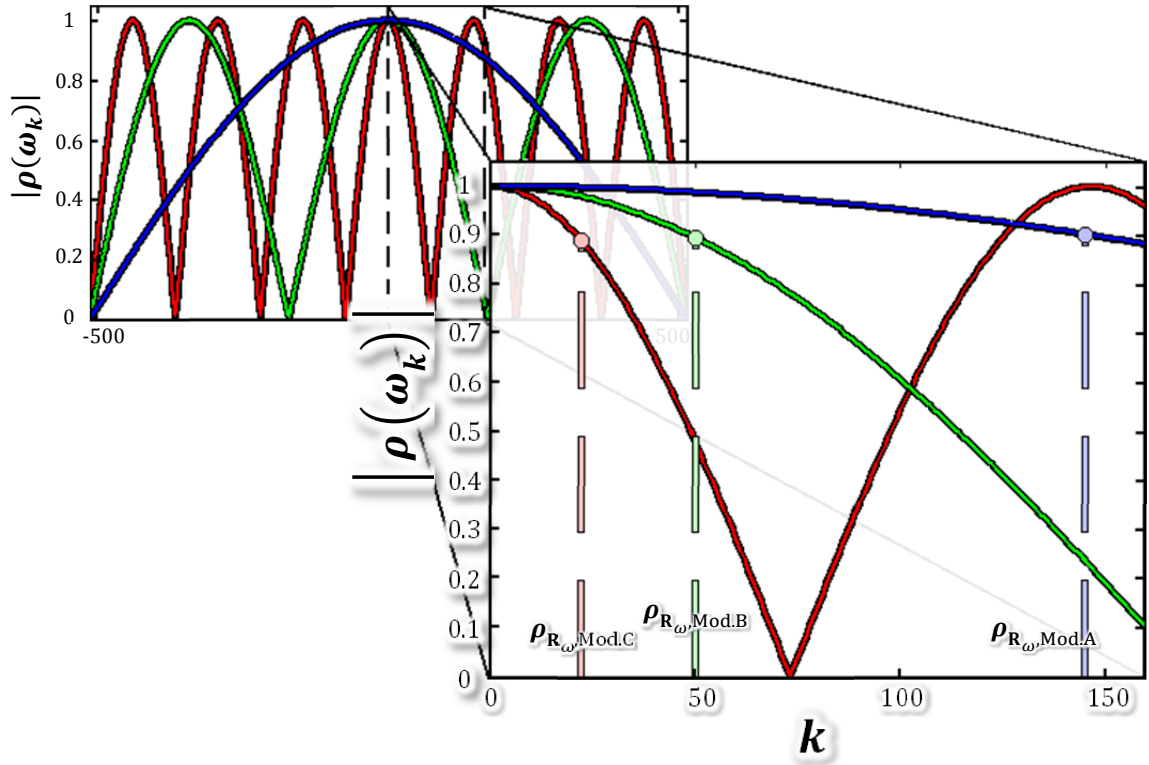


Figure 9.3: Correlation in the angular-frequency domain and normalize coherence bandwidth.

One thing to take away from the graph is that Model C has a smaller coherence bandwidth because the two taps have the largest spacing in the delay domain. Another thing to note in the case of Models B and C, is that in these models there are parts of the band that are more than one coherence bandwidth apart but are highly correlated with one another. This is a very important concept. This goes to the heart of why the ICM technique works.

Take the case shown in Figure 9.4, where the ICM technique performs extremely well. The multipath model is the SRWC Model shown in Figure 7.4.

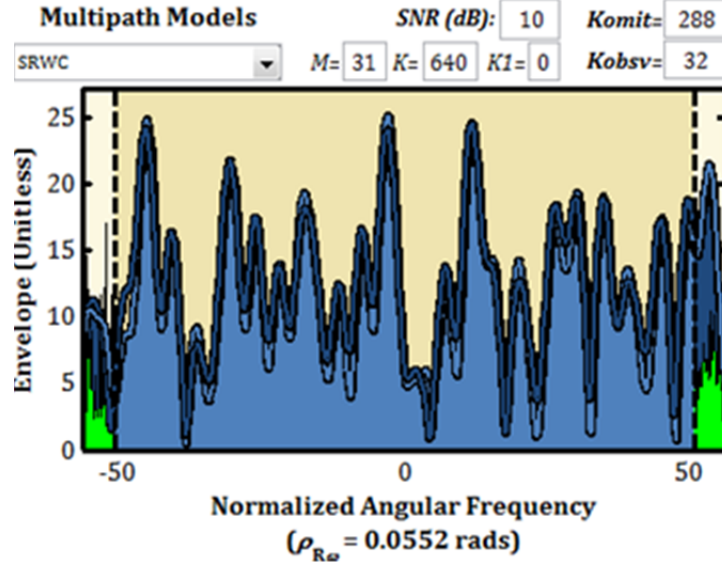


Figure 9.4: EESIM case 1 of a great MP model, the SRWC model, for the ICM technique.

The angular-frequency correlation for this model is shown in Figure 9.4. Only half of the spectrum is shown since it is symmetric about ω_0 .

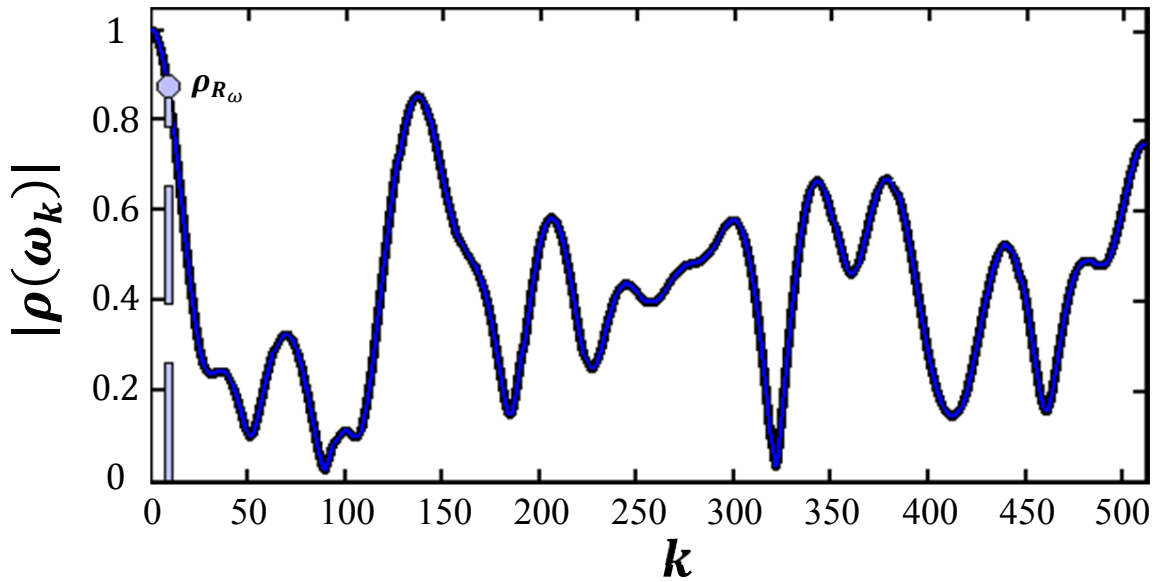


Figure 9.5: The SRWC model angular-frequency domain correlation.

As can be seen in Figure 9.5, there are many frequencies beyond a coherence bandwidth apart that are more than 50% correlated. This is why the ICM technique works so well for

the SRWC model. This allows the out-of-band portion of the channel to be used to determine the in-band portion, because the OOB channel contains a significant amount of information about the IB channel.

In contrast, the worst model, the EDT model with a 90 degree slope, has the following angular-frequency domain correlation shown in Figure 9.6. With this model there are no two frequencies with significant separation (i.e. multiple coherence bandwidths apart) that are highly correlated. In these cases, the OOB channel does not contain enough information about the IB channel. Therefore the IB channel cannot be accurately extrapolated while omitting a significant amount of bandwidth. The performance in these cases is similar or the same as the performance that is seen from the NCM technique.

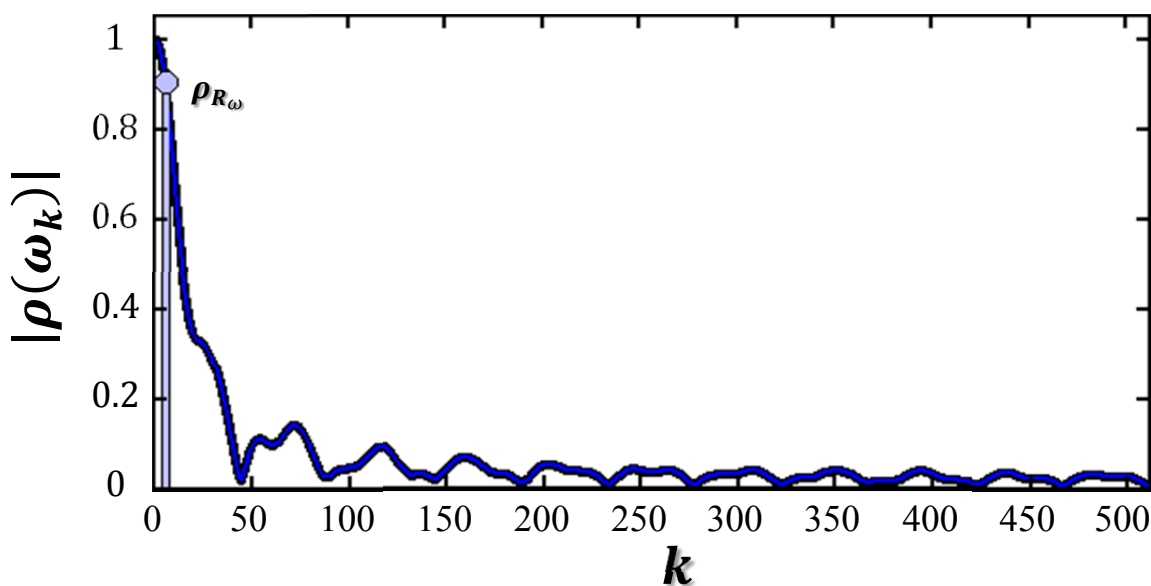


Figure 9.6: The EDT with 90 degree slope model angular-frequency domain correlation.

If the slope of the EDT Model is increased to 36 degrees, shown in Figure 7.7, the performance significantly improves, because the angular-frequency domain correlation becomes more favorable for the ICM technique, as seen in Figure 9.7.

Through the case study it was discovered that each of these cases the SWRC, EDT 90° and EDT 36° all have coherence bandwidths that are approximately equal, but their performance varies drastically. Through this research what has been observed is that the coherence bandwidth, as define in this thesis, is not a good indicator of the performance of the ICM technique. In the case of the EDT models the slope of the model has the most effect on the ICM technique performance. This is highlighted in the next simulator section in its case study. Furthermore, with respect to the delay model (i.e. CIR), for the ICM technique it is most desirable to have a CIR or delay model where there are multiple samples between delay taps. This creates a situation where there is a small coherence bandwidth and an extremely desirable angular-frequency domain correlation for the ICM technique. This allows the omission of several coherence bandwidths as seen in Figure 9.4.

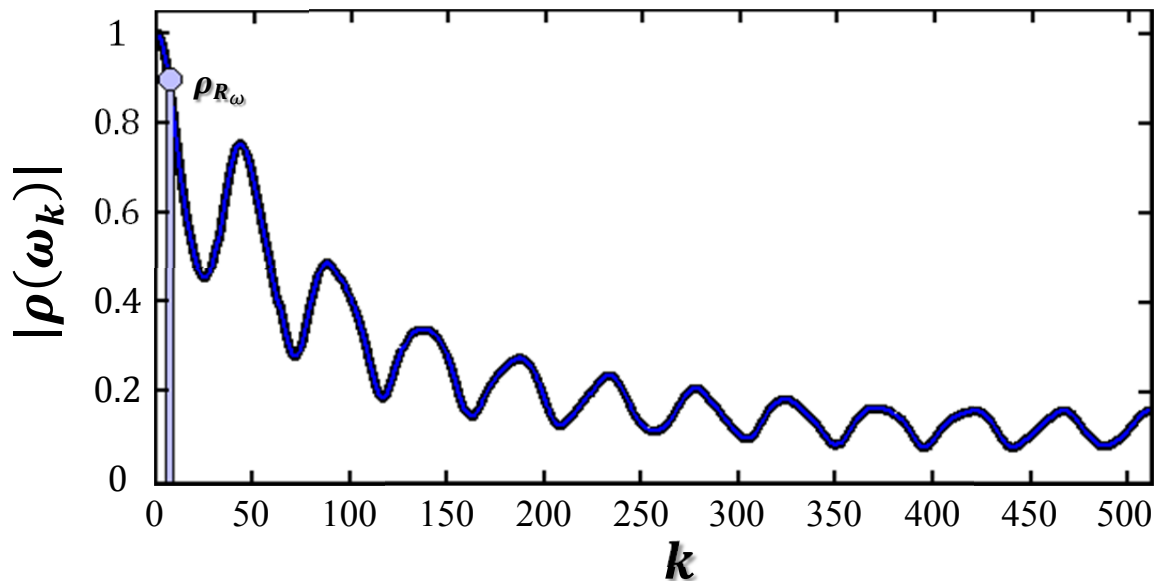


Figure 9.7: The EDT with 36 degree slope model angular-frequency domain correlation.

9.3 RMSE-SE Simulator

The RMSE-SE simulator (RMSESIM) is designed to verify the RMSE-SE performance metric derived in Chapter Seven. In this section the validity and accuracy of the equations will be examined through simulations. As has been stated, these equations allow users to easily determine and compare the performance of the ICM, DCM, and NCM techniques.

RMSESIM gives a visual depiction, similar to Figure 7.9, of what performance is better based on either the theoretical RMSE-SE or sampled RMSE-SE. By using both the theoretical and sampled value the accuracy of the RMSE-SE metric can still be compared. However, the main focus of this simulation is not to compare the accuracy of the metric, but to compare the performance of the ICM and DCM technique.

This performance comparison will work in the following manner. Nature will determine the multipath and fading models. The users will select the ICM and DCM parameters based on the wireless communication system design. The initial variables based on the models and the wireless communication system can then be placed into the RMSESIM comparison simulation. From here, the user can visually see where the ICM, DCM, and/or NCM techniques are the best. These terms best, great, good, etc... are all relative. The plots generated by RMSESIM provide the basis for these qualitative comparisons.

Explanation of RMSESIM Programming

In most ways, the programming for RMSESIM is the same as EESIM. Starting with the initial variables in Table 9.1, the “# of Coh. times...” variable is not used in the RMSESIM, and the checkboxes are not present either. There is one added setting, and that is the radio

button that allows users to select the performance or comparison simulation. All the other variables in the table are the same.

The steps to create the channel statistics and the linear estimator-extrapolators are the same as in the EESIM. Unlike the EESIM after these two steps the theoretical RMSE-SE is calculated using Equations 7.30, 7.42, 7.45, and 7.46. The next two steps, the generation of the wireless channel and the calculation of the extrapolation are the same, but a following step is added. This step is the calculation of the sampled RMSE-SE. The final step with RMSESIM is also plotting. The iteration in RMSESIM occurs in the same place, but the trigger is the toggling of the simulate button and does not involve the clicking of a checkbox. Figure 9.8 shows a block diagram of the RMSESIM programming.

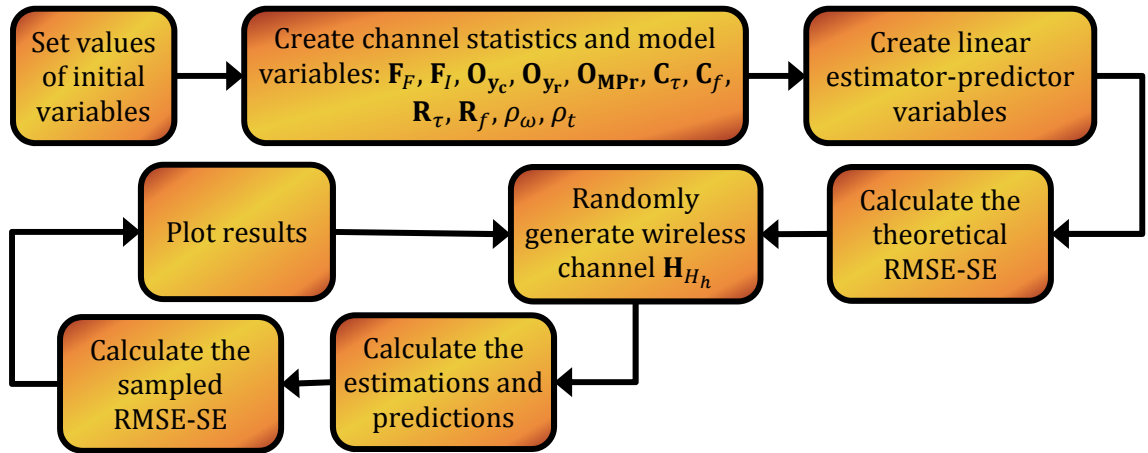


Figure 9.8: MATLAB code block diagram for RMSESIM.

There are two types of plots in this simulator, the performance and comparison plots. The performance plots are of the various theoretical and sampled RMSE-SE equations in log scale. The top plot is of the DCM and NCM with respect to time, and the bottom plot is for the ICM and NCM with respect to the angular-frequency. The legend is given in the GUI for the respective plots.

The second type of plots deals with the comparison of the three techniques. The comparisons are given in the time-angular-frequency matrix domain. Therefore Equations 9.10, 9.11, and 9.12 show the matrix forms used to create the matrix for the plot,

$$\mathbf{Z}_{ICM} \approx \mathbf{z}_{c,ICM,t_{\frac{L}{2}+1}} \mathbf{1}_L^T, \quad 9.10$$

$$\mathbf{Z}_{DCM} \approx \mathbf{1}_K \mathbf{z}_{r,DCM,\omega_0}, \quad 9.11$$

$$\mathbf{Z}_{NCM} = \sqrt{3 \text{diag}(\mathbf{R}_\omega \circ \mathbf{R}_\omega) \text{diag}(\mathbf{R}_t \circ \mathbf{R}_t)^T - 2K \text{diag}(\mathbf{R}_\omega) \text{diag}(\mathbf{R}_t)^T + K^2}. \quad 9.12$$

The matrices \mathbf{Z}_{ICM} and \mathbf{Z}_{DCM} are approximated to reduce the amount of processing needed. These approximations are accurate because the covariance matrices have minor variations with respect to the opposing domain.

These matrices are used in the following manner to create the matrices for the comparison plots. First the maximum value is determined for each of the three \mathbf{Z} matrices and the overall maximum is selected, Z_{max} . Then each matrix element is compared to determine the normalization matrix. Each element in the normalization matrix is determined by selecting the minimum value between each of the respective elements from the \mathbf{Z}_{ICM} , \mathbf{Z}_{DCM} , and \mathbf{Z}_{NCM} matrices. Equation 9.13 gives the normalization matrix,

$$\mathbf{Z}_{norm} = Z_{max} - 10 \log(\min(\mathbf{Z}_{ICM}, \mathbf{Z}_{DCM}, \mathbf{Z}_{NCM})), \quad 9.13$$

Note, the functions $\log(\cdot)$ and $\max(\cdot, \cdot, \cdot)$ are element-wise functions.

Using the norm matrix, three matrices are created. These matrices are considered to be the normalized version of the RMSE-SE matrixes for each technique.

$$\mathbf{Z}_{ICM,norm} = \text{inv}(\mathbf{Z}_{norm}) [Z_{max} - 10 \log(\mathbf{Z}_{ICM})], \quad 9.14$$

$$\mathbf{Z}_{DCM,norm} = \text{inv}(\mathbf{Z}_{norm}) [Z_{max} - 10 \log(\mathbf{Z}_{DCM})], \quad 9.15$$

$$\mathbf{Z}_{NCM,norm} = \text{inv}(\mathbf{Z}_{norm}) [Z_{max} - 10 \log(\mathbf{Z}_{NCM})]. \quad 9.16$$

The function $\text{inv}(\cdot)$ is an element-wise inverse function. Each of these normalized matrices have values in the following range, $[0\ 1]$, and any undefined value caused by division by zero is set to equal one. The RGB color scheme was used for comparison since the range of values was between zero and one, and there were three matrices to compare. Red represents the DCM technique, green represents ICM, and blue represents NCM. Figure 9.9 gives the graphical depiction of the legend, and Table 9.3 gives a discrete version of the same legend. Another discrete version is also presented in the GUI.

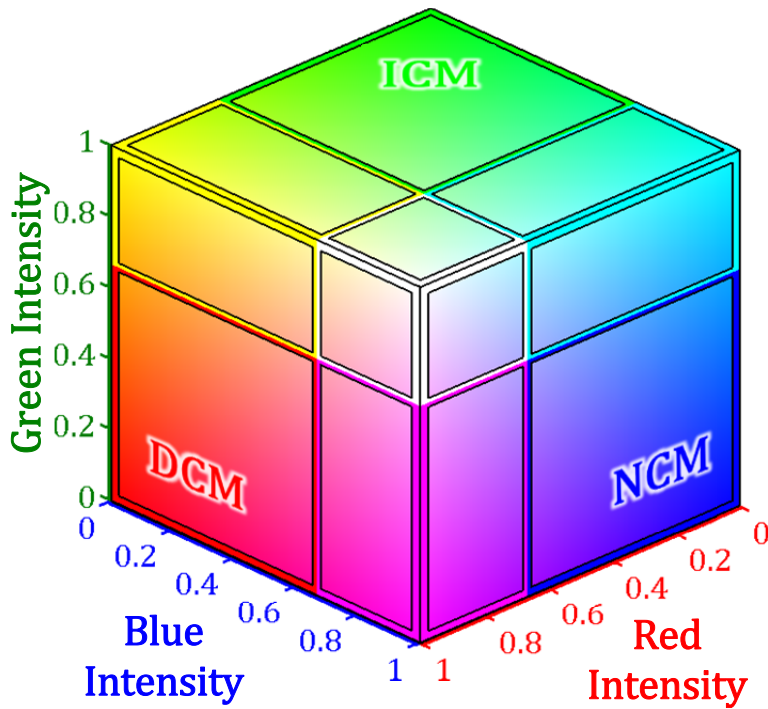


Figure 9.9: Color legend for the ICM, DCM, and NCM techniques.

R	G	B	Color	Best
1	0	0	Red	DCM
0	1	0	Green	ICM
1	1	0	Yellow	DCM or ICM
0	0	1	Blue	NCM
1	0	1	Magenta	NCM or DCM
0	1	1	Cyan	NCM or ICM
1	1	1	White	DCM, ICM, or NCM

Table 9.3: Discretize color legend for the ICM, DCM, and NCM techniques.

This type of comparison was created for this research, and the plots in this simulation will be based on this color scheme. There are three ways to read this plot. The highest level is just using the plot to determine what technique is the best. So, if a part of the plot looks green then the ICM technique is the best in that region. In this high level, only the color

readings of red, green, or blue are used. The next level the user can include the other colors, like cyan. For cyan, the ICM and NCM technique have the same performance. Note for application purposes, in cases where the performance of the NCM technique is the same as the DCM and/or ICM technique, the NCM technique will most likely be preferable since it does not require any measurements. The third and lowest level form of reading the plots is to select points on the plot and get the actual color intensities and translate them back to the performance metrics.

RMSESIM Results

In this subsection the results of RMSESIM will be presented, but before discussing some of the results a depiction of the GUI is given in Figure 9.10 and 9.11. Figure 9.10 shows the performance simulation. The plots in this figure are a great representation of the accuracy.

In the bottom left corner of the figure, the number of samples used in the average is given. As can be seen, within 128 samples the sampled RMSE-SE has approached the theoretical RMSE-SE.

Figure 9.11 shows the comparison simulator. As seen in the figure, the comparison simulator can also be used to view the accuracy of the theoretical RMSE-SE. The top plot is the theoretical RMSE-SE and the bottom plot is the sampled RMSE-SE. The main use of these plots is for comparison purposes, and in Figure 9.11 in can be seen that the DCM technique is best within approximately three coherence times of the measured DCM values. What can also be seen is that after three coherence times the performance of all three of the techniques are approximately equal, hence the whitish color. Remember, when any of the

techniques' performance is approximately equal to the performance of the NCM technique, the NCM technique will be preferable because it does not require any measurements.

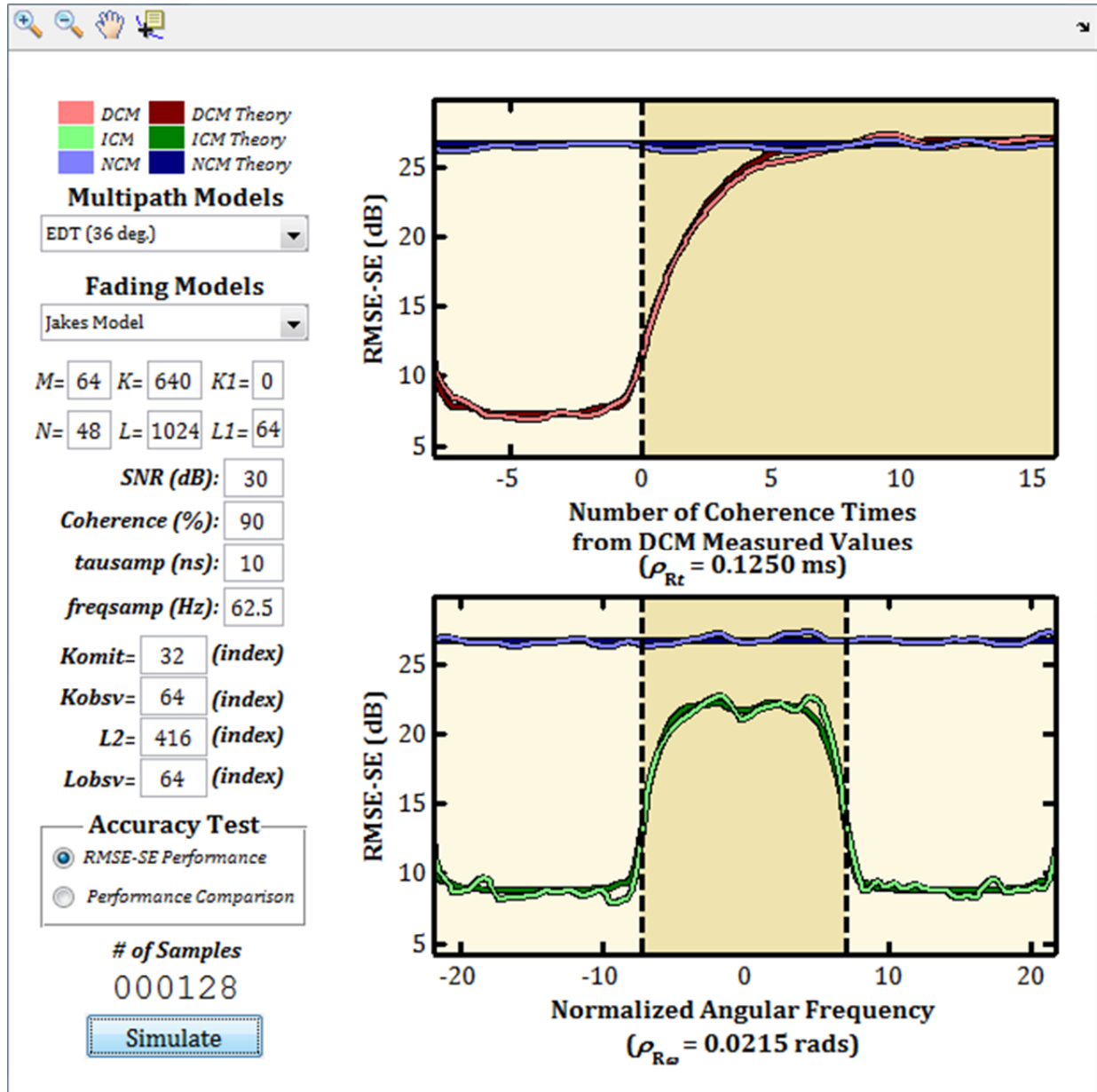


Figure 9.10: RMSESIM GUI showing the theoretical and sampled RMSE-SE.

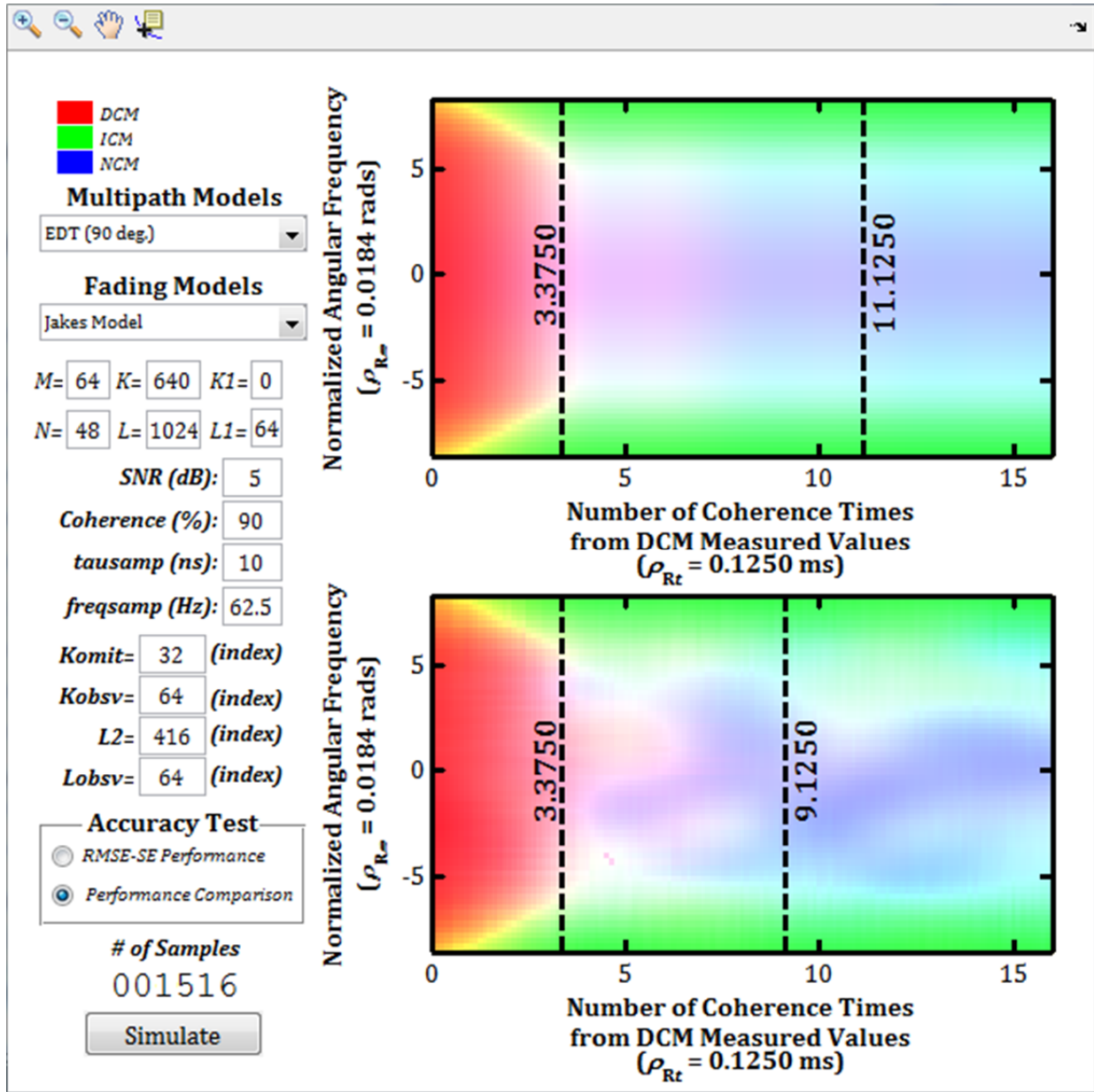


Figure 9.11: RMSESIM GUI showing the performance comparison.

The rest of this subsection will cover the performance comparison results for various variable selections, which will be referred to as cases. Instead of showing the graphical depiction as shown in Figure 9.11, the coherence times corresponding to the dotted black lines shown in Figure 9.11 are given for the performance comparison results. To get these

the GUI variables were set to the values in Table 9.4, and Tables 9.5 and 9.6 show the performance comparison results.

Table 9.5 list the results obtained from the first dotted line from the left in Figure 9.11. This dotted line is the coherence time value at which the inequality in Equation 9.17 becomes true. The second dotted line in Figure 9.11 is the coherence time value at which the inequality in Equation 9.18 becomes true, and these values are given in Table 9.6. The dotted lines in the top plot are the theoretical values and for the bottom plot the dotted lines represent the sampled version of the theoretical values.

$$\frac{1}{2K_{omit}} \begin{bmatrix} \mathbf{0}_{K_{obsrv}+K_2} \\ \mathbf{1}_{2K_{omit}} \\ \mathbf{0}_{K_{obsrv}+K_2} \end{bmatrix}^T \mathbf{z}_{c,ICM,t_l} \leq Z_{DCM,\omega_0,t_l}, \quad 9.17$$

$$Z_{ICM,\omega_0,t_l} \leq Z_{DCM,\omega_0,t_l}, \quad 9.18$$

In Equations 9.17 and 9.18 the variable Z_{LEP,ω_k,t_l} is the RMSE-SE for the respective LEE technique at angular-frequency, ω_k , and time, t_l . For the sampled version, the theoretical RMSE-SE values are replaced with the sampled values.

The values in Table 9.5 and 9.6 are indicative of the IET_{DCM} . The IET_{DCM} can be any value between the values in Table 9.5 and Table 9.6, depending on how many sub-carriers of the omitted spectrum you want to include in the inequality. Also, as can be seen in the tables IET_{DCM} is shown as it varies with respect to four of the variables given in Chapter Seven: the number of time indices observed and omitted (L_{obsrv} and L_{omit}), the average theoretical SNR ($1/\sigma_W^2$) in dB, the number of angular-frequency indices omitted (K_{omit}), and the slope of the EDT model. All the other changeable variables in the RMSE-SE GUI remain constant and are given in Table 9.4.

Wireless Channel	
Fading Model: Jakes'	
$\tau_s = NA$	
$f_s = NA$	
ICM Technique	DCM Technique
$K = 640$	$L = 1024$
$M = 64$	$N = 48$
$K_1 = 0$	$L_1 = \frac{L - 2L_{obsrv} - L_{omit}}{2}$
$K_{obsrv} = 64$	$L_{omit} = 480 - L_{obsrv}$

Table 9.4: Constant initial variables and settings used in IET_{DCM} calculation.

		L_{obsrv}	8 ($L_{omit} = 472$)			32 ($L_{omit} = 448$)			128 ($L_{omit} = 352$)		
		SNR	10	30	50	10	30	50	10	30	50
K_{omit}	MPM										
16	EDT 18°		0.125	0.125	0.375	0.125	0.250	0.625	0.125	0.375	0.750
	EDT 36°		0.375	0.875	1.125	0.625	1.375	1.500	0.875	1.625	1.875
	EDT 90°		1.500	1.625	1.125	2.250	2.500	1.625	2.500	2.875	2.000
32	EDT 18°		0.125	0.375	0.750	0.125	0.625	1.125	0.125	0.875	1.375
	EDT 36°		0.750	1.375	2.125	1.250	2.125	2.875	1.500	2.500	3.250
	EDT 90°		2.375	2.750	3.500	3.250	4.000	4.625	3.875	4.750	5.125
64	EDT 18°		0.375	1.000	1.625	0.750	1.500	2.250	0.875	1.750	2.500
	EDT 36°		1.375	2.125	3.000	2.000	3.125	4.000	2.375	3.625	4.500
	EDT 90°		3.250	3.750	4.750	4.375	5.250	6.125	7.750	6.375	7.125

Table 9.5: The IET_{DCM} obtained from the first dotted line in Figure 9.11.

In Table 9.5 there are three colors shown: green, blue, and cyan. Green states that after the coherence time shown, the ICM technique has better performance if the inequality in Equation 9.17 is false. Blue signifies all the techniques or just the ICM and NCM have equal performance, but the NCM technique is considered better because it does not require any measurements. With respect to performance, the cyan color means that the ICM and NCM

techniques have the same performance, but either the ICM or NCM techniques could be considered to be better than the DCM technique.

In Tables 9.5 and 9.6 MPM stands for multipath model, and the numbers in the parentheses in the L_{obsrv} row are the L_{omit} values as given in Table 9.4. The three dashes in Table 9.6 means that there are no lines in the respective cases.

		L_{obsrv}	8 ($L_{omit} = 472$)			32 ($L_{omit} = 448$)			128 ($L_{omit} = 352$)		
		SNR	10	30	50	10	30	50	10	30	50
K_{omit}	MPM										
16	EDT 18°		0.125	0.125	0.500	0.125	0.250	0.750	0.125	0.375	0.875
	EDT 36°		0.375	1.125	1.375	0.875	1.750	2.000	1.000	2.000	2.250
	EDT 90°		2.250	2.250	1.500	3.125	3.375	2.125	3.625	3.875	2.500
32	EDT 18°		0.125	0.375	0.750	0.250	0.750	1.125	0.375	0.875	1.375
	EDT 36°		0.875	1.500	2.500	1.375	2.250	3.250	1.625	2.625	3.750
	EDT 90°		4.250	3.625	4.375	8.000	5.125	5.750	11.375	6.250	6.500
64	EDT 18°		0.625	1.125	1.750	1.125	1.750	2.500	1.375	2.125	2.875
	EDT 36°		1.750	2.500	3.625	2.625	3.625	4.750	3.000	4.250	5.375
	EDT 90°		---	8.375	---	---	---	11.500	19.375	18.125	15.625

Table 9.6: The IET_{DCM} obtained from the second dotted line in Figure 9.11.

Furthermore, these results were used to show which technique has the best performance in several different cases. In the next section this case study is discussed in further detail.

9.4 RMSESIM Case Study

The purpose of this case study is to inform users which cases are best for the ICM, DCM, or NCM techniques. The metrics used to make this determination are the IUT_{DCM} and the

IET_{DCM} given in Chapter Eight. If the inequality in Equation 9.19 is true then the DCM technique is the best. If the inequality is false then the ICM or NCM technique is the best.

$$\frac{IUT_{DCM}}{\frac{R_{DCM}}{0.125 \text{ ms}}} \leq \frac{IET_{DCM}}{\frac{2b_{sc}K_{omit}}{\rho_{R_t} IET_{DCM}}}. \quad 9.19$$

This inequality is evaluated in 972 different cases in which seven parameters are varied. These parameters are shown in Table 9.7.

Parameters	Qualifiers	Quantifiers
The dynamic nature of the DWE	Very dynamic Moderately dynamic Slightly dynamic	$\rho_{R_t} = 0.125 \text{ ms}$ $\rho_{R_t} = 1.25 \text{ ms}$ $\rho_{R_t} = 12.5 \text{ ms}$
The number of feedback bits per coherence time	A few bits More than a few bits Many more than a few bits	$R_{DCM} = 16 \rho_{R_t}/0.125 \text{ ms}$ $R_{DCM} = 128 \rho_{R_t}/0.125 \text{ ms}$ $R_{DCM} = 1024 \rho_{R_t}/0.125 \text{ ms}$
Multipath Models	Great Model for ICM Good Model for ICM Bad Model for ICM	EDT 18° EDT 36° EDT 90°
Number of information and overhead bits need per subcarrier	Several bits A few bits	$b_{DCM}/K_{omit} = 16$ $b_{DCM}/K_{omit} = 4$
SNR	Low Medium High	0 dB 30 dB 50 dB
RX Memory Capacity	Minimum Large	$L_{obsrv} = 8$ $L_{obsrv} = 128$
Bandwidth Omission with respect $K_{obsrv} = 64$	Fifth Third Half	$K_{omit} = 16$ $K_{omit} = 32$ $K_{omit} = 64$

Table 9.7: Initial variables and settings used in theoretical probability calculation.

Some of these parameters are also used in Tables 9.5 and 9.6. These parameters give rise to the IET_{DCM} values, and the IET_{DCM} values only vary with these parameters because of how the RMSESIM is designed.

The parameters listed in Table 9.7 are varied and the inequality is calculated for each of the respective cases, and placed into Tables 9.8 – 9.10. These tables are color coded using the legend in Figure 9.9 and Table 9.3. In this instance, the colors indicate what technique is best based on the inequality.

Several conclusions can be drawn from these tables. This section will cover the most important ones. One thing to know about the parameters in the tables is that they are arranged in descending order from left to right with respect to how much the inequality varies with respect to the parameter's variation. So, the inequality in Equation 9.19 varies most when the dynamic nature of the DWE changes, and varies the least when the bandwidth omission changes. Before presenting these tables, an explanation will be given on how to read the tables. Table 9.8 will be used for the explanation.

First, in the table the qualifiers are used for the respective parameters. As stated, there are a total of 972 cases, one for each qualifier combination. In the text the qualifier combinations will be written in the following form, *{Dynamic nature of the DWE, Number of feedback bits per coherence time, MP model, Info bits needed per subcarrier, SNR, RX memory capacity, Bandwidth omission}*. The italicize parameter represents the respective qualifiers, for example, {Very, A Few, Great, Several, Low, Minimum, Fifth}. {Very, A Few, Great, Several, Low, Minimum, Fifth} represents one case, the case where: the DWE is very dynamic, there are a few feedback bits that need to be sent to the transmitter per coherence time, the MP model is great for the ICM technique, there are several bits needed per

subcarrier, the SNR is low, there is a minimum amount of memory capacity needed at the receiver for the DCM technique, and a fifth of the bandwidth is omitted for the ICM technique. In the tables “All” takes the place of some of the qualifiers, such as {Very, A Few, All, All, All, All, All}. In this instance {Very, A Few, All, All, All, All, All} represents all cases for which the DWE is very dynamic and there are a few feedback bits that need to be sent to the transmitter per coherence time.

The qualifier combinations given by the text in the braces can be obtained by reading the table from the far left column in the table to the last parameter column, “Bandwidth omission”. The far left column gives the “Dynamic nature of the DWE” qualifier. Since the tables are split into three this qualifier will always be the same for each respective table, (i.e. “Very” for the very dynamic DWE case studies, “Moderately” for the moderately dynamic DWE case studies, etc...). Moving to the next column, the first column from the leftmost column will give the qualifier for the “Number of feedback bits per coherence time” parameter, and the next column’s qualifiers for the parameter, “MP Model” will be with respect to the previous qualifier from the “Number of feedback bits per coherence time” parameter. So, if “More” is selected in the “Number of feedback bits per coherence time” column, then the respective qualifiers of the “MP Model” parameter will be the ones that fit within the cells height. This is true for all subsequent qualifiers and parameters.

The far right columns in the table is the number of cases for which the DCM (D), ICM (I), and/or NCM (N) technique is preferred based on the inequality and colors in Table 9.5. In text these numbers will be presented in brackets as such, $[D, I, N]$ and referred to as the NOC. For example, the first row in the far right columns in Table 9.8 has an NOC of $[0, 90, 18]$. This NOC corresponds to the following cases: {Very, A Few, All, All, All, All, All}.

The next NOC is [0, 18, 0] and it corresponds to cases: {Very, More, Great, Several, All, All, All}. The NOC for the following cases, {Very, All, All, All, All, All, All}, can be obtain from summing together the respective NOC. For {Very, All, All, All, All, All, All} the NOC is the sum of all the NOCs in Table 9.8, [141,156,27]. For the following cases, {Very, More, Bad, Several, High, All, All}, the NOC is [2,2,2]. The NOCs are used to determine the colors using the legend in Figure 9.9,

$$[\text{Red, Green, Blue}] = \frac{\text{NOC}}{\max(\text{NOC})}. \quad 9.20$$

So, the color legend values for the leftmost cell in the Table 9.8, “Very”, represented by {Very, All, All, All, All, All, All}, is [$\sim 0.9, 1, \sim 0.17$]. Using these values and the legend in Figure 9.9, the respective color for the “Very” cell was obtained. For {Very, More, Bad, Several, High, All, All} the color legend values are [1, 1, 1]. That is why the respective cell is white.

The original table created was broken into three tables because of its length. This first table, Table 9.8, covers DWEs that are very dynamic. If the nature of the DWE is very dynamic then most of the cases are best for the ICM technique. Thus occurs when there are a few or more than a few feedback bits per coherence time.

Dynamic nature of the DWE	Number of feedback bits per coherence time	MP model	Info bits needed per subcarrier	SNR	RX memory capacity	Bandwidth omissions	Number of Cases		
							D	I	N
Very	A Few	All	All	All	All	All	0	90	18
	More	Great	Several	All	All	All	0	18	0
			A Few	Low	All	All	0	6	0
				Medium	All	All	0	6	0
				High	Minimum	All	0	3	0
					Large	All	3	0	0
		Good	Several	All	All	All	0	15	3
			A Few	Low	Minimum	All	0	2	1
				Large	All	3	0	0	
				Medium	All	All	6	0	0
				High	All	All	6	0	0
		Bad	Several	Low	Minimum	All	0	2	1
					Large	Fifth	1	0	0
						Third	0	1	0
				Half		0	1	0	
				Medium	Minimum	All	0	2	1
					Large	Fifth	1	0	0
						Third	1	0	0
				Half		0	0	1	
				High	Minimum	All	0	2	1
					Large	Fifth	1	0	0
	Third	1	0			0			
	Half	0	0			1			
	Many More	Great	A Few	All	All	All	18	0	0
			Several	Low	All	All	0	6	0
				Medium	Minimum	Fifth	0	1	0
					Third	0	1	0	
					Half	1	0	0	
		High	Large	All	3	0	0		
		Good	A Few	All	All	All	6	0	0
			All	All	All	All	18	0	0
Bad			All	All	All	36	0	0	
			All	All	All	36	0	0	

Table 9.8: Case studies for a very dynamic DWE.

Tables 9.9 is for the moderately dynamic wireless environment, and in Table 9.10 the DWE is slightly dynamic. In most of these cases the DCM technique is considered to be the best. In moderately dynamic cases where there are a few information bits per subcarrier, and the multipath model is great, the ICM technique will most likely be best. The same can be said if the multipath model was changed to a good model and the radio needed to send back several information bits per subcarrier.

Dynamic Nature of the DWE	Number of feedback bits per coherence Time	MP models	Info bits needed per subcarrier	Noise level	RX Memory Capacity	Bandwidth omissions	Number of Cases			
							D	I	N	
Moderately	A Few	Great	Several	All	All	All	0	18	0	
				Low	All	All	0	6	0	
				Medium	Minimum	All	0	3	0	
					Large	Fifth	0	1	0	
						Third	1	0	0	
						Half	1	0	0	
			A Few	High	Minimum	Fifth	0	1	0	
						Third	0	1	0	
					Half	1	0	0		
					Large	All	3	0	0	
		Good		Several	Low	All	All	0	4	2
			Medium		Minimum	All	0	2.5	0.5	
					Large	Fifth	1	0	0	
						Third	0	1	0	
						Half	0	0.5	0.5	
			High	Minimum	All	0	2	1		
				Large	Fifth	1	0	0		
					Third	1	0	0		
					Half	0	1	0		
					A Few	Low	Minimum	All	0	2
		Medium	Large	All		3	0	0		
			All	All		6	0	0		
		High	All	All		6	0	0		
		Bad	Several	Low		Minimum	All	0	2	1
				Large		All	3	0	0	
						Medium	Fifth	1	0	0
				Third			0	1	0	
				Half	0		0	1		
				Large	Fifth		1	0	0	
					Third		1	0	0	
	Half				0	0	1			
	High			Minimum	Fifth	0	1	0		
					Third	1	0	0		
			Half		0	0	1			
			Large	All	3	0	0			
				All	All	18	0	0		
	More		Great	Several	Low	Minimum	All	0	3	0
						Large	Fifth	0	1	0
					Third		0	1	0	
					Half		1	0	0	
					Medium	Minimum	Fifth	0	1	0
				Third			0	1	0	
				Half			1	0	0	
		Large		All		3	0	0		
				All		6	0	0		
		A Few		All	All	18	0	0		
	Good		All	All	All	36	0	0		
			Bad	All	All	All	36	0	0	
		Many More	All	All	All	All	108	0	0	

Table 9.9: Case studies for a moderately dynamic DWE.

Dynamic Nature of the DWE	Number of feedback bits per coherence Time	MP models	Info bits needed per subcarrier	Noise level	RX Memory Capacity	Bandwidth omissions	Number of Cases		
							D	I	N
Slightly	A Few	Great	Several	Low	Minimum	All	0	3	0
					Large	Fifth	0	1	0
						Third	0	1	0
						Half	1	0	0
						Fifth	0	1	0
				Medium	Minimum	Third	1	0	0
						Half	1	0	0
					Large	All	3	0	0
				High	All	All	6	0	0
			A Few	All	All	All	18	0	0
		Good	All	All	All	All	36	0	0
		Bad	All	All	All	All	36	0	0
	More	All	All	All	All	All	108	0	0
	Many More	All	All	All	All	All	108	0	0

Table 9.10: Case studies for a slightly dynamic DWE.

There are some other important special cases. Whenever there are many more than a few information bits that can be sent back over the feedback channel, in most cases the DCM technique will be the best. Another special case is when there are a few information bits that can be sent over the feedback channel per coherence time, a great multipath model for the ICM technique, several bits that need to be sent back per subcarrier, and high noise level. Most of these cases will be best for the ICM technique.

The proof of the initial statement that the ICM technique is best in very dynamic wireless environments is shown in these tables. These tables also break the channel and techniques into 937 cases that are qualitatively defined by seven parameters. Users can use these qualifications and outcomes of the inequality to make general statements about what techniques are best.

9.5 Summary

This chapter covered two simulations and a case study based on one of the simulations. The first simulation, EESIM, gives the user a way to visualize the extrapolated waveform for four of the LEEs. It is a GUI that users can use to change variables pertaining to the wireless environment and view the extrapolated waveforms, “at a click of a button.” The second simulation RMSESIM gives the users the ability to view the RMSE-SE performance metric for the ICM and DCM technique, and shows its accuracy by comparing it to a sampled version of the same metric. Also, RMSESIM allows users to compare the performance of the ICM and NCM technique with respect to the angular-frequency and time.

One of the most valuable parts of this chapter is the case study based on the RMSESIM performance comparison. From the performance comparison the user can determine the IET_{DCM} . The IET_{DCM} and IUT_{DCM} can then be used in the inequality in Equation 9.19. The results of the inequality can be varied by changing seven parameters. Each of these variations is referred to as cases, and the inequality in each of these cases determines if the ICM, DCM, or NCM technique is the best. This is captured in Tables 9.8 – 9.10. Listed below are a few of the things to take away from these tables. Note, these statements and the determination of what technique is best are based on the logical outcome of the inequalities or the variation of these outcomes.

- The performance outcome (i.e. which techniques are the best) varies the most with the dynamic nature of the DWE.
- The performance outcome varies the least with the bandwidth omission. This is interesting because the RMSE-SE varies a lot with respect to the omitted bandwidth.
- If the DWE is very dynamic then in most of the cases the ICM technique will be the best.

- If the receiver can send much more than a few information bits back to the transmitter per coherence time then in most of the cases the DCM technique will be best.
- If the DWE is moderately dynamic and the receiver can only send back a few information bits per coherence time and the multipath model is great for the ICM technique then even in the moderately dynamic environment ICM technique will be best in most cases.

CHAPTER TEN

INDIRECT CHANNEL MEASUREMENTS EXPERIMENT

10.1 Introduction

This chapter will cover an experiment that was conducted during the course of this research which used the ICM and the full channel measurement (FCM) technique. This experiment used universal software radio peripherals (USRPs) to show how the ICM technique can measure a portion of the wireless channel, the OOB channel, and extrapolate another portion, the IB channel. These experiments used the FCM technique to approximate the actual channel. By using the estimation obtained from the FCM technique, the ICM technique can be visually compared to the best estimate of the actual wireless channel.

Also, the experiment presented in this thesis captures some of the aspects and features of EESIM. The ability to view the extrapolated and estimated waveform is the main feature that is actualized through this experiment. Another feature that will be discussed is the ability to vary the different parameters defined in Chapter Seven and generate different

case studies for other experiments. This thesis only covers one of the case studies. Another important and informative feature shown through this experiment is a comparison of the theoretical RMSE-SE calculated by using the theoretical values and the sampled RMSE-SE calculated with experimental values.

The rest of this chapter covers the setup and results of the experiment. The setup of the experiment given in this thesis covers the USRP transmitter and receiver design for the ICM technique and the ICM post processing. The results from the experiment resemble the results obtained from the EESIM and RMSESIM simulation tools, but are limited to the ICM and FCM techniques. The next section in this chapter discusses the experiment setup.

10.2 Estimator and Extrapolator Simulator

In Chapter 5 a depiction of a wireless communication system is given in Figure 5.1. The experimental setup is derived from this basic system. The linear system block diagram in Figure 5.1 is adapted to suit the ICM technique and is shown in Figure 10.1.

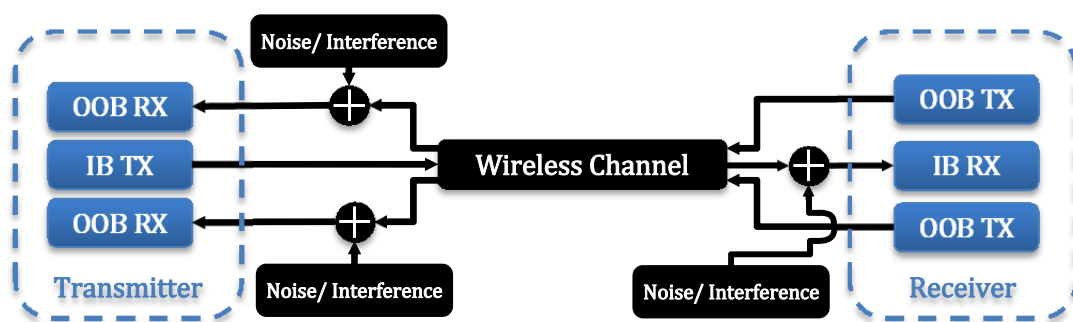


Figure 10.1: Wireless communication system model for a system that is using the ICM technique.

Figure 10.1 shows the actual linear model for a wireless communication system that uses the ICM technique in a full-duplex fashion. The transmitter and receiver are

full-duplex. The transmitter is able to transmit on the IB channel and receive on the OOB channels. The receiver can receive on the IB channel and transmit on the OOB channels. The wireless channel consists of the IB and OOB channels. The IB and OOB channels are in the same temporal and spatial domains but different spectral domains.

Portions of the linear model in Figure 10.1 were implemented in the experiment setup. The experiment setup used two laptops each connected to a USRP. One laptop was used to emulate an impulse sent through the wireless channel, and the other laptop measured the OOB channels or the full channel. This setup is shown in Figure 10.2.

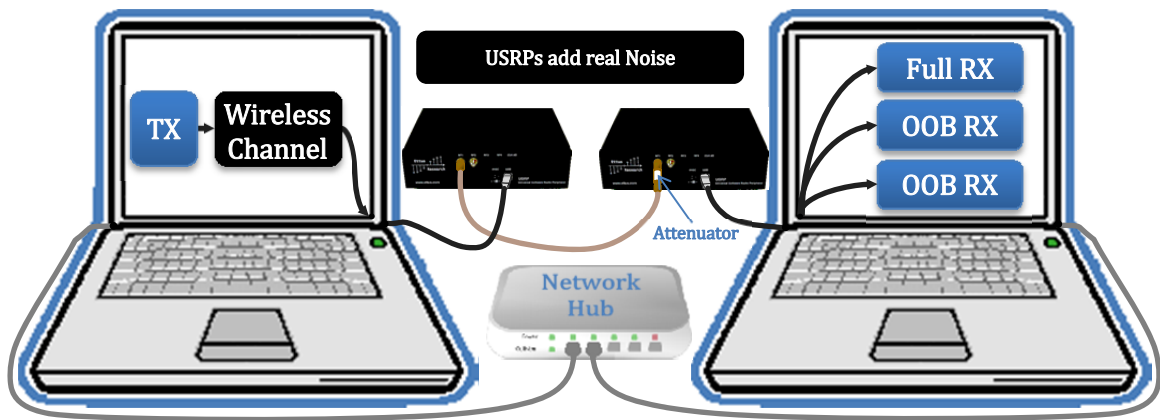


Figure 10.2: ICM experiment setup.

As seen in Figure 10.2 the computer on the left creates the wireless channel excited by a transmitted signal. Part of the transmit signal also contains overhead used to conduct the experiments. This overhead will be discussed in the subsequent subsection. The signal to transmit is sent to the USRP. The USRP begins transmitting the signal via coax cable to the other USRP. The signal transmitted is attenuated to prevent clipping. The received signal is obtained by observing either of the OOB channels or the full channel. The network hub is

used to automate the experiment. The USRP transmitter and receiver are explained in further detail in the next section.

USRP Transmitter and Receiver Design

The transmitter is a software defined radio (SDR). The SDR hardware is the USRP and the software is GNURadio run using the Pipeline software setup designed by a group at Carnegie Mellon University [23]. The transmitting USRP was set to have a center frequency of 2402 MHz and an interpolation rate of 32. The interpolation rate of 32 means the USRP has a bandwidth of 4 MHz with respect to complex samples. The 4 MHz bandwidth does not suggest the multipath nature of the wireless channel. The channel used can be and was more frequency selective than what is typically seen for a 4 MHz channel. The 4 MHz channel will be treated as if it were a 100 MHz channel with respect to its frequency selectiveness.

The transmit signal is an OFDM signal, and when viewed in the time-angular-frequency matrix domain the variable K is equal to 320. The channel model used for the transmitted signal is the EDT 16° multipath model. Only part of the transmitted signal is used to show the effects of the channel. The transmit signal had multiple parts shown in Figure 10.3: synchronization and training signals, and spaces. There was also a transmission signal for initial frequency synchronization shown in Figure 10.4

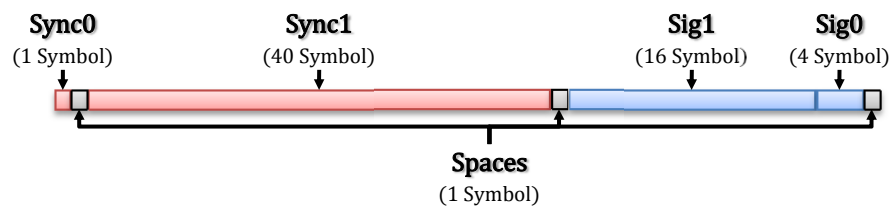


Figure 10.3: USRP transmit signal.

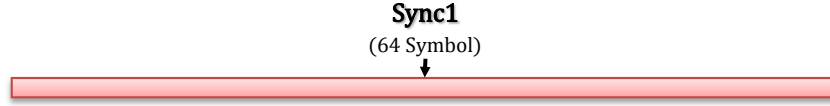


Figure 10.4: USRP transmit signal for initial frequency synchronization.

For the transmit signal a symbol length was 400 samples. The guard interval was 80 samples, hence $K = 320$. The total length of the transmitted signal is 25600 complex samples.

The synchronization signal Sync0 was used for time synchronization and was a CI-OFDM symbol that uses all 320 subcarriers. Sync1 was used for frequency synchronization and it is also a CI-OFDM symbol but it uses only 20 evenly space subcarriers. The spaces had no signal and were used to estimate the noise floor as well as to avoid settling time effects from the receiver. The training signal Sig1 was used to determine the receiving USRP filter and Sig0 was used to determine the wireless channel. Sig1 and Sig0 were both CI-OFDM symbols that used all 320 subcarriers. Sig0 was the only part of the signal that included the effects of the channel.

When obtaining the received signal for the FCM technique, the receiving USRP captured 102400 complex samples at a decimation rate of 16. This means that the bandwidth was 4 MHz. The center frequency for the receiving USRP was also set to be 2402 MHz plus any necessary frequency adjustments obtained from initial frequency synchronization. Unlike the FCM technique, in the ICM technique the decimation rate, number of complex samples, and center frequency of the receiving USRP can be equal to several different values in this experiment setup. The decimation rate and center frequency for the ICM technique were determined from the variables K_{obsrv} , K_{omit} , K , the FCM receive decimation rate and the number of complex samples used in the FCM technique. Using these variables, tables where

created to determine the variables for the ICM technique. Table 10.1 shows the outline of the tables and Tables 10.2 – 10.4 shows the tables with actual values. Equations 10.1 – 10.6 show the calculation for the values in Table 10.1. The variables and values in the grey shaded cells were used to determine the green blocks. The dark and lighter colors are just used to group similar variables.

	Actual USRP Bandwidth	K_{obsrv}	ICM Decimation Rate		ICM Number of Complex Samples
K_{omit}	Actual Omitted USRP Bandwidth	Center Frequencies	Left OOB Channel Beginning and Ending Indices	IB Channel Beginning and Ending Indices	Right OOB Channel Beginning and Ending Indices

Table 10.1: Table outline for receiving USRP variable for the ICM technique.

$$\text{Actual USRP Bandwidth} = \frac{64000\text{kHz} (K_{obsrv})}{\underbrace{K}_{320} \underbrace{dec_{FCM}}_{16}} = 12.5\text{kHz} (K_{obsrv}) \quad 10.1$$

$$\text{Actual Omitted USRP Bandwidth} = 12.5\text{kHz} (2K_{omit}) \quad 10.2$$

$$\text{Center Frequencies} = \pm 12.5\text{kHz} \left(\frac{K_{obsrv} + 2K_{omit}}{2} \right) \quad 10.3$$

$$dec_{ICM} = \frac{K(dec_{FCM})}{2K_{omit}} \quad 10.4$$

$$\text{Number of Complex Samples ICM} = \frac{\left(\frac{\text{Number of Complex Samples FCM}}{dec_{FCM}} \right) (dec_{FCM})}{dec_{ICM}} \quad 10.5$$

$$\begin{bmatrix} \text{Left OOB Channel Beginning Index} \\ \text{Left OOB Channel End Index} \\ \text{IB Channel Beginning Index} \\ \text{IB Channel End Index} \\ \text{Right OOB Channel Beginning Index} \\ \text{Right OOB Channel End Index} \end{bmatrix} = \begin{bmatrix} 161 - K_{omit} - K_{obsrv} \\ 160 - K_{omit} \\ 161 - K_{omit} \\ 160 + K_{omit} \\ 161 + K_{omit} \\ 160 + K_{omit} + K_{obsrv} \end{bmatrix} \quad 10.6$$

Using these equations the subsequent tables were generated. A total of 180 cases were conceived for the ICM technique by varying K_{omit} , K_{obsrv} , and K . The variables K_{omit} , K_{obsrv} , and K must obey the inequalities in Equations 7.4 – 7.6. The variables K_{omit} and K_{obsrv} must be a factor of 640 because the USRP requires an even decimation rate and the fact that K equals 320 or 640 in this research and experiments. Tables 10.2 – 10.4 show 37 of the 180 cases. In the tables $K = 320$, $dec_{FCM} = 16$, and the number of complex samples for FCM is 102400.

	1600.00 kHz	(128)	40		40960		
1	25.00 kHz	±812.50 kHz	[32	159	160	161	162 289]
2	50.00 kHz	±825.00 kHz	[31	158	159	162	163 290]
4	100.00 kHz	±850.00 kHz	[29	156	157	164	165 292]
5	125.00 kHz	±862.50 kHz	[28	155	156	165	166 293]
8	200.00 kHz	±900.00 kHz	[25	152	153	168	169 296]
10	250.00 kHz	±925.00 kHz	[23	150	151	170	171 298]
16	400.00 kHz	±1000.00 kHz	[17	144	145	176	177 304]
20	500.00 kHz	±1050.00 kHz	[13	140	141	180	181 308]
32	800.00 kHz	±1200.00 kHz	[1	128	129	192	193 320]

Table 10.2: Receiving USRP variable for the ICM technique and $K_{obsrv} = 128$.

	500.00 kHz	(40)	128		12800		
1	25.00 kHz	±262.50 kHz	[120	159	160	161	162 201]
2	50.00 kHz	±275.00 kHz	[119	158	159	162	163 202]
4	100.00 kHz	±300.00 kHz	[117	156	157	164	165 204]
5	125.00 kHz	±312.50 kHz	[116	155	156	165	166 205]
8	200.00 kHz	±350.00 kHz	[113	152	153	168	169 208]
10	250.00 kHz	±375.00 kHz	[111	150	151	170	171 210]
16	400.00 kHz	±450.00 kHz	[105	144	145	176	177 216]
20	500.00 kHz	±500.00 kHz	[101	140	141	180	181 220]
32	800.00 kHz	±650.00 kHz	[89	128	129	192	193 232]
40	1000.00 kHz	±750.00 kHz	[81	120	121	200	201 240]
64	1600.00 kHz	±1050.00 kHz	[57	96	97	224	225 264]

Table 10.3: Receiving USRP variable for the ICM technique and $K_{obsrv} = 40$.

	200.00 kHz	(16)	320		5120			
1	25.00 kHz	±112.50 kHz	[144	159	160	161	162	177]
2	50.00 kHz	±125.00 kHz	[143	158	159	162	163	178]
4	100.00 kHz	±150.00 kHz	[141	156	157	164	165	180]
5	125.00 kHz	±162.50 kHz	[140	155	156	165	166	181]
8	200.00 kHz	±200.00 kHz	[137	152	153	168	169	184]
10	250.00 kHz	±225.00 kHz	[135	150	151	170	171	186]
16	400.00 kHz	±300.00 kHz	[129	144	145	176	177	192]
20	500.00 kHz	±350.00 kHz	[125	140	141	180	181	196]
32	800.00 kHz	±500.00 kHz	[113	128	129	192	193	208]
40	1000.00 kHz	±600.00 kHz	[105	120	121	200	201	216]
64	1600.00 kHz	±900.00 kHz	[81	96	97	224	225	240]
80	2000.00 kHz	±1100.00 kHz	[65	80	81	240	241	256]
128	3200.00 kHz	±1700.00 kHz	[17	32	33	288	289	304]

Table 10.4: Receiving USRP variable for the ICM technique and $K_{obsrv} = 16$.

The sending and receiving of the transmitted signal can be automated after obtaining all the desired transmitter and receiver values. The automation was done in MATLAB. For this experiment $K_{obsrv} = 128$ and $K_{omit} = 32$. Therefore, the decimation rate was 40, the center frequencies were ± 1200 kHz plus initial frequency adjustment, and the number of received complex samples for each OOB channel was 40960. The transmitter values were not varied.

The MATLAB automation procedure and USRP setup is given in Figure 10.5. This automation was done after determining the frequency adjustment needed at the receiver using the transmit signal designed for the initial frequency synchronization.

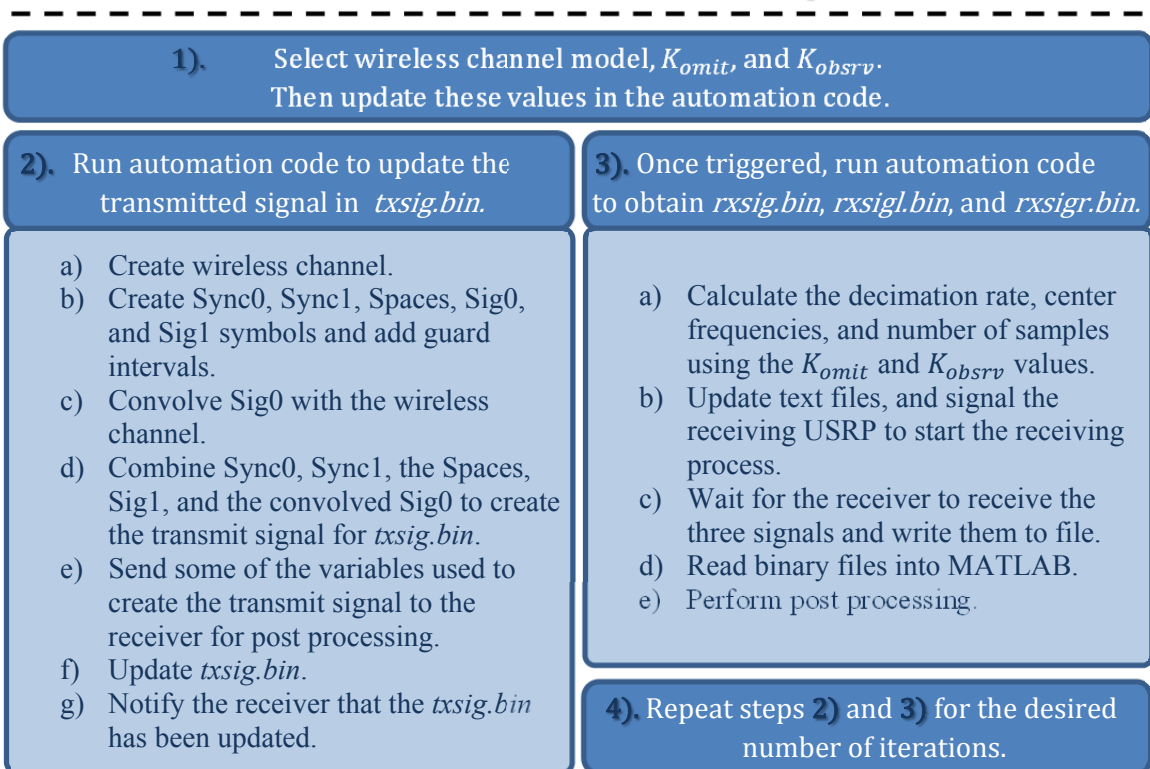
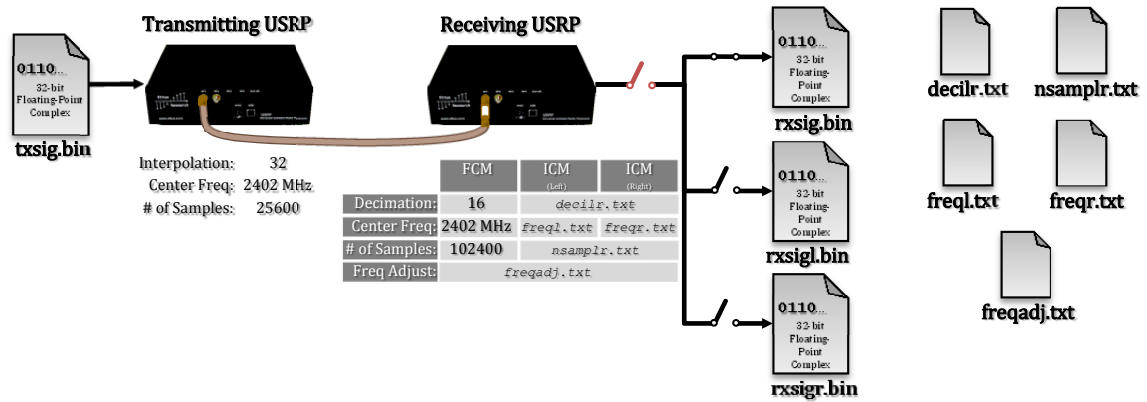


Figure 10.5: USRP transmit signal for initial frequency synchronization.

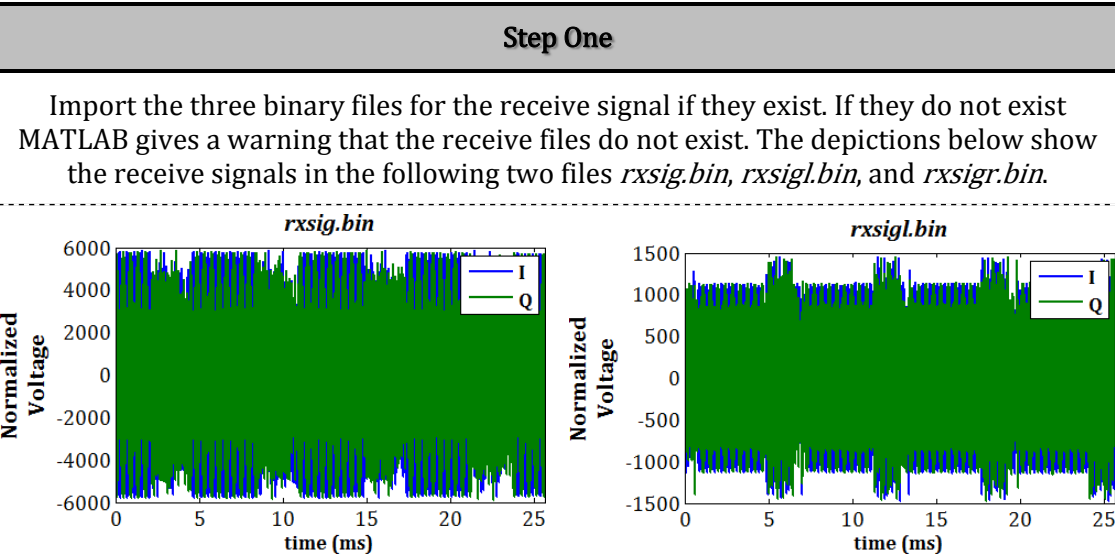
The transmitting USRP was always sending the binary file in the figure. The receiving USRP received and stored the binary file when it was signaled to do so. This signaling is represented by the red switch in the figure. When the switch is closed, the receiving USRP goes through and flips each of the black switches to obtain the respective receive binary files. After obtaining these files the red switch is flipped to the open position. Note that the

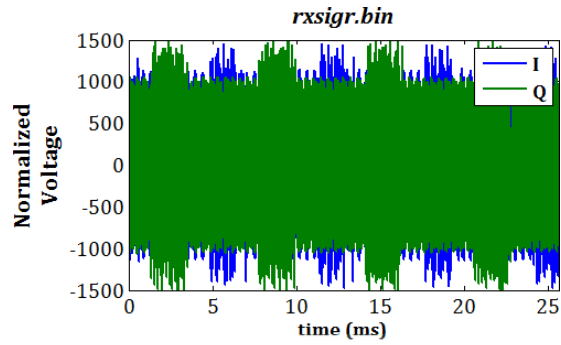
signaling is done in software and not hardware. The SDR process and the pipeline method are explained in [23].

In this experiment there were 990 iterations performed. Through the post-processing the ICM technique’s performance was viewed. In the next subsection the post-processing is discussed.

Post Processing

In this section the post processing will be broking in to steps and listed in the unlabeled tables below. These tables give a description of the step in the process and a depiction illustrating the signal during the step in the process. Note that the “l” or “r” at the end of a variable or file signifies the variable or file for the left or right OOB channel respectively.



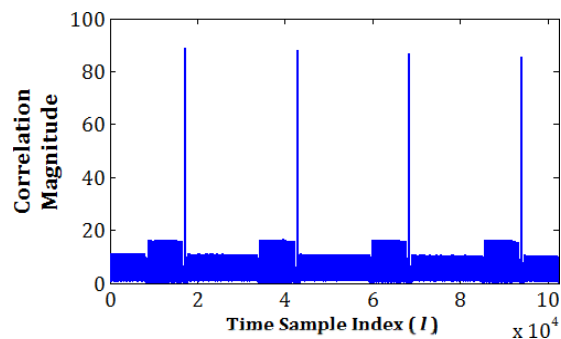


Step Two

Use the variables sent via the network hub from the transmitting USRP computer to reconstruct the signals Sync0, Sync1, Sig1, and the unconvoluted Sig0. These signals are also created for the left and right OOB channel

Step Three

Correlate Sync0, Sync0l, and Sync0r with the respective receive signals rxsig, rxsigl, and rxsigr. Then pick the maximum peak. This peak determines the part of the received signal to use for the rest of the processing. However if the max correlation value falls below a certain threshold. MATLAB stops the processing and gives a warning. Depicted below is rxsig convolved with Sync0 for time synchronization.

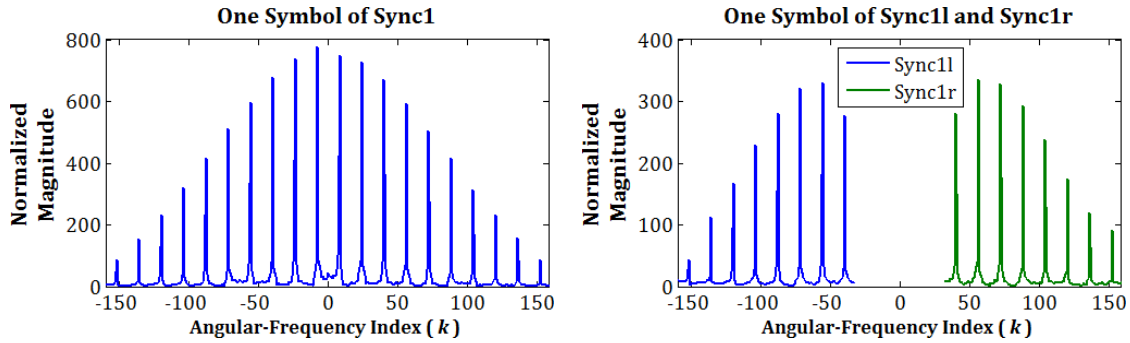


Step Four

Divide the extracted part of rxsig, rxsigl, and rxsigr into the five respective parts: Sync0, Sync1, Sig0, Sig1, and Spaces.

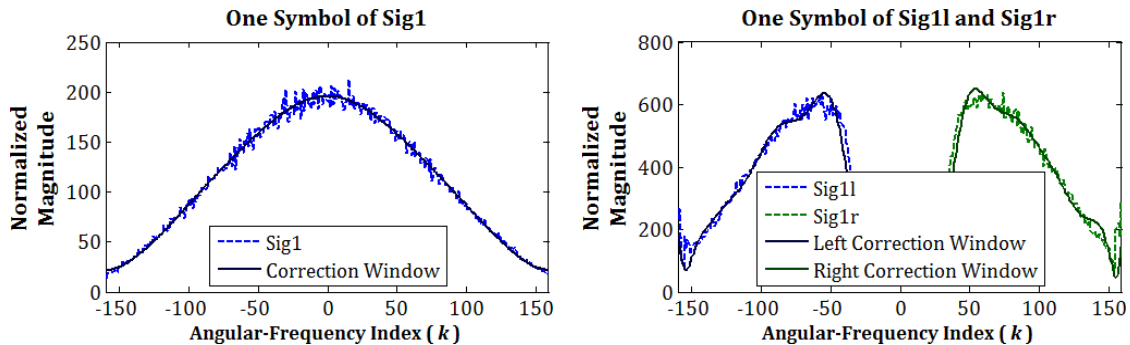
Step Five

Use Sync1 to do more frequency synchronization and remove any frequency shifts. Depicted is one of the Sync1 symbols for rxsig, rxsigl, and rxsigr.



Step Six

Use Sig1 to determine the correction window to account for the filtering from the USRP. Depicted is one symbol from Sig1, Sig1l, Sig1r, and the respective correction windows.

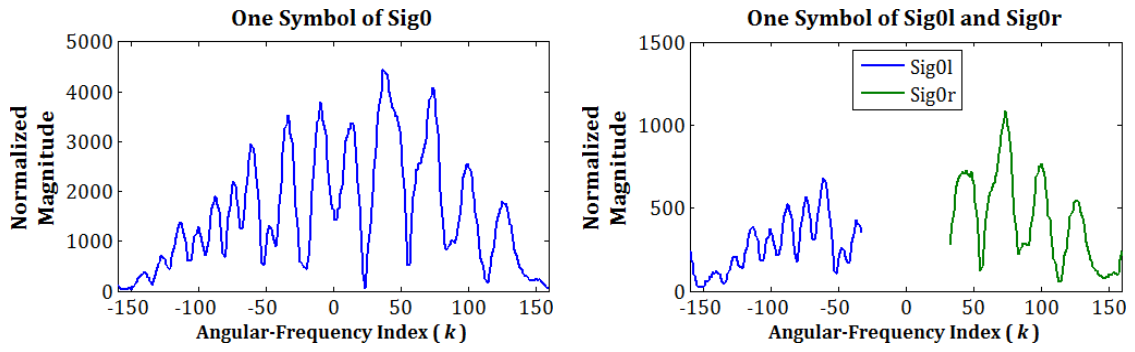


Step Seven

From the Spaces estimate the noise floor

Step Eight

Obtain the measured values from Sig0. Depicted are the measured values for the FCM and ICM techniques. The FCM uses Sig0 and ICM uses Sig0l and Sig0r. So, one symbol of these signal are shown



Step Nine

Save MATLAB workspaces and all the variables to calculate results for the ICM and FCM techniques. Then notify the transmitter to transmit update the channel.

This concludes the post processing procedures. In the next section the calculation of the results and the results themselves will be discussed.

10.3 Experiment Results

The main purpose of the post processing is to obtain the correction windows in Step Six, the noise floor in Step Seven, and the measured values in Step Eight. With these values and the predetermine values of K_{omit} and K_{obsrv} , Equations 7.23, 7.24, and 7.26 can be used to estimate and extrapolate the wireless channel using the ICM technique. Similarly, Equations 7.24 and 7.26 can be used to estimate the wireless channel using the FCM technique by setting $K_{omit} = 0$. Note, in the equations $K_2 = 0$ and $R_{t,t_l} = 1$ for the ICM and FCM techniques.

The introduction of the correction window introduces a new term to Equation 7.24. For the FCM technique, Equation 10.7 shows the Schur complement with correction window term \mathbf{V}_{full} , and Equation 10.8 shows the Schur complement for the ICM technique with the

correction window term \mathbf{V}_{lr} . The correction window terms are diagonal matrices. In the case of \mathbf{V}_{lr} it is the diagonal concatenation of the left and right correction windows,

$$\mathbf{P}_{\tau,FCM} = \left[\mathbf{R}_{\tau}^{-1} + (\mathbf{V}_{full} \mathbf{X}_{X_x} \mathbf{F}_F)^H \underbrace{\mathbf{R}_{W_w}^{-1}}_{\substack{\text{Noise} \\ \text{Term} \\ \text{Full}}} (\mathbf{V}_{full} \mathbf{X}_{X_x} \mathbf{F}_F) \right]^{-1}, \quad 10.7$$

$$\mathbf{P}_{\tau,ICM} = \left[\mathbf{R}_{\tau}^{-1} + (\mathbf{V}_{lr} \mathbf{O}_{y_c} \mathbf{X}_{X_x} \mathbf{F}_F)^H \underbrace{(\mathbf{O}_{y_c} \mathbf{R}_{W_w} \mathbf{O}_{y_c}^T)^{-1}}_{\substack{\text{Noise Term for} \\ \text{Left and Right}}} (\mathbf{V}_{lr} \mathbf{O}_{y_c} \mathbf{X}_{X_x} \mathbf{F}_F) \right]^{-1}. \quad 10.8$$

Equations 10.7 and 10.8 are created from Equations 7.23, 7.24, and 7.26 to estimate and/or extrapolate the wireless channel Equation.

$$\hat{\mathbf{h}}_{c,FCM} = \mathbf{F}_F \mathbf{P}_{\tau,FCM} (\mathbf{V}_{full} \mathbf{X}_{X_x} \mathbf{F}_F)^H \mathbf{R}_{W_w}^{-1} \underbrace{\mathbf{y}_{c,full}}_{\text{Sig0}}. \quad 10.9$$

$$\hat{\mathbf{h}}_{c,ICM} = \mathbf{F}_F \mathbf{P}_{\tau,ICM} (\mathbf{V}_{lr} \mathbf{O}_{y_c} \mathbf{X}_{X_x} \mathbf{F}_F)^H (\mathbf{O}_{y_c} \mathbf{R}_{W_w} \mathbf{O}_{y_c}^T)^{-1} \underbrace{\mathbf{y}_{c,lr}}_{\substack{\text{Sig0l and} \\ \text{Sig0r}}}. \quad 10.10$$

Figure 10.6 was created using Equations 10.9 and 10.10. Shown in the figure are the estimation and/or extrapolation obtained from using the FCM or ICM technique for the respective received signal(s). It also shows the channel used at the transmitter, but it is not visible because the FCM technique, as stated, estimates the channel very well. At the end of this section there are three other figures similar to Figure 10.6 but they use different receive signal(s).

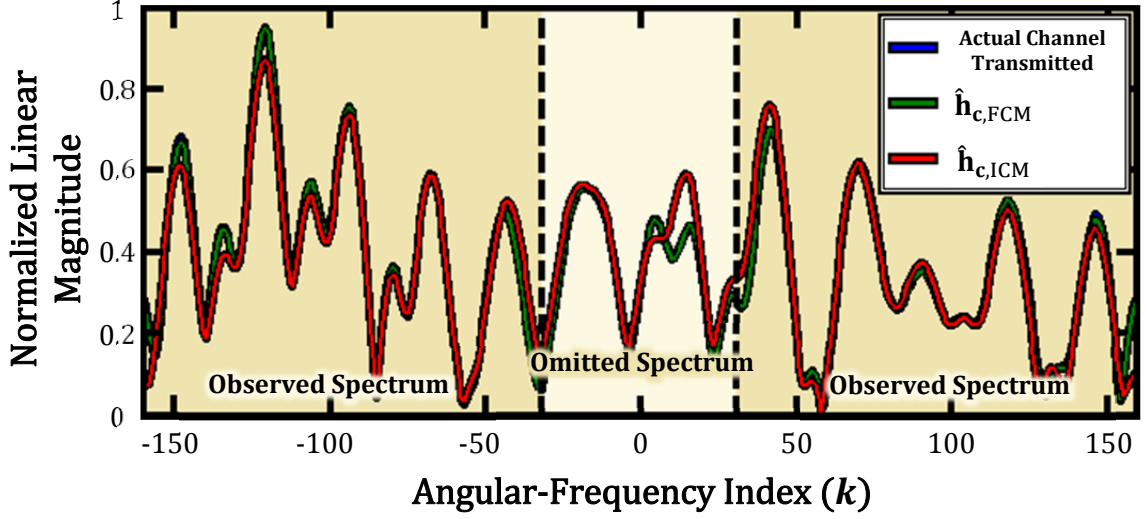


Figure 10.6: Wireless channel estimation and extrapolations calculated in case one.

Similar to the EESIM, this experiment and the figures show that the ICM technique is able to extrapolate the omitted spectrum. This begs the question, “What is the accuracy of the ICM technique in this experiment?” RMSE-SE can be used to determine the accuracy of the ICM technique. The equation to calculate this metric is given in Chapter Seven and rewritten here in Equation 10.11,

$$\mathbf{z}_{c,ICM,t_l} = \sqrt{\text{diag} \left(2(\mathbf{R}_\omega - \mathbf{P}_{\omega,ICM}) \circ \mathbf{P}_{\omega,ICM} + (\mathbf{P}_{\omega,ICM} \circ \mathbf{P}_{\omega,ICM}^*) + \text{diag}(\mathbf{P}_{\omega,ICM})\text{diag}(\mathbf{P}_{\omega,ICM})^H \right)}, \quad 10.11$$

$$\mathbf{P}_{\omega,ICM} = \mathbf{F}_F \mathbf{P}_{\tau,ICM} \mathbf{F}_F^H. \quad 10.12$$

Through simulations, the simulator RMSESIM shows how accurate this metric is in determining the performance of the ICM technique. It compares the theoretical RMSE-SE to the sampled RMSE-SE. This experiment was used to further prove the accuracy of the RMSE-SE. This was done by comparing Equation 10.11, which is used for the theoretical RMSE-SE, to the sampled RMSE-SE. The sampled RMSE-SE was obtained by estimating and extrapolating the channel for all 990 iterations using the ICM and FCM technique. Once the

channel estimation and extrapolations were obtained they were used to calculate the square root of the average of the difference between the squared envelopes obtained from the ICM and FCM techniques. Figure 10.7 shows this comparison.

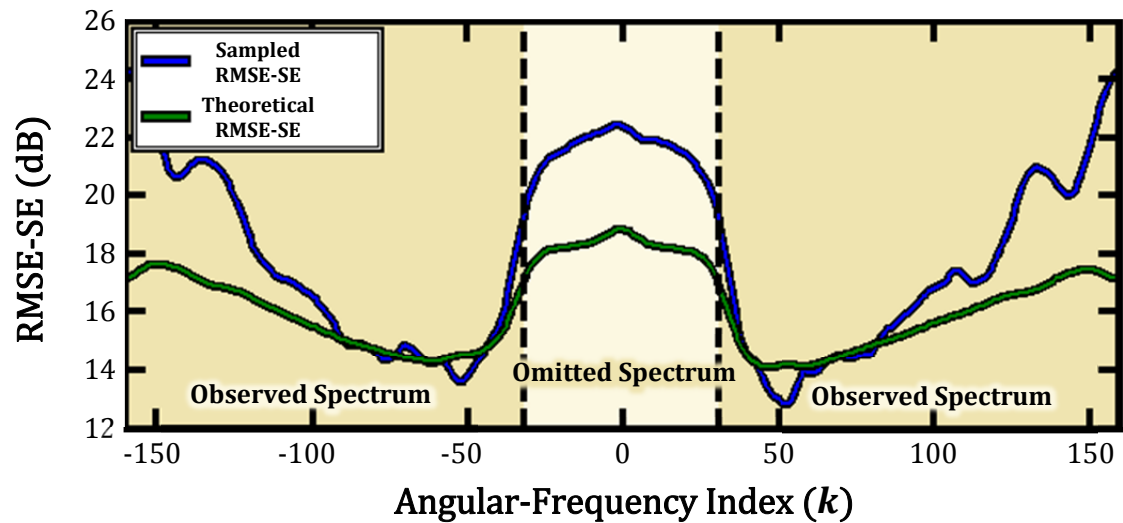


Figure 10.7: Theoretical and sampled RMSE-SE comparison obtained through experimentation

In Figure 10.7 a difference of approximately 3.5 dB can be seen between the sampled and theoretical RMSE-SE in the omitted spectrum band. For RMSESIM, there is approximately no difference between the sampled and theoretical. This difference in Figure 10.7 can be attributed to the estimation of the correction windows and the noise floors. These values are used in the equations as if they were the exact values, but they actually possess some error. This error causes the difference that is seen in the figure. Even given this difference between the sampled and the theoretical, this experiment further demonstrates the accuracy of the RMSE-SE metric. With sound theory, validated through simulations and experiment, it can be stated that the RMSE-SE can be used to accurately determine the performance of the ICM technique. This section will be concluded with more channel estimations and extrapolations similar to that in Figure 10.6.

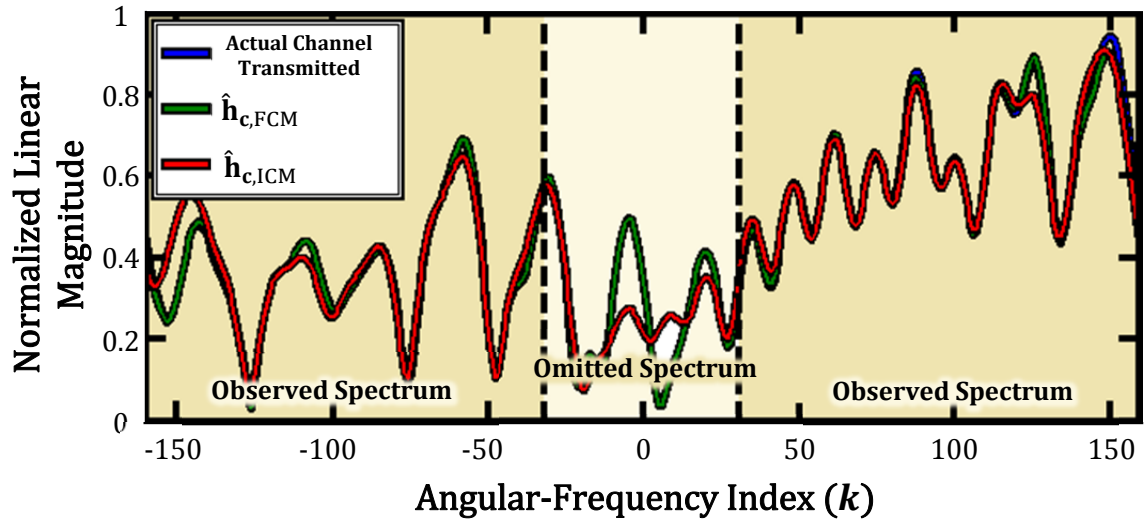


Figure 10.8: Wireless channel estimation and extrapolations calculated in case two.

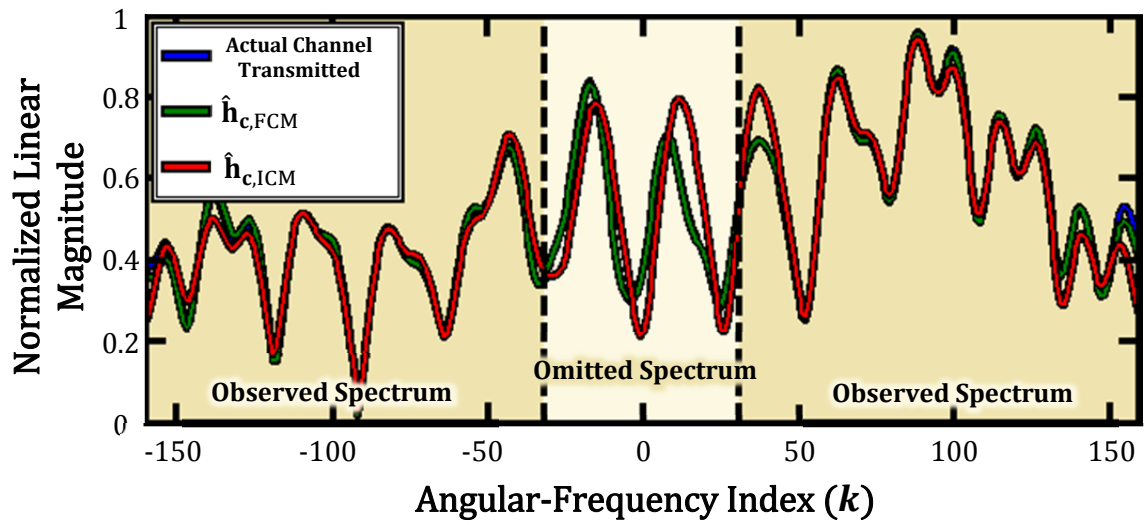


Figure 10.9: Wireless channel estimation and extrapolations calculated in case three.

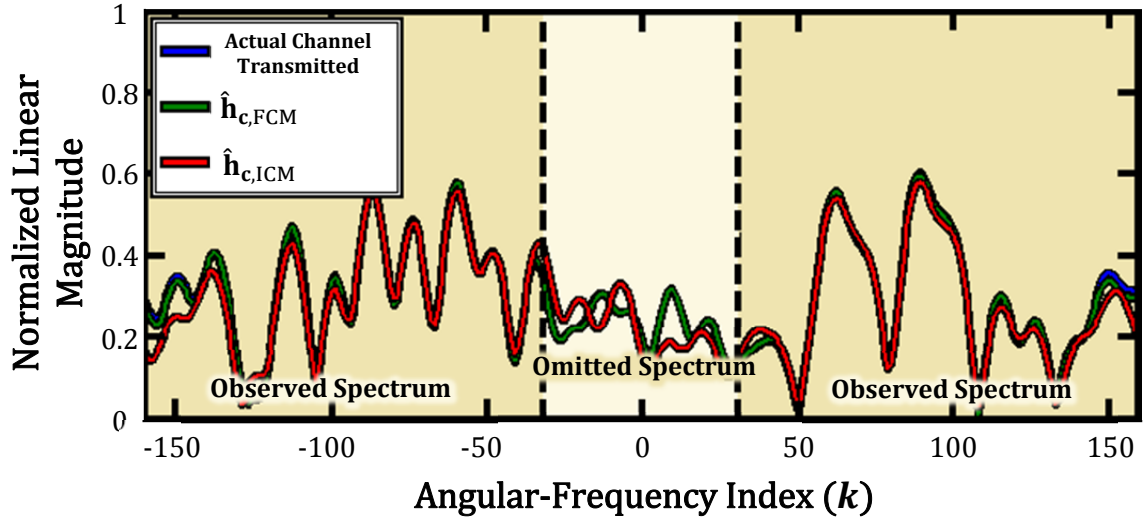


Figure 10.10: Wireless channel estimation and extrapolations calculated in case four

10.4 Summary

In summary, this chapter has explained the experiment that was design to verify that the ICM technique works with real hardware. This experiment used USRPs and the Pipeline interface to transmit a signal that had already been convolved with the channel. This signal was received and processed by another USRP using the Pipeline interface. After post processing, results were generated to show that the ICM technique works and to verify the ICM performance metric.

The results from the experiment showed that the ICM technique worked as theorized and simulated. Since real hardware was used, the effects of this hardware had to be accounted for by using a correction window to aid in determining the estimation and/or extrapolation.

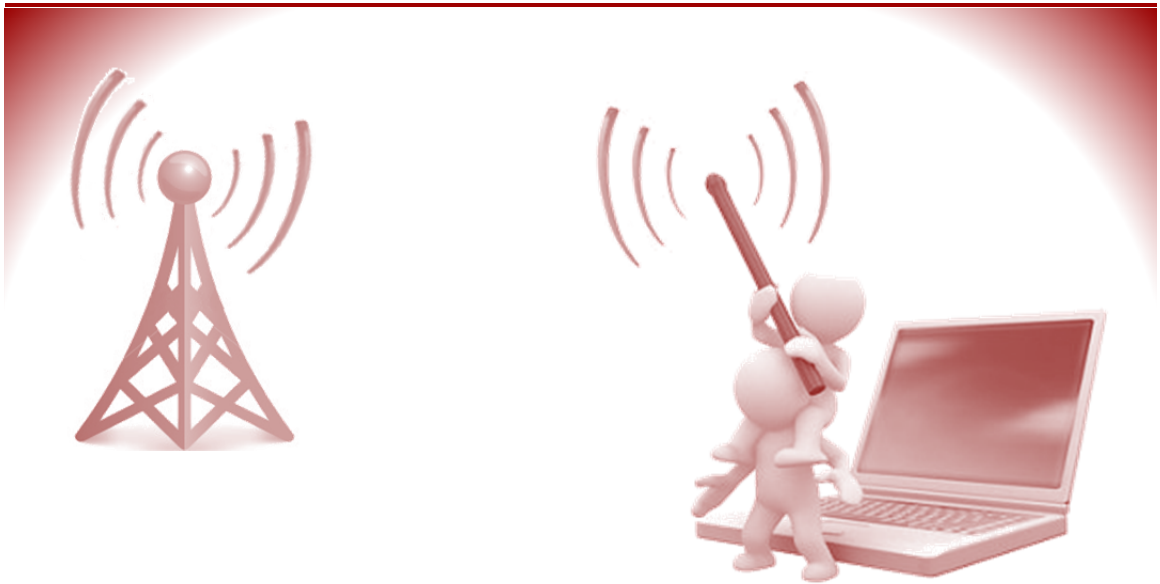
As in other chapters, the accuracy of the estimated and extrapolated channel was measured with the RMSE-SE. The theory behind this metric was given in Chapter Seven and

verified through simulations using the RMSESIM. In this chapter this metric was verified through experimentation using a similar method to that in the RMSESIM. With minor errors due to the estimation of the correction window and noise floor, the experiment verified that the equation for the RMSE-SE is an accurate calculation of the performance metric.

Overall, these experiments showed that the idea of extrapolating IB wireless channel from the OOB channels works and its performance can be verified through the use of the RMSE-SE equations. This is a major step towards designing a system that can fully implement the technique shown in Figure 10.1 or the network in Figure 8.5.

PART IV

CONCLUSION



Part IV is the last part of this thesis. The first chapter in this part will begin to conclude the thesis by giving a review of all that has been presented, a clear overview of all the contributions made during the course of this research, and the meaning of the contributions to the body of work in the respective research area. The final chapter will discuss how to further the research that has been presented through future work. This part will cover:

- A review of the thesis.
- A highlighting of the contributions.
- The meaning of the contributions with respect to the area of research.
- A discussion of future research.

CHAPTER ELEVEN

THESIS REVIEW

11.1 Thesis Summary and Research Questions

In Chapter One the background and scope was given. With respect to the scope, this thesis covered sensing and learning techniques that could be used in cognitive radios and/or networks to obtain the instantaneous channel state information (ICSI) needed for radio network effectiveness (RNE) in dynamic wireless environments (DWEs). In this thesis the channel state information (CSI) could be statistical CSI (SCSI) like the covariance matrices of the channel, noise variance, SNR, and/or other statistical values, or the CSI could be the ICSI, such as the channel impulse response (CRI) or transfer function (TF). The RNE in this thesis was the end-to-end objectives associated with cognitive radios and/or networks trying to increase their throughput or capacity through implementing a rate adaptation system that varied the modulation scheme(s) used.

First Research Question

In Chapter Two the research methodology was given. At the end of the chapter three questions were presented. The first question was “How can radios obtain the ICSI in a timely and accurate manner in DWEs?” The timely and accurate sensing and learning of the ICSI can be done through deploying three techniques: indirect channel measurements (ICM) technique, direct channel measurements (DCM) technique, or the no channel measurement (NCM) technique. The ICM technique uses measurements from the present and future out-of-band (OOB) channel along with the SCSi to learn the ICSI for the present and future in-band (IB) channel. In contrast, the DCM technique uses past and present IB channel measurements along with SCSi to obtain the ICSI for the present and future IB channel, and the NCM technique only uses SCSi to obtain the present and future IB channel. These techniques can be summarized with the depiction in Figure 11.1.

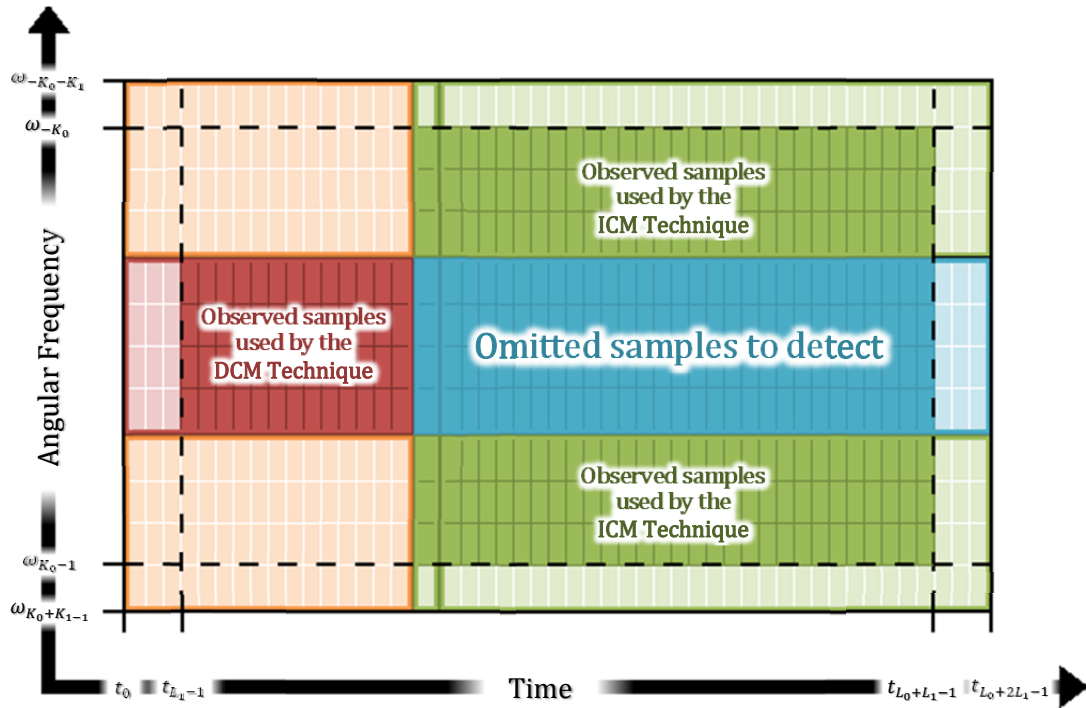


Figure 11.1: Wireless channel two dimensional block diagram that indicates how total coherence blocks are used.

In Figure 11.1 the red color blocks are used by the DCM technique, the green colored blocks by the ICM technique, and the blue blocks are extrapolated. Similar to Figure 4.2, this figure shows blocks that are in the time-angular-frequency domain, and each block represents multiple total coherence blocks, as defined in Chapter Four. The figure shows what part of the channel that is measured by the ICM and DCM techniques, and the part of the channel that is extrapolated by all three techniques.

The linear estimator and extrapolators used in the ICM and DCM techniques can be categorized as angular-frequency or time linear estimators and extrapolators. This thesis defines estimators and extrapolators as any technique that uses a set of channel total coherence blocks to determine the same (estimator) or different (extrapolator) set of channel total coherence blocks. The estimators and extrapolators in this thesis are used to estimate or extrapolate the statistical definition of the channel derived in Chapter Four and represented here in Equation 11.1,

$$\mathbf{H}_{H_h} = \mathbf{B}_{A_a} = \mathbf{F}_F \mathbf{C}_\tau \mathbf{N}_{(M \times N)} \mathbf{C}_f \mathbf{F}_I = \mathbf{F}_F \mathbf{B}_{a_A}. \quad 11.1$$

In Chapter Six Equations 11.2 and 11.3 was presented.

$$\underbrace{\mathbf{O}_{\hat{\mathbf{h}}_{c,(LEE),t_l}} \hat{\mathbf{h}}_{c,H_h,t_l}}_{\hat{\mathbf{h}}_{c,(LEE),H_h,t_l}} = \mathbf{G}_{\mathbf{y}_{c,(LEE),t_l}} \underbrace{\mathbf{O}_{\mathbf{y}_{c,(LEE),t_l}} \mathbf{y}_{c,Y_y,t_l}}_{\mathbf{y}_{c,(LEE),Y_y,t_l}}. \quad 11.2$$

$$\underbrace{\hat{\mathbf{h}}_{r,H_h,\omega_k} \mathbf{O}_{\hat{\mathbf{h}}_{r,(LEE),\omega_k}}}_{\hat{\mathbf{h}}_{r,(LEE),H_h,\omega_k}} = \underbrace{\mathbf{y}_{r,Y_y,\omega_k} \mathbf{O}_{\mathbf{y}_{r,(LEE),\omega_k}}}_{\mathbf{y}_{r,(LEE),Y_y,\omega_k}} \mathbf{G}_{\mathbf{y}_{r,(LEE),\omega_k}}. \quad 11.3$$

The variables $\mathbf{G}_{\mathbf{y}_{c,(LEE),t_l}}$ and $\mathbf{G}_{\mathbf{y}_{r,(LEE),\omega_k}}$ define the type of linear estimator and/or extrapolator used. Given Equation 11.1, statistically the most accurate $\mathbf{G}_{\mathbf{y}_{c,(LEE),t_l}}$ and $\mathbf{G}_{\mathbf{y}_{r,(LEE),\omega_k}}$ is the one created from using Bayesian analysis. Chapter Six gives several other ways to create these matrices but in this thesis the focus is on the most accurate estimator and extrapolator for the angular-frequency and time domains. Listed in Table 11.1 are other

angular-frequency and time estimators and extrapolators along with the ICM and DCM techniques.

Technique	Type	Linear Matrix	Omission Matrices
LSEP	Ang.-Freq. Extrapolator	$\mathbf{G}_{y_c, \text{LSEP}}$ (Equation 7.7)	\mathbf{O}_{y_c} (Equation 7.3)
LSEP w/MP Reduction	Ang.-Freq. Extrapolator	$\mathbf{G}_{y_c, \text{LSEP} \setminus \text{MPr}}$ (Equation 7.17)	\mathbf{O}_{y_c} and \mathbf{O}_{MPr} (Equation 7.16)
SRWC	Ang.-Freq. domain Extrapolator	$\mathbf{G}_{y_c, \text{SRWC}}$ (Equation 7.11)	\mathbf{O}_{y_c}
SRWC w/MP Reduction	Ang.-Freq. Domain Extrapolator	$\mathbf{G}_{y_c, \text{SRWC} \setminus \text{MPr}}$ (Equation 7.19)	\mathbf{O}_{y_c} and \mathbf{O}_{MPr}
ICM	Ang.-Freq. Domain Extrapolator	\mathbf{G}_ω (Equation 7.23)	\mathbf{O}_{y_c}
DCM	Time Domain Extrapolator	\mathbf{G}_t (Equation 7.36)	\mathbf{O}_{y_r} (Equation 7.31)
NCM	Ang.-Freq. and Time Domain Extrapolator	Constant value	$\mathbf{0}_{(\text{Row} \times \text{Col})}$
FCM	Ang.-Freq. or Time Domain Extrapolator	\mathbf{G}_ω or \mathbf{G}_t	\mathbf{O}_{y_c} or \mathbf{O}_{y_r}

Table 11.1: Summary of the estimators and/or extrapolators in Chapter Seven.

Equations 11.2 and 11.3 also have omission matrix pairs. These matrix pairs can be used to determine if the technique is an estimator or extrapolator.

Second Research Question

The second research question was “what method was the best in DWEs?” To answer this question, the mean squared error (MSE) and the root mean squared error of the squared envelope (RMSE-SE) performance metrics were used. Each of these metrics gives a numerical value that is correlated with the estimation and/or extrapolation performance of

each of the three techniques. These values from the MSE or the RMSE-SE can be used in various types of wireless environments to compare the ICM, DCM, and NCM techniques. For DWEs there are situations where the ICM technique is best and there are situations where the DCM technique is the best. Figure 11.2 shows these situations for one case.

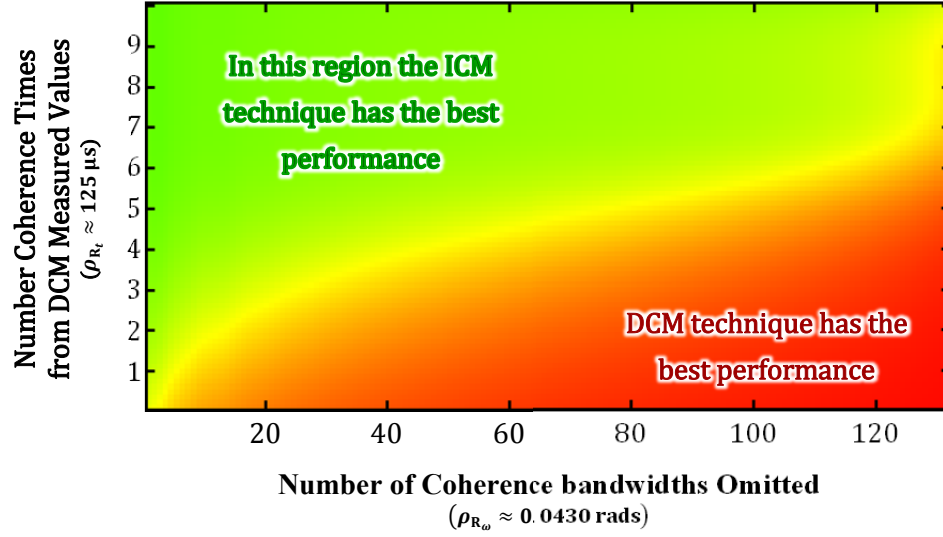


Figure 11.2: Optimal performance color map of the ICM and DCM techniques for ED delay channel model with a slope decline of 36 degrees; and a Jakes spectral model for the frequency taps with a 1 kHz Doppler shift.

The MSE comparison for the ICM and DCM estimator-extrapolator is shown in Figure 11.2. The y-axis is the number of coherence times the extrapolation is away from the DCM estimates. The x-axis is the number of coherence bandwidths omitted. In this thesis and for this DWE case, in situations where the extrapolation is several coherence times away from the estimate the ICM technique will outperform the DCM technique.

Not shown in the Figure 11.2, but discussed in the thesis is the comparison of the ICM and DCM techniques to the NCM technique. The ICM and DCM techniques performances are always better than or approximately equal to the performance of the NCM technique. In cases where the performance of the NCM technique is approximately the same to that of the

ICM and/or DCM technique, the NCM technique will be preferred because it does not require any measurements.

For any DWE case, a similar analysis with the RMSE-SE and MSE can be done to determine which technique has the best performance for that DWE case.

Third Research Question

The third question asked how the answers from the first and second questions relate to the RNE of the cognitive radios and /or networks. This question was addressed in Chapter Eight. Chapter Eight gave a detailed explanation on how the ICM and DCM techniques can be used to improve RNE. Also, Chapter Eight presented some more metrics related to rate adaptation: the information update time (IUT) and expiration time (IET), bits per sub carrier (BPS), bits in error (BIE), and bit error rate (BER).

The IUT and IET for the respective measurement technique will indicate if the technique will work for rate adaptation. If the time it takes to update the ICSI, IUT, is greater than the amount of time the information is considered valid, IET, then the measurement technique will not work or will have poor performance for rate adaptation. IET and IUT can be used to give a basic understanding of how the performance of each measurement technique compares with respect to rate adaptations.

The other metrics (i.e. BPS, BIE, and BER) in Chapter Eight give a more in-depth understanding of the measurement techniques' effect on rate adaptation. BPS, BIE, and BER are more closely related to the end-to-end objective. The cognitive radio and/or network may have a desired data rate or link quality it wishes to maintain, and the BPS, BIE, and BER

are direct indicators of things like the data rate and link quality. In Chapter Eight the probability of obtaining a particular BPS and BER is given and rewritten here,

$$\Pr\{\hat{S}_{l,k} \in \mathbb{S}_{T_{BPS}}, S_{l,k} \in \mathbb{S}_{T_{BER,BPS}}\} = \sum_{n=0}^{\infty} \left[\frac{\beta_n}{4(\alpha_s^2 \alpha_r^2)^{n+1}} \right] \Gamma(n+1, \alpha_s^2 \hat{s}_r^2) \Big|_{\hat{s}_{r,0}}^{\hat{s}_{r,1}} \cdots \cdots \Gamma(n+1, \alpha_s^2 s_r^2) \Big|_{s_{r,0}}^{s_{r,1}}. \quad 11.4$$

Given the square root of the extrapolated SNR or SNIR obtained from one of the measurement techniques and the square root of the actual SNR or SNIR, the probability of obtaining a particular BPS and/or BER can be determined using Equation 11.4. This is a powerful equation. Researchers and engineers can pre-calculate a system's performance before designing and/or deploying it by using Equation 11.4. Along with the IUT and IET, this equation also answers the third question by showing how the measurement techniques affect RNE.

Simulations and Experiments

Chapters One, Two, and Three gave the background for and scope of the research. Chapters Four and Five gave the notational framework and conceptual understanding to answer the research questions. Chapter Six and part of Chapter Seven addressed the first research question. The rest of Chapter Seven covered the second research question, and Chapter Eight answered the third question. Chapters Nine and Ten presented the simulations and experiment to support the theory presented in the other chapters.

To support the theories developed in Chapters 6 – 8, two simulators were created: EESIM and RMSESIM. Through simulation, EESIM allows users to change the parameters of the DWE and see the actual estimated and extrapolated waveforms of a few of the

estimators and extrapolators in this thesis. A snapshot of the program interface is given in Figure 11.3.

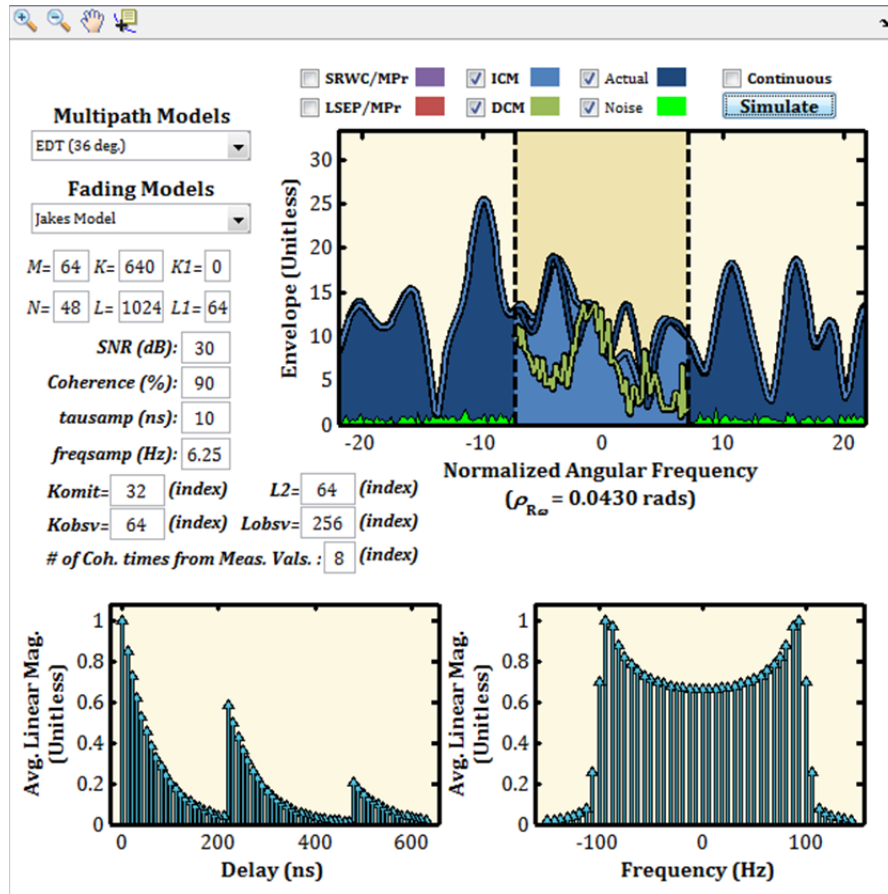


Figure 11.3: EESIM GUI.

The simulator RMSESIM gives users the ability to verify and view the accuracy of the RMSE-SE performance metric for the ICM, DCM, and NCM technique. RMSESIM also allows users to do a performance comparison of the three techniques as well. Snapshots of the simulator interface are given in Figures 11.4 and 11.5.

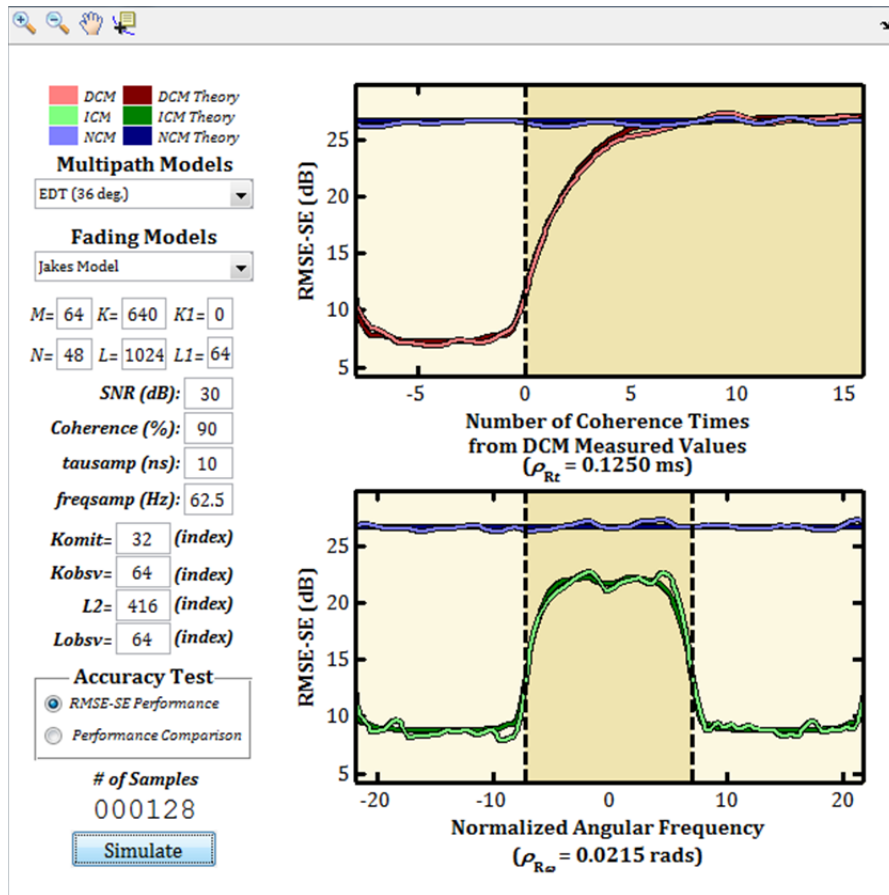


Figure 11.4: RMSESIM GUI showing the theoretical and sampled RMSE-SE.

These simulations showed that the theory for the measurement techniques were sound. It also gave users the ability to see how these measurement techniques performed in various DWE cases.

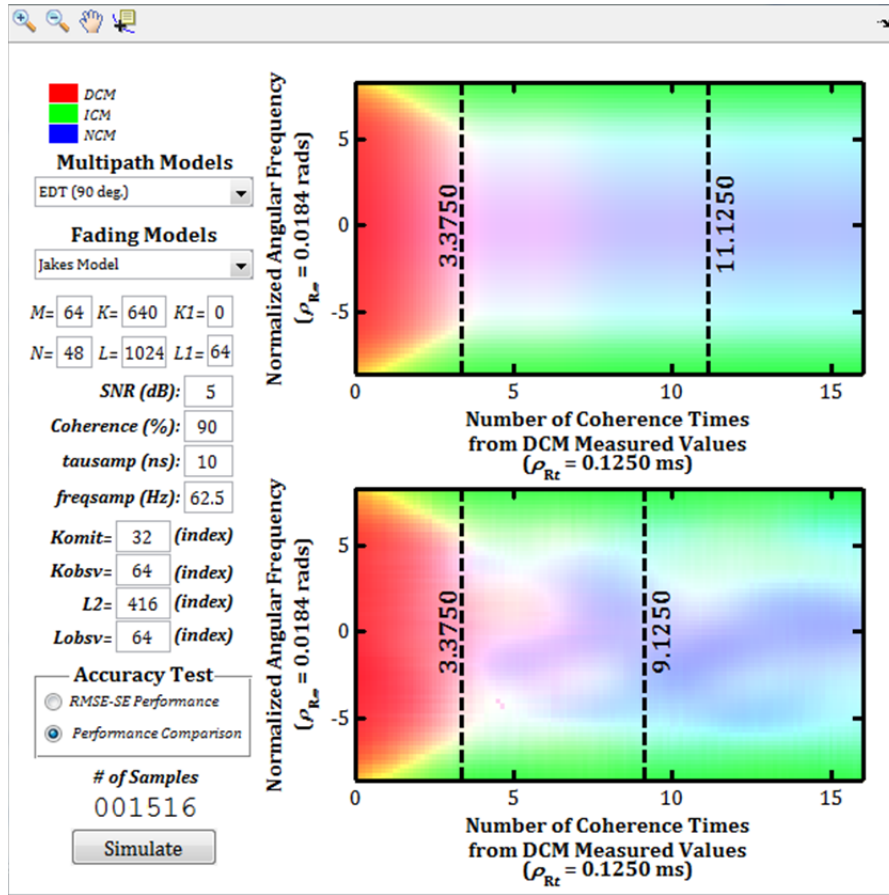


Figure 11.5: RMSESIM GUI showing the performance comparison.

To further verify the ICM technique and to show its ability to be implemented in hardware the experiment presented in Chapter Ten was conducted. Similar to EESIM, this experiment showed the actual estimated and extrapolated waveform from the ICM technique, shown in Figures 10.6 and 10.8 – 10.10. In the experiment real hardware was used and not a simulation. This showed the accuracy of the technique as well as how hardware implementation might work.

The experiment also showed the accuracy of the RMSE-SE performance metric. The sampled performance metric obtained through the experiment was slightly skewed because

of the estimation of some of the constant terms in the theory. Figure 10.7 shows the experimental and theoretical RMSE-SE.

11.2 Thesis Contributions

To conclude the thesis review a clear and detailed account of the contributions and their value to the respective research area will be given. In this thesis there are many contributions, some minor. The main contribution of this thesis is the indirect channel measurement technique. Unlike conventional thinking of having to measure the spectrum of interest directly to obtain the ICSI, the ICM technique shows that ICSI of the spectrum of interest can be obtained through indirect measurements.

Intuitively, one might say an indirect measurement would only be able to determine the ICSI for a spectrum equal to approximately one or two coherence bandwidths, but this research shows that this is not the case. The ICM technique can omit much more than two coherence bandwidths and in some cases it can omit more than 50% of the modeled spectrum containing several coherence bandwidths. Having a technique, like the ICM technique, that can indirectly measure the channel can benefit communication systems greatly.

Conventionally, systems that directly measure the spectrum of interest suffer from delayed updates of the ICSI. Mainly due to the need of feeding the information back to the radio that needs the information. Given the reciprocity of the wireless channel, the ICM technique removes the need for that type of information feedback, and this can greatly help wireless communication systems that use ICSI, especially with regards to cognitive radios or networks.

Researchers at Mitsubishi Electric Research Laboratories also had a similar idea to the ICM technique, labeled as the SRWC technique in this thesis, and their paper was published during the course of this research [109]. This thesis showed that the SRWC technique is less accurate than the ICM technique.

There are other differences between the two sets of research, and Table 11.2 gives a side-by-side comparison of these two techniques. Listing only some of the similarities and differences.

	SRWC Research	ICM Research
Researched Angular-Frequency Estimator and Extrapolator	✓	✓
Used classical estimation and extrapolation	✓	✓
Used Bayesian estimation and extrapolation		✓
Does not assume a prior knowledge about the wireless channel statistics	✓	
Uses PN schemes	✓	
Uses MCM Sequences		✓
Studies many different wireless channels		✓
Compares time and angular-frequency extrapolators		✓
Accuracy Analysis		✓
Describes usage of the technique in wireless communication systems		✓
Provides closed form equations		✓

Table 11.2: Side-by-side comparison of the SRWC and ICM research.

ICM Technique Contribution

As stated, the ICM Technique is the main contribution of this thesis, and there are many parts to this contribution. These contributive parts are listed and discussed in the bulleted list below.

- **The Equations for the ICM, DCM, and NCM techniques:** As mentioned, the ICM technique is the most important contribution of this thesis. With regards to the ICM technique as well as the DCM and NCM techniques, there were numerous equations given: equations that gave the estimated and extrapolated waveforms for the wireless channel, ones that gave the respected MSEs, and there are many other equations in Chapter Seven created for this research. These equations give researchers a means to develop these techniques by using this theoretical framework created in Chapter Seven. Unlike the ICM technique, the DCM technique and NCM technique are not considered to be novel. However, presenting the equations using the linear notation in Chapter Six is novel, and it can give researchers a way to directly compare these techniques.
- **RMSE-SE Metric:** The RMSE-SE Metric Equations for the ICM, DCM, and NCM techniques are also given in Chapter Seven. Typically the RMSE or MSE of the envelope is used, but in this research the squared envelope was used. This allowed the creation of a closed form equation that can be used to set a value to the performance of the respective techniques. In contrast, the RMSE or MSE of the envelope did not allow for an easy calculation for the closed form equation. This closed form equation can be used by researchers to quickly and accurately place a value on the technique's performance.

- **EESIM**: Chapter Nine presents two simulators. One of the simulators is EESIM. EESIM allows users to see the estimated and extrapolated waveforms from the ICM, DCM, and a couple other techniques. This simulator also shows which technique has the best performance in the spectrum of interest. The simulators were created by the author and will be made available on request. This simulator gives users the ability to simulate how these techniques will perform in various DWE cases.
- **RMSESIM**: The second simulation in Chapter Nine is RMSESIM. RMSESIM was used to verify the accuracy of the RMSE-SE metrics created for the ICM, DCM, and NCM techniques. It also compared the three techniques and gave indications on which technique had the best performance. Also, this simulator was created by the author and will be made available upon request.
- **ICM Technique Hardware Implementation and Analysis**: There has not been any prior hardware implementation or analysis with respect to the ICM technique, because the ICM technique was created during this research. Chapter Ten details this implementation and analysis.
- **Comparison of the ICM and DCM Techniques**: Another major contribution of this thesis is this comparison of the ICM and DCM techniques that is presented throughout the thesis. There has not been any literature discovered during this research that compares angular-frequency estimators and extrapolators (represented by the ICM technique) to time estimators and extrapolators (represented by the DCM technique). This thesis gives contrasting equations for the two techniques, compares performance metrics, compares their ability in rate adaptation systems, and gives many other ways to compare the ICM and DCM techniques. For many different cases, this thesis shows researchers and engineers

what technique is preferred, or gives them the tools to discern which technique they would prefer for a given case.

- **Wireless Communication Channel Notation:** In Chapter Four the wireless communication channel is reviewed. The underlining concepts presented are not new, but the total coherence block diagram and easily calculated statistical model are. In Chapter Four the equation in Equation 11.1, the statistical model of the channel, was given. All the notation and views that accompany this equation have made simulating the channel easier. As shown in Chapter Four, typically the wireless channel is modeled using conventional two-dimensional matrix analysis. Instead, Equation 11.1 was used to represent the time-angular-frequency domain matrix. This allowed for reduction of the variables needed to model the channel. The use of this type of notation and modeling may be useful to other researchers and engineers in simulating similar systems. This method was conceived through viewing the channel using the total coherence block diagram view instead of the traditional tap delay line model view.
- **Linear Estimator and Extrapolator Notation:** The Linear estimators and extrapolators presented in Chapter Six aids in unifying many different techniques. the notation associated with Equations 11.2 and 11.3 gives a general form that was applied to all the estimation and extrapolation techniques in this thesis, and this general form can aid research and engineers in comparing other estimation and/or extrapolation techniques, as well give an indication what type of technique it is (i.e. estimator or extrapolator, classical or Bayesian, etc...)

Rate Adaptation Contributions

Along with the ICM technique the rate adaption research present also have some meaningful contributions. The ICM technique and rate adaptation methods present are the two main contributions of the thesis. Like the ICM technique research, the rate adaptation research also has contributive parts that are listed below.

- **Rate Adaptation Implementation for the ICM and DCM Techniques:** Chapter Eight gives the basic blueprints on how to develop a rate adaptation system that uses the ICM or DCM techniques. The structure of the wireless communication system, the adaptive modulation scheme, the threshold values used in the selection process, and other things related to the rate adaptation system were discussed and derived. This rate adaptation can potentially be placed into radios, and the biggest benefit of this scheme is that it successfully uses the ICM and DCM techniques in making its adaptive decisions.
- **The IUT and IET Metrics:** Also in Chapter Eight there were a few metric or tools given to aid researchers and engineers in creating rate adaptation systems the same as or similar to what was presented in the chapter. The first metrics were the time it takes to update the ISCSI, the IUT, and the amount of time for which the ICSI is considered valid, the IET. These metrics gave the basic foundation in assessing the performance of the ICM and DCM techniques. For example, if the IUT for the DCM technique is greater than the IET determined by the performance of the ICM and DCM techniques then the ICM technique will be preferred over the DCM technique. These metrics were created during the course of this research to aid similar assessments. This provides researchers with an easy heuristic to make a determination on what technique to use in similar rate adaptation systems.

- **The Joint pdf for the BPS and BER:** There are few other metrics given in Chapter Eight. All the other metrics in the chapter are either a part of or can be obtained from the joint pdf for the BPS and BER: BPS, BER, BIE, the most probable BER and BPS, and the expected BER and BPS. The Joint pdf presented is a powerful equation. Imagine being able to design a rate adaptation system and knowing the probability of this system having particular BPS and BER values. The possibilities are vast. For example, if a system must always operate with a certain BPS and BER value, an Engineer can use this equation to determine how much SNR or SNIR is needed and/or whether or not to use the ICM or DCM techniques, neither, or a combination of the two.

CHAPTER TWELVE

FUTURE RESEARCH

During the course of this research there have been many ideas that were not able to be explored due to time constraints. From reading this thesis some of these ideas may be obvious and others may not. This chapter will not inundate the reader with a medley of ideas, but instead present one idea to push this research forward. That idea is the actual experimental implementation of a cognitive radio network that can deploy the ICM, DCM, and NCM techniques.

First, the dynamic wireless environment (DWE) in the experimental setup will be explained. Note some of these assumptions were given in Chapter Eight: the assumption that the network has a star topology. In the network there is a base station or access point and multiple user nodes. The uplink and downlink channels operate in different spectral channels. Each channel experiences Rayleigh fading and possibly interference from the primary user of the spectrum.

The DWE could be implemented using Carnegie Mellon University's Emulator System or a system like it. This would allow for the simulation of various channels that could be seen in a DWE. It could also simulate the transition from one type of DWE to another. The emulator allows for the connection of real radio hardware, in particular software defined radios (SDRs) for cognitive radio networks.

Some researchers see software defined radios (SDR) as being the radio of the future because of their reconfigurable nature [116-119]. However the vision that will be presented here goes a bit beyond reconfigurable software. It is envisioned that there will be software (SW) cores or RF processing units to do necessary signal processing, protocol management, etc... It is also imagined that future SDRs will have multiple SW cores each connected to RF hardware (ADC, DAC, filters, amplifiers, and other analog devices) or hardware cores working in parallel. The SDR will also have multiple antennas, and each SW core could have sub cores and respective RF hardware that could transmit and receive from each antenna. Each core may or may not be synchronized; the same goes for the RF hardware (HW). This is the vision of future software defined radios presented in this chapter, and a generic depiction of this configuration is shown in Figure 12.1. Using this generic depiction, an explanation of the radios that could be used in the experiment will be given.

To reflect this vision, the experimental setup would have a maximum of four SW cores for the user nodes and the base station. There are two possible RF hardware setups using different universal software radio peripherals (USRPs), shown in Figure 12.2, and the RF HW would be synchronized. One of the setups could use USRP1s and the other could use USRP2s or USRP N200s.

Looking at Figure 12.2 you can see how the radio setup used in this research fits into the vision of future radios.

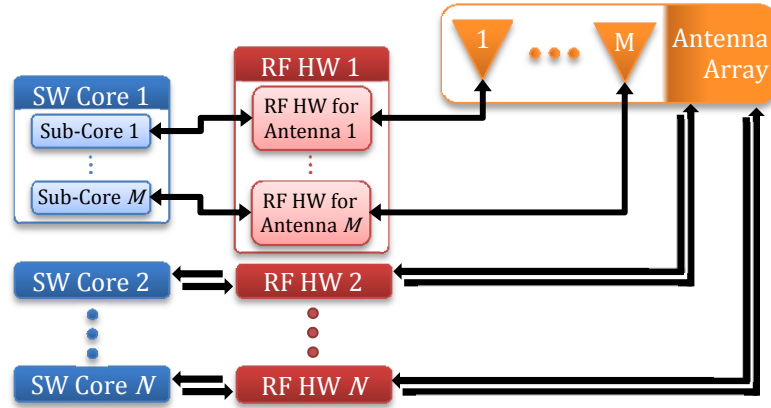


Figure 12.1: Generic block diagram of the author's vision of future radios.

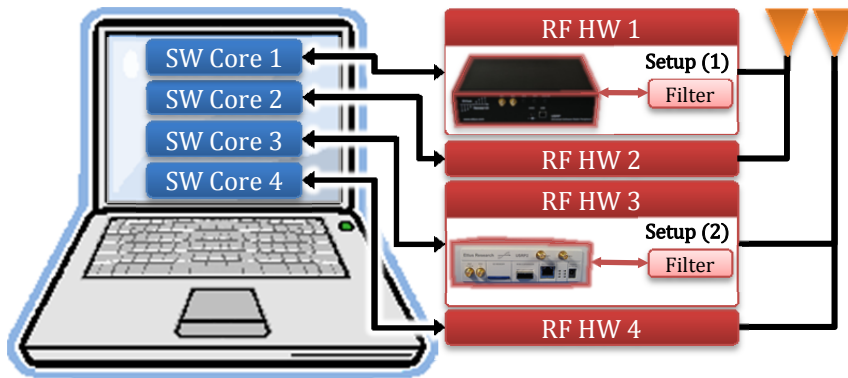


Figure 12.2: Experimental radio setup 1 (USRP1s) and 2 (USRP2s or N200s).

In the overall network, shown in Figure 12.3, there would be a minimum of three radios with one of the above setups. That means there will be one base station and at least two users. The wireless channel could be simulated by the Emulator system. Using the above assumptions and system setup the ICM and DCM technique would be fully implemented along with the rate adaptation schemes in Chapter Eight. Several sensor nodes could also be

used for other cognitive radio/network sensing. The sensor nodes would not have the same functionality as the radio in Figure 12.2, but they would use USRPs.

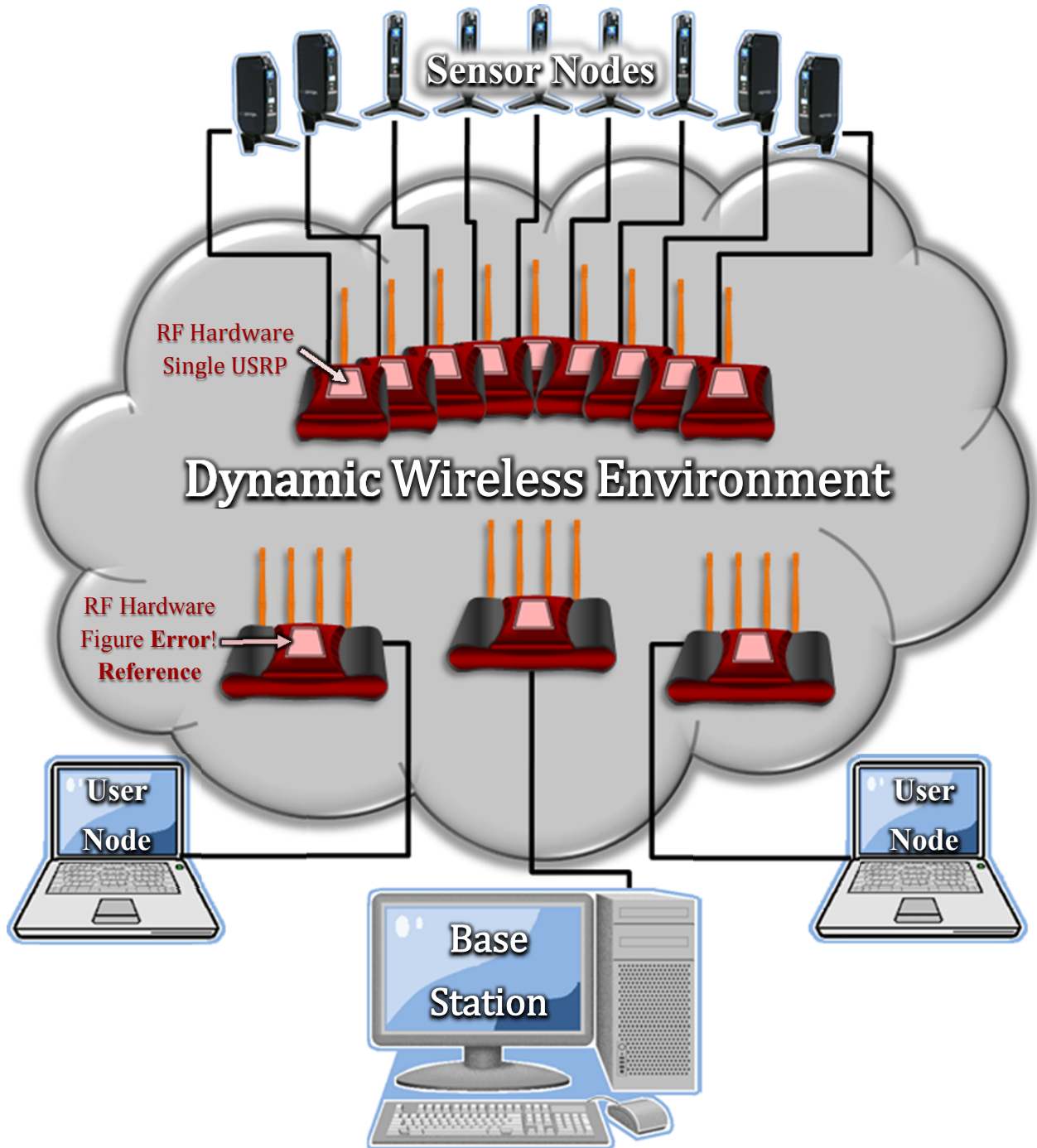


Figure 12.3: Diagram of experimental network setup.

This experimental setup could be ran over several days and data collected to prove some of the metrics given in Chapter Seven and Eight, and to create some new ones. It could also be used to show a functional rate adaptation system that could implement the respective techniques in a cognitive manner. For example, in one DWE the ICM technique could be the best and another DWE the DCM technique could be the best. A cognitive system would be able to determine what type of DWE it is in and reconfigure itself for the respective DWE.

There are many other ideas in this thesis that could be implemented given the time, and may still be implemented in future work. However, this experiment has the greatest potential for furthering and expanding the scope of this research by implementing what has been presented in an actual communication system.

BIBLIOGRAPHY

- [1] B. A. Fette, *Cognitive Radio Technology*, 2nd ed. Burlington, MA: Elsevier Academic Press, 2009.
- [2] S. Haykin, "Cognitive Radio: Brain-Empowered Wireless Communications," *Selected Areas in Communications, IEEE Journal*, vol. 23, pp. 201-220, February 2005 2005.
- [3] S. Haykin, "Cognitive Dynamic Systems," in *Acoustics, Speech and Signal Processing, 2007. ICASSP 2007. IEEE International Conference on*, 2007, pp. IV-1369-IV-1372.
- [4] J. Mitola, III, "Cognitive Radio: An Integrated Agent Architecture for Software Defined Radio," Doctor of Technology, Teleinformatics, Royal Institute of Technology (KTH), Sweden, 2000.
- [5] W. Beibei and K. J. R. Liu, "Advances in cognitive radio networks: A survey," *Selected Topics in Signal Processing, IEEE Journal of*, vol. 5, pp. 5-23, 2011.
- [6] P. Pawelczak, K. Nolan, L. Doyle, S. W. Oh, and D. Cabric, "Cognitive radio: ten years of experimentation and development," *Communications Magazine, IEEE*, vol. 49, pp. 90-100, 2011.
- [7] T. Keller and L. Hanzo, "Adaptive Multicarrier Modulation: A Convenient Framework for Time-Frequency Processing in Wireless Communications," *Proceedings of the IEEE*, vol. 88, pp. 611-640, 2000.

- [8] S. Ye, R. S. Blum, and L. J. Cimini Jr, "Adaptive modulation for variable-rate OFDM systems with imperfect channel information," in *Vehicular Technology Conference, 2002. VTC Spring 2002. IEEE 55th*, 2002, pp. 767-771.
- [9] J. Gross and M. Bohge, "Dynamic mechanisms in OFDM wireless systems: A survey on mathematical and system engineering contributions," *TU-Berlin, Tech. Rep. TKN-06-001*, 2006.
- [10] M. Bohge, J. Gross, A. Wolisz, and M. Meyer, "Dynamic resource allocation in OFDM systems: an overview of cross-layer optimization principles and techniques," *Network, IEEE*, vol. 21, pp. 53-59, 2007.
- [11] D. J. Love, R. W. Heath, Jr., V. K. N. Lau, D. Gesbert, B. D. Rao, and M. Andrews, "An Overview of Limited Feedback in Wireless Communication Systems," *Selected Areas in Communications, IEEE Journal on*, vol. 26, pp. 1341-1365, 2008.
- [12] T. L. Marzetta and B. M. Hochwald, "Fast Transfer of Channel State Information in Wireless Systems," *Signal Processing, IEEE Transactions on*, vol. 54, pp. 1268-1278, 2006.
- [13] M. K. Ozdemir and H. Arslan, "Channel Estimation for Wireless OFDM Systems," *Communications Surveys & Tutorials, IEEE*, vol. 9, pp. 18-48, 2007.
- [14] A. Kawam and M. Ahmed, "Limited Feedback in Wireless Communications and Networks," *INTERNATIONAL JOURNAL OF ADVANCED ELECTRONICS AND COMMUNICATION SYSTEMS*, vol. 2, 2012.
- [15] S. Falahati, A. Svensson, T. Ekman, and M. Sternad, "Adaptive modulation systems for predicted wireless channels," *Communications, IEEE Transactions on*, vol. 52, pp. 307-316, 2004.
- [16] J. Marinho and E. Monteiro, "Cognitive radio: survey on communication protocols, spectrum decision issues, and future research directions," *Wireless Networks*, vol. 18, pp. 147-164, 2012.

- [17] I. F. Akyildiz, W. Y. Lee, M. C. Vuran, and S. Mohanty, "NeXt generation/dynamic spectrum access/cognitive radio wireless networks: a survey," *Computer Networks*, vol. 50, pp. 2127-2159, 2006.
- [18] P. Sutton, L. E. Doyle, and K. E. Nolan, "A reconfigurable platform for cognitive networks," in *Cognitive Radio Oriented Wireless Networks and Communications, 2006. 1st International Conference on*, 2006, pp. 1-5.
- [19] J. Mitola, *Software Radio*: Wiley Online Library, 2003.
- [20] M. Dardaillon, K. Marquet, T. Risset, and A. Scherrer, "Software defined radio architecture survey for cognitive testbeds," in *Wireless Communications and Mobile Computing Conference (IWCMC), 2012 8th International*, 2012, pp. 189-194.
- [21] J. Mitola III, "Software radios: Survey, critical evaluation and future directions," *Aerospace and Electronic Systems Magazine, IEEE*, vol. 8, pp. 25-36, 1993.
- [22] Q. Zhao and B. M. Sadler, "A survey of dynamic spectrum access," *Signal Processing Magazine, IEEE*, vol. 24, pp. 79-89, 2007.
- [23] R. L. Cooper, K. C. Borries, X. Wang, and D. D. Stancil, "A Spatial and Temporal Spectrum Sensing System for Interference Avoidance in Dynamic Spectrum Access," in *SDR Forum*, Washington, D.C., 2009.
- [24] V. D. Chakravarthy, "Evaluation of Overlay/Underlay Waveform via SD-SMSE Framework for Enhancing Spectrum Efficiency," Doctor of Philosophy, Electrical Engineering, Wright State University, Dayton, OH, 2008.
- [25] J. O. Neel, "Analysis and Design of Cognitive Radio Networks and Distributed Radio Resource Management Algorithms," Doctor of Philosophy, Electrical Engineering, Virginia Polytechnic Institute and State University, Blacksburg, Virginia, 2006.
- [26] R. W. Thomas, "Cognitive Networks," Doctor of Philosophy, Computer Engineering, Virginia Polytechnic Institute and State University, Blacksburg, Virginia, 2007.
- [27] T. S. Rappaport, *Wireless Communications Principles and Practice*. Upper Saddle River, New Jersey: Prentice Hall PTR, 1996.

- [28] T. Yucek and H. Arslan, "A survey of spectrum sensing algorithms for cognitive radio applications," *Communications Surveys & Tutorials, IEEE*, vol. 11, pp. 116-130, 2009.
- [29] Q. Liang, M. Liu, and D. Yuan, "Channel estimation for opportunistic spectrum access: uniform and random sensing," *Mobile Computing, IEEE Transactions on*, vol. 11, pp. 1304-1316, 2012.
- [30] E. Hossain, D. Niyato, and Z. Han, *Dynamic spectrum access and management in cognitive radio networks*. Cambridge University Press, 2009.
- [31] M. Haddad, M. Debbah, and A. Menouni Hayar, "Diversity-Multiplexing Tradeoff for Frequency Fading Channels with CSIT," in *Cognitive Radio Oriented Wireless Networks and Communications, 2006. 1st International Conference on*, 2006, pp. 1-5.
- [32] Y. G. Li, L. J. Cimini, Jr., and N. R. Sollenberger, "Robust Channel Estimation for OFDM Systems with Rapid Dispersive Fading Channels," *Communications, IEEE Transactions on*, vol. 46, pp. 902-915, 1998.
- [33] V. Tarokh, N. Seshadri, and A. R. Calderbank, "Space-Time Codes for High Data Rate Wireless Communication: Performance Criterion and Code Construction," *Information Theory, IEEE Transactions on*, vol. 44, pp. 744-765, 1998.
- [34] M. O. Pun, A. F. Molisch, P. Orlik, and A. Okazaki, "Super-Resolution Blind Channel Modeling," in *Communications (ICC), 2011 IEEE International Conference on*, 2011, pp. 1-5.
- [35] A. J. Paulraj and C. B. Papadias, "Space-time processing for wireless communications," *Signal Processing Magazine, IEEE*, vol. 14, pp. 49-83, 1997.
- [36] J. B. Andersen, T. S. Rappaport, and S. Yoshida, "Propagation measurements and models for wireless communications channels," *Communications Magazine, IEEE*, vol. 33, pp. 42-49, 1995.
- [37] D. Tse and P. Viswanath, *Fundamentals of wireless communication*. Cambridge university press, 2005.

- [38] B. P. Lathi, *Modern Digital and Analog Communication Systems 3e* Osece: Oxford university press, 1998.
- [39] G. L. Stüber, *Principles of mobile communication*: Springer, 2011.
- [40] W. G. Newhall, "Wideband propagation measurement results, simulation models, and processing techniques for a sliding correlator measurement system," Citeseer, 1997.
- [41] M. C. Jeruchim, P. Balaban, and K. S. Shanmugan, *Simulation of communication systems: modeling, methodology and techniques*: Springer, 2000.
- [42] B. Sklar, "Rayleigh fading channels in mobile digital communication systems. I. Characterization," *Communications Magazine, IEEE*, vol. 35, pp. 90-100, 1997.
- [43] M. D. Yacoub, *Foundations of mobile radio engineering*: CRC, 1993.
- [44] W. Jakes, *Mobile radio propagation*: Wiley-IEEE Press, 2009.
- [45] J. Parsons and A. Turkmani, "Characterisation of mobile radio signals: model description," in *Communications, Speech and Vision, IEE Proceedings I*, 1991, pp. 549-556.
- [46] A. Turkmani and J. Parsons, "Characterisation of mobile radio signals: base station crosscorrelation," in *Communications, Speech and Vision, IEE Proceedings I*, 1991, pp. 557-565.
- [47] M. K. Simon and M. S. Alouini, *Digital communication over fading channels* vol. 86: Wiley-IEEE Press, 2004.
- [48] B. Sklar, *Digital communications* vol. 2: Prentice Hall, 2001.
- [49] A. V. Oppenheim, R. W. Schaffer, and J. R. Buck, *Discrete-time signal processing* vol. 2: Prentice hall Englewood Cliffs, NJ:, 1989.
- [50] J. P. M. G. Linnartz, "JPL's Wireless Communication Reference Website," ed, 2006.

- [51] H. Schulze and C. Lüders, *Theory and Applications of OFDM and CDMA: Wideband Wireless Communications*. Wiley, 2005.
- [52] H. Liu and G. Li, *OFDM-based broadband wireless networks: design and optimization*. Wiley-Interscience, 2005.
- [53] K. Fazel and S. Kaiser, *Multi-Carrier and Spread Spectrum Systems*. Wets Sussex, England: John Wiley & Sons Ltd, 2003.
- [54] D. A. Wiegandt, Z. Wu, and C. R. Nassar, "High-throughput, high-performance OFDM via pseudo-orthogonal carrier interferometry spreading codes," *Communications, IEEE Transactions on*, vol. 51, pp. 1123-1134, 2003.
- [55] Z. Wu and C. R. Nassar, "Narrowband interference rejection in OFDM via carrier interferometry spreading codes," *Wireless Communications, IEEE Transactions on*, vol. 4, pp. 1491-1505, 2005.
- [56] D. A. Wiegandt, C. R. Nassar, and Z. Wu, "The elimination of peak-to-average power ratio concerns in OFDM via carrier interferometry spreading codes: a multiple constellation analysis," in *System Theory, 2004. Proceedings of the Thirty-Sixth Southeastern Symposium on*, 2004, pp. 323-327.
- [57] L. L. Scharf, *Statistical Signal Processing: Detection, Estimation, and Time Series Analysis*. Reading, MA: Addison-Wesley Publishing Company, Inc., 1991.
- [58] A. Papoulis and R. V. Probability, *Stochastic processes* vol. 3: McGraw-hill New York, 1991.
- [59] X. Cai and G. B. Giannakis, "Adaptive PSAM accounting for channel estimation and prediction errors," *Wireless Communications, IEEE Transactions on*, vol. 4, pp. 246-256, 2005.
- [60] I. C. Wong and B. L. Evans, "Joint channel estimation and prediction for OFDM systems," in *Global Telecommunications Conference, 2005. GLOBECOM'05. IEEE*, 2005, pp. 5 pp.-2259.

- [61] M. Sternad and D. Aronsson, "Channel estimation and prediction for adaptive OFDMA/TDMA uplinks, based on overlapping pilots," in *Acoustics, Speech, and Signal Processing, 2005. Proceedings.(ICASSP'05). IEEE International Conference on*, 2005, pp. iii/861-iii/864 Vol. 3.
- [62] M. Sternad and D. Aronsson, "Channel estimation and prediction for adaptive OFDM downlinks [vehicular applications]," in *Vehicular Technology Conference, 2003. VTC 2003-Fall. 2003 IEEE 58th*, 2003, pp. 1283-1287.
- [63] Z. Shen, J. G. Andrews, and B. L. Evans, "Short range wireless channel prediction using local information," in *Signals, Systems and Computers, 2003. Conference Record of the Thirty-Seventh Asilomar Conference on*, 2003, pp. 1147-1151.
- [64] A. Duel-Hallen, "Fading Channel Prediction for Mobile Radio Adaptive Transmission Systems," *Proceedings of the IEEE*, vol. 95, pp. 2299-2313, 2007.
- [65] T. Eyceoz, A. Duel-Hallen, and H. Hallen, "Deterministic channel modeling and long range prediction of fast fading mobile radio channels," *Communications Letters, IEEE*, vol. 2, pp. 254-256, 1998.
- [66] O. Edfors, M. Sandell, J. J. Van de Beek, S. K. Wilson, and P. O. Borjesson, "OFDM channel estimation by singular value decomposition," *Communications, IEEE Transactions on*, vol. 46, pp. 931-939, 1998.
- [67] J. J. Van de Beek, O. Edfors, M. Sandell, S. K. Wilson, and P. O. Borjesson, "On channel estimation in OFDM systems," in *Vehicular Technology Conference, 1995 IEEE 45th*, 1995, pp. 815-819.
- [68] Y. Li, L. J. Cimini Jr, and N. R. Sollenberger, "Robust channel estimation for OFDM systems with rapid dispersive fading channels," *Communications, IEEE Transactions on*, vol. 46, pp. 902-915, 1998.
- [69] Y. Li, "Simplified channel estimation for OFDM systems with multiple transmit antennas," *Wireless Communications, IEEE Transactions on*, vol. 1, pp. 67-75, 2002.
- [70] T. Hwang, C. Yang, G. Wu, S. Li, and G. Ye Li, "OFDM and its wireless applications: a survey," *Vehicular Technology, IEEE Transactions on*, vol. 58, pp. 1673-1694, 2009.

- [71] Y. Sun, L. Yu, Q. Zhang, and L. Tang, "Wireless channel estimation based on B-spline interpolation in OFDM system," in *Natural Computation (ICNC), 2010 Sixth International Conference on*, 2010, pp. 3243-3247.
- [72] K. J. Kim, J. Yue, R. A. Iltis, and J. D. Gibson, "A QRD-M/Kalman filter-based detection and channel estimation algorithm for MIMO-OFDM systems," *Wireless Communications, IEEE Transactions on*, vol. 4, pp. 710-721, 2005.
- [73] S. Haykin, D. J. Thomson, and J. H. Reed, "Spectrum sensing for cognitive radio," *Proceedings of the IEEE*, vol. 97, pp. 849-877, 2009.
- [74] H. Minn and N. Al-Dhahir, "Optimal training signals for MIMO OFDM channel estimation," *Wireless Communications, IEEE Transactions on*, vol. 5, pp. 1158-1168, 2006.
- [75] Y. Liu and S. Sezginer, "Simple iterative channel estimation in LTE systems," in *Multi-Carrier Systems & Solutions (MC-SS), 2011 8th International Workshop on*, 2011, pp. 1-5.
- [76] M. D. Larsen, A. L. Swindlehurst, and T. Svantesson, "Performance bounds for MIMO-OFDM channel estimation," *Signal Processing, IEEE Transactions on*, vol. 57, pp. 1901-1916, 2009.
- [77] F. Foroughi, J. Lofgren, and O. Edfors, "Channel estimation for a mobile terminal in a multi-standard environment (LTE and DVB-H)," in *Signal Processing and Communication Systems, 2009. ICSPCS 2009. 3rd International Conference on*, 2009, pp. 1-9.
- [78] F. F. Abari, J. Löfgren, and O. Edfors, "Channel estimation for a mobile terminal in a multi-standard environment (LTE and DVB-H)," *Low-complexity and filter-tap memory optimized channel estimation in multi-mode and multi-standard OFDM systems*, p. 39, 2011.
- [79] F. F. Abari, F. K. Sharifabad, and O. Edfors, "Low Complexity Channel Estimation for LTE in Fast Fading Environments for Implementation on Multi-Standard Platforms,"

- in *Vehicular Technology Conference Fall (VTC 2010-Fall)*, 2010 IEEE 72nd, 2010, pp. 1-5.
- [80] S. Sorrentino, D. Greco, and L. Reggiani, "Least Squares Channel Estimation for IEEE 802.16e Systems Based on Adaptive Taps Selection," in *Vehicular Technology Conference, 2008. VTC Spring 2008. IEEE*, 2008, pp. 1524-1528.
 - [81] U. Tureli, H. Liu, and M. D. Zoltowski, "OFDM blind carrier offset estimation: ESPRIT," *Communications, IEEE Transactions on*, vol. 48, pp. 1459-1461, 2000.
 - [82] A. K. Bera and Y. Biliass, "The MM, ME, ML, EL, EF and GMM approaches to estimation: a synthesis," *Journal of Econometrics*, vol. 107, pp. 51-86, 2002.
 - [83] E. Ertin, U. Mitra, and S. Siwamogsatham, "Maximum-likelihood-based multipath channel estimation for code-division multiple-access systems," *Communications, IEEE Transactions on*, vol. 49, pp. 290-302, 2001.
 - [84] R. Negi, "Title," unpublished].
 - [85] A. L. Toledo, T. Vercauteren, and W. Xiaodong, "Adaptive Optimization of IEEE 802.11 DCF Based on Bayesian Estimation of the Number of Competing Terminals," *Mobile Computing, IEEE Transactions on*, vol. 5, pp. 1283-1296, 2006.
 - [86] B. Dong and W. Xiaodong, "Sampling-based soft equalization for frequency-selective MIMO channels," *Communications, IEEE Transactions on*, vol. 53, pp. 278-288, 2005.
 - [87] K. Huber and S. Haykin, "Improved bayesian MIMO channel tracking for wireless communications: incorporating a dynamical model," *Wireless Communications, IEEE Transactions on*, vol. 5, pp. 2458-2466, 2006.
 - [88] D. T. M. Slock, "Bayesian blind and semiblind channel estimation," in *Sensor Array and Multichannel Signal Processing Workshop Proceedings, 2004*, 2004, pp. 417-421.
 - [89] W. Wei, J. Xin, C. Yueming, and W. Xiaoxue, "Bayesian Cramer-rao Bound for channel estimation in cooperative OFDM," in *Wireless Communications and Signal Processing (WCSP), 2010 International Conference on*, 2010, pp. 1-6.

- [90] T. Ghirmai, M. F. Bugallo, J. Miguez, and P. M. Djuric, "A sequential Monte Carlo method for adaptive blind timing estimation and data detection," *Signal Processing, IEEE Transactions on*, vol. 53, pp. 2855-2865, 2005.
- [91] L. Huang, J. W. M. Bergmans, and F. M. J. Willems, "Low-complexity LMMSE-based MIMO-OFDM channel estimation via angle-domain processing," *Signal Processing, IEEE Transactions on*, vol. 55, pp. 5668-5680, 2007.
- [92] K. Yu, J. S. Evans, and I. B. Collings, "Performance analysis of LMMSE receivers for M-ary QAM in Rayleigh faded CDMA channels," *Vehicular Technology, IEEE Transactions on*, vol. 52, pp. 1242-1253, 2003.
- [93] S. Changyong, J. G. Andrews, and E. J. Powers, "An Efficient Design of Doubly Selective Channel Estimation for OFDM Systems," *Wireless Communications, IEEE Transactions on*, vol. 6, pp. 3790-3802, 2007.
- [94] C. Ming-Xian, "A new derivation of least-squares-fitting principle for OFDM channel estimation," *Wireless Communications, IEEE Transactions on*, vol. 5, pp. 726-731, 2006.
- [95] M. Latva-Aho and M. J. Juntti, "LMMSE detection for DS-CDMA systems in fading channels," *Communications, IEEE Transactions on*, vol. 48, pp. 194-199, 2000.
- [96] I. Tolochko and M. Faulkner, "Real time LMMSE channel estimation for wireless OFDM systems with transmitter diversity," in *Vehicular Technology Conference, 2002. Proceedings. VTC 2002-Fall. 2002 IEEE 56th*, 2002, pp. 1555-1559 vol.3.
- [97] J. F. Schmidt, J. E. Cousseau, R. Wichman, and S. Werner, "Low-Complexity Channel Prediction Using Approximated Recursive DCT," *Circuits and Systems I: Regular Papers, IEEE Transactions on*, vol. 58, pp. 2520-2530, 2011.
- [98] L. Wei, Y. Lie-Liang, and L. Hanzo, "Wideband channel estimation and prediction in single-carrier wireless systems," in *Vehicular Technology Conference, 2005. VTC 2005-Spring. 2005 IEEE 61st*, 2005, pp. 543-547 Vol. 1.

- [99] J. Tsao, D. Porrat, and D. Tse, "Prediction and Modeling for the Time-Evolving Ultra-Wideband Channel," *Selected Topics in Signal Processing, IEEE Journal of*, vol. 1, pp. 340-356, 2007.
- [100] Z. Yatong, W. Rui, and X. Kewen, "Nonlinear prediction of fast fading channel based on minimax probability machine," in *Industrial Electronics and Applications (ICIEA), 2011 6th IEEE Conference on*, 2011, pp. 451-454.
- [101] T. Ekman and G. Kubin, "Nonlinear prediction of mobile radio channels: measurements and MARS model designs," in *Acoustics, Speech, and Signal Processing, 1999. Proceedings., 1999 IEEE International Conference on*, 1999, pp. 2667-2670 vol.5.
- [102] S. Jiancheng, Z. Taiyi, and L. Feng, "Nonlinear prediction of mobile-radio fading channel using recurrent least squares support vector machines and embedding phase space," in *Communications, Circuits and Systems, 2004. ICCCAS 2004. 2004 International Conference on*, 2004, pp. 282-286 Vol.1.
- [103] S. Zukang, J. G. Andrews, and B. L. Evans, "Short range wireless channel prediction using local information," in *Signals, Systems and Computers, 2003. Conference Record of the Thirty-Seventh Asilomar Conference on*, 2003, pp. 1147-1151 Vol.1.
- [104] Y. Isukapalli and B. D. Rao, "Ergodicity of Wireless Channels and Temporal Prediction," in *Signals, Systems and Computers, 2006. ACSSC '06. Fortieth Asilomar Conference on*, 2006, pp. 473-477.
- [105] M. F. Iskander and Y. Zhengqing, "Propagation prediction models for wireless communication systems," *Microwave Theory and Techniques, IEEE Transactions on*, vol. 50, pp. 662-673, 2002.
- [106] D. Schafhuber and G. Matz, "MMSE and adaptive prediction of time-varying channels for OFDM systems," *Wireless Communications, IEEE Transactions on*, vol. 4, pp. 593-602, 2005.

- [107] S. Semmelrodt and R. Kattenbach, "Investigation of different fading forecast schemes for flat fading radio channels," in *Vehicular Technology Conference, 2003. VTC 2003-Fall. 2003 IEEE 58th*, 2003, pp. 149-153 Vol.1.
- [108] I. C. Wong and B. L. Evans, "Sinusoidal Modeling and Adaptive Channel Prediction in Mobile OFDM Systems," *Signal Processing, IEEE Transactions on*, vol. 56, pp. 1601-1615, 2008.
- [109] J. Tao, A. Duel-Hallen, and H. Hallen, "Performance of adaptive coded modulation enabled by long-range fading prediction with data-aided noise reduction," in *Military Communications Conference, 2008. MILCOM 2008. IEEE*, 2008, pp. 1-7.
- [110] A. Svensson, "An Introduction to Adaptive QAM Modulation Schemes for Known and Predicted Channels," *Proceedings of the IEEE*, vol. 95, pp. 2322-2336, 2007.
- [111] M. R. Souryal and R. L. Pickholtz, "Adaptive modulation with imperfect channel information in OFDM," in *Communications, 2001. ICC 2001. IEEE International Conference on*, 2001, pp. 1861-1865 vol.6.
- [112] R. K. Mallik, "On multivariate Rayleigh and exponential distributions," *Information Theory, IEEE Transactions on*, vol. 49, pp. 1499-1515, 2003.
- [113] N. C. Beaulieu and K. T. Hemachandra, "Novel Simple Forms for Multivariate Rayleigh and Rician Distributions with Generalized Correlation," in *Global Telecommunications Conference (GLOBECOM 2010), 2010 IEEE*, 2010, pp. 1-6.
- [114] C. C. Tan and N. C. Beaulieu, "Infinite series representations of the bivariate Rayleigh and Nakagami-m distributions," *Communications, IEEE Transactions on*, vol. 45, pp. 1159-1161, 1997.
- [115] D. A. Zogas and G. K. Karagiannidis, "Infinite-series representations associated with the bivariate rician distribution and their applications," *Communications, IEEE Transactions on*, vol. 53, pp. 1790-1794, 2005.
- [116] J. Mitola, III, *Software Radio Architecture: Object-Oriented Approaches to Wireless Systems Engineering*. West Sussex, England: John Wiley & Sons, Ltd, 2000.

- [117] J. Mitola, III and Z. Zvonar, *Software Radio Technologies: Selected Readings*. West Sussex, England: John Wiley & Sons, Ltd, 2001.
- [118] W. Tuttlebee, *Software Defined Radio: Enabling Technologies*. West Sussex, England: John Wiley & Sons, Ltd, 2002.
- [119] W. Tuttlebee, *Software Defined Radio: Origins, Drivers and International Perspectives*. West Sussex, England: John Wiley & Sons, Ltd, 2002.

APPENDIX A

MULTIPATH AND FADING MODELS

HiperLAN/2 Channel Model Standards	209
LTE Channel Model Standards	211
ITU Channel Model Standards	212
The SRWC Channel Model	213
Exponential Decaying Tap Model with Three Sets of Decaying Taps	213
Generating Multipath Models Cholesky Matrix	215
Jakes' and Flat Doppler Models Cholesky Matrix	215

In Appendix A the various multipath models and fading models will be presented using the MATLAB code used in the generation process. In the case of the multipath model, MATLAB code is used to generate a three column matrix containing all the parameters needed for a Rician model: delays normalized to 1 ns (first column), average power in dB (second column), and K factor (third column). The standards and all other models are given below.

MATLAB CODE BEGIN

```
%% HiperLAN/2 Channel Model Standards 209

% Model A: A typical large open space and office environments for
%           NLOS conditions and 100ns average rms delay spread.
HL2.ChA = [...
    0      0.0    0
   10    -0.9    0
   20    -1.7    0
   30    -2.6    0
   40    -3.5    0
   50    -4.3    0
   60    -5.2    0]
```

```

70    -6.1    0
80    -6.9    0
90    -7.8    0
110   -4.7    0
140   -7.3    0
170   -9.9    0
200  -12.5    0
240  -13.7    0
290  -18.0    0
340  -22.4    0
390  -26.7    0];

% Model B: A typical office environment for NLOS conditions
%           and 50ns average rms delay spread
HL2.ChB = [...
0      -2.6    0
10     -3.0    0
20     -3.5    0
30     -3.9    0
50      0.0    0
80     -1.3    0
110    -2.6    0
140    -3.9    0
180    -3.4    0
230    -5.6    0
280    -7.7    0
330    -9.9    0
380   -12.1    0
430   -14.3    0
490   -15.4    0
560   -18.4    0
640   -20.7    0
730   -24.6    0];

% Model C: A typical large open space environment for NLOS
%           conditions and 150ns average rms delay spread.
HL2.ChC = [...
0      -3.3    0
10     -3.6    0
20     -3.9    0
30     -4.2    0
50      0.0    0
80     -0.9    0
110    -1.7    0
140    -2.6    0
180    -1.5    0
230    -3.0    0
280    -4.4    0
330    -5.9    0
400    -5.3    0
490    -7.9    0
600    -9.4    0
730   -13.2    0
880   -16.3    0
1050  -21.2    0];

```

```

% Model D: A typical large open space environment for NLOS
%           conditions and 250ns average rms delay spread.
HL2.ChD = [...
    0      -4.9    0
   10     -5.1    0
   20     -5.2    0
   40     -0.8    0
   70     -1.3    0
  100     -1.9    0
  140     -0.3    0
  190     -1.2    0
  240     -2.1    0
  320      0.0    0
  430     -1.9    0
  560     -2.8    0
  710     -5.4    0
  880     -7.3    0
 1070     -1.6    0
 1280    -13.4    0
 1510    -17.4    0
 1760    -20.9    0];

```

%% LTE Channel Model Standards

```

% Model A: Extended Pedestrian A model (EPA)
LTE.ChA = [...
    0      0.0    0
   30     -1.0    0
   70     -2.0    0
   90     -3.0    0
  110     -8.0    0
  190    -17.2    0
  410    -20.8    0];

```

```

% Model B: Extended Vehicular A model (EVA)
LTE.ChB = [...
    0      0.0    0
   30     -1.5    0
  150     -1.4    0
  310     -3.6    0
  370     -0.6    0
  710     -9.1    0
 1090     -7.0    0
 1730    -12.0    0
 2510    -16.9    0];

```

```

% Model C: Extended Typical Urban model (ETU)
LTE.ChC = [...
    0      -1    0
   50      -1    0
  120      -1    0
  200       0    0
  230       0    0
  500       0    0
 1600      -3    0
 2300      -5    0

```

```
5000 -7 0];
```

%% ITU Channel Model Standards 212

```
% -----
```

	Channel A	Channel B
Test environment	RMS(ns)	RMS(ns)
Indoor office	35	100
Outdoor to indoor and pedestrian	45	750
Vehicular - high antenna	370	4000

```
% -----
```

```
% Model A: Indoor office test environment tapped-delay-line parameters
```

```
% Channel A
```

```
ITU.ChA = [...
    0     0     0
   50    -3     0
  110   -10     0
  170   -18     0
  290   -26     0
  310   -32     0];
```

```
% Model B: Indoor office test environment tapped-delay-line parameters
```

```
% Channel B
```

```
ITU.ChB = [...
    0     0     0
   100   -3.6   0
   200   -7.2   0
   300  -10.8   0
   500  -18.0   0
   700  -25.2   0];
```

```
% Model C: Outdoor to indoor and pedestrian test environment tapped
% delay-line parameters Channel A
```

```
ITU.ChC = [...
    0     0     0
   110    -3     0
   190   -10     0
   410   -32     0];
```

```
% Model D: Outdoor to indoor and pedestrian test environment tapped
% delay-line parameters Channel B
```

```
ITU.ChD = [...
    0     0.0     0
   200    -0.9     0
   800    -4.9     0
  1200    -8.0     0
  2300    -7.8     0
  3700   -23.9     0];
```

```

% Model E: Vehicular test environment, high antenna, tapped-delay-line
% parameters Channel A
ITU.ChE = [...
    0      0      0
   310    -3      0
   710   -10      0
  1090   -18      0
  1730   -26      0
  2510   -32      0];

% Model F: Vehicular test environment, high antenna, tapped-delay-line
% parameters Channel B
% ITU.ChF = [...
%     0      -2.5      0
%    300      0.0      0
%   8900   -12.8      0
%  12900   -10.0      0
%   17100  -25.2      0
%   20000  -16.0      0];

```

%% MCM This channel is feature in the SRWC Paper

```

MCM.ChA = [...
    0      0      0
   60      0      0
  140      0      0
  210     -3      0
  300     -3      0];

```

%% Exponential decaying tap models 213

```

EDT0 = [0;22;48];
EDT0(:,2) = [0;-4.7;-13.7];
Q0 = [1 1 1]*18/90;
Q1 = [1 1 1]*36/90;
Q2 = [1 1 1]*54/90;
Q3 = [1 1 1]*72/90;
Q4 = [1 1 1]*90/90;

M = 64;

dynrang = 50;
maxtappwr = max(EDT0(:,2));

space0 = diff([EDT0(:,1);M]);
ind0 = {...
    (1:space0(1))';...
    (space0(1)+1:sum(space0(1:2)))';...
    (sum(space0(1:2))+1:sum(space0))'};

EDT.Q18 = (0:M-1)';
EDT.Q36 = (0:M-1)';
EDT.Q54 = (0:M-1)';

```

```

EDT.Q72 = (0:M-1)';
EDT.Q90 = (0:M-1)';

for i1=1:3;
    if Q0(i1) == 0;
        EDT.Q18(ind0{i1},2) = [EDT0(i1,2);-Inf*ones(space0(i1)-1,1)];
        EDT.Q36(ind0{i1},2) = [EDT0(i1,2);-Inf*ones(space0(i1)-1,1)];
        EDT.Q54(ind0{i1},2) = [EDT0(i1,2);-Inf*ones(space0(i1)-1,1)];
        EDT.Q72(ind0{i1},2) = [EDT0(i1,2);-Inf*ones(space0(i1)-1,1)];
        EDT.Q90(ind0{i1},2) = [EDT0(i1,2);-Inf*ones(space0(i1)-1,1)];
    elseif Q0(i1) == 1;
        EDT.Q18(ind0{i1},2) = EDT0(i1,2)*ones(space0(i1),1);
        EDT.Q36(ind0{i1},2) = EDT0(i1,2)*ones(space0(i1),1);
        EDT.Q54(ind0{i1},2) = EDT0(i1,2)*ones(space0(i1),1);
        EDT.Q72(ind0{i1},2) = EDT0(i1,2)*ones(space0(i1),1);
        EDT.Q90(ind0{i1},2) = EDT0(i1,2)*ones(space0(i1),1);
    else
        EDT.Q18(ind0{i1},2) = (0:-1:-
space0(i1)+1)'/tan(pi*Q0(i1)/2)+EDT0(i1,2);
        EDT.Q36(ind0{i1},2) = (0:-1:-
space0(i1)+1)'/tan(pi*Q1(i1)/2)+EDT0(i1,2);
        EDT.Q54(ind0{i1},2) = (0:-1:-
space0(i1)+1)'/tan(pi*Q2(i1)/2)+EDT0(i1,2);
        EDT.Q72(ind0{i1},2) = (0:-1:-
space0(i1)+1)'/tan(pi*Q3(i1)/2)+EDT0(i1,2);
        EDT.Q90(ind0{i1},2) = (0:-1:-
space0(i1)+1)'/tan(pi*Q4(i1)/2)+EDT0(i1,2);
    end
end

EDT.Q18(:,1) = EDT.Q18(:,1)*10;
EDT.Q36(:,1) = EDT.Q36(:,1)*10;
EDT.Q54(:,1) = EDT.Q54(:,1)*10;
EDT.Q72(:,1) = EDT.Q72(:,1)*10;
EDT.Q90(:,1) = EDT.Q90(:,1)*10;
EDT.Q18(:,3) = 0;
EDT.Q36(:,3) = 0;
EDT.Q54(:,3) = 0;
EDT.Q72(:,3) = 0;
EDT.Q90(:,3) = 0;

%% Store all Models

save ChMods.mat HL2 LTE ITU MCM EDT
clear all

```

MATLAB CODE END

For the multipath models created in the code above, the code below can be used to create the Cholesky matrix for the respective multipath model in MATLAB.

MATLAB CODE BEGIN

```
%% Generate Multipath Models Cholesky Matrix 215
% List of Potential Channel Models
% HL2.ChA LTE.ChA ITU.ChA EDT.Q18 MCM.ChA
% HL2.ChB LTE.ChB ITU.ChB EDT.Q36
% HL2.ChC LTE.ChC ITU.ChC EDT.Q54
% HL2.ChD           ITU.ChD EDT.Q72
%                   ITU.ChE EDT.Q90

load ChMods.mat % load all channel models
MPMod = EDT.Q36; % select channel model to generate the Cholesky matrix

tapin = MPMod;
tapin(:,1) = tapin(:,1)/10;
M = max(tapin(:,1))+1;
K = 640; % Select the number of angular-frequency samples in the model

Ompr = eye(M);
Ompr = Ompr(tapin(:,1)+1,:);
Ctau = sqrt(10.^(tapin(:,2)/10)./(2*tapin(:,3)+2));
Ctau = diag(Ctau/sqrt(sum(Ctau.^2)/(K)));
```

MATLAB CODE END

The next MATLAB code is used to generate the fading models in this thesis. This code creates the Cholesky matrix as describe in the thesis after inputting the necessary variables.

MATLAB FUNCTION BEGIN

```
%% Jakes' and Flat Doppler Models Cholesky Matrix 215
function C = DFCovMtxGen(type,M0,M1,M2)
% type = type of fading model, Jakes' or Flat
% M0 = number of samples between the max a min doppler shift not the
number
%       of frequency taps
% M1 = total number of time samples including the samples not observed.
% M2 = the number of unobserved samples in the begining and thend of
the
%       fading signal

fd = 1;
M3 = M1-2*M2;
c0 = 1.5;

if strcmpi(type,'jakes')
    x = 2*pi*fd*abs(-M3/2:M3/2-1)/(2*M0);
```

```

x(x==0) = 1e-200;
h = [2^(1/4)*pi^(1/2)*gamma(3/4)*fd*...
      x.^(-1/4).*besselj(1/4,x).*...
      (0.54+0.46*cos(2*pi*((0:M3-1)-M3/2)/M3)) 0];

elseif strcmpi(type,'flat')
    x = fd*(-M3/2:M3/2-1)/M0;
    h = [2*sinc(x).*...
          (0.54+0.46*cos(2*pi*((0:M3-1)-M3/2)/M3)) 0];
else
    error('Incorrect Type')
end

h = convmtx(h,M3);
w = hamming(M2*2);
h = h(:,M3/2+(1-M2:M3+M2))*diag([w(1:M2);ones(M3,1);w(M2+1:end)]);
h = h*fft(eye(M1),[],2)*diag([ones(1,sqrt(M1)*c0/2) zeros(1,M1-
sqrt(M1)*c0) ones(1,sqrt(M1)*c0/2)])*ifft(eye(M1),[],2);
H = h*fft(eye(M1),[],2)/(M1);
H = H/sqrt(sum(sum(abs(H).^2)));
C = ifftshift(H(:,[1:sqrt(M1)*c0/2 end-sqrt(M1)*c0/2+1:end]),2);
C = C'*C;
C = chol(C);
C = C/sqrt(2*sum(sum(abs(C).^2)));

```

MATLAB FUNCTION END

APPENDIX B

RATE ADAPTATION LOOK-UP TABLE

$\begin{matrix} j \\ i \end{matrix}$		Modulation Schemes											
		00	01	02	03	04	05	06	07	08	09	10	11
BER Limits	00	11.31	14.32	19.03	21.22	25.32	27.37	31.35	33.37	37.33	39.34	43.30	45.31
	01	11.24	14.25	18.96	21.15	25.25	27.30	31.28	33.30	37.25	39.27	43.22	45.23
	02	11.16	14.17	18.89	21.07	25.17	27.22	31.20	33.22	37.17	39.19	43.14	45.15
	03	11.09	14.10	18.81	21.00	25.10	27.14	31.12	33.14	37.09	39.11	43.06	45.07
	04	18.73	20.92	25.02	27.06	31.04	33.06	37.01	39.03	42.98	44.99	18.73	20.92
	05	18.66	20.84	24.94	26.98	30.96	32.98	36.93	38.94	42.89	44.91	18.66	20.84
	06	18.58	20.76	24.86	26.90	30.88	32.90	36.85	38.86	42.81	44.82	18.58	20.76
	07	18.50	20.68	24.78	26.82	30.80	32.81	36.76	38.77	42.72	44.73	18.50	20.68
	08	18.41	20.59	24.69	26.73	30.71	32.72	36.68	38.68	42.63	44.64	18.41	20.59
	09	18.33	20.51	24.61	26.65	30.62	32.64	36.59	38.60	42.54	44.55	18.33	20.51
	10	18.24	20.42	24.52	26.56	30.53	32.55	36.50	38.50	42.45	44.46	18.24	20.42

$\begin{matrix} j \\ i \end{matrix}$		Modulation Schemes											
		00	01	02	03	04	05	06	07	08	09	10	11
BER Limits	11	18.16	20.34	24.43	26.47	30.44	32.45	36.40	38.41	42.36	44.37	18.16	20.34
	12	18.07	20.24	24.34	26.38	30.35	32.36	36.31	38.32	42.26	44.27	18.07	20.24
	13	17.98	20.15	24.25	26.28	30.26	32.27	36.21	38.22	42.16	44.17	17.98	20.15
	14	17.88	20.06	24.15	26.19	30.16	32.17	36.11	38.12	42.06	44.07	17.88	20.06
	15	17.79	19.97	24.05	26.09	30.06	32.07	36.01	38.02	41.96	43.97	17.79	19.97
	16	17.69	19.87	23.96	25.99	29.96	31.97	35.91	37.91	41.86	43.86	17.69	19.87
	17	17.60	19.77	23.86	25.89	29.86	31.86	35.81	37.81	41.75	43.75	17.60	19.77
	18	17.49	19.67	23.75	25.79	29.75	31.76	35.70	37.70	41.64	43.64	17.49	19.67
	19	17.39	19.56	23.65	25.68	29.64	31.65	35.59	37.59	41.53	43.53	17.39	19.56
	20	17.29	19.46	23.54	25.57	29.53	31.54	35.47	37.47	41.41	43.41	17.29	19.46
	21	17.18	19.35	23.43	25.46	29.42	31.42	35.36	37.36	41.29	43.29	17.18	19.35
	22	17.07	19.24	23.31	25.34	29.30	31.30	35.24	37.24	41.17	43.17	17.07	19.24
	23	16.95	19.12	23.20	25.22	29.18	31.18	35.12	37.11	41.05	43.05	16.95	19.12
	24	16.84	19.00	23.08	25.10	29.06	31.06	34.99	36.99	40.92	42.92	16.84	19.00
	25	16.72	18.88	22.96	24.98	28.93	30.93	34.86	36.86	40.79	42.78	16.72	18.88
	26	16.60	18.76	22.83	24.85	28.80	30.80	34.73	36.72	40.65	42.65	16.60	18.76

$\begin{matrix} j \\ i \end{matrix}$		Modulation Schemes											
		00	01	02	03	04	05	06	07	08	09	10	11
BER Limits	27	16.47	18.63	22.70	24.72	28.67	30.66	34.59	36.58	40.51	42.50	16.47	18.63
	28	16.34	18.50	22.57	24.59	28.53	30.52	34.45	36.44	40.37	42.36	16.34	18.50
	29	16.21	18.37	22.43	24.45	28.39	30.38	34.31	36.29	40.22	42.21	16.21	18.37
	30	16.07	18.23	22.29	24.30	28.25	30.23	34.16	36.14	40.06	42.05	16.07	18.23
	31	15.93	18.08	22.14	24.15	28.10	30.08	34.00	35.98	39.90	41.89	15.93	18.08
	32	15.78	17.94	21.99	24.00	27.94	29.92	33.84	35.82	39.74	41.72	15.78	17.94
	33	15.63	17.78	21.83	23.84	27.78	29.76	33.67	35.65	39.57	41.55	15.63	17.78
	34	15.48	17.62	21.67	23.68	27.61	29.59	33.50	35.48	39.39	41.37	15.48	17.62
	35	15.32	17.46	21.51	23.51	27.44	29.41	33.32	35.30	39.21	41.18	15.32	17.46
	36	15.15	17.29	21.33	23.33	27.26	29.23	33.14	35.11	39.01	40.99	15.15	17.29
	37	14.98	17.12	21.15	23.15	27.07	29.04	32.94	34.91	38.81	40.78	14.98	17.12
	38	14.80	16.93	20.97	22.96	26.88	28.84	32.74	34.70	38.60	40.57	14.80	16.93
	39	14.61	16.74	20.77	22.76	26.67	28.63	32.53	34.49	38.39	40.35	14.61	16.74
	40	14.42	16.54	20.57	22.55	26.46	28.42	32.31	34.26	38.16	40.12	14.42	16.54
	41	14.21	16.34	20.35	22.33	26.24	28.19	32.07	34.02	37.91	39.87	14.21	16.34
	42	14.00	16.12	20.13	22.10	26.00	27.95	31.83	33.78	37.66	39.61	14.00	16.12

$\begin{matrix} j \\ i \end{matrix}$		Modulation Schemes											
		00	01	02	03	04	05	06	07	08	09	10	11
BER Limits	43	13.78	15.89	19.90	21.86	25.76	27.70	31.57	33.51	37.39	39.34	13.78	15.89
	44	13.55	15.65	19.65	21.61	25.50	27.43	31.30	33.23	37.11	39.05	13.55	15.65
	45	13.3	15.40	19.39	21.35	25.22	27.15	31.01	32.94	36.80	38.74	13.30	15.40
	46	13.04	15.14	19.12	21.06	24.93	26.85	30.70	32.62	36.48	38.41	13.04	15.14
	47	12.77	14.86	18.83	20.76	24.62	26.53	30.38	32.29	36.14	38.05	12.77	14.86
	48	12.48	14.56	18.52	20.45	24.29	26.19	30.03	31.93	35.76	37.67	12.48	14.56
	49	12.17	14.24	18.18	20.10	23.94	25.83	29.65	31.54	35.36	37.26	12.17	14.24
	50	11.84	13.90	17.83	19.74	23.56	25.43	29.24	31.11	34.92	36.81	11.84	13.90
	51	11.49	13.54	17.45	19.34	23.14	25.00	28.79	30.65	34.45	36.31	11.49	13.54
	52	11.11	13.14	17.03	18.91	22.69	24.53	28.30	30.14	33.92	35.76	11.11	13.14
	53	10.70	12.72	16.58	18.44	22.19	24.01	27.76	29.58	33.33	35.15	10.70	12.72
	54	10.25	12.25	16.08	17.91	21.64	23.44	27.15	28.94	32.66	34.45	10.25	12.25
	55	9.76	11.73	15.53	17.33	21.03	22.79	26.46	28.22	31.9	33.65	9.76	11.73
	56	9.21	11.16	14.92	16.68	20.33	22.05	25.68	27.38	31.01	32.71	9.21	11.16
	57	8.60	10.51	14.22	15.94	19.52	21.19	24.75	26.40	29.96	31.60	8.60	10.51
	58	7.91	9.78	13.41	15.07	18.58	20.18	23.66	25.23	28.72	30.28	7.91	9.78

$\begin{matrix} j \\ i \end{matrix}$		Modulation Schemes											
		00	01	02	03	04	05	06	07	08	09	10	11
BER Limits	59	7.11	8.92	12.47	14.05	17.47	18.97	22.36	23.85	27.26	28.75	7.11	8.92
	60	6.18	7.91	11.34	12.83	16.13	17.55	20.85	22.26	25.60	27.04	6.18	7.91
	61	5.06	6.70	10.00	11.38	14.58	15.92	19.14	20.49	23.75	25.11	5.06	6.70
	62	3.69	5.25	8.40	9.71	12.81	14.08	17.21	18.45	21.59	22.80	3.69	5.25
	63	2.00	3.51	6.55	7.80	10.79	11.94	14.89	15.96	18.85	19.83	2.00	3.51
	64	-0.11	1.45	4.35	5.51	8.28	9.22	11.87	12.65	15.24	15.95	-0.11	1.45
	65	-2.93	-1.23	1.41	2.43	4.79	5.47	7.73	8.23	10.42	10.81	-2.93	-1.23
	66	-7.71	-5.78	-3.57	-2.59	-0.77	-0.22	1.47	1.78	3.41	3.55	-7.71	-5.78

Table B.1: SNR threshold look-up table.

